



HAL
open science

Identification of interacting mitochondrial enzymes involved in pyrroline-5-carboxylate metabolism in *Arabidopsis thaliana*

Yao Zheng

► **To cite this version:**

Yao Zheng. Identification of interacting mitochondrial enzymes involved in pyrroline-5-carboxylate metabolism in *Arabidopsis thaliana*. Biochemistry, Molecular Biology. Sorbonne Université, 2021. English. NNT: 2021SORUS269 . tel-04206678

HAL Id: tel-04206678

<https://theses.hal.science/tel-04206678v1>

Submitted on 14 Sep 2023

HAL is a multi-disciplinary open access archive for the deposit and dissemination of scientific research documents, whether they are published or not. The documents may come from teaching and research institutions in France or abroad, or from public or private research centers.

L'archive ouverte pluridisciplinaire **HAL**, est destinée au dépôt et à la diffusion de documents scientifiques de niveau recherche, publiés ou non, émanant des établissements d'enseignement et de recherche français ou étrangers, des laboratoires publics ou privés.

Sorbonne Université

Ecole doctorale 515 – Complexité du vivant

Institut d'Écologie et des Sciences de l'Environnement de Paris (iEES)

Equipe Adaptation des Plantes aux Contraintes Environnementales (APCE)

Identification of interacting mitochondrial enzymes involved in pyrroline-5-carboxylate metabolism in *Arabidopsis thaliana*

Par Yao ZHENG

Thèse de doctorat de Biologie Moléculaire et Biochimie

Dirigée par Dr. Sandrine LANFRANCHI et Dr. Arnould SAVOURÉ

Présentée et soutenue publiquement le 13 Septembre 2021

Devant un jury composé de :

| | | |
|--------------------------------|-------------------------------------|--------------------|
| Mme. MASCLAUX-DAUBRESSE Céline | DR, INRAE, IJPB | Rapporteur |
| M. BATOKO Henri | PR, University of Louvain (Belgium) | Rapporteur |
| Mme. LISZKAY Anja | DR, CNRS, I2BC | Examinatrice |
| Mme. AVILAN Luisana | CR, University of Portsmouth (UK) | Examinatrice |
| M. HENRI Julien | MCF, Sorbonne Université, IBPS | Examineur |
| M. BAILLY Christophe | PR, Sorbonne Université, IBPS | Examineur |
| Mme. LANFRANCHI Sandrine | MCF, Sorbonne Université, iEES | Co-encadrante |
| M. SAVOURÉ Arnould | PR, Sorbonne Université, iEES | Directeur de thèse |

Acknowledgements

I still remember the first day I arrived at campus Jussieu of Sorbonne Université in September 2017. At that moment, it is still called Université Pierre et Marie Curie.

Le temps passe si vite!

Right now, it is already my fourth and the last year for my PhD in France. Hence, I cannot help feeling a little bit melancholy. During the past 4 years of my study, I have received many supports and help from other people. Therefore, there are many people that I would like to thank for.

At first, I want to show my sincere appreciation for my jury:

Mme. Céline MASCLAUX-DAUBRESSE

M. Henri BATOKO

Mme. Anja LISZKAY

Mme. Luisana AVILAN

M. Julien HENRI

M. BAILLY Christophe

It is my honour and pleasure to let them be the member of my jury and thank for their presence and remarks. Special thanks to my two rapporteurs Mme. Céline MASCLAUX-DAUBRESSE and M. Henri BATOKO for their inspiring comments for my thesis.

Secondly, I would like to express my great gratitude to my two supervisors—Dr. Arnould SAVOURÉ and Dr. Sandrine LEBRETON—who are sophisticated scientists with benevolent heart and creative mind. Dr. Sandrine LEBRETON guided my experiments with great patience, and she is always able to bring new ideas for my PhD project to guide me. Dr. Arnould SAVOURÉ is always supportive and kind. His optimistic attitude and inspiring ideas enlighten and lead me to conquer all the difficulties during my study. With the generous help and critical thinking from my two supervisors, I became to know better about how to do scientific research and how to optimize time management for the project. I know I am not a perfect student, but my supervisors are always kind and patient about my mistakes and shortcomings. My gratitude to them is beyond my words.

Next, I would like to express my deep thanks for everyone in our team APCE who are supportive and give me a warm welcome in the lab:

Anne GUIVARC'H

Régis MALDINEY

Cécile CABASSA-HOURTON

Emilie CRILAT

Pierre CAROL

Marianne BORDENAVE-JACQUEMIN

Séverine PLANCHAIS

Katia AMI

Luc RICHARD

Corentin DOURMAP

Mariem KSIAA

Iry ANDRIANJARA

Rabaa HIDRI

Sabrina GUERIDI

Ahmed EL MOUKHTARI

I will never forget the day that we gather to fill up tips for the pipette. I wish I were able to join your lovely chatting in French. Special thanks to Anne who is a kind and benevolent friend to me and helps me a lot to adapt myself to the life in Paris. I also appreciate the generous help from Cécile who kindly and efficiently instruct me in mitochondria related experiments. Thank Emilie for her skilled technical support in plasmid construction and Western blots. I also want to show my appreciation to the secretary team of iEES. Special thanks for Mme. Carole BOUSQUET.

Next, I want to show my sincere appreciation to Prof. Hans-Peter BRAUN from Institute of Plant Genetics, Leibniz Universität Hannover, Germany. Thanks for him and his team to help me perform MS and related analysis. Moreover, I am also very grateful for Susanne BOLTE, Jean-François GILLES, and France LAM from the IBPS imaging facility for their help with confocal microscopy and 3D rendering on mitochondria. I would also express my gratitude for Stéphanie AGYS, Patrick DUMONT, Emilie DAVEAU, and Carina RODRIGUES MENDES from the growth chamber team of IBPS. Special thanks to my friend Wei ZHANG (张炜) from IBPS who helped me during my study in Paris.

I am also grateful to Mme. Emmanuèle MOUCHEL-VIELH, M. Frederic DEVAUX and Mme. Samira ERRAJI from Ecole Doctorale "Complexité du Vivant" (ED515) for their help during my study.

Next, I would like to express my deep gratitude to my motherland—China. It is a great pleasure for me to receive the Chinese National Scholarship issued by China Scholarship Council (CSC). Without the financial help from CSC, I could not accomplish my study in France.

At last, I want to thank all my family. My dear girlfriend Lin ZHANG (张琳) is always there understanding and supporting me. Our encounter is an unexpectedly beautiful gift for me during my study in France. I am extremely grateful to both my mother Xiuying XIA (夏秀英) and father Yunlong ZHENG (郑云龙) whose love protect and support me forever. Thank them for bringing me to this splendid world.

The words I can write here is limited, but my gratitude in my heart is unlimited.

September 2021

Paris

Table of Contents

| | |
|---|------|
| Acknowledgements | i |
| Table of Contents | iii |
| List of Figures and Tables | vi |
| Abbreviations | viii |
| General Introduction | 1 |
| Chapter 1. State of the Art..... | 5 |
| 1.1 Proline is a multifunctional amino acid..... | 5 |
| 1.2 Proline Metabolism | 6 |
| 1.2.1 Proline biosynthesis | 6 |
| 1.2.2 Proline catabolism..... | 9 |
| 1.2.3 Subcellular localization of proline metabolic enzymes..... | 11 |
| 1.2.4 Proline transport in plants | 12 |
| 1.2.5 Proline/P5C cycle | 14 |
| 1.3 Regulation of proline metabolism in plants | 15 |
| 1.3.1 Regulation of proline biosynthesis..... | 15 |
| 1.3.2 Regulation of proline catabolism | 21 |
| 1.3.3 Post-translational modification of proline metabolic enzymes | 23 |
| 1.4 Proline catabolism is tightly linked to energy metabolism | 24 |
| 1.4.1 Proline catabolism and mitochondrial respiration..... | 24 |
| 1.4.2 Proline catabolism and dark-induced leaf senescence | 27 |
| 1.5 Structural biology of ProDH, P5CDH, and OAT..... | 29 |
| 1.5.1 Structure diversity and oligomerization | 29 |
| 1.5.2 Metabolon and substrate channelling..... | 31 |
| 1.6 Scientific questions | 33 |
| Chapter 2. The proline cycle as a eukaryotic redox valve | 37 |
| Chapter 3. Different fate of mitochondrial enzymes involved in pyrroline-5-carboxylate metabolism during dark-induced leaf senescence in <i>Arabidopsis thaliana</i> | 51 |
| Article..... | 52 |
| Abstract | 53 |
| Introduction | 53 |
| Methods and Materials | 56 |
| Results | 60 |

| | |
|---|------------|
| Knockout <i>Arabidopsis prodh1prodh2</i> and <i>p5cdh</i> mutants accumulate proline during dark-induced senescence | 60 |
| Involvement of P5C metabolism enzymes during DIS | 61 |
| Significant metabolic reprogramming of <i>prodh1prodh2</i> and <i>p5cdh</i> mutants during DIS evidenced by metabolomic profiling analysis..... | 62 |
| Discussion | 65 |
| Figures and tables..... | 69 |
| References | 78 |
| Chapter 4. Pyrroline-5-carboxylate metabolism protein complex detected in <i>Arabidopsis thaliana</i> leaf mitochondria..... | 85 |
| Article..... | 86 |
| Abstract | 87 |
| Introduction..... | 87 |
| Materials and Methods | 90 |
| Results..... | 96 |
| ProDH1, P5CDH and OAT interact in plant mitochondria | 96 |
| ProDH1, P5CDH and OAT are present in different sub-mitochondrial fractions during DIS in <i>Arabidopsis thaliana</i> | 98 |
| Proteomic evidence for interactions between ProDH1, P5CDH and OAT during DIS in <i>Arabidopsis</i> leaves..... | 99 |
| Identification of a P5CDH-interacting complex by complexome profiling..... | 100 |
| ProDH1 and OAT co-immunoprecipitate with P5CDH-GFP..... | 101 |
| Discussion | 102 |
| ProDH1, P5CDH, and OAT interact in mitochondria during DIS..... | 102 |
| ProDH, P5CDH, and OAT can form a complex with other partners during DIS | 103 |
| Figures and tables..... | 106 |
| References | 117 |
| 4.1 Supplementary results | 121 |
| 4.1.1 Heat map for proteins co-migrate with P5CDH..... | 121 |
| 4.1.2 Putative interaction between ProDH1 and SDH1-1 is strengthened by 1D BN-PAGE followed with MS | 121 |
| 4.1.3 DSP crosslinking reveals high molecular weight complex of ProDH1, P5CDH, and OAT | 123 |
| 4.1.4 ProDH2 may interact with ProDH1 and P5CDH in mitochondrial membrane..... | 125 |
| 4.1.5 Figures | 126 |
| 4.1.6 Supplementary materials and methods..... | 128 |
| Chapter 5. General discussion and perspectives | 131 |
| 5.1 Temporal and spatial identification of ProDH1, P5CDH, and OAT..... | 131 |
| 5.1.1 DIS triggers all three ProDH1, P5CDH, and OAT catabolic enzymes | 131 |
| 5.1.2 ProDH1, P5CDH, and OAT presents different submitochondrial localization..... | 133 |
| 5.2 ProDH1, P5CDH, and OAT interact to form a P5C metabolic complex | 134 |

| | |
|---|-----|
| 5.3 Proline catabolism has a close relationship with ETC and energy production | 135 |
| 5.4 Mitochondrial P5C metabolic complex may allow P5C/GSA sequestration and fine regulation of proline catabolism | 136 |
| 5.4.1 Substrate channelling | 137 |
| 5.4.2 Co-regulation through interactions | 138 |
| 5.4.3 P5CDH may function as a regulatory funnel during DIS | 139 |
| 5.5 Perspectives | 139 |
| 5.5.1 Identify other partners of P5C metabolic complex | 139 |
| 5.5.2 Substrate channelling | 140 |
| 5.5.3 Relationship with Complex II | 140 |
| 5.5.4 PTMs | 141 |
| Annexes | 145 |
| Annex I: Multiple sequence alignments | 145 |
| Alignments for OAT | 145 |
| Alignments for ProDH | 147 |
| Alignments for P5CDH | 149 |
| References | 151 |
| Abstract | 164 |
| Résumé | 164 |

List of Figures and Tables

| | | Title | Page |
|-------------|--------------|--|-------|
| Chapter I | Figure I-1. | Venn diagram of multiple functions of proline metabolism in plants and animals | 5 |
| | Figure I-2. | Simplified proline metabolism in higher plants. | 7 |
| | Figure I-3. | Representative diagram for proline catabolic enzymes in different living organisms. | 9 |
| | Figure I-4. | Unrooted phylogenic tree of eukaryotic proline dehydrogenase | 10 |
| | Figure I-5. | Working model of trifunctional PutA. | 11 |
| | Figure I-6. | Correlation between proline catabolism and the ETC | 25 |
| | Table I-1. | Oligomeric state of proline catabolic enzymes and OAT | 30 |
| | Figure I-7. | Substrate channeling of GsPutA. | 32 |
| Chapter II | Figure II-1. | Proline metabolism in plants and its links to the ornithine and pentose phosphate pathways. | 40 |
| | Figure II-2. | The glycerol-3-phosphate (G3P) (A) and the malate–aspartate (B) shuttles for transporting reducing equivalents from cytosolic NADH into the mitochondrial matrix or mitochondrial oxidative phosphorylation pathway, respectively. | 42 |
| | Figure II-3. | Malate-oxaloacetate shuttle, or the malate valve, involves the intercon-version of malate and oxaloacetate by malate dehydrogenase (MDH). | 44 |
| Chapter III | Figure 1. | Total chlorophyll contents during dark-induced senescence in Arabidopsis. | 79 |
| | Figure 2. | Proline contents during dark-induced senescence in Arabidopsis. | 79 |
| | Figure 3. | Transcript levels of P5CS1, <i>ProDH1</i> , <i>P5CDH</i> , and <i>OAT</i> during DIS. | 80 |
| | Figure 4. | <i>ProDH1</i> , <i>P5CDH</i> , <i>OAT</i> and <i>SAG12</i> protein levels during DIS in Arabidopsis. | 81 |
| | Figure 5. | Protein amounts and enzymatic activities of <i>ProDH</i> and <i>OAT</i> were reduced in <i>p5cdh</i> at Day 4 of DIS. | 81 |
| | Figure 6. | Principle component analysis (PCA) of metabolome during 0-5 days of DIS in Arabidopsis. | 82 |
| | Figure 7. | Contents of amino acids (AA), AA derived metabolites, and TCA metabolites in different genotypes during DIS. | 83/84 |

| | | | |
|-------------|-------------------------|--|-----|
| Chapter III | Figure 8. | Correlation between glutamate and proline (A) as well as P5C and proline (B) during DIS in Arabidopsis. | 85 |
| | Supplemental Figure S1. | Photographs of dark-induced leaf senescence during dark-induced leaf senescence in Arabidopsis. | 86 |
| | Supplemental Figure S2. | TGX Stain-Free membranes of total proteins extracted from Col-0, as well as <i>prodh1prodh2</i> , <i>p5cdh</i> , <i>oat</i> mutants after 0-5 days of DIS. | 86 |
| | Supplemental Figure S3. | P5CS and P5CR protein contents at D3 of DIS in Arabidopsis | 87 |
| | Supplementary Table S1. | List of primers | 87 |
| | Supplementary Table 2. | Distribution of the 117 metabolites across the 3 PCs | 88 |
| Chapter IV | Figure 1. | BiFC assays with ProDH1, P5CDH, and OAT in <i>Nicotiana benthamiana</i> | 116 |
| | Figure 2. | Sub-mitochondrial localization of ProDH1, P5CDH, and OAT in <i>Arabidopsis thaliana</i> during DIS | 117 |
| | Figure 3. | Proteomic analysis of ProDH1, P5CDH, and OAT in mitochondrial fractions of <i>Arabidopsis thaliana</i> using 2D BN/SDS-PAGE, immunoblotting and MS | 118 |
| | Figure 4. | ProDH1, P5CDH, and OAT expressed during DIS in <i>Arabidopsis thaliana</i> co-migrate on 2D native/SDS gels | 118 |
| | Figure 5. | Comparative complexome profiling of mitochondria from two Arabidopsis lines | 119 |
| | Figure 6. | Co-immunoprecipitation (Co-IP) of ProDH1 and OAT with P5CDH-tGFP | 120 |
| | Supplemental Figure S1. | Proline sensitivity of <i>p5cdh</i> was complemented in <i>35S:P5CDH-tGFP/p5cdh</i> plants. | 121 |
| | Supplemental Figure S2. | Controls and additional BiFC assays in <i>Nicotiana benthamiana</i> . | 122 |
| | Supplemental Figure S3. | Protein expression of BiFC infiltrated <i>Nicotiana benthamiana</i> leaves. | 123 |
| | Supplemental Figure S4. | Migration pattern of selected proteins not affected by P5CDH-tGFP. | 124 |
| | Supplemental Figure S5. | Complexome profiling for SDH1-1. | 125 |
| | Supplemental Table S1. | List of primers used for cloning | 126 |

Abbreviations

| ABBREVIATION | MEANING |
|---------------------|--|
| AAP | Amino Acid Permease |
| AAT | Aspartate Aminotransferase |
| ABA | Abscisic Acid |
| ABF | ABRE Binding Factor |
| ABRE | ABA-Responsive Elements |
| ALDH | Aldehyde dehydrogenase |
| AP2/ERF | APETALA2/Ethylene-Responsive Factor |
| AREB | ABA-Responsive Element Binding Protein |
| ASN1 | ASPARAGINE SYNTHETASE1 |
| CaM | Calmodulin |
| CaMTA | CaM binding Transcription Activator |
| ChIP | Chromatin Immunoprecipitation |
| ChIP-chip | Chromatin Immunoprecipitation-DNA chip hybridization |
| CO | CONSTANS |
| Complex I | NADH-Ubiquinone Oxidoreductase |
| CRT | C-Repeats |
| DFR1 | Drought and Freezing Responsive gene 1 |
| DHAP | Dihydroxyacetone Phosphate |
| DIS | Dark-Induced Senescence |
| DLS | Developmental Leaf Senescence |
| DRE | Dehydration-Responsive Elements |
| DSP | Dithiobis(Succinimidylpropionate) |
| ETC | Electron Transport Chain |
| ETF | Electron Transfer Flavoprotein |
| ETF-QO | Electron Transfer Flavoprotein-Ubiquinone Oxidoreductase |
| FLC | FLOWERING LOCUS C |
| FRI | FRIGIDA |
| G3P | Glycerol-3-Phosphate |
| GAPDH | Glyceraldehyde 3-Phosphate Dehydrogenase |
| GDH | Glutamate Dehydrogenase |
| GK | γ -Glutamyl Kinase |
| GP | γ -Glutamyl Phosphate |
| GPDH | Glycerol-3-Phosphate Dehydrogenase |
| GPR | γ -Glutamyl Phosphate Reductase |
| GSA/GSAL | γ -Glutamyl Semialdehyde |
| HY5 | ELONGATED HYPOCOTYL 5 |
| iN | Internal NAD(P)H Dehydrogenase |

ABBREVIATIONS

| ABBREVIATION | MEANING |
|---------------------|--|
| IVDH | Isovaleryl-Coenzyme A Dehydrogenase |
| LHT | Lysine-Histidine Transporter |
| MDH | Malate Dehydrogenase |
| MOT | Malate/OAA Translocators |
| NAC | NAM, ATAF, and CUC |
| nat-siRNA | natural small interfering RNA |
| OAA | Oxaloacetate |
| OxPPP | Oxidative Pentose Phosphate Pathway |
| P5C | Δ^1 -Pyrroline-5-carboxylate |
| P5CDH/GSALDH | Δ^1 -Pyrroline-5-Carboxylate Dehydrogenase/ γ -Glutamyl Semialdehyde Dehydrogenase |
| P5CR/PYCR | Δ^1 -Pyrroline-5-Carboxylate Reductase |
| P5CS | Δ^1 -Pyrroline-5-Carboxylate Synthetase |
| PCD | Programmed Cell Death |
| PEP | Phosphoenolpyruvate |
| PLC | Phospholipase C |
| PLD | Phospholipase D |
| PLP | Pyridoxal-5-phosphate |
| PP2C | Type 2C protein phosphatase |
| PRE | Proline/Hypoosmolarity-Responsive Element |
| ProDH/POX | Proline Dehydrogenase/Proline Oxidase |
| ProT | Proline Transporters |
| PutA | Proline utilization A |
| ROS | Reactive Oxygen Species |
| SDH/Complex II | Succinate Dehydrogenase |
| SIS | Shade-Induced Senescence |
| SnRK | Sucrose Nonfermenting-1-Related Kinase |
| SRO5 | SIMILAR TO RCD ONE 5 |
| TCA | Tricarboxylic Acid |
| TFs | Transcription Factors |
| TIM barrel | ($\beta\alpha$) ₈ barrel |
| TOR | TARGET OF RAPAMYCIN |
| UQ | Ubiquinone |
| OAT | Ornithine δ -Aminotransferase |

General Introduction

Plants are the most selfless living organisms on Earth. They not only bring solar energy and oxygen into biosphere by photosynthesis, but they also participate in the global biogeochemical cycles that influence and maintain our climate system through vegetation-climate interaction (Schulze, 2001; Piao *et al.*, 2019). Besides, plants are the most thriving taxa on Earth, constituting about 80% of the global biomass (represented by carbon) (Bar-On *et al.*, 2018). They provide food, medicine, shelter, and materials for animals including human.

However, plants live in dynamic environments that are often unfavourable or stressful for plant growth and development. Hostile environmental conditions for plants include biotic stress, such as pathogen infection and herbivore attack, and abiotic stress, such as drought, heat, cold, nutrient deficiency, salt, and heavy metals. Among them, drought, salt, and temperature stresses are major environmental factors that constrain the geographical distribution of plants in nature, limit agricultural productivity, and consequently threaten food security (Zhu, 2016). However, climate change will exacerbate the adverse effects of these abiotic stresses on agriculture, by causing increased occurrence of extreme weather (Fedoroff *et al.*, 2010).

Overall, proline accumulation is recognized as a common response to variable stresses in living organisms. As a proteinogenic amino acid, proline is essential for primary metabolism and versatile among species. It contributes to biotic/abiotic stress responses, osmotic adjustment, protein chaperoning, reactive oxygen species (ROS) signalling, redox homeostasis, and energy metabolism. Hence, study on proline metabolism will be instructive for future crop engineering, furthermore, improving human society's ability to cope with climate change.

In plants, proline is mainly synthesized from glutamate. Proline is synthesized from glutamate by the sequential action of Pyrroline-5-Carboxylate (P5C) Synthetase (P5CS) and P5C Reductase (P5CR). Proline is oxidized to glutamate in mitochondria by the sequential action of Proline Dehydrogenase (ProDH) and P5C Dehydrogenase (P5CDH). Both proline anabolism and catabolism use P5C as an intermediate. In addition, Ornithine δ -Aminotransferase (OAT) also participates in P5C production, which converts ornithine and α -ketoglutarate to glutamate and P5C in mitochondria. So far, extensive studies have shown multiple biological features of proline and its biosynthetic pathway in the past decades, however, details of the regulation of proline catabolism are still largely unknown.

Intriguingly, the structure of proline catabolic enzymes is diverse among species. In Gram-negative bacteria, ProDH and P5CDH are combined into one bifunctional enzyme known

as Proline utilization A (PutA). But in some other bacteria such as *Thermus thermophilus*, ProDH and P5CDH are monofunctional enzymes. However, only monofunctional ProDH and P5CDH are found in eukaryotes (Tanner, 2008; Servet *et al.*, 2012).

A substrate-channelling mechanism has been found in bifunctional PutA allowing P5C/GSA sequestration in *Geobacter sulfurreducens* and *Bradyrhizobium japonicum* (Srivastava *et al.*, 2010; Singh *et al.*, 2014). Moreover in *T. thermophilus*, monofunctional ProDH and P5CDH have been reported to interact with each other, forming a similar substrate channel as PutA (Sanyal *et al.*, 2015). Recently, Cabassa-Hourton *et al.*, (2016) have reported that ProDH is involved in a putative protein complex in proline-treated *Arabidopsis thaliana* (*Arabidopsis*). So far, it is still unknown whether eukaryotic proline catabolic enzymes form a substrate channel.

Thus, this study aims at characterizing the organization and the regulation of eukaryotic proline catabolic enzymes—ProDH and P5CDH. As OAT is also involved in proline metabolism through the generation of P5C, the relationship between OAT, ProDH, and P5CDH has been investigated in *Arabidopsis*.

The major scientific issues that this study wants to address are:

1. To precisely define the sub-mitochondrial localizations of ProDH1, P5CDH, and OAT.
2. To determine whether eukaryotic ProDH1, P5CDH, and OAT form a protein complex
3. To unravel the physiological importance of the presence of such complex *in planta*.

CHAPTER I.

State of the Art

Chapter 1. State of the Art

1.1 Proline is a multifunctional amino acid

Proline is a proteinogenic amino acid that is essential for primary metabolism and versatile among living organisms (Fig. I-1). Overall, proline contributes to stress response, osmotic adjustment, protein chaperoning, ROS signalling, redox homeostasis and energy metabolism (Szabados and Savouré, 2010; Liu and Phang, 2012; Ben Rejeb *et al.*, 2014; Silao *et al.*, 2019).

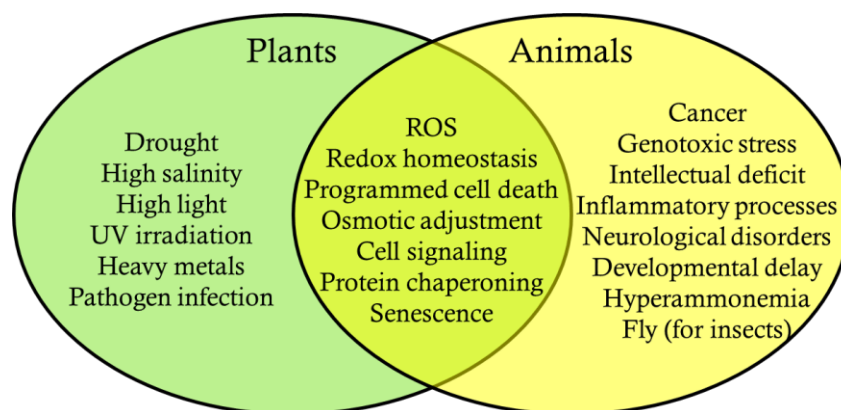


Figure I-1. Venn diagram of multiple functions of proline metabolism in plants and animals (Szabados and Savouré, 2010; Cecchini *et al.*, 2011; Fichman *et al.*, 2015; Phang, 2019).

Stress-induced proline accumulation in plants has been reported first in wilting *Lolium perenne* (rye grass) (Kemble and Macpherson, 1954). To date, proline accumulation in plants has been reported in responses to a broad array of stimuli including drought (Choudhary *et al.*, 2005), high salinity (Ghars *et al.*, 2008; Yoshiba *et al.*, 1995), cold (Savouré *et al.*, 1997), high light and UV irradiation (Saradhi *et al.*, 1995), heavy metals (Schat *et al.*, 1997), oxidative stress (Yang *et al.*, 2009), and biotic stress (Fabro *et al.*, 2004; Haudecoeur *et al.*, 2009).

In humans, proline metabolism has been reported to play an important role in cancer, aging, programmed cell death, pathogen virulence, ROS production, inflammatory processes, and response to genotoxic stresses (Fichman *et al.*, 2015; Tanner, 2017; Phang, 2019).

Proline accumulation has been originally implicated in osmotic stress tolerance in bacteria (Christian, 1955; Csonka and Hanson, 1991) and this role has been further demonstrated in plants (Delauney and Verma, 1993), fungi (Takagi, 2008), and invertebrates (Gilles and Schoffeniels, 1969; Fyhn, 1976). It has been demonstrated since a long time that proline can

act as a beneficial compatible solute buffering the cellular osmolarity under osmotic stress (Szabados and Savouré, 2010).

Other than being an osmoprotectant, proline can also act as a potent nonenzymatic antioxidant. Proline is able to quench hydroxyl radicals (Smirnoff and Cumbes, 1989), preventing cells from oxidative damage caused by ROS. Accordingly, it has been reported that ROS is able to induce proline accumulation in both plants (Fabro *et al.*, 2004) and animals (Krishnan *et al.*, 2008).

Besides, ROS are also known to act as secondary messengers in intracellular signaling cascades, triggering both abiotic and biotic stresses responses in plants (Ben Rejeb *et al.*, 2014) and cell death in humans (Liu and Phang, 2012). In agreement with the role of proline in ROS signalling, proline catabolism has been reported to participate in the regulation of programmed cell death, including tumour cell apoptosis (Liu and Phang, 2012) in humans, dark-induced leaf senescence (Launay *et al.*, 2019) and hypersensitive response (Monteoliva *et al.*, 2014) in plants.

In addition, plant abiotic stress signaling has been proposed to evolve from energy sensing pathways (Zhu, 2016), emphasizing the connection between abiotic stress response and energy metabolism. Coherent with a critical role in abiotic stress response, proline and proline metabolism could also participate in energy metabolism in various organisms. In some insects, such as *Apis mellifera* (honeybee), proline is a respiratory fuel for flight (Teulier *et al.*, 2016). In *Arabidopsis*, proline has been identified as an alternative respiratory substrate during dark-induced leaf senescence (Launay *et al.*, 2019).

Taken together, both proline *per se* and proline metabolism play critical and regulatory roles in large range of cellular processes among living organisms. The study on proline and proline metabolism will be beneficial for both crops yielding improvement under changing environment and new cancer therapeutic strategy designing.

1.2 Proline Metabolism

1.2.1 Proline biosynthesis

1.2.1.1 Main pathway for proline biosynthesis

Generally, proline is synthesized from glutamate via phosphorylation to γ -glutamyl phosphate (GP) by γ -Glutamyl Kinase (GK), which is reduced to γ -glutamyl semialdehyde (GSA/GSAL) by γ -Glutamyl Phosphate Reductase (GPR). GSA is spontaneous cyclized to Δ^1 -pyrroline-5-carboxylate (P5C), followed by the reduction to proline by P5C reductase (P5CR,

a.k.a. PYCR) (Csonka and Leisinger, 2007)(Fig. I-2). GP is inherently unstable and can be hydrolysed spontaneously to 5-oxopyrrolidine-2-carboxylate (Katchalsky and Paecht, 1954).

In prokaryotes, proline biosynthetic enzymes are as mentioned above. While vascular plants and animals possess orthologs of the same three enzymes for proline biosynthesis, except their GK and GPR are fused together, forming a bifunctional Δ^1 -pyrroline-5-carboxylate synthase (P5CS), in which the GK domain is N-terminal and the GPR domain is C-terminal (Fig. I.2-2). But the presence of bifunctional P5CS is not a universal feature for eukaryotes, because some unicellular green algae, such as *Chlamydomonas reinhardtii*, *Micromonas* sp. RCC299, and *Ostreococcus lucimarinus*, and fungi have separate GKs and GPRs. However, the oomycete *Phytophthora sojae* and the photosynthetic diatom *Phaeodactylum tricoratum*, which belong to the kingdom Stramenopiles, are exceptional among eukaryotic microbes that have bifunctional P5CSs (Fichman *et al.*, 2015).

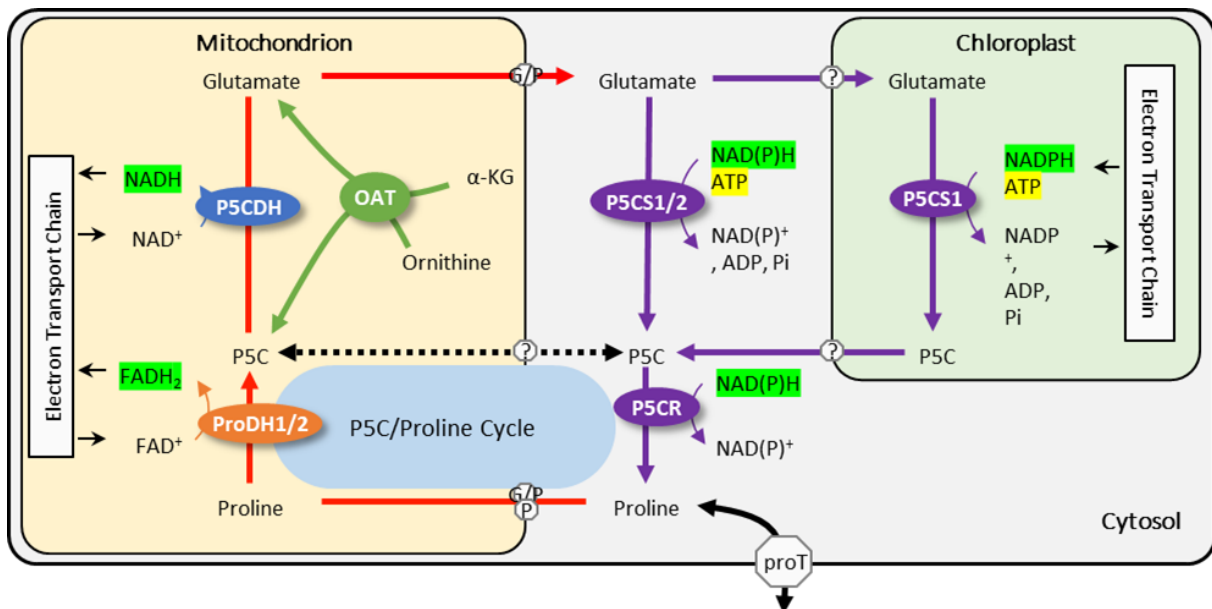


Figure I-2. Simplified proline metabolism in higher plants. Glutamate is reduced to P5C by P5CS, afterwards P5CR further reduces the P5C intermediate to proline. As an alternative pathway, proline can be also synthesized from ornithine by OAT. Proline oxidized by ProDH to P5C leading to the release of electrons, which might be transferred to electron transport chain through CoQ. After, P5CDH converts P5C to glutamate. G/P, mitochondrial glutamate/proline antiporter; P, mitochondrial proline transporter; ProT, plasma membrane proline transporter; ?, predicted transporters. Modified from Szabados and Saviouré (2010).

In most higher plants, two isoforms of *P5CS* and one isoform of *P5CR* have been found (Szabados and Saviouré, 2010). For example, *A. thaliana* has two isoforms of *P5CS*: one house-keeping isoform *AtP5CS2* and one stress-specific isoform *AtP5CS1*. In addition, some vascular plants have more than two isoforms of *P5CS*. For example, *Sorghum bicolor*, *Zea mays* (maize),

and the partially diploidized tetraploid *Glycine max* (soybean) have three, four and seven partial- or full-length copies of annotated *P5CS* genes, respectively (Fichman *et al.*, 2015). Although two isoforms of *AtP5CS* are highly similar in sequences, their expression are remarkably different. Transcripts of both *P5CS* genes can be detected in most organs, but *AtP5CS2* is more abundant in dividing and meristematic tissues, such as shoot and root tips, embryos, and developing inflorescences, whereas *AtP5CS1* is expressed at a high level in leaves, floral tissues, desiccating pollen grains, and embryos (Mattioli *et al.*, 2009b).

1.2.1.2 Alternative pathway for proline biosynthesis

Alternatively, proline may be synthesized from ornithine through Ornithine δ -Aminotransferase (OAT). OAT is a nuclear encoded and pyridoxal-5-phosphate (PLP)-dependent enzyme among living organisms (Stránská *et al.*, 2008; You *et al.*, 2012; Fichman *et al.*, 2015). OAT is encoded by a single-copy gene in eukaryotes (You *et al.*, 2012). It catalyzes the transfer of δ -amino group from ornithine to α -ketoglutarate, forming glutamate and GSA/P5C. The resulting GSA/P5C is either oxidized by P5C dehydrogenase (P5CDH) forming glutamate or reduced by P5CR forming proline (Fig. I-2).

This alternative ornithine-derived proline biosynthesis pathway is likely to occur in animals (Mezl and Knox, 1977; Smith and Phang, 1979; Adams and Frank, 1980; Fichman *et al.*, 2015), however, it is still controversial in plants. The first *OAT* gene from plants has been identified in *Vigna aconitifolia* by functional complementation to an *E. coli* proline auxotroph strain (Delauney *et al.*, 1993). Besides, application of the OAT inhibitor gabaculine reduces stress-induced proline accumulation in *Raphanus sativus* (radish)(Hervieu *et al.*, 1995) and *Oryza sativa* (rice)(Yang and Kao, 1999). Moreover, overexpression of the Arabidopsis *OAT* gene in *Nicotiana plumbaginifolia* (Roosens *et al.*, 2002) and rice (Wu *et al.*, 2003) resulted in increased proline content and stress tolerance, supporting the putative involvement of OAT in proline synthesis.

But the role of OAT in plant proline biosynthesis is challenged by its subcellular localization. In both animals and plants, OAT is recognized as a mitochondrial protein. Human, for example, has two P5CR isoforms in mitochondria named PYCR1/2 and one in cytosol named PYCRL (Reversade *et al.*, 2009; Ingeniis *et al.*, 2012). However, plant P5CR has been shown to be localized in cytosol (Szoke *et al.*, 1992). The sequential action of OAT and P5CR is fundamental for ornithine-derived proline biosynthesis. But the subcellular isolation of plant OAT and P5CR may impair this action. Because the transportation of GSA/P5C between

mitochondria and cytosol has not been proved yet. In addition, Funck *et al.*, (2008) has reported that salt stress-induced proline accumulation is not affected in *Arabidopsis oat* mutants.

In contrast, exogenous supply of ornithine is effectively inducing proline accumulation in intact plants and leaf discs of *Anacardium occidentale* (cashew), in which proline contents were several times higher than glutamate-fed or salt-treated cashew (da Rocha *et al.*, 2012). Therefore, the contribution of OAT in plant proline biosynthesis needs further investigation.

1.2.2 Proline catabolism

Proline is oxidized by the sequential action of proline dehydrogenase (ProDH) and P5CDH. ProDH, a.k.a. proline oxidase (POX), catalyzes the first and rate-limiting step of proline catabolism, using FAD as a cofactor. Proline, when oxidized by ProDH, is converted to P5C. Subsequently, P5CDH, a.k.a. GSAL dehydrogenase (GSALDH), converts GSA to glutamate, using NAD^+ as a cofactor (Fig. I-2).

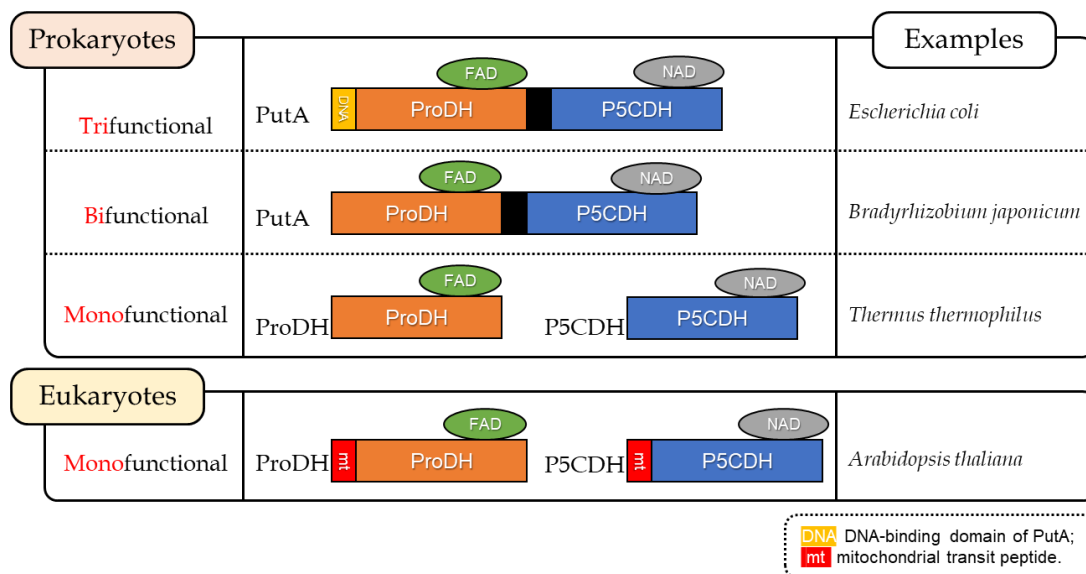


Figure I-3. Representative diagram for proline catabolic enzymes in different living organisms. FAD is the cofactor for monofunctional ProDH and ProDH domain of PutA. NAD^+ is the cofactor for monofunctional P5CDH and P5CDH domain of PutA. The position of FAD and NAD^+ in the diagram does not represent the real position of their binding domain.

Intriguingly, in Gram-negative bacteria ProDH and P5CDH are combined into one bifunctional enzyme known as Proline utilization A (PutA) (Fig. I-3). The ProDH and P5CDH domains are in the N-terminus and C-terminus of PutA, respectively. In some bacteria such as *E.coli*, PutA is trifunctional because it harbours a DNA-binding domain in the N-terminal part of the PutA, which enables EcPutA to act as a transcriptional repressor of proline utilization

operon (Gu *et al.*, 2004). But in some other bacteria such as *Thermus thermophilus*, ProDH and P5CDH are monofunctional enzymes (Fig. I-3). In contrast, only monofunctional ProDH and P5CDH are found in eukaryotes (Tanner, 2008; Servet *et al.*, 2012).

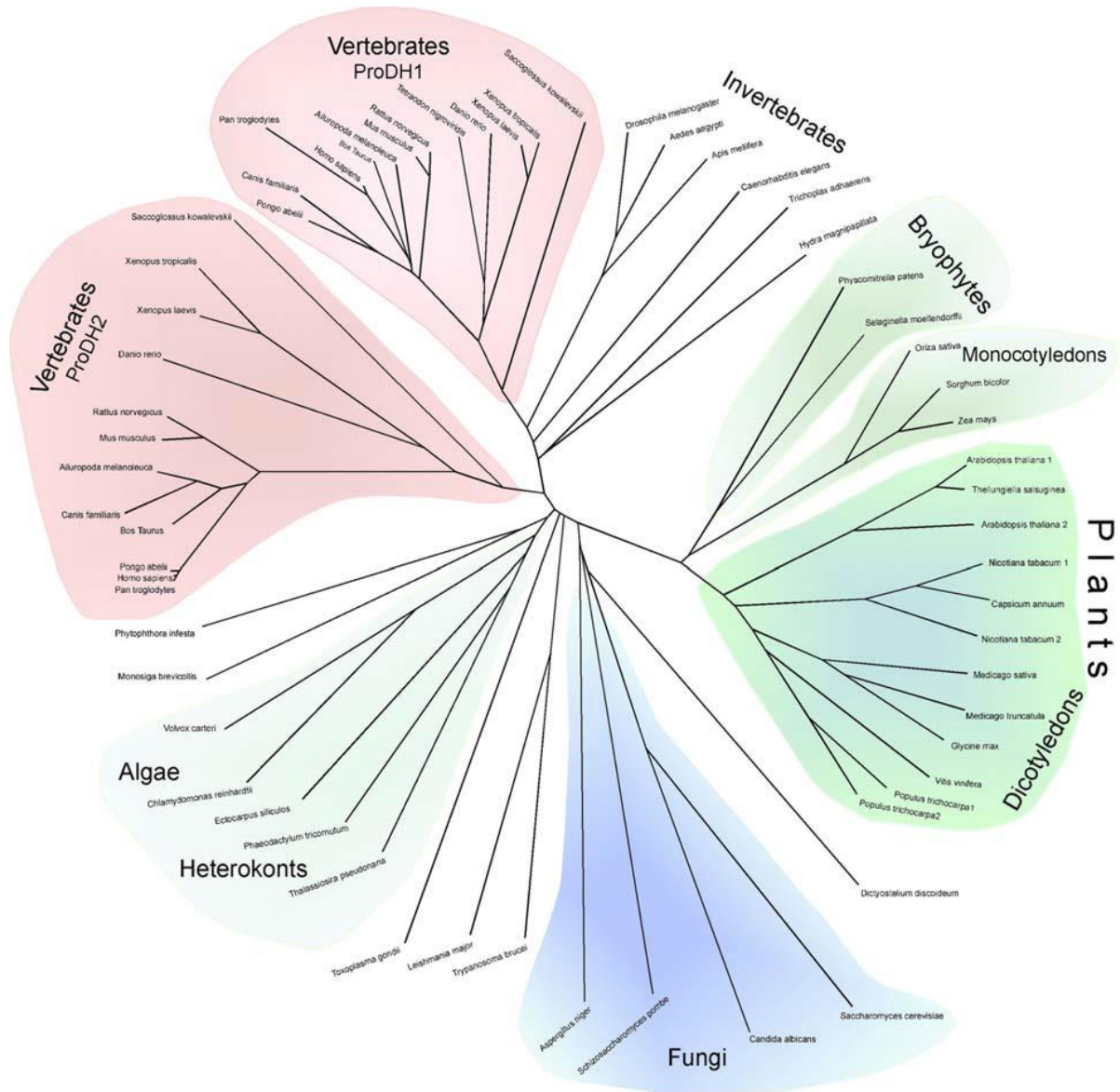


Figure I-4. Unrooted phylogenetic tree of eukaryotic proline dehydrogenase. From Servet *et al.*, (2012).

So far, two ProDH isoforms are found in dicotyledon plants and vertebrates, whereas only one ProDH was found in monocotyledon plants, algae, fungi, and invertebrate genomes (Fig. I-4)(Servet *et al.*, 2012). In dicotyledonous plants, the two ProDH isoforms are closely related (for example, two ProDH isoforms in *Arabidopsis* share 75% sequence identity), in contrast to the vertebrate ProDH isoforms, which are distantly related (for example, 45%

sequence identities between human ProDHs) (Servet *et al.*, 2012). Human ProDH1 oxidizes proline whereas the substrate of ProDH2 is hydroxyproline (Phang *et al.*, 2010).

In Arabidopsis, the two *ProDH* isoforms are non-redundant (Funck *et al.*, 2010): *ProDH1* (AT3G30775, also known as *ERD5*) and *ProDH2* (AT5G38710). *AtProDH1* acts as the major isoform, which is induced by proline or hypo-osmolarity, and downregulated by dehydration (Kiyosue *et al.*, 1996). In contrast, *AtProDH2* was specifically upregulated during salt stress when *ProDH1* was repressed (Funck *et al.*, 2010).

Only one *P5CDH* is characterized in eukaryotic organisms (Deuschle *et al.*, 2001). As a member of aldehyde dehydrogenase (ALDH) gene superfamily, plant *P5CDH* belongs to the ALDH12 family. Therefore *AtP5CDH* is also named *AtALDH12A1* (Brocker *et al.*, 2013). Depending on amino acid sequence identity, *P5CDH* in bacteria, fungus, and animals are classified as ALDH4 family (for example *HsALDH4A1* in humans) (Korasick *et al.*, 2019).

1.2.3 Subcellular localization of proline metabolic enzymes

1.2.3.1 In prokaryotes

Localization of prokaryotic proline biosynthetic enzymes is believed to be cytosolic (Fichman *et al.*, 2015). However, proline catabolic PutAs and monofunctional ProDHs were shown to be peripheral membrane-associated enzymes (Fig. I-5)(Spicer and Maloy, 1993).

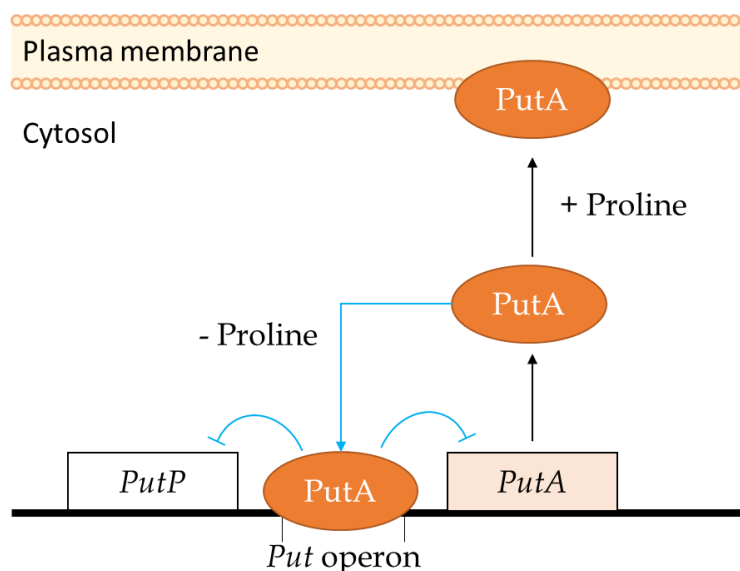


Figure I-5. Working model of trifunctional PutA. Ellipses represent the PutA protein. Rectangles represent the gene encoding sequences of either *PutP* or *PutA*. Modified from Spicer and Maloy (1993).

In *E. coli* and *Salmonella typhimurium*, trifunctional PutA controls the transcription of proline utilization operon, including two genes: *PutA* (encoding PutA enzyme) and *PutP* encoding the high-affinity Na⁺-proline transporter (Spicer and Maloy, 1993; Zhou *et al.*, 2008). According to proline level, trifunctional PutA switches between a DNA-binding transcriptional repressor and a membrane-associated enzyme (Fig. I-5). In absence of proline, trifunctional PutA is localized in the cytosol, where it represses *PutA* and *PutP* gene expression. In presence of proline, trifunctional PutA binds to the inner cytoplasmic membrane, where it catalyzes the oxidation of proline and transfer electrons to membrane-associated electron transfer chain (Spicer and Maloy, 1993; Zhou *et al.*, 2008).

1.2.3.2 In eukaryotes

Unlike prokaryotes, enzymes involved in eukaryotic proline metabolism exhibit diverse compartmentation (Szabados and Savouré, 2010). For proline anabolism in plants, P5CS was found in the cytosol and likely chloroplasts, while P5CR is only found in the cytosol (Székely *et al.*, 2008; Szabados and Savouré, 2010). In humans, P5CS is observed in mitochondria, while two isoforms of P5CR (PYCR1/2) are found in mitochondria and one (PYCRL) in cytosol (Fichman *et al.*, 2015; Phang, 2019).

Proline catabolism has been reported in mitochondria in both animals, yeasts, and plants (Fichman *et al.*, 2015). ProDH has been described to localize in the matrix side of the mitochondrial inner membrane in both animals and plants (Brunner and Neupert, 1969; Elthon and Stewart, 1981; Cabassa-Hourton *et al.*, 2016). P5CDH was reported to associate with mitochondrial inner membrane in *Zea mays* (maize)(Elthon and Stewart, 1981) and parasitic protozoon *Trypanosoma cruzi* (Mantilla *et al.*, 2015) but in mitochondrial matrix in mouse (Brunner and Neupert, 1969). Meanwhile, OAT is believed to localize in the mitochondrial matrix in both animals (Doimo *et al.*, 2013) and plants (Winter *et al.*, 2015).

1.2.4 Proline transport in plants

1.2.4.1 Long-distance translocation of proline

Land plants have evolved complex adaptation strategies to survive in dynamic water status, among which transport of compatible solutes by membrane transport system is critical for plant adaptation (Jarzyniak and Jasiński, 2014).

Under low water availability, high levels of proline have been found in the phloem sap of *Medicago sativa* (alfalfa) (Girousse *et al.*, 1996), indicating that proline is subjected to long-distance transport in phloem elements under water constraints. In addition, tissue-specific proline biosynthesis and catabolism have been reported to be vital for plant growth and redox balance at low water potential in *Arabidopsis* (Sharma *et al.*, 2011). At low water potential (-1.2 MPa), *AtProDH1* maintains high expression in root apex and shoot meristem, whereas *AtP5CS1* is mostly induced in shoot tissue (Sharma *et al.*, 2011).

In addition, transport of proline is also essential under normal growth conditions. For example, developing fruit of *Vitis vinifera* (grapevine) contains increasingly high levels of free proline. However, both mRNA and protein levels of domestic *VvP5CS* stay uniform during the development of grapevine fruit (Stines *et al.*, 1999). In *Solanum lycopersicum* previously named as *Lycopersicon esculentum* (tomato), high proline accumulation in pollen has been reported to be independent of *LeP5CS* expression (Fujita *et al.*, 1998). Another example of proline transportation is that exogenous proline supply can rescue the morphological abnormality of antisense-*AtP5CS* transgenic *Arabidopsis*, in which proline biosynthesis has been severely impaired in the whole transgenic plants (Nanjo *et al.*, 1999).

Plant transporters mediating proline uptake across the plasma membrane have been identified in the amino acid transporter (ATF) or amino acid/auxin permease (AAP) family (Lehmann *et al.*, 2010). In the ATF/AAP family, proline transporters have been classified into different subfamilies, namely the amino acid permease (AAP) family, the lysine-histidine transporter (LHT) family and the proline transporter (ProT) family.

AAPs mediate proton-coupled uptake of glutamate/aspartate and neutral amino acids, including proline (Frommer *et al.*, 1993; Fischer *et al.*, 1995). LHTs transport neutral amino acids, including proline, and acidic amino acids with high affinity (Lee and Tegeder, 2004). In contrast to AAPs and LHTs, ProTs exhibit higher selectivity for proline, transporting both proline and glycine betaine (Rentsch *et al.*, 1996; Grallath *et al.*, 2005). So far, ProTs have been identified in many plants, including *Arabidopsis* (*AtProT1/2/3*)(Rentsch *et al.*, 1996; Grallath *et al.*, 2005), tomato (*LeProT1/2/3*)(Schwacke *et al.*, 1999), rice (*Oryza sativa*; *OsProT*)(Igarashi *et al.*, 2000), barley (*Hordeum vulgare*; *HvProT*)(Ueda *et al.*, 2001), and mangrove (*Avicennia marina*; *AmProT1/2/3*)(Waditee *et al.*, 2002).

Expression of several members of the ProT family is often correlated with stress or high proline concentrations in plants. The mRNA levels of *AtProT2* and *AmProT1/2/3* have been reported to increase under salt stress conditions and high concentrations of proline and glycine betaine (Waditee *et al.*, 2002). Furthermore, *HvProT* expression in barley roots is increased by

salt stress treatments (Ueda *et al.*, 2001). In tomato, expression of *LeProT1* has been shown to be confined to pollen and expression correlated with elevated proline levels (Schwacke *et al.*, 1999). In contrast, *AtProT1* and *OsProT* have not been shown to be induced under stress conditions (Rentsch *et al.*, 1996; Igarashi *et al.*, 2000).

Moreover, it has been reported that all three *AtProTs* localize in the plasma membrane. The affinity of all three *AtProTs* are highest for glycine betaine, lower for proline, and lowest for γ -aminobutyric acid (Grallath *et al.*, 2005). Although subcellular localization and substrate affinity are the same, *AtProTs* are not redundant *in planta*. *AtProT1* expression has been detected only in the phloem or phloem parenchyma cells throughout the whole plant, indicating its role in long-distance transport of compatible solutes (Grallath *et al.*, 2005). *AtProT2* expression is restricted to the epidermis and the cortex cells in roots, whereas induced by wounding in leaves (Grallath *et al.*, 2005). In contrast, *AtProT3* expression is restricted to the above-ground parts of the plant and could be detected in the leaf epidermal cells (Grallath *et al.*, 2005).

1.2.4.2 Intracellular proline transport

As proline metabolism exhibits diverse compartmentation in both higher plants and animals, intracellular proline translocation is of great importance. However, organellar proline transporters are largely unknown. So far, in *Triticum durum* (durum wheat), two mitochondrial inner membrane localized proline transporters have been identified based on a biochemical analysis, i.e., a proline uniporter and a proline/glutamate antiporter (Di Martino *et al.*, 2006). Accordingly, one proline/glutamate antiporter has been identified in rat kidney mitochondria (Atlante *et al.*, 1996).

1.2.5 Proline/P5C cycle

In plants, mitochondrial P5C is supposed to be exported into the cytosol (Miller *et al.*, 2009) under certain physiological conditions. However, experimental evidence is still lacking for the existence of P5C specific carrier/transporter on the mitochondrial inner membrane. In cytosol, mitochondrial P5C, either derived from ProDH or OAT, can replenish the cytosolic proline biosynthesis, bypassing the ATP utilization mediated by P5CS activity. There, P5C is reduced by P5CR into proline, which is transported back into mitochondria and degraded by ProDH. Hence, the process described above is termed as “Proline/P5C cycle”, which was previously reported in animal cells (Hagedorn and Phang, 1986).

In this cycle, one molecule of proline is oxidized by ProDH into one P5C reducing FAD^+ . Afterwards, one P5C is exported into cytosol and reduced by P5CR into one proline leading to the oxidation of NAD(P)H into NAD(P)^+ . In summary, the net amount of proline and P5C is not altered by this cycle. However, NAD(P)H is consumed in the cytosol, while FADH_2 is formed in the mitochondria. Thus, reducing power is shuttled in a single direction from cytosol to the mitochondrial matrix.

One function of the ETC is to regenerate NAD^+ for glycolysis in the cytosol, however, mitochondrial inner membrane is impermeable to NAD(P)H and NAD(P)^+ (Berg *et al.*, 2015). NAD(P)^+ can be directly shuttled between subcellular compartments via NAD^+ -carrier proteins localized in mitochondrial inner membrane (Palmieri *et al.*, 2009). As for NAD(P)H , NAD(P)H is oxidized by external NAD(P)H dehydrogenase (Edman *et al.*, 1985; Schertl and Braun, 2014). On the other hand, the electrons from NAD(P)H , rather than NAD(P)H *per se*, can be shuttled across the mitochondrial inner membrane in eukaryotic systems, including the Glycerol-3-Phosphate (G3P) shuttle, Malate/Aspartate shuttle, and Malate/Oxaloacetate (OAA) shuttle (McKenna *et al.*, 2006; Rasmusson and Møller, 2015), as well as Proline/P5C cycle.

Moreover, it has been shown that Proline/P5C cycle is able to regenerate NADP^+ which is needed for the oxidative pentose phosphate pathway (OxPPP), due to the NADPH consumption by P5CR in the cytosol in both animals (Liu *et al.*, 2015) and plants (Shetty, 2004). Proline/P5C cycle has also been shown to regenerate NAD^+ for glycolysis in animals (Liu *et al.*, 2015). In plants, this issue is not clear yet and needs additional research.

Taken together, Proline/P5C cycle can irreversibly transform cytosolic NAD(P)H to FADH_2 on the matrix side of mitochondrial inner membrane, therefore contributing to the cellular redox state adjustment. A detailed review about this topic entitled “The proline cycle as a eukaryotic redox valve” was published in *Journal of Experimental Botany* and is presented in Chapter 2.

1.3 Regulation of proline metabolism in plants

1.3.1 Regulation of proline biosynthesis

Although proline metabolism in plants has been studied over decades, the regulation of proline metabolism is still far from fully understood.

In *Arabidopsis*, *P5CSI* transcript is subjected to intron-mediated alternative splicing, which is responsible for the natural variation of proline metabolism in different *Arabidopsis*

ecotypes and climate adaptation (Kesari *et al.*, 2012). As a geographical widely distributed species, different ecotypes of *Arabidopsis* exhibit variable proline accumulation responses to drought stress, which are related to the adaptation of a particular accession to specific ecological conditions. For example, drought-induced proline accumulation in *Arabidopsis* accession Shakdara (Sha) was threefold less than that of Landsberg *erecta* (*Ler*). It has been reported that, unlike *Ler*, Sha *P5CS1* has additional four TA repeats in intron 2 and a G-to-T transversion in intron 3 that are sufficient to promote alternative splicing, resulting a non-functional *P5CS1* transcript lacking exon 3 (termed as exon 3-skip *P5CS1*)(Kesari *et al.*, 2012). In Sha and other accessions with the same intron polymorphisms, the non-functional exon 3-skip *P5CS1* transcript constituted as half amount of the total *P5CS1* transcript. Further analysis by Kesari *et al.*, (2012) suggests a role of *P5CS1* in local adaptation to environment in *Arabidopsis*.

1.3.1.1 Regulation of proline biosynthesis under drought or salt stress

In response to drought or salt stress, proline accumulation is ensured by the activation of proline biosynthesis and inhibition of proline catabolism. In *Arabidopsis*, transcriptional activation of *P5CS1* was observed under desiccation, drought, high salinity and cold, but not under heat stress (Yoshida *et al.*, 1995; Saviouré *et al.*, 1997; Abraham *et al.*, 2003). Stress-induced *P5CS* transcription has also been reported in other plants, such as *Medicago sativa* (alfalfa)(Ginzberg *et al.*, 1998) and rice (Hur *et al.*, 2004). It is likely to be one of the major regulatory mechanisms that controls proline accumulation in plants.

In *Arabidopsis*, *AtP5CS1* and *AtP5CS2* have non-redundant roles in stress-induced and developmental control of proline biosynthesis. Knockout mutations of *AtP5CS1* result in the reduction of stress-induced proline synthesis, hypersensitivity to salt stress, and accumulation of ROS. By contrast, *AtP5CS2* mutations cause embryo abortion during late stages of seed development (Székely *et al.*, 2008).

Besides, transcriptional activation of *P5CS* is necessary but not sufficient for proline accumulation. In some plants, proline contents are not correlated with *P5CS* transcriptional levels in salt-treated *Lycopersicon esculentum* (tomato) (Fujita *et al.*, 1998) and mature fruit of *Vitis vinifera* (grapevine) (Stines *et al.*, 1999). This lack of correlation maybe due to the allosteric inhibition of *P5CS* by proline (Fichman *et al.*, 2015).

In addition, mutants in *Cytochrome P450, Family 86, Subfamily A, Polypeptide2* (*CYP86A2*) and *Long Chain Acyl Synthetase2* (*LACS2*), which catalyze two successive steps in very-long-chain fatty acid (VLCFA) synthesis, exhibit increased proline accumulation, with

unchanged ProDH1 and P5CS1 on both protein and mRNA level in Arabidopsis under low water potential (Shinde *et al.*, 2016). Moreover, it has been reported that the NADPH oxidase inhibitor diphenyleneiodonium (DPI) induces high levels of proline accumulation. *cyp86a2* and *lacs2* mutants have been reported to be hypersensitive to DPI but this can be reverted by ROS scavengers (Shinde *et al.*, 2016). In parallel, RNA sequencing of *p5cs1-4* shows altered expression of chloroplast and mitochondria electron transport genes compared to wild-type in Arabidopsis (Shinde *et al.*, 2016). These results show that proline metabolism coordinates with fatty acid synthesis and redox metabolism of chloroplast and mitochondria in an unknown manner (Shinde *et al.*, 2016).

In both Arabidopsis and rice, analysis of the promoter regions of *P5CS1*, *P5CS2*, and *P5CR* predicted impressive amount of putative *cis*-acting elements of various transcriptional factors (Fichman *et al.*, 2015; Zarattini and Forlani, 2017). The diversity of these *cis*-acting elements suggests the expression of these genes is controlled by conjugated upstream signaling, although the role of these *cis*-acting elements remains to be determined. In the following context, stress-induced transcriptional regulation of proline biosynthesis is reviewed, which is mediated by either abscisic acid (ABA)-dependent or independent pathway.

1.3.1.1.1 ABA-dependent proline biosynthesis

In plants, drought triggers the production of the phytohormone ABA, which in turn promotes stomatal closure and induces down-stream gene expression to counteract the hostile influence of drought. At transcriptional level, ABA-responsive elements (ABRE), belonging to the G-BOX family (ACGTGG/TC) and characterized by an ACGT core sequence, are considered to be the major *cis*-acting elements in ABA regulated genes (Shinozaki and Yamaguchi-Shinozaki, 2007).

In Arabidopsis, the promoter of *AtP5CS1/2* and *AtP5CR* contain typical ABREs, which is the binding site of two bZIP transcription factors (TFs): ABRE binding factor (ABF) and ABA-responsive element binding protein (AREB)(Fichman *et al.*, 2015). Thus, the presence of ABREs in the promoter of these proline synthetic genes could be responsible for the ABA-mediated activation of proline biosynthesis.

Salt-induced activation of *AtP5CS1* is controlled by ABI1-dependent signalling (Strizhov *et al.*, 1997). The *ABI1* encodes a type 2C protein phosphatase (PP2C), which is a component of the ABA receptor complex integrating ABA and Ca²⁺ signals (Ma *et al.*, 2009; Park *et al.*, 2009), and regulates downstream gene expression through the control of phosphorylation

of ABF-type TFs by the Sucrose Nonfermenting-1-Related Kinase 2 (SnRK2)(Fujii *et al.*, 2009).

Moreover, the conserved bZIP-binding sites predicted in the *AtP5CS* promoter could also be involved in light and hormone pathways. The bZIP transcription factor ELONGATED HYPOCOTYL 5 (HY5) has been shown to integrate light and ABA signals. HY5-binding sites have been detected in the promoters of *AtP5CS1/2* by chromatin immunoprecipitation (ChIP) coupled with DNA chip hybridization (Lee *et al.*, 2007). Moreover, it has been demonstrated that HY5 binds to G-box and C-box elements of *AtP5CS1* under salt stress (Kovács *et al.*, 2019).

1.3.1.1.2 ABA-independent proline biosynthesis

ABA-independent stress-responsive gene expression is mediated by dehydration-responsive elements (DRE), DRE-related motifs such as C-repeats (CRT) and low-temperature-responsive elements (Zarattini and Forlani, 2017).

It has been reported that the gene expression of *AtP5CS* and *AtP5CR* is ABA-independent upon cold and osmotic treatments (Savouré *et al.*, 1997). Accordingly, *AtP5CS1/2* and *AtP5CR* promoters contain predicted APETALA2/Ethylene-Responsive Factor (AP2/ERF) binding sites (Fichman *et al.*, 2015). AP2/ERF TFs are encoded by a plant-specific gene family, which has 147 members in Arabidopsis and 163 members in rice (José L. and Elliot M., 1998). Members of AP2/ERF family participate in the regulation of abiotic stress responses, including drought, cold, and hypoxia (Zhu *et al.*, 2010; Dietz *et al.*, 2010). The conserved GCC motif found in the *P5CS* promoters is closely related to the DRE/CRT, which is the binding site for the AP2/ERF family TFs namely DREB1/CBF and DREB2. In particular, the DREB1-type TFs are involved in cold-responsive pathways, whereas DREB2-type TFs play a role in osmotic-responsive pathways (Zarattini and Forlani, 2017).

Another group of plant-specific TFs, namely the NAM, ATAF, and CUC (NAC) proteins, is involved in the ABA-independent pathway under stress. Overexpression of NAC proteins is able to induce proline accumulation and drought resistance in rice (Hong *et al.*, 2016) and tobacco (Liu *et al.*, 2013). Consistently, NAC binding motifs have been identified in *OsP5CS2* and *OsP5CR* promoters (Zarattini and Forlani, 2017), suggesting NAC TFs might directly regulate proline biosynthesis under stress condition.

1.3.1.2 Regulation of proline biosynthesis in reproductive development

Apart from stress response, proline is also important for plant development and growth (Mattioli *et al.*, 2009a). In the literature, high proline content has been reported in the reproductive organs of different plant species, revealing the role of proline in development under physiological non-stressed conditions (Chiang and Dandekar, 1995; Nanjo *et al.*, 1999; Funck *et al.*, 2012). In *Arabidopsis*, proline constitutes 17–26% of the total free amino acid in reproductive tissues (floret and seed), but only 1–3% of the total free amino acid in vegetative tissues such as rosette, leaf and root (Chiang and Dandekar, 1995).

Interestingly, proline synthesis also participates in flower transition (Mattioli *et al.*, 2009a). It has been reported that the inhibition of *P5CS1* in *Arabidopsis* can inhibit bolting—the fast stem elongation occurring immediately after flower transition (Nanjo *et al.*, 1999). Moreover, knock-out *p5cs1* mutant behaved as late flowering, but overexpression of *P5CS1* leads to early flowering under both long-day and short-day condition (Mattioli *et al.*, 2008). Besides, it has been reported that *P5CS2* also plays a role in flowering (Mattioli *et al.*, 2009b). Accordingly, exogenous proline treatment accelerates organ growth and meristem formation, and stimulates expression of the cell cycle-related protein CYCB1;1 (Mattioli *et al.*, 2009b).

However, the upstream regulatory pathway upon P5CS mediated flowering transition is yet unknown. As a clue, *P5CS2* was identified as an early target induced by CONSTANS (CO), a predominant flowering promoting transcriptional factor in photoperiodic pathway (Samach *et al.*, 2000). Moreover, another key flowering regulatory gene *FRIGIDA* (*FRI*) has been reported to enhance drought tolerance by activating *P5CS1* expression and promoting proline accumulation in *Arabidopsis*. This *FRI*-mediated *P5CS1* induction is depending on a functional *FLOWERING LOCUS C* (*FLC*) (Chen *et al.*, 2018).

1.3.1.3 Other regulatory pathways upon proline biosynthesis

1.3.1.3.1 WRKYs

The WRKY family TFs have been thoroughly reported to play important roles in biotic stress response, yet its emerging role in abiotic stress has been revealed by recent studies (Banerjee and Roychoudhury, 2015). Some studies have shown WRKY TFs may regulate proline metabolism. Overexpression of *Triticum aestivum* (wheat) *WRKY10* in tobacco results in enhanced drought and salt tolerance with higher intracellular proline contents (Wang *et al.*, 2013). Overexpressing *AtWRKY57* in rice results in enhanced drought tolerance with high

proline contents and increased *OsP5CS1* expression (Jiang *et al.*, 2016). Consistently, WRKY binding sites have been predicted in promoters of *AtP5CS2* (Fichman *et al.*, 2015) and *OsP5CR* (Zarattini and Forlani, 2017).

1.3.1.3.2 Calcium and lipid signaling

Calmodulin (CaM), as a major Ca^{2+} sensor, plays an important role in biotic and abiotic stress signaling. Under drought, salt, and cold stresses, microarray data has shown CaM binding Transcription Activator 1 (CaMTA1) upregulating both *AtP5CS1* and *AtP5CS2* expression in roots, but not in leaves (Pandey *et al.*, 2013). In addition, in Arabidopsis, salt-inducible CaM4 has been found to interact with AtMYB2, inducing *AtP5CS1* expression and enhancing salt tolerance (Yoo *et al.*, 2005).

Consistently, several MYB recognition sites have been identified in the promoter of proline biosynthesis genes in both rice (Zarattini and Forlani, 2017) and Arabidopsis (Fichman *et al.*, 2015). Apart from Ca^{2+} signaling, MYB family TFs have been found to participate in plant response to various abiotic stresses including salt, drought, cold, and excessive light (Li *et al.*, 2015). Overexpression of *MYB2* induces proline accumulation in Arabidopsis (Yoo *et al.*, 2005), wheat (Mao *et al.*, 2011), and rice (Yang *et al.*, 2012). Similarly, *OsMYB48-1* overexpressing rice plants have higher *OsP5CS1* and *OsP5CS2* expression, and accumulate higher amounts of proline under drought and salt stress (Xiong *et al.*, 2014).

Lipid signaling mediated by phospholipases plays essential roles in plant responses to abiotic stresses and phytohormones. Under non-stressed conditions, Phospholipase D (PLD) acts as a negative regulator of proline biosynthesis in Arabidopsis (Thiery *et al.*, 2004). Inhibition of PLD by primary butanol treatment leads to increased *AtP5CS1* transcripts and proline accumulation (Thiery *et al.*, 2004). In addition, Phospholipase C (PLC)-mediated lipid signaling pathway has been reported to enable plant to discriminate between ionic and nonionic stresses (Parre *et al.*, 2007). Application of a specific inhibitor of PLCs, U73122, inhibits salt-induced proline accumulation by reducing *AtP5CS1* on both mRNA and protein levels. Moreover, application of cyclopiazonic acid (CPA), an inhibitor of calcium ATPase, can partially restore U73122-inhibited salt-induced proline accumulation, indicating the involvement of calcium signaling in PLC-mediated ionic stress induced proline accumulation (Parre *et al.*, 2007).

In addition, halophyte *Eutrema salsugineum*, previously named as *Thellungiella halophila*, which is close related to Arabidopsis phylogenetically, has a high capacity in proline accumulation under both water-stressed and non-stressed conditions (Taji *et al.*, 2004; Ghars *et*

al., 2008). In contrast to *Arabidopsis*, *T. halophila* PLD functions as a positive regulator of proline accumulation, whereas ThPLC exerts a negative control on proline biosynthesis (Ghars *et al.*, 2012), revealing that differential regulation of lipid signaling pathways is critical to explain the differentiated proline accumulation between *T. halophila* and the *Arabidopsis*.

1.3.2 Regulation of proline catabolism

Transcriptional regulations of *ProDH* has been studied since 1990s (Kiyosue *et al.*, 1996). Accumulated studies have depicted an intricate regulation network, which can integrate multiple signals to regulate the precise expression of *ProDH* in *Arabidopsis*. In the following paragraphs, transcriptional regulation of proline catabolism in response to hypoosmolarity, low-energy condition, and light signals is reviewed.

1.3.2.1 Heterodimer of group C/S₁ bZIPs regulate ProDH in response to hypoosmolarity and energy homeostasis

ProDH1 transcriptional expression has been reported to be induced by hypoosmolarity, post-drought rehydration and exogenous proline treatment. It was shown to be inhibited by drought, osmotic stress and sucrose (Kiyosue *et al.*, 1996; Hanson *et al.*, 2008).

Transcriptional regulation of *ProDH* is depending on a core *cis*-acting element ACTCAT, termed as proline/hypoosmolarity-responsive element (PRE) present in the promoter region. PRE is necessary for proline-responsive and hypoosmolarity-responsive expression of not only *ProDH* but also other 21 proline-inducible genes in *Arabidopsis* (Sato *et al.*, 2002). Besides, group S₁ of bZIP transcription factors, such as bZIP53, was demonstrated to bind to the ACTCAT *cis*-element on the *ProDH* promoter and function as *ProDH* transcriptional activator (Sato *et al.*, 2004). Moreover, in the context of *ProDH* regulation, Weltmeier *et al.* (2006) shows that bZIP53 does not preferentially form dimers with its own group S bZIPs but strongly interacts with members of group C bZIPs, such as bZIP63. Therefore, *ProDH* has been shown to be regulated by an elaborate heterodimer network of group C/S₁ bZIPs (Weltmeier *et al.*, 2006). Recent studies on the C/S₁ network suggest it acts as central regulators of plant low-energy response under extended darkness, working downstream of SnRK1 (Mair *et al.*, 2015; Pedrotti *et al.*, 2018).

Energy homeostasis is crucial to all living organisms. Thus, it is managed by an evolutionarily conserved system consisting of two counteracting kinases, SnRK1 and TARGET OF

RAPAMYCIN (TOR) (Dröge-Laser and Weiste, 2018). SnRK1 is induced by energy deprivation conditions, such as dark-induced senescence (DIS), and inhibited by sucrose (Baena-González *et al.*, 2007; Baena-González and Sheen, 2008). The principal processes activated by SnRK1s are major energy-preserving catabolic pathways related to carbohydrate, lipid, and amino acid metabolism, as well as autophagy or general stress responses (Baena-González and Sheen, 2008). In contrast to SnRK1, TOR is activated by both nitrogen and carbon metabolites and promotes energy-consuming processes and repressing nutrient remobilization through autophagy (Dobrenel *et al.*, 2016).

bZIP11, a group S₁ bZIP, is repressed by sucrose. In Arabidopsis, *ASPARAGINE SYNTHETASE1 (ASNI)* and *ProDH1/2* have been identified as targets that are rapidly activated by bZIP11. Increased *bZIP11* expression leads to decreased proline and increased phenylalanine levels. Hence, bZIP11 is proposed to be a bridge between sugar signals and amino acid metabolism (Hanson *et al.*, 2008). Additionally, *bzip63* knock-out mutant exhibits a delayed DIS phenotype and altered primary metabolism. bZIP63 was also found to be phosphorylated by the SnRK1 through direct interaction in an energy-dependent manner. Thus, the role of bZIP63 in energy/carbon starvation response has been established (Mair *et al.*, 2015).

Hence, together with the fact that proline oxidation can produce FADH₂ and NADH, proline catabolism might also play an important role in energy homeostasis maintenance during DIS.

1.3.2.2 HY5 suppresses both ProDH and P5CDH in response to light signal

More importantly, light can control proline metabolism directly. Light has been found to affect both proline biosynthesis and degradation in plants since 1970s (Hanson and Tully, 1979; Sanada *et al.*, 1995).

In Arabidopsis, some studies suggest that light/dark cycle is responsible for the oscillation expression of *ProDH* at both mRNA and protein levels under stress or non-stress conditions (Hayashi *et al.*, 2000; Dubois *et al.*, 2017). Both mRNA and protein of *ProDH1* were found to be induced and stabilized under continuous darkness (Hayashi *et al.*, 2000). Moreover, Dubois *et al.* (2017) has reported that the expression of *AtProDH1* oscillates in young leaves under well-watered growth condition. Under this condition, *AtProDH1* expression has a mild peak in the day and a more predominant peak in the night. Unexpectedly, gradually mild drought only inhibits diurnal *AtProDH1* expression, not the nocturnal, suggesting the drought response might be gated by circadian clock (Dubois *et al.*, 2017).

Recent research improves our understanding on the interaction between light signaling pathway and proline catabolism. It is reported that HY5, a bZIP-type transcription factor, which was found to be a high hierarchical regulator of the photomorphogenesis (Lee *et al.*, 2007, page 5), can directly bind to the C-box motif on the *ProDH1* promoter (Kovács *et al.*, 2019). HY5 can down-regulate the expression of *ProDH1* under salt stress in a red and blue light dependent manner (Kovács *et al.*, 2019). Additionally, *P5CDH* transcriptional expression is also regulated by HY5. In Arabidopsis, *P5CDH* mRNA is degraded by its own antisense overlapping gene *SIMILAR TO RCD ONE 5 (SRO5)* (AT5G62520) derived natural small-interfering RNA (nat-siRNA) under salt stress (Borsani *et al.*, 2005). Moreover, researchers found that *SRO5* is not only a HY5 binding target but also positively regulated by HY5, by using chromatin immunoprecipitation-DNA chip hybridization (ChIP-chip) associated with genome-wide expression analysis (Lee *et al.*, 2007).

1.3.3 Post-translational modification of proline metabolic enzymes

Protein posttranslational modifications (PTMs) represent a key means of regulating cellular processes and diversifying the proteome (Park *et al.*, 2013). In bacteria *S. typhimurium*, trifunctional PutA (StPutA) has been reported to autophosphorylate on several threonine, serine, and tyrosine residues (Ostrovsky and Maloy, 1995). The rate of dephosphorylation of StPutA protein is positively correlated with its interaction with membranes and the availability of proline. Dephosphorylated StPutA protein has a higher DNA binding affinity than the phosphorylated StPutA (Ostrovsky and Maloy, 1995).

So far, PTMs of eukaryotic proline metabolic enzymes are major reported in animals. It has been reported that *Mus musculus* (mouse) P5CS subject to lysine succinylation identified by quantitative lysine succinylation proteome (Park *et al.*, 2013). In addition, human PYCR has been reported to subject to lysine acetylation and serine phosphorylation (Zhou *et al.*, 2013) identified by mass spectrometry (MS)-based phosphoproteomics. Recently, HsPYCR1 has been reported to directly bind to sirtuin SIRT3, a mitochondrial NAD⁺-dependent deacetylase, both *in vivo* and *in vitro* (Chen *et al.*, 2019). Moreover, CREB-binding Protein (CBP) is the acetyltransferase for HsPYCR1, whereas SIRT3 deacetylates HsPYCR1. Acetylation of HsPYCR1 at K228 reduces its enzymatic activity by impairing the formation of the decamer of HsPYCR1 (Chen *et al.*, 2019). In addition, it has been reported that mouse P5CDH (MmP5CDH) subject to lysine succinylation (Park *et al.*, 2013), lysine acetylation (Rardin *et al.*, 2013), and serine phosphorylation (Zhou *et al.*, 2013; Bian *et al.*, 2014) identified by large-scale

approaches. MmProDH1 has been reported to subject to lysine acetylation identified by quantitative proteomics (Rardin *et al.*, 2013).

However, direct study is unavailable for PTMs of plant proline metabolic enzymes so far. By searching the Arabidopsis protein phosphorylation site database (PhosPhAt 4.0)(Durek *et al.*, 2010), there is one phosphorylation site experimentally confirmed for ProDH1, 5 for ProDH2, 2 for P5CS2, and 1 for P5CR. Furthermore, disulphide bonds have been speculated to stabilize the quaternary structure of AtProDH (Fabro *et al.*, 2020). According to sequence alignments, many conserved cysteine residues have been found in both OAT, ProDH, and P5CDH (see Annex). Moreover, AtP5CDH has been reported to be a target of thioredoxin in Arabidopsis roots (Marchand *et al.*, 2010).

1.4 Proline catabolism is tightly linked to energy metabolism

1.4.1 Proline catabolism and mitochondrial respiration

1.4.1.1 General introduction of mETC

The electron transport chain (ETC) is fundamental to mitochondria function. The electrons from redox reactions—such as proline oxidation—enter the ECT either via NAD(P)H or via flavine nucleotides (FADH₂, FMNH₂) (Schertl and Braun, 2014). Flavine nucleotides are generally bound to proteins—such as ProDH—which termed as flavoproteins.

Some dehydrogenases can directly transfer electrons to ubiquinone (UQ), such as succinate dehydrogenase (SDH, a.k.a. Complex II) and glyceraldehyde 3-phosphate dehydrogenase (GAPDH) (Fig. I-6) (Schertl and Braun, 2014). On the contrary, many dehydrogenases can indirectly donate electrons into ETC. There are two inner mitochondrial membrane-localized UQ-targeted electron entry points of ETC, i.e., the NAD(P)H dehydrogenase complexes and the electron transfer flavoprotein-ubiquinone oxidoreductase (ETF-QO) system in eukaryotes. On the one hand, many dehydrogenases in the mitochondrial matrix, such as P5CDH, can generate NAD(P)H which is oxidized by NADH-ubiquinone oxidoreductase (Complex I) or internal NAD(P)H dehydrogenase (iN), to finally donate electrons to UQ (Schertl and Braun, 2014). On the other hand, some dehydrogenases, such as isovaleryl-coenzyme A dehydrogenase (IVDH), transfer electrons to the electron transfer flavoprotein (ETF) in the mitochondrial matrix, then to ETF-QO, and finally to UQ (Ishizaki *et al.*, 2005). Hence, the ETF/ETF-QO system is recognized as a short branch of the ETC (Ishizaki *et al.*, 2005; Schertl and Braun, 2014).

1.4.1.2 Relationship between proline catabolism and mETC

As a flavoenzyme, ProDH has been speculated to transfer electrons to ETC (Fig. I-6). The connection between ProDH and ETC is first found in *Saccharomyces cerevisiae* (Wang and Brandriss, 1987). It has been reported that a functional ETC is necessary for yeast to utilize proline as a nitrogen source (Wang and Brandriss, 1987).

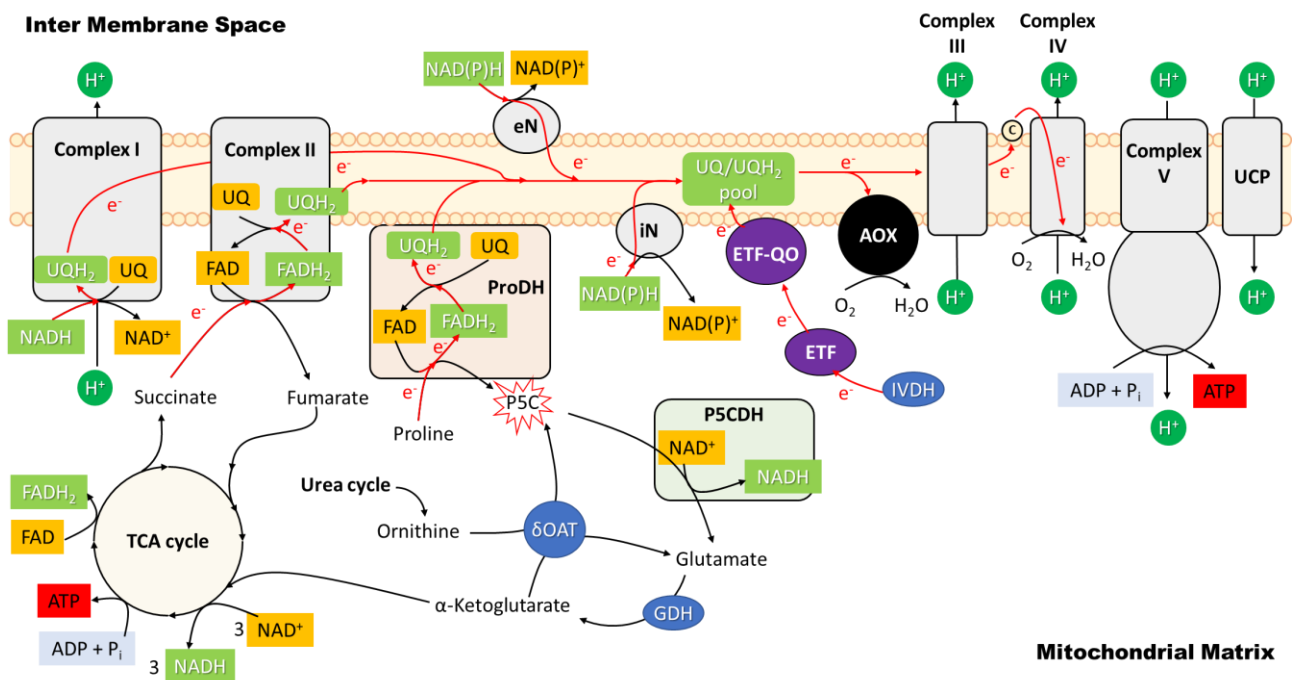


Figure I-6. Correlation between proline catabolism and the ETC. The transfer route of electrons is depicted in red lines with arrow. e⁻, electron; H⁺, proton; P_i, inorganic phosphate; ADP, adenosine diphosphate; ATP, adenosine triphosphate; UQ/UQH₂, oxidized/reduced ubiquinone; NAD(P)⁺/NAD(P)H, oxidized/reduced nicotinamide adenine dinucleotide (phosphate); FAD/FADH₂, oxidized/reduced flavin adenine dinucleotide; P5C, δ¹-pyrroline-5-carboxylate. Complex I, NADH-ubiquinone oxidoreductase; SDH1-4, 1-4 subunits of succinate dehydrogenase (Complex II); 3x[Fe-S], three iron–sulfur clusters of SDH2; eN, external NAD(P)H dehydrogenase; iN, internal NAD(P)H dehydrogenase; ETF, electron transfer flavoprotein; ETF-QO, electron transfer flavoprotein-ubiquinone oxidoreductase; AOX, alternative oxidase; Complex III, ubiquinone-cytochrome c oxidoreductase; c, cytochrome c; Complex IV, cytochrome c oxidase; Complex V, ATP synthase; UCP, uncoupling protein; TCA cycle, tricarboxylic acid cycle; ProDH, proline dehydrogenase; P5CDH, P5C dehydrogenase; OAT, ornithine δ-aminotransferase; GDH, glutamate dehydrogenase; IVDH, isovaleryl-coenzyme A dehydrogenase.

In *Arabidopsis*, a detailed respiratory study—using mitochondria isolated from Col-0 (wild-type, WT), *prodh1*, *prodh2*, and *p5cdh*—has been performed by Cabassa-Hourton *et al.*, (2016). It has been shown that proline treatment can increase both protein content and enzymatic activity of ProDH, which can further provide electrons to ETC resulting in elevated respiratory rate in WT plants (Cabassa-Hourton *et al.*, 2016). In addition, L-proline related

substrates like D-proline or L-hydroxyproline (substrate for vertebrate ProDH2) did not lead to any ETC-dependent O₂ consumption in plants (hereafter, L-proline is referred to as proline). Besides, proline dependent respiration has been observed in mitochondria isolated from WT, *p5cdh*, and *prodh2* plants instead of *prodh1*, which demonstrated that electron transfer from proline to ETC is mediated by ProDH1 in Arabidopsis (Cabassa-Hourton *et al.*, 2016).

To date, several studies have shown that the oxidation of proline by ProDH is coupled with the reduction of UQ. There are two possible mechanisms by which ProDH can transfer electrons to UQ. One hypothesis is that ProDH can transfer electrons to UQ indirectly through ETF/ETF-QO system, like IVDH. Another possibility is that ProDH can bind directly with UQ, like Complex II.

However, the possibility of the ETF/ETF-QO system as an electron mediator between ProDH and UQ has been ruled out by a study in yeast (Wanduragala *et al.*, 2010). It has been reported that ProDH can bind directly to UQ by its evolutionary conserved catalytic core ($\beta\alpha$)₈ barrel (a.k.a. TIM barrel) in *E. coli* (Moxley *et al.*, 2011), yeast (Wanduragala *et al.*, 2010), *Mus musculus* (mouse), and *Homo sapiens* (human) colorectal cancer cell culture (Hancock *et al.*, 2016). Therefore, we can speculate the plant ProDH should have a similar UQ binding capacity, even lacking experimental evidence *in planta*.

As the final product of proline catabolism, glutamate can be converted to α -ketoglutarate by glutamate dehydrogenase (GDH). After, α -ketoglutarate can possibly replenish the TCA cycle to produce succinate, which can subsequently fuel the ETC through Complex II. Thus, it is straightforward to hypothesize that there should be a functional connection between proline catabolism and Complex II.

In Arabidopsis cell culture, external addition of proline has been shown to induce the activity of GDH (Schertl *et al.*, 2014). Furthermore, it has been reported that the mRNA level, protein level, and enzymatic activity of ProDH are substantially increased during DIS in the detached rosette leaves of Arabidopsis (Launay *et al.*, 2019). Meanwhile, a higher respiration capacity of Complex I and II has been observed in mitochondria isolated from wild-type (Col-0) at the late stage of DIS. Consistently, the respiratory rate of Complex II has been found decreased significantly in *prodh1prodh2* double mutant plants, compared with wildtype (Launay *et al.*, 2019).

In parallel, succinate has been found to be an uncompetitive inhibitor of ProDH in human DLD colorectal cancer cell culture (Hancock *et al.*, 2016). Furthermore, by using a membrane-permeable crosslinker dithiobis succinimidyl propionate (DSP) in mitochondria isolated from mouse liver, it has been reported that ProDH can co-immunoprecipitate with both SDH1

and SDH2 subunits of Complex II (Hancock *et al.*, 2016). This is consistent with the finding that ProDH1 is associated with unknown low-molecular-mass complexes in mitochondria isolated from proline-treated *Arabidopsis* cell culture (Cabassa-Hourton *et al.*, 2016). However, the interacting partner(s) of ProDH still needs further investigation. Taken together, these findings strongly support a speculated link between proline catabolism and Complex II in both plant and animal.

1.4.2 Proline catabolism and dark-induced leaf senescence

Leaf, the most important photosynthetic organ, is not only the place of carbon fixation but also the destination of nitrogen allocation during vegetative growth (Schulze *et al.*, 1994; Makino *et al.*, 1997). Leaf senescence, as a form of programmed cell death (PCD), is the final stage of leaf development and vital for the remobilization of valuable nutrients to other organs to increase plant fitness (Lim *et al.*, 2007; Havé *et al.*, 2016; Liebsch and Keech, 2016; Woo *et al.*, 2019). As a highly organized and active physiological process, leaf senescence is essential to optimize nutrient reallocation for plant reproductive growth and supporting plant adaptation under adverse environmental conditions (Noodén and Penney, 2001; Avila-Ospina *et al.*, 2014; Liebsch and Keech, 2016). It is controlled by integrated various internal and external signals including developmental age, nutrition status, hormone signal, water status, light, hypoxia, and temperature change (Woo *et al.*, 2019; Izumi and Ishida, 2019).

During senescence, leaf cells are subject to dramatic structural and metabolic changes. The breakdown of the chloroplast is the earliest and the most significant cellular structural alteration during senescence (Chrobok *et al.*, 2016). In contrast, the mitochondrial integrity and energy status are maintained until the final stage of senescence, even the number of mitochondria decreased by 30% (Keech *et al.*, 2007; Chrobok *et al.*, 2016) and mitochondrial morphology is altered (Ruberti *et al.*, 2014) in senescing cells. Alongside with the structural alteration, metabolic reprogramming from anabolism to catabolism is taking place in senescing leaf cells. Metabolically, as the degradation of chloroplast, the senescing leaf cells are changing from photo-autotrophy to heterotrophy. Most of nitrogen in leaves reside in chloroplasts (Makino and Osmond, 1991). In C_3 plants, for example, the chloroplast proteins account for about 75% to 80% of the total leaf nitrogen (Makino and Osmond, 1991). Recent studies suggest that, when photosynthesis is inhibited, chloroplast degradation through autophagy is required for the production of free amino acids, instead of amino acid biosynthesis. This constitutes an alternative energy source in mitochondria (Chen *et al.*, 2017; Izumi and Ishida, 2019).

During developmental leaf senescence (DLS), it has been reported that mitochondria orchestrate catabolic processes and become energy-producing and metabolic hubs, facilitating the retrieval of nutrients from the senescing organ to the rest of the plant (Chrobok *et al.*, 2016). Moreover, many amino acid catabolic processes have been up-regulated during DLS to produce glutamate, including lysine-ketoglutarate reductase/saccharopine dehydrogenase (LKR/SDH) in lysine catabolism, enzymes in branched-chain amino acids (BCAA) catabolism, OAT in arginine catabolism, ProDH1/2 and P5CDH in proline catabolism (Chrobok *et al.*, 2016). As the common final product of these catabolic pathways, glutamate has been proposed to play a central role in nitrogen remobilization during DLS (Chrobok *et al.*, 2016).

In accordance with the key role of leaves in photosynthesis and light sensing, light quantity and quality play an essential role in leaf senescence regulation. Light deprivation in form of severe shading or darkening on leaves leads to rapid senescence, termed as shade- or dark-induced senescence (SIS and DIS, respectively) (Liebsch and Keech, 2016). As a commonly used and useful tool to study senescence, DIS has many features common to DLS, sharing a high number of commonly regulated genes, although with considerable differences as well (Buchanan-Wollaston *et al.*, 2005; Graaff *et al.*, 2006). Furthermore, it has been reported that senescence is induced in individually darkened *Arabidopsis* leaves, but inhibited in whole darkened plants (Weaver and Amasino, 2001). DIS treatment of detached leaves is highly effective in inducing senescence-associated genes (SAGs) and chlorophyll loss (Weaver and Amasino, 2001).

Proline accumulation has been reported in excised rice leaves during DIS (Wang *et al.*, 1982; Mondal *et al.*, 1985). In parallel, a recent study suggests that the proteolysis of chloroplast proteins during DIS contributes to amino acid accumulation in dark-treated *Camellia sinensis* (tea) leaves, which is a common and effective industrial practice to improve free amino acids in preharvest tea leaves (Chen *et al.*, 2017).

Furthermore, recent studies have shown that proline catabolism is induced during DIS in *Arabidopsis* (Chrobok *et al.*, 2016; Launay *et al.*, 2019), where proline acts as an alternative respiratory substrate in responding to energy deprivation (Launay *et al.*, 2019). Meanwhile, both mRNA and protein levels of *AtProDH* and *AtP5CDH* have been shown to be enhanced during DIS (Launay *et al.*, 2019). Therefore, DIS is a promising physiological condition to investigate putative interaction between ProDH, OAT, and P5CDH.

1.5 Structural biology of ProDH, P5CDH, and OAT

In the past decades, proline biosynthesis has been studied extensively. However, the regulation of proline catabolism and its biological role are largely unknown. Therefore, this study is focusing on the proline catabolic enzymes and OAT.

1.5.1 Structure diversity and oligomerization

The oligomeric state of proline catabolic enzymes is unexpectedly diverse (Tab. I-1). Dimeric PutA structures were observed in some bacteria such as *E. coli* (Singh *et al.*, 2011) and *Geobacter sulfurreducens* (Singh *et al.*, 2014). But in *Sinorhizobium meliloti* and *Corynebacterium freiburgense*, PutA was found to exist as monomer-dimer equilibrium (Luo *et al.*, 2016; Korasick *et al.*, 2017). Moreover, PutA was reported to form a ring-shaped tetramer in *Bradyrhizobium japonicum* (Srivastava *et al.*, 2010).

The oligomeric state of monofunctional P5CDH has been extensively studied (Tab. I-1). Dimeric P5CDH was found in human, mouse, *Bacillus halodurans*, and *B. licheniformis* (Srivastava *et al.*, 2012; Luo *et al.*, 2013; Pemberton and Tanner, 2013). In lower plant *Physcomitrella patens* and higher plant *Zea mays*, P5CDH exists as equilibrium between a domain-swapped dimer and a dimer-of-dimer tetramer (Korasick *et al.*, 2019). Trimer-of-dimers hexameric P5CDH were found in *Saccharomyces cerevisiae*, *Thermus thermophilus*, *Deinococcus radiodurans*, and *Mycobacterium tuberculosis* (Luo *et al.*, 2013; Pemberton *et al.*, 2014; Lagautriere *et al.*, 2015).

However, the oligomeric state of monofunctional ProDH has not been thoroughly studied (Tab. I-1). Dimeric ProDH has been found in *Trypanosoma cruzi* (Paes *et al.*, 2013) and human (Tallarita *et al.*, 2012). The oligomeric state of ProDH remains ambiguous in *T. thermophilus* (TtProDH). N-terminally His-tagged TtProDH solubilized with non-ionic detergent *n*-octyl- β -D-glucopyranoside (BOG) has been described as a mixture of dimers and monomers in crystals (White *et al.*, 2007). In contrast, when using maltose-binding protein (MBP) as a solubility tag, MBP-tagged and MBP-clipped TtProDH have been found to form oligomers and soluble aggregates through non-native self-association, in both the absence and presence of BOG in solution (Huijbers and Berkel, 2015).

Furthermore, it has been reported that the hydrophobic N-terminal helix of TtProDH is important for that self-association process. The more polar MBP-tagged F10E/L12E TtProDH variant exclusively forms tetramers and maintains catalytic activity over a wide range of temperatures (Huijbers and Berkel, 2016). Taken together, TtProDH is likely to form dimer and

monomer in crystals, whereas it will form active tetramer complex in solution. So far, structure of eukaryotic ProDHs have not been solved. AtProDH1 has been found to form part of a low-molecular-mass (70–140 kDa) complex in the mitochondrial membrane in proline treated *Arabidopsis* suspension cells (Cabassa-Hourton *et al.*, 2016). Recently, heterologous expression of AtProDH1 and AtProDH2 in *E. coli* showed that the first N-terminal α -helix of AtProDH is necessary for its enzyme activity and oligomerization. AtProDH is likely to form tetramers in solution, which may be stabilized by disulphide bonds (Fabro *et al.*, 2020).

Table I-1. Oligomeric state of proline catabolic enzymes and OAT

| | Organism | Oligomeric state | PDB code | Reference |
|-------|-------------------------------------|----------------------------|------------|------------------------------------|
| PutA | <i>Escherichia coli</i> | Dimer | 2GPE | (Singh <i>et al.</i> , 2011) |
| | <i>Geobacter sulfurreducen</i> | Dimer | 4NM9 | (Singh <i>et al.</i> , 2014) |
| | <i>Sinorhizobium meliloti</i> | Monomer-dimer equilibrium | 5KF6 | (Luo <i>et al.</i> , 2016) |
| | <i>Corynebacterium freiburgense</i> | Monomer-dimer equilibrium | 5UX5 | (Korasick <i>et al.</i> , 2017) |
| | <i>Bradyrhizobium japonicum</i> | Ring-shaped tetramer | 3HAZ | (Srivastava <i>et al.</i> , 2010) |
| P5CDH | <i>Bacillus licheniformis</i> | Dimer | 3RJL | (Luo <i>et al.</i> , 2013) |
| | <i>Bacillus halodurans</i> | Dimer | 3QAN | (Luo <i>et al.</i> , 2013) |
| | <i>Thermus thermophilus</i> | Trimer-of-dimers hexamer | 2BHQ | (Luo <i>et al.</i> , 2013) |
| | <i>Deinococcus radiodurans</i> | Trimer-of-dimers hexamer | - | (Luo <i>et al.</i> , 2013) |
| | <i>Mycobacterium tuberculosis</i> | Trimer-of-dimers hexamer | 4LEM, 4NS3 | (Lagautriere <i>et al.</i> , 2015) |
| | <i>Homo sapiens</i> | Dimer | 3V9G | (Srivastava <i>et al.</i> , 2012) |
| | <i>Mus musculus</i> | Dimer | 3V9J | (Srivastava <i>et al.</i> , 2012) |
| | <i>Zea mays</i> | Dimer-tetramer equilibrium | 6D97 | (Korasick <i>et al.</i> , 2019) |
| | <i>Physcomitrella patens</i> | Dimer-tetramer equilibrium | - | (Korasick <i>et al.</i> , 2019) |
| | <i>Saccharomyces cerevisiae</i> | Trimer-of-dimers hexamer | 4OE6 | (Pemberton <i>et al.</i> , 2014) |
| ProDH | <i>Thermus thermophilus</i> | Monomer and dimer | 2G37 | (White <i>et al.</i> , 2007) |
| | | Tetramer | - | (Huijbers and Berkel, 2016) |
| | <i>Trypanosoma cruzi</i> | Dimer | - | (Paes <i>et al.</i> , 2013) |
| | <i>Homo sapiens</i> | Dimer | - | (Tallarita <i>et al.</i> , 2012) |
| OAT | <i>Plasmodium falciparum</i> | Dimer | 3LG0 | (Jortzik <i>et al.</i> , 2010) |
| | <i>Vigna aconitifolia</i> | Monomer | - | (Sekhar <i>et al.</i> , 2007) |
| | <i>Pisum sativum</i> | Monomer | - | (Stránská <i>et al.</i> , 2010) |
| | <i>Homo sapiens</i> | Tetramer-dimer equilibrium | 1OAT | (Montioli <i>et al.</i> , 2017) |

Diverse oligomeric states of OAT have been reported but only from a limited number of living organisms (Tab. I-1). So far, monomeric OAT has been reported in two plant species *Vigna aconitifolia* (Sekhar *et al.*, 2007) and *Pisum sativum* (Stránská *et al.*, 2010). In bacteria *Plasmodium falciparum*, OAT has been found dimeric (Jortzik *et al.*, 2010). In human, OAT has been reported as tetramer-dimer equilibrium (Montioli *et al.*, 2017).

1.5.2 Metabolon and substrate channelling

Protein complexes of sequential metabolic enzymes, often termed as metabolons, may permit direct channelling of substrates and intermediates between enzymes, providing increased control over metabolic fluxes (Srere, 1985; Zhang *et al.*, 2017). Dynamic assemblies of consecutive enzymes have been observed in a wide range of metabolic pathways, such as Calvin–Benson cycle (Huege *et al.*, 2011), TCA cycle (Robinson and Srere, 1985), glycolysis (Graham *et al.*, 2007), mitochondrial electron transport chain (Lapuente-Brun *et al.*, 2013), oxidative pentose phosphate pathway (Debnam *et al.*, 1997), fatty acid β -oxidation (Ishikawa *et al.*, 2004), and branched chain amino acid metabolism (Islam *et al.*, 2007).

Some studies suggest that the intermediate P5C or most probably its tautomeric form GSA, shared by proline metabolism and ornithine pathways, is toxic for the cell. Exogenous proline supply are lethal in both yeast and *Arabidopsis p5cdh* mutants, causing a burst of reactive oxygen species (ROS) (Deuschle *et al.*, 2001). Furthermore, P5C/GSA was reported to react with metabolites (Farrant *et al.*, 2001), to inhibit the mitochondrial respiration and to trigger the burst of superoxide anions in mitochondria (Nishimura *et al.*, 2012), and, last but not least, participate in apoptosis signaling pathway (Maxwell and Davis, 2000).

In connection with the role of P5C/GSA, it was found in *Geobacter sulfurreducens* and *Bradyrhizobium japonicum* that dimerization of PutA enables substrate-channelling to sequester P5C/GSA inside PutA (Srivastava *et al.*, 2010; Singh *et al.*, 2014)(Fig. I-7). Moreover in *Thermus thermophilus*, monofunctional TtProDH and TtP5CDH have been reported to interact with each other, also forming a similar substrate channel as PutA (Sanyal *et al.*, 2015). A dissociation constant of 3 μ M has been estimated for TtProDH-TtP5CDH interaction, indicating these two proteins form a weak and transient protein complex (Sanyal *et al.*, 2015). Furthermore, the interaction between TtProDH and TtP5CDH is orientation-specific, TtP5CDH specifically binds to the top face of the TtPRODH $\beta_8\alpha_8$ barrel (Sanyal *et al.*, 2015).

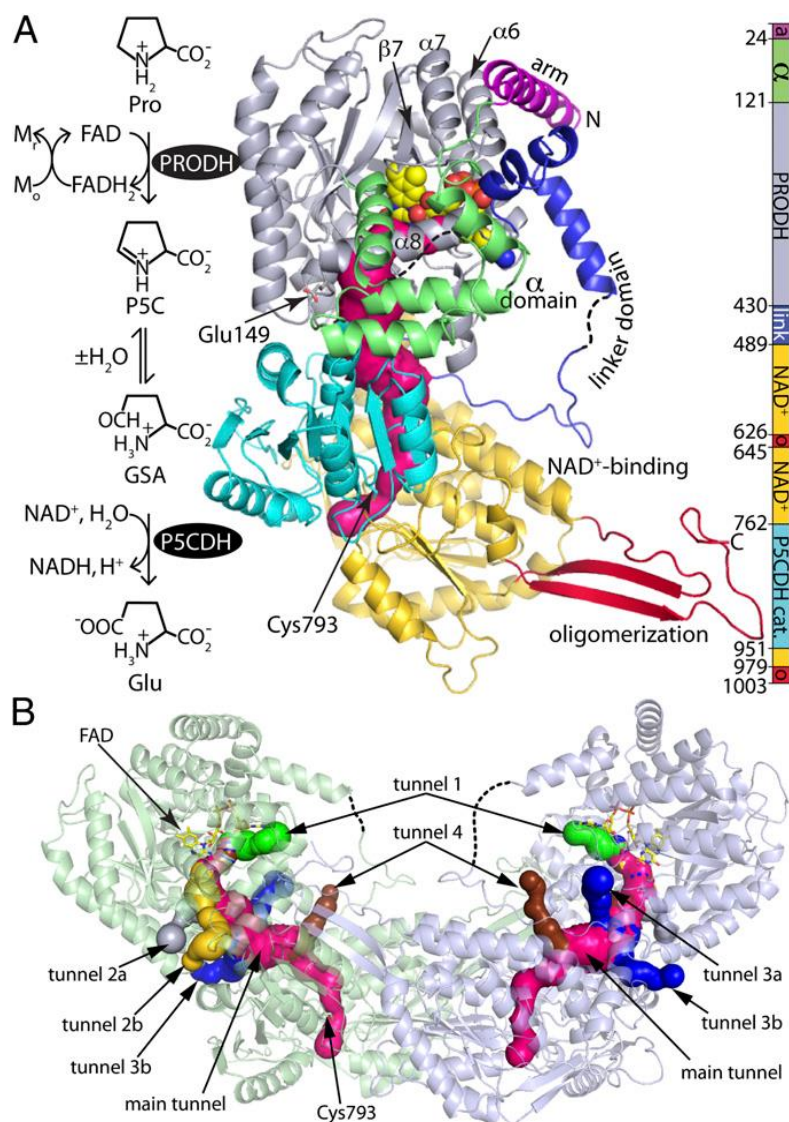


Figure I-7. Substrate channeling of GsPutA. (A) Reactions catalyzed by GsPutA and a ribbon drawing of the monomer of GsPutA (PDB: 4NM9). The pink surface represents the substrate-channelling tunnel. The domains are colored according to the legend on the right. The dashes denote disordered sections of the α and linker domains. (B) Ribbon drawing of the GsPutA dimer, with the two monomers colored green and blue. The surfaces represent the substrate channelling tunnel system. The main substrate-channelling tunnel is colored pink. From Singh *et al.*, (2014).

Overall, P5C/GSA channelling could be beneficial to avoid toxicity of P5C/GSA, but also to exert tight regulation of proline catabolic flux protecting cells from proline-P5C futile cycling between proline biosynthesis and catabolism. This mechanism has already been found in both bifunctional and monofunctional prokaryotic proline catabolic enzymes, thus eukaryotic proline catabolic enzymes might also follow the same regime.

1.6 Scientific questions

In the previous contents, the importance of proline and proline metabolism in different aspects has been discussed. Proline biosynthesis has drawn many scientists' attention in the past decades. However, little is known about the biological role and regulation of proline catabolism in eukaryotes. Therefore, in this study, the relationship between OAT, ProDH, and P5CDH during DIS has been investigated.

The major scientific issues that this study wants to address are:

1. To precisely define the sub-mitochondrial localizations of ProDH1, P5CDH, and OAT.
2. To determine whether eukaryotic ProDH1, P5CDH, and OAT form a protein complex
3. To unravel the physiological importance of the presence of such complex *in planta*.

CHAPTER II.

The proline cycle as a
eukaryotic redox valve

The impact of the proline metabolism goes beyond regulating the actual levels of the product proline or the intermediate P5C. Recent works have shown the importance of proline metabolism in energy metabolism and redox homeostasis. However, the role of proline metabolism in these biological processes are not well understood. Thus, we believed that it was a key time to summarize our understanding of the relationship between proline cycle and redox status. Our review in this topic was already accepted by *Journal of Experimental Botany* (in press). This review highlights the putative role of proline cycle in redox status in cells in relation to other redox shuttles and its importance for energy metabolism. We also addressed the role of the proline-P5C cycle *in planta*.

Chapter 2. The proline cycle as a eukaryotic redox valve

Yao Zheng, Cécile Cabassa-Hourton, Séverine Planchais, Sandrine Lebreton, Arnould Savoure¹

Sorbonne Université, UPEC, CNRS, IRD, INRAE, Institute of Ecology and Environmental Sciences of Paris (iEES), Paris, France

¹Corresponding author, arnould.savoure@sorbonne-universite.fr

Journal of Experimental Botany, in Press: 31 July 2021, <https://doi.org/10.1093/jxb/erab361>



Journal of Experimental Botany
<https://doi.org/10.1093/jxb/erab361> Advance Access Publication 31 July, 2021



REVIEW PAPER

The proline cycle as a eukaryotic redox valve

Yao Zheng, Cécile Cabassa-Hourton, Séverine Planchais, Sandrine Lebreton and Arnould Savoure*

Sorbonne Université, UPEC, CNRS, IRD, INRAE, Institute of Ecology and Environmental Sciences of Paris (iEES), F-75005 Paris, France

* Correspondence: arnould.savoure@sorbonne-universite.fr

Received 1 July 2021; Editorial decision 27 July 2021; Accepted 29 July 2021

Editor: Graham Noctor, Université Paris-Sud, France

Abstract

The amino acid proline has been known for many years to be a component of proteins as well as an osmolyte. Many recent studies have demonstrated that proline has other roles such as regulating redox balance and energy status. In animals and plants, the well-described proline cycle is concomitantly responsible for the preferential accumulation of proline and shuttling of redox equivalents from the cytosol to mitochondria. The impact of the proline cycle goes beyond regulating proline levels. In this review, we focus on recent evidence of how the proline cycle regulates redox status in relation to other redox shuttles. We discuss how the interconversion of proline and glutamate shuttles reducing power between cellular compartments. Spatial aspects of the proline cycle in the entire plant are considered in terms of proline transport between organs with different metabolic regimes (photosynthesis versus respiration). Furthermore, we highlight the importance of this shuttle in the regulation of energy and redox power in plants, through a particularly intricate coordination, notably between mitochondria and cytosol.

Keywords: Mitochondria, proline cycle, proline metabolism, proline transport, redox shuttle, redox status, redox valve

Introduction

Redox homeostasis during development is vital for all branches of the tree of life, particularly in response to environmental changes (Scheibe *et al.*, 2005). Compartmentalization of metabolism and other cellular functions in eukaryotic cells implies that pools of metabolites, ions, and reducing equivalents are concentrated locally in a regulated manner (Lunn, 2006). Maintenance of metabolism as environmental conditions vary, whether regularly, rapidly, or to extremes, is a challenge for all eukaryotic organisms, and particularly plants for several reasons. As sessile organisms, plants cannot move away to more clement conditions, so they are subject to dynamic environmental alterations. In eukaryotic photosynthetic organisms, the regulation of energy metabolism is particularly complex because it

involves two organelles, the mitochondrion and the chloroplast, as major sources of ATP and reducing power in the form of the pyridine nucleotides NADH and NADPH (Foyer and Noctor, 2020). Additional complexity of redox and energy metabolism arises from the daily cycles of light and dark periods, and the presence of green and non-green tissues within the same individual. In daylight, photon energy is transformed in green tissues by photosystems into ATP and NADPH, which in turn are used to fix CO₂ by the Calvin–Benson cycle. In mitochondria, oxidative phosphorylation breaks down carbohydrates to generate ATP in all tissues at any time, but remains the only powerhouse system operative during the night and in non-green tissues. Tight spatiotemporal coordination of supply

and demand to the two powerhouse systems of plant cells is required to meet the energy needs of anabolic processes such as primary assimilation of carbon and nitrogen, as well as transport of substrates, intermediates, and products.

Specific translocators enable the direct or indirect exchange of reducing power between cell compartments (Palmieri *et al.*, 2009). The cofactor NAD^+ , the oxidized form of NADH, is synthesized in the cytosol and must be imported into organelles to ensure timely supply to many enzymatic reactions. In *Arabidopsis*, the two NAD^+ carrier proteins NDT1 and NDT2 have been shown to respectively localize in plastid and mitochondrial membranes, allowing direct transport of NAD^+ into these organelles (Palmieri *et al.*, 2009). Recent data locate NDT1 exclusively in the mitochondrial membrane (de Souza Chaves *et al.*, 2019). On the contrary, no transporter has been identified as a carrier of reduced form NADH from one subcellular compartment to another. Membranes are also impermeable to both NADPH cofactor and its oxidized form NADP^+ . An NADP^+ carrier has not been identified yet, suggesting that this compound is likely to be formed by an NAD^+ kinase. Indeed NAD^+ kinases have been found to be localized in the cytosol and chloroplasts (Gakière *et al.*, 2018; Dell'Aglio *et al.*, 2019). Furthermore, NAD^+ kinase has been also detected in the mitochondrial matrix of yeasts and mammals (Outten and Culotta, 2003; Ohashi *et al.*, 2012), but not of plants (Gakière *et al.*, 2018).

As organellar membranes are not permeable to reduced forms of pyridine nucleotides, the compartmentalized redox couples (NAD^+/NADH and $\text{NADP}^+/\text{NADPH}$) rely on shuttles for their translocation between subcellular compartments. A shuttle system is a series of biochemical interconversions that temporarily bind the redox or other molecular entity in a permeant form that can be ferried across the membrane barrier, releasing or reconstituting the entity on the other side of the barrier. The number of steps, enzymes, substrates, and transporters involved depends on the type, site and function of the shuttle. Shuttles are thus dynamic control systems that redirect metabolic flux so certain compounds can be overproduced. Organellar and cytosolic NADH and NADPH pools have been shown to be regulated by multiple shuttles or metabolic valves, such as the glycerol-3-phosphate (G3P) shuttle and the malate–aspartate shuttle for the NADH pools, and the malate–oxaloacetate (OAA) shuttle for NADPH pools. The concept of a metabolic valve is that build-up of an entity, such as a reducing equivalent, on one side of a membrane barrier can be released or purged in a regulated manner, redistributing the entity in the cell while resetting the conditions on either side of the barrier. In this sense, a valve might not be expected to operate stoichiometrically. Such shuttle and valve mechanisms enable redox and energy homeostasis in both normal and stressed states. Proline metabolism involves the interconversion of glutamate and proline in a process linked to cellular compartments and energetics. Therefore, enzymes involved in proline metabolism could participate in $\text{NAD(P)}^+/\text{NAD(P)}$

H homeostasis in a shuttle mechanism with a valve function during plant development and in stress conditions.

Proline metabolism

Abiotic stresses perturb cellular redox homeostasis, and proline metabolism is thought to act as an important redox buffer in both plants and animals (Krishnan *et al.*, 2008; Sharma *et al.*, 2011; Ben Rejeb *et al.*, 2014, 2015; Phang, 2019). Proline plays important roles in various developmental stages of plants as well as in stress tolerance (Kavi Kishor and Sreenivasulu, 2014; Bhaskara *et al.*, 2015; Trovato *et al.*, 2019). Indeed most plant species have been shown to accumulate proline in response to abiotic and biotic stresses. In plants, proline biosynthesis occurs in the cytosol starting from glutamate (Fig. 1). Glutamate is phosphorylated and reduced by Δ^1 -pyrroline-5-carboxylate synthetase (P5CS) using NADPH as a cofactor to form glutamate semialdehyde (GSA) in equilibrium with pyrroline-5-carboxylate (P5C). P5C is further reduced to proline by P5C reductase (P5CR) also using NAD(P)H as a cofactor. Székely *et al.* (2008) presented evidence that P5CS1 may be localized in chloroplasts during salt stress, indicating that proline may also be synthesized in this organelle. Recent work using spectrally resolved fluorescence imaging showed exclusive cytosolic localization of P5CS1 and P5CS2 in *Arabidopsis* protoplasts, suggesting that plastids do not contribute to P5CS-mediated proline biosynthesis (Funck *et al.*, 2020). The subcellular localization of P5CS1 therefore remains ambiguous and may depend on growth and/or stress conditions. Further research is required to unravel these discrepancies.

In animals, the conversion of P5C to proline is also mediated by P5CR, commonly named PYCR. The organization of the proline biosynthesis pathway is more complex, at least in humans, where PYCR is encoded by three different genes, *PYCR1*, 2, and *L*, with both *PYCR1* and *PYCR2* localized in mitochondria and *PYCR1* in the cytosol (De Ingeniis *et al.*, 2012). P5CR was shown to be exclusively cytosolic in *Arabidopsis* cells (Funck *et al.*, 2012).

When stress is relieved, proline is rapidly transported from the cytosol into mitochondria by either a mitochondrial proline symporter or a proline/glutamate antiporter (Di Martino *et al.*, 2006); however, genes encoding these transporters have yet to be identified. Mitochondrial proline is then oxidized by the sequential action of proline dehydrogenase (ProDH) and P5C dehydrogenase (P5CDH) to release glutamate. Mitochondrial glutamate transporters ‘a bout de souffle’ (BOU) and mitochondrial uncoupling proteins UCP1/2 have now been identified and it is conceivable that they could participate in the shuttling of glutamate during the proline cycle (Monné *et al.*, 2018; Porcelli *et al.*, 2018). ProDH, also known as proline oxidase (POX), catalyses the first and rate-limiting step of proline catabolism using FAD as a cofactor (Servet *et al.*, 2012). In both animals and plants, ProDH is localized on the matrix side of

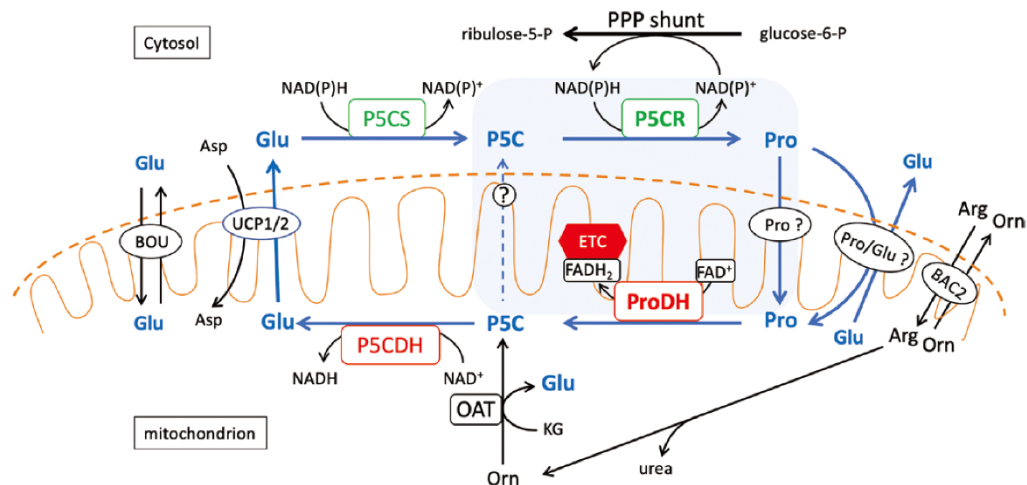


Fig. 1. Proline metabolism in plants and its links to the ornithine and pentose phosphate pathways. The proline cycle is highlighted by blue arrows and the putative proline–P5C cycle with light blue shading. ‘?’ indicates unknown transporter(s). Asp, aspartate; BAC, basic amino acid carrier; BOU, a bout de souffle; ETC, electron transport chain; Glu, glutamate; KG, α -ketoglutarate; OAT, ornithine δ -aminotransferase; Orn, ornithine; PPP shunt, pentose phosphate pathway; P5C, pyrroline-5-carboxylate; P5CDH, P5C dehydrogenase; P5CS, P5C synthetase; Pro, proline; ProDH, proline dehydrogenase; UCP, mitochondrial uncoupling protein.

the mitochondrial inner membrane (Elthon and Stewart, 1981; Cabassa-Hourton *et al.*, 2016) where it transfers electrons released from proline oxidation to the mitochondrial electron transport chain. While P5CDH activity was detected in the mitochondrial inner membrane in *Zea mays* (maize) (Elthon and Stewart, 1981), this enzyme is localized in the mitochondrial matrix in animals (Brunner and Neupert, 1969) and other plants (Deuschle *et al.*, 2001). Recently, Ren *et al.* (2018) have shown that the two enzymes may physically interact with the inhibitory protein DFR1 in *Arabidopsis* to regulate proline catabolism.

In mitochondria, ornithine δ -aminotransaminase (OAT) contributes to the formation of GSA and glutamate by transferring the ornithine δ -amino group to α -ketoglutarate (KG). There have been some reports of proline biosynthesis from ornithine in plants (Delauney *et al.*, 1993; Roosens *et al.*, 1998) and in animals (De Ingeniis *et al.*, 2012). An increase in proline content was also shown to be correlated with higher OAT activity in salt-stressed cashew plants (da Rocha *et al.*, 2012) and in rice overexpressing OAT (You *et al.*, 2012). In comparison, Funck *et al.* (2008) demonstrated that, at least in *Arabidopsis*, P5C is involved in glutamate formation through the action of P5CDH rather than proline biosynthesis.

In bacteria, invertebrates, and plants such as halophytes, proline accumulation has been shown to contribute to osmotic adjustment of cells to counterbalance water loss (Slama *et al.*, 2015; Forlani *et al.*, 2019). Proline can act as a metabolic signaling molecule to modulate mitochondrial functions and influence cell death (Szabados and Savouré, 2010; Senthil-Kumar and Mysore, 2012; Zhang and Becker, 2015; Rizzi *et al.*, 2016; Phang, 2019). Proline has also been shown to participate

in the redox balance and energy status of the cell. Proline metabolism may provide stress protection by maintaining the NADPH/NADP⁺ balance and the levels of antioxidants (Ben Rejeb *et al.*, 2014). On a cellular scale, proline metabolism may bridge compartments to allow redox changes across membranes. Given this reach and multifunctionality, we now focus on the characteristics of three redox shuttle systems to provide a framework in which to consider whether proline metabolism could fulfil a similar purpose in eukaryotes.

Eukaryotic redox shuttles

The glycerol-3-phosphate shuttle

In mitochondria, electrons released from NADH oxidation are transferred to the electron transport chain, which in turn feeds the energy necessary to pump protons across the inner mitochondrial membrane. This creates an electrochemical proton gradient that drives ATP synthesis. In addition to ATP generation, mitochondrial membrane potential drives the transport of metabolites between mitochondrial and cytosolic compartments. In yeasts, plants, and animals, a G3P shuttle involved in redox homeostasis has been described (Ansell *et al.*, 1997; Shen *et al.*, 2003, 2006; Mráček *et al.*, 2013). A key component of the shuttle is a G3P dehydrogenase on the outer surface of the inner mitochondrial membrane that donates electrons directly to the ubiquinone pool. The G3P shuttle irreversibly consumes cytosolic NADH generating mitochondrial FADH₂ (Fig. 2A; Shen *et al.*, 2006; McKenna *et al.*, 2006). Briefly, electrons from NADH are transferred to dihydroxyacetone phosphate (DHAP) via the cytosolic G3P dehydrogenase (cGPDH) to

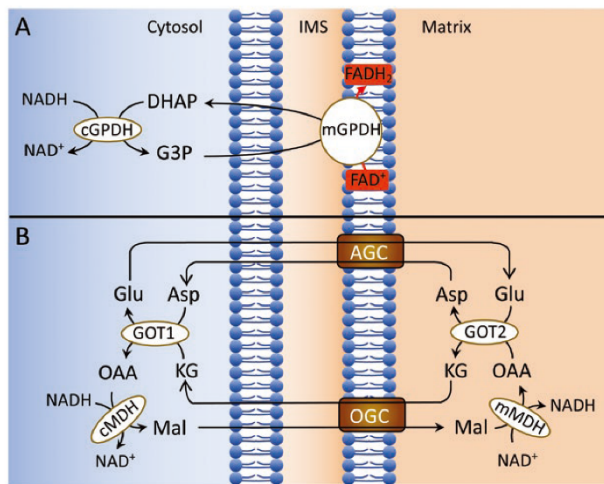


Fig. 2. The glycerol-3-phosphate (G3P) (A) and the malate–aspartate (B) shuttles for transporting reducing equivalents from cytosolic NADH into the mitochondrial matrix or mitochondrial oxidative phosphorylation pathway, respectively. AGC, aspartate–glutamate carrier; Asp, aspartate; DHAP, dihydroxyacetone phosphate; GPDH, glycerol-3-phosphate dehydrogenase; G3P, glycerol-3-phosphate; Glu, glutamate; GOT, glutamate oxaloacetate aminotransferase; IMS, intermembrane space; KG, α -ketoglutarate; Mal, malate; MDH, malate dehydrogenase; OAA, oxaloacetate; OGC, KG–malate carrier.

form G3P. Then, G3P is converted to DHAP on the outer surface of the inner mitochondrial membrane by mitochondrial G3P dehydrogenase (mGPDH). Next, electrons are transferred to FAD to form FADH₂ within the mitochondria, coupled with the reduction of ubiquinone (McKenna *et al.*, 2006). This G3P shuttle is especially prominent in muscle cells enabling an extremely high rate of oxidative phosphorylation to be sustained. Some insects that lack lactate dehydrogenase are completely dependent on the G3P shuttle for the regeneration of cytoplasmic NAD⁺ (Mráček *et al.*, 2013). Generally, the G3P shuttle provides a less important mechanism of redox state regulation in mammalian cells than the malate–aspartate shuttle (described in detail below) because most tissues have only low levels of mGPDH (Mráček *et al.*, 2013). In plants, the *FAD-GPDH* gene has been reported to be highly expressed during seed germination and repressed upon water stress (Shen *et al.*, 2006; Quettier *et al.*, 2008). However, the role of the G3P shuttle remains elusive in plants.

The malate–aspartate shuttle

Like the G3P shuttle, the more complex malate–aspartate shuttle acts to irreversibly transfer reducing equivalents from cytosolic NADH to mitochondria (Borst, 2020), but in contrast it transfers NADH from the cytosol into the mitochondrial matrix forming NADH again. This system involves two cytosolic and two matrix enzymes as well as two inner membrane transporters. In the cytosol, electrons from NADH

are transferred to OAA by cytosolic malate dehydrogenase (cMDH) to generate malate (Fig. 2B). Malate is multifunctional because it is an intermediate in energy metabolism that is also involved in the transfer of reducing equivalents, and possibly metabolic trafficking between different cell types in eukaryotes. Malate enters the mitochondrial matrix via the malate–KG carrier (OGC) in exchange for KG. The mitochondrial malate dehydrogenase (mMDH) converts malate to OAA, transferring the electrons to NAD⁺ to form NADH in the matrix. Subsequently, OAA is transaminated to aspartate via mitochondrial glutamate OAA aminotransferase (GOT) with the simultaneous conversion of glutamate to KG. Finally, aspartate is exported from the mitochondria via the aspartate–glutamate carrier (AGC) in exchange for cytosolic glutamate, which brings one proton into the mitochondria.

The efflux of aspartate from mitochondria is stoichiometric with entry of glutamate plus a proton in an electrogenic exchange that provides directionality while controlling the rate (LaNoue *et al.*, 1974a, b). Consequently, the malate–aspartate shuttle is powered by the electrochemical proton gradient to export aspartate and so aids the import of reducing equivalents into mitochondria. It is not clear what regulates the balance between the malate–aspartate shuttle and the G3P shuttle.

The malate–aspartate shuttle is found in yeast and animals (Cavero *et al.*, 2003; McKenna *et al.*, 2006; Sarrústegui and Bak, 2015); however, it is still unclear whether this shuttle also occurs in plant mitochondria. There is evidence for this type of shuttle in plant–bacteria interactions in root nodules of *Alnus glutinosa* (Akkermans *et al.*, 1981) and *Pisum sativum* with an associated role in nitrogen fixation (Appels and Haaker, 1991). This shuttle has also been described as operating between glyoxysomes and mitochondria from the endosperm of germinating castor bean (Mettler and Becvers, 1980).

The malate–OAA shuttle

In plant cells, the regulation of energy metabolism is particularly complex because both mitochondria and chloroplasts are involved. The malate–OAA shuttle, sometimes referred to as the malate valve, is a powerful system for balancing metabolic fluxes through indirect transport of reducing equivalents. The valve is composed of cytosolic, mitochondrial, plastid, and peroxisomal malate dehydrogenases (MDH) in cooperation with malate–OAA translocators (MOT) (Fig. 3). For example, higher levels of NAD(P)H drive plastid MDH to convert OAA to malate. Then, malate is transferred to the cytosol or mitochondria by MOTs. In the mitochondrial matrix, malate is oxidized by mitochondrial MDH, which reduces NAD⁺ to NADH (Selinski and Scheibe, 2019). Theoretically, the malate–OAA shuttle should be able to transfer reducing equivalents in either direction depending on the prevailing redox conditions on either side of the membrane. Oxidation of malate to OAA by mitochondrial MDH generates NADH, which is then oxidized by complex I producing reactive oxygen species (ROS).

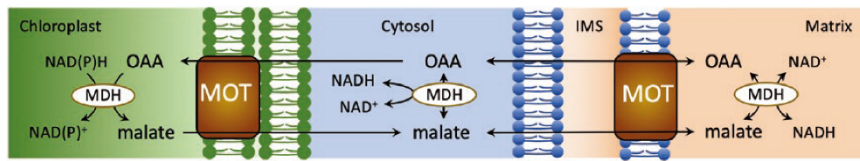


Fig. 3. Malate–oxaloacetate shuttle, or the malate valve, involves the interconversion of malate and oxaloacetate by malate dehydrogenase (MDH). Isoenzymes of MDH are present in each cellular compartment, the cytosol, chloroplasts, and mitochondria. MDH, malate dehydrogenase; OAA, oxaloacetate; MOT, malate- α -ketoglutarate transporter.

Generation of ROS from malate oxidation can trigger cell death in both animals and plants suggesting that such mechanisms are conserved (Zhao *et al.*, 2020). However, in plant cells this shuttle may only serve to export reducing equivalents from mitochondria and plastids in normal growth conditions (Selinski and Scheibe, 2019). It should be noted that the exchange of malate and OAA mediated by MOTs across different cellular compartments is not driven by the electrochemical proton gradient, so this exchange can only move reducing equivalents from a relatively reduced compartment to a relatively oxidized compartment. Since the mitochondrial matrix is much more reduced than the cytosol with respect to the NADH/NAD⁺ ratio, the OAA transporter is likely to work primarily to export reducing equivalents from mitochondria to the cytosol (Selinski and Scheibe, 2019).

The proline cycle as a reducing-equivalent shuttle

Considering that metabolism of proline involves the oxidation of NAD(P)H in the cytosol and the reduction of NAD⁺ in mitochondria, we postulate that proline metabolism may also play an important role as a redox regulator in eukaryotic cells. Indeed, P5CS and P5CR oxidize NAD(P)H in the cytosol, while in mitochondria ProDH and P5CDH reduce FAD and NAD⁺, respectively.

In the cytosol, induction of P5CS and/or P5CR expression may help to maintain a low NADPH/NADP⁺ ratio (Liang *et al.*, 2013). Coordination between proline and redox metabolism can be deduced from the phenotype of the Arabidopsis *p5cs1* mutant because it displays hypersensitivity to salt stress, accumulation of ROS, and strongly enhanced expression of genes involved in redox metabolism of the mitochondria and chloroplasts (Székely *et al.*, 2008; Shinde *et al.*, 2016). Using a forward genetic screen based on a *ProDH1*-promoter luciferase reporter, Shinde *et al.* (2016) found that mutants affected in the synthesis of very-long-chain fatty acids (VLCFAs) or in cuticle deposition also accumulate more proline. This implies a strong coordination between proline and lipid metabolism in relation to redox status. Proline and lipid metabolism both help buffer cellular redox status under stress.

Regulation of P5CR activity in Arabidopsis seems to depend on a complex pattern of regulation including the ratios

of reduced to oxidized pyridine nucleotides, the preference for phosphorylated over non-phosphorylated pyridine nucleotides, and the presence of ions (Giberti *et al.*, 2014; Ruszkowski *et al.*, 2015). Equimolar concentrations of NADP⁺ completely suppress the NADH-dependent activity of P5CR, whereas the NADPH-dependent reaction is mildly affected (Giberti *et al.*, 2014). Moreover, NADH-dependent but not NADPH-dependent activity of P5CR is inhibited by an excess of proline. Excess of salt inhibits the NADH-dependent and activates the NADPH-dependent activity of P5CR. Similarly, in the protozoan *Trypanosoma cruzi*, TcP5CR is an NADPH-dependent cytosolic enzyme whose activity is fine-tuned by NADPH cytosolic pools (Marchese *et al.*, 2020). Thus, the reduced status of the cytosol dependent on proline cycle functioning would be mostly driven by regulation of NADPH homeostasis.

In mitochondria, regulation of the reduced state by the proline cycle occurs through the production of both NADH and FADH₂, which impact electron transport chain functioning as well as ROS production. Several studies in both animal and plant cells have shown that increasing the reduced state of mitochondria by metabolic or mutational manipulation leads to proline biosynthesis, while decreasing mitochondrial reduced state and/or ATP synthesis impairs proline accumulation (Huang *et al.*, 2013; Schwörer *et al.*, 2020). A decrease in the activity of the mitochondrial electron transport chain caused by a defect in one of its superprotein complexes leaves cells prone to the damage of excess reducing power. Enhancing proline biosynthesis and down-regulating its degradation would be an alternative way to trap reducing power and limit saturation of the electron transport chain and formation of ROS. Recently, SSR1, a mitochondrial protein with a tetratricopeptide repeat domain, was shown to be involved in maintaining the function of the mitochondrial electron transport chain (Han *et al.*, 2021). When the *ssr1-1* mutant was treated with proline, the ROS content was higher, the ATP level was lower, and AOX function was enhanced. ProDH was hypothesized to directly generate ROS because this enzyme was shown to reduce oxygen *in vitro* (White *et al.*, 2007) and its overexpression increased ROS production in cancers and apoptosis (Pandhare *et al.*, 2009; Moxley *et al.*, 2011). However, Goncalves *et al.* (2014) demonstrated that superoxides are not produced by ProDH itself but by specific components of the electron transport chain. ProDH/POX was found to bind directly to coenzyme Q suggesting that proline-derived electrons can directly reduce

oxygen at complex III to generate superoxides (Hancock *et al.*, 2016). On the other hand, *p5cs1-4*, an Arabidopsis mutant impaired in stress-induced proline accumulation, was shown to be associated with strongly up-regulated expression of a number of genes encoding NAD(P)H dehydrogenases and/or related to mitochondrial respiration (Shinde *et al.*, 2016). Similarly, Lovell *et al.* (2015) revealed that proline concentration was strongly affected by cytoplasmic genome variation in an Arabidopsis mapping population in response to drought. Mitochondrial DNA polymorphisms were linked to two genes encoding NADH dehydrogenase subunits indicating that proline accumulation is tightly regulated by cellular redox status and that proline catabolism is important in drought tolerance. These results combined support the idea of a tight regulation between proline metabolism and cellular redox status with mitochondria having a key role, possibly dissipating energy for drought stress tolerance (Atkin and Macherel, 2009). This would be consistent with the view that the dynamics of proline metabolism, probably through a proline cycle between biosynthesis and catabolism, is important for cell homeostasis.

The importance of the proline cycle in development and stress

Various environmental stresses such as drought or salt stress have been shown to trigger proline accumulation by up-regulating proline biosynthesis and down-regulating proline catabolism (Peng *et al.*, 1996; Parre *et al.*, 2007; Leprince *et al.*, 2015). If ProDH is absent, the proline cycle may not be active in such stress conditions, although a low level of ProDH may be sufficient to allow cycling between proline and glutamate to support the maintenance of a proper NAD(P)⁺ to NAD(P)H ratio. For example, expression of ProDH2 has been shown to be triggered by salt stress whereas ProDH1 expression is repressed (Funck *et al.*, 2010). Other studies have shown the importance of mitochondrial proline catabolism in the regulation of cell redox status in response to drought stress (Sharma *et al.*, 2011). In such stress conditions, the presence of ProDH1, including some with putative post-translational modifications, was observed in western blots of protein extracts (Bhaskara *et al.*, 2015). This discrepancy could be due to the different growth conditions and/or sensitivities of the antibodies used, and it would be important to determine the activity of ProDH with an appropriate assay to clarify this issue (Lebreton *et al.*, 2020). In addition, transcriptome analyses have revealed that *ProDH1* transcript levels oscillate during light–dark cycles, being down-regulated during the day and up-regulated during the night. Drought down-regulates *ProDH1* transcript levels but only during the day. Interestingly, VLCFA biosynthesis genes had a similar expression profile to the *ProDH1* gene (Dubois *et al.*, 2017), which corroborates the idea that proline metabolism is coordinated with VLCFA biosynthesis when cellular redox status is altered.

Transgenic plants overexpressing *P5CS1* under the control of a heat shock promoter accumulated proline in a heat-dependent manner and, interestingly, were less tolerant to heat shock. Indeed, higher *ProDH1* expression and ROS contents were measured in these transgenic plants suggesting that the proline cycle had been stimulated (Lv *et al.*, 2011). High levels of P5C were also detected in the yeast *put2* mutant (mutated in the yeast gene for P5CDH) (Nomura and Takagi, 2004) and the Arabidopsis *p5cdh* mutant in addition to high levels of ROS upon proline treatment (Deuschle *et al.*, 2004; Miller *et al.*, 2009). This work revealed the importance of the proline cycle in maintaining cellular ROS homeostasis.

The proline cycle is also involved in NADP⁺/NADPH homeostasis during plant development through a spatial and temporal compartmentalization of proline synthesis and proline degradation. Such a distribution of metabolism between different organs implies that proline as well as glutamate must be transported somehow. Proline is known to move between tissues through vascular vessels (Girousse *et al.*, 1996) and from cell to cell by plasma membrane transporters such as the amino acid/auxin permease and proline transporter (ProT) (Schwacke *et al.*, 1999; Hirner *et al.*, 2006; Lehmann *et al.*, 2011).

Interestingly proline is mainly synthesized in photosynthetically active tissues, although its oxidation is localized in non-green sink tissues (Sharma *et al.*, 2011). Proline is transported from source to sink tissues such as growing regions of root and shoot where the oxidation of proline will provide energy to support growth. Source–sink interactions are also key determinants of leaf senescence (Dellero *et al.*, 2020). During plant senescence, specific degradation of Calvin cycle enzymes is triggered, lowering the NADPH levels in chloroplasts or senescent organs. Expression of *ProDH1* and to a lesser extent *ProDH2* has been shown to be triggered when leaf senescence is induced by darkness, leading to higher ProDH activity (Launay *et al.*, 2019). In addition, proline was demonstrated to be an alternative metabolic substrate whose oxidation fuels the electron transport chain to generate energy (Launay *et al.*, 2019). Proline oxidation is therefore important for restoring the NADP⁺ to NADPH ratio of the cell.

In another example, transport of proline was shown to be important during the formation of plant reproductive organs. Proline was 56 times more concentrated in flowers (sink organs) than in source leaves (Schwacke *et al.*, 1999). Proline accumulated in pollen grains accounted for 70% of the total free amino acids and was essential for pollen fertility (Mattioli *et al.*, 2018). The *LeProT1* gene, which encodes a proline transporter, is expressed in the germinating pollen tube. However, the proline transport through this route is insufficient to fulfill the demand of developing microspore cells (Mattioli *et al.*, 2018). The proline that accumulates in pollen derives from local synthesis inside developing microspores and mature pollen grains. In this case, it was also suggested that proline would have a role in supplying energy during the rapid growth of the pollen tube.

Proline accumulation may also be a very important mechanism to balance redox potential oscillation during the day.

Indeed, light is known to affect transcript levels of both proline biosynthesis and degradation genes in plants (Hanson and Tully, 1979; Sanada *et al.*, 1995). *P5CS* gene expression is promoted during the light period and repressed during dark periods, whereas *ProDH* transcript levels show the opposite behavior (Hayashi *et al.*, 2000; Dubois *et al.*, 2017). It is conceivable that light regulation also occurs at the protein level. By using a proteomic approach, Marchand *et al.* (2010) have shown that P5CDH could be a target of thioredoxin. Thioredoxins (Trx) are ubiquitous proteins catalysing reversible disulfide-bond formation involved in enzyme redox and activity regulation. Different Trx isoforms are present in mitochondria (Trx o, Trx h) and cytosol (Trx h), and the reducing power for Trx reduction is provided by NADPH through NADPH-thioredoxin reductase (NTR) (Geigenberger *et al.*, 2017). Interestingly, less proline and more glutamate and malate accumulated in *trxo1* and *ntra ntrb* double mutants compared with the wild type (Daloso *et al.*, 2015). A 30% reduction in proline accumulation was also observed in a *trxo1* mutant under low water potential conditions by Verslues *et al.* (2014). All these data reflect a probable regulation of proline metabolic enzymes by Trxs, which are able to transmit the light signal from the chloroplast to other organelles like mitochondria. Moreover, as the proline cycle may shuttle reducing power from cytosol to mitochondria, we can hypothesize that it also contributes to the control of the NTR/Trx system. Thus, the proline cycle may be important during the night when photosynthesis is not active to generate redox power and energy.

The proline–pyrroline-5-carboxylate cycle and its functions

Interestingly, when it is in equilibrium with GSA in a reversible non-enzymatic reaction, P5C is an intermediate for both proline biosynthesis from either glutamate or ornithine and proline oxidation. It is a product of ProDH activity in mitochondria and a substrate of P5CR in the cytosol. If P5C could move back and forth between the cytosol and the mitochondrial matrix, P5CR and ProDH could then be said to form a metabolic ring, the proline–P5C cycle. Notionally, a prerequisite for a functional proline–P5C cycle is for both P5CR and ProDH to be expressed at the same time and for either GSA or P5C to be transported through mitochondrial membranes. The existence of this cycle in plants is far from proven, not least because no transporter of P5C has been identified yet.

The proline–P5C cycle was first proposed by Hagedorn and Phang (1986) when they demonstrated the catalytic functioning of the shuttle to generate cytosolic NADP⁺ without stoichiometric consumption of proline. Proline is exported to mitochondria by a transporter whose gene has not been identified yet. Proline is then oxidized to P5C, which may be transported back into the cytosol, with the help of a putative unknown transporter, to be further reduced to proline

by P5CR. By this route, mitochondrial P5C would replenish cytosolic proline biosynthesis and avoid at the same time the consumption of cytosolic ATP and production of mitochondrial NADH by bypassing P5CS and P5CDH, respectively. This proline–P5C cycle would then allow NADPH to be consumed in the cytosol, while FAD⁺ would be reduced in mitochondria. Thus, reducing power would be shuttled in a single direction from the cytosol to the mitochondrial matrix in this cycle (Fig. 1). The proline–P5C cycle has been proposed to maintain the redox balance between mitochondria and the cytosol.

In animals, the proline–P5C cycle has been shown to play important roles in the regulation of cell growth and cell death. This cycle acts by transferring the reducing power formed by the pentose phosphate pathway into mitochondria for the production of either ROS or ATP. ROS signaling mediated by ProDH was shown to trigger apoptosis, suggesting that ProDH is a mitochondrial tumor suppressor (Liu and Phang, 2012).

Miller *et al.* (2009) proposed that a proline–P5C cycle also operates in plants with P5C transport. This plant biochemical cycle may support the preferential accumulation of proline as well as the shuttling of redox equivalents from the cytosol to mitochondria. This cycle would maintain a high cellular proline to P5C ratio and direct electrons to the electron transport chain.

Increases in ProDH expression and activity have been observed when the oxidative burst occurs during the hypersensitive response (Cecchini *et al.*, 2011; Monteoliva *et al.*, 2014). In this instance, ProDH was proposed to participate in the hypersensitive response through the proline–P5C cycle by generating ROS to trigger cell death in order to prevent pathogen spread in plants. It is possible that proline toxicity may be due to an overflow of electrons in the mitochondrial electron transport chain.

P5C may also originate from the arginine pathway. In most organisms, arginine catabolism contributes to the formation of ornithine and urea through the action of arginase. In general, OAT catalyses the transfer of the δ -amino group from ornithine to KG yielding GSA/P5C and glutamate, contributing to P5C input into mitochondria to serve as the substrate for P5CDH (Fig. 1). In intestinal cells, OAT also participates in the degradation of ornithine to form citrulline, which results in a consumption of P5C (Ginguay *et al.*, 2017). In plants, a direct contribution of OAT to stress-induced proline accumulation is still debated. A study of salt-stressed *Arabidopsis oat* knockout mutants provided strong evidence that OAT does not contribute to stress-induced proline accumulation (Funck *et al.*, 2008). Therefore, it is unlikely that the OAT pathway contributes to the proline–P5C cycle, at least in salt stress conditions. It has nevertheless been proposed that high concentrations of free arginine may increase the affinity of P5CDH for P5C, possibly influencing the balance between P5C export into the cytosol and its mitochondrial oxidation to glutamate (Forlani *et al.*, 2015).

Conclusions and perspectives

As mitochondrial membranes are not permeable to NAD(P)⁺ or NAD(P)H, eukaryotes have evolved redox shuttles, like the G3P, malate–aspartate, and malate–OAA shuttles, to allow transfer of reducing power from one compartment to another. It is not clear yet whether a malate–aspartate shuttle operates in plant cells.

The availability of a redox shuttle that allows redox exchange between cytosol and mitochondria is of particular interest for plant cells. Proline metabolism is a unique pathway because it involves the interconversion of proline and glutamate, a process linked to consumption of reducing power for proline biosynthesis in the cytosol. The existence of the proline cycle allows the biosynthesis of proline and concomitant oxidation of NADPH molecules in the cytosol. Furthermore, glucose oxidation from the pentose phosphate pathway in the cytosol can be linked to ATP production via the sequential transfer of the generated NADPH to proline, which would be then oxidized by ProDH in the mitochondrion.

When proline is transported into mitochondria, its oxidation supports oxidative phosphorylation by a mechanism independent of NADH oxidation because electrons enter the electron transport system at the level of the flavoenzyme ProDH, which directly feeds the mitochondrial electron transport chain and drives the synthesis of ATP. This proline cycle enables electrons from cytosolic NADPH to be transported into mitochondria against the NADH concentration gradient. It is unlikely that the proline cycle acts as a continuous major source of energy because firstly ProDH has to be expressed and active, and secondly this cycle produces only a limited amount of the ATP produced by succinate entering the tricarboxylic acid cycle. Nevertheless, there may be special conditions when this shuttle acts as a transient yet significant source of energy for development or survival. The proline cycle may be required when the tricarboxylic acid cycle cannot operate maximally, as postulated to occur during the initiation of leaf senescence. The proposed proline cycle appears to play an important role in regulating both cytosolic and mitochondrial redox states. Regulation at the level of ProDH and P5CR enzymes and/or transport of proline, P5C, and glutamate across mitochondrial membranes requires more study, but given the influence and reach of the proline shuttle, any new findings may be relevant in the study and development of resilient crops.

Acknowledgements

We would like to thank the reviewers for their constructive comments and efforts for improving our review. Members of the APCE, iEES team are gratefully acknowledged for their stimulating discussions.

Author contributions

AS conceived and planned the review topic. AS wrote the manuscript with support from YZ, CC, SP and SL. All authors approved the final version of the manuscript.

Conflict of interest

The authors declare that this research was conducted in the absence of any commercial or financial relationships that would cause any potential conflicts of interest.

Funding

This work received financial support from Sorbonne Université and a PhD fellowship to YZ from the China Scholarship Council.

References

- Akkermans ADL, Huss-Danell K, Roelofsen W.** 1981. Enzymes of the tricarboxylic acid cycle and the malate–aspartate shuttle in the N₂-fixing endophyte of *Alnus glutinosa*. *Physiologia Plantarum* **53**, 289–294.
- Ansell R, Granath K, Hohmann S, Thevelein JM, Adler L.** 1997. The two isoenzymes for yeast NAD⁺-dependent glycerol 3-phosphate dehydrogenase encoded by *GPD1* and *GPD2* have distinct roles in osmoadaptation and redox regulation. *The EMBO Journal* **16**, 2179–2187.
- Appels MA, Haaker H.** 1991. Glutamate oxaloacetate transaminase in pea root nodules: participation in a malate/aspartate shuttle between plant and bacteroid. *Plant Physiology* **95**, 740–747.
- Atkin OK, Macherel D.** 2009. The crucial role of plant mitochondria in orchestrating drought tolerance. *Annals of Botany* **103**, 581–597.
- Ben Rejeb K, Abdely C, Savouré A.** 2014. How reactive oxygen species and proline face stress together. *Plant Physiology and Biochemistry* **80**, 278–284.
- Ben Rejeb K, Lefebvre-De Vos D, Le Disquet I, Leprince AS, Bordenave M, Maldiney R, Jdey A, Abdely C, Savouré A.** 2015. Hydrogen peroxide produced by NADPH oxidases increases proline accumulation during salt or mannitol stress in *Arabidopsis thaliana*. *New Phytologist* **208**, 1138–1148.
- Bhaskara GB, Yang TH, Verslues PE.** 2015. Dynamic proline metabolism: importance and regulation in water limited environments. *Frontiers in Plant Science* **6**, 484.
- Borst P.** 2020. The malate–aspartate shuttle (Borst cycle): How it started and developed into a major metabolic pathway. *IUBMB Life* **72**, 2241–2259.
- Brunner G, Neupert W.** 1969. Localisation of proline oxidase and Δ -pyrroline-5-carboxylic acid dehydrogenase in rat liver. *FEBS Letters* **3**, 283–286.
- Cabassa-Hourton C, Schertl P, Bordenave-Jacquemin M, et al.** 2016. Proteomic and functional analysis of proline dehydrogenase 1 link proline catabolism to mitochondrial electron transport in *Arabidopsis thaliana*. *The Biochemical Journal* **473**, 2623–2634.
- Cavero S, Vozza A, del Arco A, et al.** 2003. Identification and metabolic role of the mitochondrial aspartate–glutamate transporter in *Saccharomyces cerevisiae*. *Molecular Microbiology* **50**, 1257–1269.
- Cecchini NM, Monteoliva MI, Alvarez ME.** 2011. Proline dehydrogenase contributes to pathogen defense in *Arabidopsis*. *Plant Physiology* **155**, 1947–1959.
- Daloso DM, Müller K, Obata T, et al.** 2015. Thioredoxin, a master regulator of the tricarboxylic acid cycle in plant mitochondria. *Proceedings of the National Academy of Sciences, USA* **112**, E1392–E1400.
- da Rocha IM, Vitorello VA, Silva JS, Ferreira-Silva SL, Viégas RA, Silva EN, Silveira JA.** 2012. Exogenous ornithine is an effective precursor and the δ -ornithine amino transferase pathway contributes to proline accumulation under high N recycling in salt-stressed cashew leaves. *Journal of Plant Physiology* **169**, 41–49.
- De Ingeniis J, Ratnikov B, Richardson AD, et al.** 2012. Functional specialization in proline biosynthesis of melanoma. *PLoS ONE* **7**, e45190.

- Delauney AJ, Hu CA, Kishor PB, Verma DP.** 1993. Cloning of ornithine δ -aminotransferase cDNA from *Vigna aconitifolia* by *trans*-complementation in *Escherichia coli* and regulation of proline biosynthesis. *The Journal of Biological Chemistry* **268**, 18673–18678.
- Dell'Aglio E, Giustini C, Kraut A, et al.** 2019. Identification of the *Arabidopsis* calmodulin-dependent NAD⁺ kinase that sustains the elicitor-induced oxidative burst. *Plant Physiology* **181**, 1449–1458.
- Dellero Y, Clouet V, Marnet N, Pellizzaro A, Dechaumet S, Niogret MF, Bouchereau A.** 2020. Leaf status and environmental signals jointly regulate proline metabolism in winter oilseed rape. *Journal of Experimental Botany* **71**, 2098–2111.
- de Souza Chaves I, Feitosa-Araújo E, Florian A, et al.** 2019. The mitochondrial NAD⁺ transporter (NDT1) plays important roles in cellular NAD⁺ homeostasis in *Arabidopsis thaliana*. *The Plant Journal* **100**, 487–504.
- Deuschle K, Funck D, Forlani G, Stransky H, Biehl A, Leister D, van der Graaff E, Kunze R, Frommer WB.** 2004. The role of Δ^1 -pyrroline-5-carboxylate dehydrogenase in proline degradation. *The Plant Cell* **16**, 3413–3425.
- Deuschle K, Funck D, Hellmann H, Daschner K, Binder S, Frommer WB.** 2001. A nuclear gene encoding mitochondrial Δ^1 -pyrroline-5-carboxylate dehydrogenase and its potential role in protection from proline toxicity. *The Plant Journal* **27**, 345–356.
- Di Martino C, Pizzuto R, Pallotta ML, De Santis A, Passarella S.** 2006. Mitochondrial transport in proline catabolism in plants: the existence of two separate translocators in mitochondria isolated from durum wheat seedlings. *Planta* **223**, 1123–1133.
- Dubois M, Claeys H, Van den Broeck L, Inzé D.** 2017. Time of day determines *Arabidopsis* transcriptome and growth dynamics under mild drought. *Plant, Cell & Environment* **40**, 180–189.
- Eithon TE, Stewart CR.** 1981. Submitochondrial location and electron transport characteristics of enzymes involved in proline oxidation. *Plant Physiology* **67**, 780–784.
- Forlani G, Bertazzini M, Zarattini M, Funck D.** 2015. Functional characterization and expression analysis of rice δ^1 -pyrroline-5-carboxylate dehydrogenase provide new insight into the regulation of proline and arginine catabolism. *Frontiers in Plant Science* **6**, 591.
- Forlani G, Trovato M, Funck D, Signorelli S.** 2019. Regulation of proline accumulation and its molecular and physiological functions in stress defence. In: Hossain MA, Kumar V, Burritt DJ, Fujita M, Mäkelä PSA, eds. *Osmoprotectant-mediated abiotic stress tolerance in plants: recent advances and future perspectives*. Cham: Springer International Publishing, 73–97.
- Foyer CH, Noctor G.** 2020. Redox homeostasis and signaling in a higher-CO₂ world. *Annual Review of Plant Biology* **71**, 157–182.
- Funck D, Baumgarten L, Stiff M, von Wirén N, Schönemann L.** 2020. Differential contribution of P5CS isoforms to stress tolerance in *Arabidopsis*. *Frontiers in Plant Science* **11**, 565134.
- Funck D, Eckard S, Müller G.** 2010. Non-redundant functions of two proline dehydrogenase isoforms in *Arabidopsis*. *BMC Plant Biology* **10**, 70.
- Funck D, Stadelhofer B, Koch W.** 2008. Ornithine- δ -aminotransferase is essential for arginine catabolism but not for proline biosynthesis. *BMC Plant Biology* **8**, 40.
- Funck D, Winter G, Baumgarten L, Forlani G.** 2012. Requirement of proline synthesis during *Arabidopsis* reproductive development. *BMC Plant Biology* **12**, 191.
- Gakière B, Hao J, de Bont L, Pétriacoq P, Nunes-Nesi A, Fernie AR.** 2018. NAD⁺ biosynthesis and signaling in plants. *Critical Reviews in Plant Sciences* **37**, 259–307.
- Geigenberger P, Thormählen I, Daloso DM, Fernie AR.** 2017. The unprecedented versatility of the plant- thioredoxin system. *Trends in Plant Science* **22**, 249–262.
- Giberti S, Funck D, Forlani G.** 2014. Δ^1 -Pyrroline-5-carboxylate reductase from *Arabidopsis thaliana*: stimulation or inhibition by chloride ions and feedback regulation by proline depend on whether NADPH or NADH acts as co-substrate. *New Phytologist* **202**, 911–919.
- Ginguy A, Cynober L, Curis E, Nicolis I.** 2017. Ornithine aminotransferase, an important glutamate-metabolizing enzyme at the crossroads of multiple metabolic pathways. *Biology* **6**, 18.
- Girousse C, Bournoville R, Bonnemain JL.** 1996. Water deficit-induced changes in concentrations in proline and some other amino acids in the phloem sap of alfalfa. *Plant Physiology* **111**, 109–113.
- Goncalves RL, Rothschild DE, Quinlan CL, Scott GK, Benz CC, Brand MD.** 2014. Sources of superoxide/H₂O₂ during mitochondrial proline oxidation. *Redox Biology* **2**, 901–909.
- Hagedorn CH, Phang JM.** 1986. Catalytic transfer of hydride ions from NADPH to oxygen by the interconversions of proline and Δ^1 -pyrroline-5-carboxylate. *Archives of Biochemistry and Biophysics* **248**, 166–174.
- Han HL, Liu J, Feng XJ, Zhang M, Lin QF, Wang T, Qi SL, Xu T, Hua XJ.** 2021. *SSR1* is involved in maintaining the function of mitochondria electron transport chain and iron homeostasis upon proline treatment in *Arabidopsis*. *Journal of Plant Physiology* **256**, 153325.
- Hancock CN, Liu W, Alvord WG, Phang JM.** 2016. Co-regulation of mitochondrial respiration by proline dehydrogenase/oxidase and succinate. *Amino Acids* **48**, 859–872.
- Hanson AD, Tully RE.** 1979. Light stimulation of proline synthesis in water-stressed barley leaves. *Planta* **145**, 45–51.
- Hayashi F, Ichino T, Osanai M, Wada K.** 2000. Oscillation and regulation of proline content by P5CS and ProDH gene expressions in the light/dark cycles in *Arabidopsis thaliana* L. *Plant & Cell Physiology* **41**, 1096–1101.
- Hirner A, Ladwig F, Stransky H, Okumoto S, Keinath M, Harms A, Frommer WB, Koch W.** 2006. *Arabidopsis* LHT1 is a high-affinity transporter for cellular amino acid uptake in both root epidermis and leaf mesophyll. *The Plant Cell* **18**, 1931–1946.
- Huang S, Taylor NL, Ströher E, Fenske R, Millar AH.** 2013. Succinate dehydrogenase assembly factor 2 is needed for assembly and activity of mitochondrial complex II and for normal root elongation in *Arabidopsis*. *The Plant Journal* **73**, 429–441.
- Kavi Kishor PB, Sreenivasulu N.** 2014. Is proline accumulation *per se* correlated with stress tolerance or is proline homeostasis a more critical issue? *Plant, Cell & Environment* **37**, 300–311.
- Krishnan N, Dickman MB, Becker DF.** 2008. Proline modulates the intracellular redox environment and protects mammalian cells against oxidative stress. *Free Radical Biology & Medicine* **44**, 671–681.
- LaNoue KF, Bryla J, Bassett DJ.** 1974a. Energy-driven aspartate efflux from heart and liver mitochondria. *The Journal of Biological Chemistry* **249**, 7514–7521.
- LaNoue KF, Meijer AJ, Brouwer A.** 1974b. Evidence for electrogenic aspartate transport in rat liver mitochondria. *Archives of Biochemistry and Biophysics* **161**, 544–550.
- Launay A, Cabassa-Hourton C, Eubel H, et al.** 2019. Proline oxidation fuels mitochondrial respiration during dark-induced leaf senescence in *Arabidopsis thaliana*. *Journal of Experimental Botany* **70**, 6203–6214.
- Lebreton S, Cabassa-Hourton C, Savouré A, Funck D, Forlani G.** 2020. Appropriate activity assays are crucial for the specific determination of proline dehydrogenase and pyrroline-5-carboxylate reductase activities. *Frontiers in Plant Science* **11**, 602939.
- Lehmann S, Gumy C, Blatter E, Boeffel S, Fricke W, Rentsch D.** 2011. *In planta* function of compatible solute transporters of the AtProT family. *Journal of Experimental Botany* **62**, 787–796.
- Leprince AS, Magalhaes N, De Vos D, Bordenave M, Crlat E, Clément G, Meyer C, Munnik T, Savouré A.** 2015. Involvement of phosphatidylinositol 3-kinase in the regulation of proline catabolism in *Arabidopsis thaliana*. *Frontiers in Plant Science* **5**, 772.
- Liang X, Zhang L, Natarajan SK, Becker DF.** 2013. Proline mechanisms of stress survival. *Antioxidants & Redox Signaling* **19**, 998–1011.
- Liu W, Phang JM.** 2012. Proline dehydrogenase (oxidase), a mitochondrial tumor suppressor, and autophagy under the hypoxia microenvironment. *Autophagy* **8**, 1407–1409.
- Lovell JT, Mullen JL, Lowry DB, Awole K, Richards JH, Sen S, Verslues PE, Juenger TE, McKay JK.** 2015. Exploiting differential

- gene expression and epistasis to discover candidate genes for drought-associated QTLs in *Arabidopsis thaliana*. *The Plant Cell* **27**, 969–983.
- Lunn JE. 2006. Compartmentation in plant metabolism. *Journal of Experimental Botany* **58**, 35–47.
- Lv WT, Lin B, Zhang M, Hua XJ. 2011. Proline accumulation is inhibitory to *Arabidopsis* seedlings during heat stress. *Plant Physiology* **156**, 1921–1933.
- Marchand CH, Vanacker H, Collin V, Issakidis-Bourguet E, Maréchal PL, Decottignies P. 2010. Thioredoxin targets in *Arabidopsis* roots. *Proteomics* **10**, 2418–2428.
- Marchese L, Olavarría K, Mantilla BS, Avila CC, Souza ROO, Damasceno FS, Elias MC, Silber AM. 2020. *Trypanosoma cruzi* synthesizes proline via a Δ^1 -pyrroline-5-carboxylate reductase whose activity is fine-tuned by NADPH cytosolic pools. *The Biochemical Journal* **477**, 1827–1845.
- Mattioli R, Biancucci M, El Shall A, Mosca L, Costantino P, Funck D, Trovato M. 2018. Proline synthesis in developing microspores is required for pollen development and fertility. *BMC Plant Biology* **18**, 356.
- McKenna MC, Waagepetersen HS, Schousboe A, Sonnewald U. 2006. Neuronal and astrocytic shuttle mechanisms for cytosolic-mitochondrial transfer of reducing equivalents: current evidence and pharmacological tools. *Biochemical Pharmacology* **71**, 399–407.
- Mettler IJ, Beevers H. 1980. Oxidation of NADH in glyoxysomes by a malate-aspartate shuttle. *Plant Physiology* **66**, 555–560.
- Miller G, Honig A, Stein H, Suzuki N, Mittler R, Zilberstein A. 2009. Unraveling Δ^1 -pyrroline-5-carboxylate-proline cycle in plants by uncoupled expression of proline oxidation enzymes. *The Journal of Biological Chemistry* **284**, 26482–26492.
- Monné M, Daddabbo L, Gagneul D, Obata T, Hielscher B, Palmieri L, Miniero DV, Fernie AR, Weber APM, Palmieri F. 2018. Uncoupling proteins 1 and 2 (UCP1 and UCP2) from *Arabidopsis thaliana* are mitochondrial transporters of aspartate, glutamate, and dicarboxylates. *The Journal of Biological Chemistry* **293**, 4213–4227.
- Monteoliva MI, Rizzi YS, Cecchini NM, Hajirezaei MR, Alvarez ME. 2014. Context of action of proline dehydrogenase (ProDH) in the hypersensitive response of *Arabidopsis*. *BMC Plant Biology* **14**, 21.
- Moxley MA, Tanner JJ, Becker DF. 2011. Steady-state kinetic mechanism of the proline:ubiquinone oxidoreductase activity of proline utilization A (PutA) from *Escherichia coli*. *Archives of Biochemistry and Biophysics* **516**, 113–120.
- Mráček T, Drahotová Z, Houštek J. 2013. The function and the role of the mitochondrial glycerol-3-phosphate dehydrogenase in mammalian tissues. *Biochimica et Biophysica Acta. Bioenergetics* **1827**, 401–410.
- Nomura M, Takagi H. 2004. Role of the yeast acetyltransferase Mpr1 in oxidative stress: regulation of oxygen reactive species caused by a toxic proline catabolism intermediate. *Proceedings of the National Academy of Sciences, USA* **101**, 12616–21.
- Ohashi K, Kawai S, Murata K. 2012. Identification and characterization of a human mitochondrial NAD kinase. *Nature Communications* **3**, 1248.
- Outten CE, Culotta VC. 2003. A novel NADH kinase is the mitochondrial source of NADPH in *Saccharomyces cerevisiae*. *The EMBO Journal* **22**, 2015–2024.
- Palmieri F, Rieder B, Ventrella A, *et al.* 2009. Molecular identification and functional characterization of *Arabidopsis thaliana* mitochondrial and chloroplastic NAD⁺ carrier proteins. *The Journal of Biological Chemistry* **284**, 31249–31259.
- Pandhare J, Donald SP, Cooper SK, Phang JM. 2009. Regulation and function of proline oxidase under nutrient stress. *Journal of Cellular Biochemistry* **107**, 759–768.
- Parre E, Ghars MA, Leprince AS, Thierry L, Lefebvre D, Bordenave M, Richard L, Mazars C, Abdelly C, Savouré A. 2007. Calcium signaling via phospholipase C is essential for proline accumulation upon ionic but not nonionic hyperosmotic stresses in *Arabidopsis*. *Plant Physiology* **144**, 503–512.
- Peng Z, Lu Q, Verma DP. 1996. Reciprocal regulation of Δ^1 -pyrroline-5-carboxylate synthetase and proline dehydrogenase genes controls proline levels during and after osmotic stress in plants. *Molecular and General Genetics* **253**, 334–41.
- Phang JM. 2019. Proline metabolism in cell regulation and cancer biology: Recent advances and hypotheses. *Antioxidants & Redox Signaling* **30**, 635–649.
- Porcelli V, Vozza A, Calcagnile V, Gorgoglione R, Arrigoni R, Fontanesi F, Marobbio CMT, Castegna A, Palmieri F, Palmieri L. 2018. Molecular identification and functional characterization of a novel glutamate transporter in yeast and plant mitochondria. *Biochimica et Biophysica Acta. Bioenergetics* **1859**, 1249–1258.
- Quettier AL, Shaw E, Eastmond PJ. 2008. *SUGAR-DEPENDENT6* encodes a mitochondrial flavin adenine dinucleotide-dependent glycerol-3-P dehydrogenase, which is required for glycerol catabolism and post germinative seedling growth in *Arabidopsis*. *Plant Physiology* **148**, 519–528.
- Ren Y, Miao M, Meng Y, Cao J, Fan T, Yue J, Xiao F, Liu Y, Cao S. 2018. DFR1-mediated inhibition of proline degradation pathway regulates drought and freezing tolerance in *Arabidopsis*. *Cell Reports* **23**, 3960–3974.
- Rizzi YS, Cecchini NM, Fabro G, Alvarez ME. 2016. Differential control and function of *Arabidopsis ProDH1* and *ProDH2* genes on infection with biotrophic and necrotrophic pathogens. *Molecular Plant Pathology* **18**, 1164–1174.
- Roosens NH, Thu TT, Iskandar HM, Jacobs M. 1998. Isolation of the ornithine- δ -aminotransferase cDNA and effect of salt stress on its expression in *Arabidopsis thaliana*. *Plant Physiology* **117**, 263–271.
- Ruszkowski M, Nocek B, Forlani G, Dauter Z. 2015. The structure of *Medicago truncatula* δ^1 -pyrroline-5-carboxylate reductase provides new insights into regulation of proline biosynthesis in plants. *Frontiers in Plant Science* **6**, 869.
- Sanada Y, Ueda H, Kuribayashi K, Andoh T, Hayashi F, Tamai N, Wada K. 1995. Novel light-dark change of proline levels in halophyte (*Mesembryanthemum crystallinum* L.) and glycophytes (*Hordeum vulgare* L. and *Triticum aestivum* L.) leaves and roots under salt stress. *Plant Cell Physiology* **36**, 965–970.
- Satrústegui J, Bak LK. 2015. Fluctuations in cytosolic calcium regulate the neuronal malate-aspartate NADH shuttle: implications for neuronal energy metabolism. *Neurochemical Research* **40**, 2425–2430.
- Scheibe R, Backhausen JE, Emmerich V, Holtgreve S. 2005. Strategies to maintain redox homeostasis during photosynthesis under changing conditions. *Journal of Experimental Botany* **56**, 1481–1489.
- Schwacke R, Grallath S, Breikreuz KE, Stransky E, Stransky H, Frommer WB, Rentsch D. 1999. LeProT1, a transporter for proline, glycine betaine, and γ -amino butyric acid in tomato pollen. *The Plant Cell* **11**, 377–392.
- Schwörer S, Berisa M, Violante S, Qin W, Zhu J, Hendrickson RC, Cross JR, Thompson CB. 2020. Proline biosynthesis is a vent for TGF β -induced mitochondrial redox stress. *The EMBO Journal* **39**, e103334.
- Selinski J, Scheibe R. 2019. Malate valves: old shuttles with new perspectives. *Plant Biology* **21** Suppl 1, 21–30.
- Senthil-Kumar M, Mysore KS. 2012. Ornithine- δ -aminotransferase and proline dehydrogenase genes play a role in non-host disease resistance by regulating pyrroline-5-carboxylate metabolism-induced hypersensitive response. *Plant, Cell & Environment* **35**, 1329–1343.
- Servet C, Ghelis T, Richard L, Zilberstein A, Savouré A. 2012. Proline dehydrogenase: a key enzyme in controlling cellular homeostasis. *Frontiers in Bioscience* **17**, 607–620.
- Sharma S, Villamor JG, Verslues PE. 2011. Essential role of tissue-specific proline synthesis and catabolism in growth and redox balance at low water potential. *Plant Physiology* **157**, 292–304.
- Shen W, Wei Y, Dauk M, Tan Y, Taylor DC, Selvaraj G, Zou J. 2006. Involvement of a glycerol-3-phosphate dehydrogenase in modulating the NADH/NAD⁺ ratio provides evidence of a mitochondrial glycerol-3-phosphate shuttle in *Arabidopsis*. *The Plant Cell* **18**, 422–441.
- Shen W, Wei Y, Dauk M, Zheng Z, Zou J. 2003. Identification of a mitochondrial glycerol-3-phosphate dehydrogenase from *Arabidopsis thaliana*:

- evidence for a mitochondrial glycerol-3-phosphate shuttle in plants. *FEBS Letters* **536**, 92–96.
- Shinde S, Villamor JG, Lin W, Sharma S, Verslues PE.** 2016. Proline coordination with fatty acid synthesis and redox metabolism of chloroplast and mitochondria. *Plant Physiology* **172**, 1074–1088.
- Slama I, Abdelly C, Bouchereau A, Flowers T, Saviouré A.** 2015. Diversity, distribution and roles of osmoprotective compounds accumulated in halophytes under abiotic stress. *Annals of Botany* **115**, 433–447.
- Szabados L, Saviouré A.** 2010. Proline: a multifunctional amino acid. *Trends in Plant Science* **15**, 89–97.
- Székely G, Abraham E, Cseplo A, et al.** 2008. Duplicated *P5CS* genes of *Arabidopsis* play distinct roles in stress regulation and developmental control of proline biosynthesis. *The Plant Journal* **53**, 11–28.
- Trovato M, Forlani G, Signorelli S, Funck D.** 2019. Proline metabolism and its functions in development and stress tolerance. In: Hossain MA, Kumar V, Burritt DJ, Fujita M, Mäkelä PSA, eds. *Osmoprotectant-mediated abiotic stress tolerance in plants: recent advances and future perspectives*. Cham: Springer International Publishing; 41–72.
- Verslues PE, Lasky JR, Juenger TE, Liu TW, Kumar MN.** 2014. Genome-wide association mapping combined with reverse genetics identifies new effectors of low water potential-induced proline accumulation in *Arabidopsis*. *Plant Physiology* **164**, 144–159.
- White TA, Krishnan N, Becker DF, Tanner JJ.** 2007. Structure and kinetics of monofunctional proline dehydrogenase from *Thermus thermophilus*. *The Journal of Biological Chemistry* **282**, 14316–14327.
- You J, Hu H, Xiong L.** 2012. An ornithine δ -aminotransferase gene *OsOAT* confers drought and oxidative stress tolerance in rice. *Plant Science* **197**, 59–69.
- Zhang L, Becker DF.** 2015. Connecting proline metabolism and signaling pathways in plant senescence. *Frontiers in Plant Science* **6**, 552.
- Zhao Y, Yu H, Zhou JM, Smith SM, Li J.** 2020. Malate circulation: linking chloroplast metabolism to mitochondrial ROS. *Trends in Plant Science* **25**, 446–454.

CHAPTER III.

Different fate of mitochondrial enzymes
involved in pyrroline-5-carboxylate
metabolism during dark-induced leaf
senescence in *Arabidopsis thaliana*

Chapter 3. Different fate of mitochondrial enzymes involved in pyrroline-5-carboxylate metabolism during dark-induced leaf senescence in *Arabidopsis thaliana*

Leaf senescence is the final stage of leaf development during which the remobilization of nutrients occurs from leaves to sink organs (Lim et al., 2007; Woo et al., 2019). During leaf senescence, chloroplasts are progressively degraded while the integrity and energy status of mitochondria are maintained until the final stage of senescence (Keech *et al.*, 2007; Chrobok *et al.*, 2016).

Recently, the connection between proline catabolism and energy metabolism during leaf senescence has been increasingly strengthened (Chrobok *et al.*, 2016; Pedrotti *et al.*, 2018; Launay *et al.*, 2019). It has been reported that proline catabolism plays a crucial role in DIS through proline oxidation to fuel mitochondria, thus meets the energy demands of senescent cells (Launay *et al.*, 2019). It has been reported that transcripts of *ProDH* and *P5CDH* accumulated during DLS (Chrobok *et al.*, 2016). *ProDH* transcripts were induced during dark-induced energy starvation (Dietrich *et al.*, 2011; Pedrotti *et al.*, 2018). Moreover, recent study also showed transcriptional and translational induction of ProDH and P5CDH during DIS in *Arabidopsis* (Launay *et al.*, 2019). However, the role of ProDH and P5CDH in DIS is still not fully characterized yet.

In addition, OAT has a close relationship with proline catabolism by participating in P5C/GSA production. Indeed, OAT converts ornithine which originates from arginine to P5C that will be used by P5CDH. Then, P5C connects arginine and proline metabolisms. *OAT* has also been found to be induced at the mRNA level during senescence in *Arabidopsis* (Chrobok *et al.*, 2016). However, the role of OAT during senescence is still unknown.

Thus, in this study, we aim to investigate the role of ProDH, P5CDH, and OAT during DIS in *Arabidopsis* with transcriptional, biochemical, and metabolomic approaches. Kinetics of DIS in different genotypes were followed by different parameters in *prodh1prodh2*, *oat*, *p5cdh* mutants, and Col-0.

Article

Different fate of mitochondrial enzymes involved in pyrroline-5-carboxylate metabolism during dark-induced leaf senescence in *Arabidopsis thaliana*

Yao Zheng¹, Cécile Cabassa-Hourton¹, Séverine Planchais¹, Emilie Crilat¹, Gilles Clément², Matthieu Dacher¹, Marianne Bordenvae-Jacquemin¹, Anne Guivarc'h¹, Corentin Dourmap¹, Pierre Carol¹, Sandrine Lebreton^{1,*}, Arnould Savouré^{1,*}

¹Sorbonne Université, UPEC, CNRS, IRD, INRAE, Institute of Ecology and Environmental Sciences of Paris (iEES), Paris, France

²Institut Jean-Pierre Bourgin, UMR 1318, INRAE-AgroParisTech, Centre INRAE, Versailles, 78026 Versailles Cedex, France

* Corresponding authors

sandrine.lanfranchi@sorbonne-universite.fr

arnould.savoure@sorbonne-universite.fr

Running title

Pyrroline-5-carboxylate metabolism and leaf senescence

Keywords:

Arabidopsis thaliana; Mitochondria; Metabolism; Proline; Pyrroline-5-carboxylate metabolism; Pyrroline-5-carboxylate metabolism

Abstract

During leaf senescence, mitochondria play a key role in the regulation of amino acid catabolism to replenish carbon backbones for nitrogen remobilization from senescing leaves to sink tissues. Pyrroline-5-carboxylate (P5C) connects proline and arginine catabolism in the mitochondria. Proline catabolism involves the sequential action of proline dehydrogenase (ProDH) and Δ^1 -pyrroline-5-carboxylate (P5C) dehydrogenase (P5CDH) into glutamate using P5C as an intermediate. Arginine catabolism, through arginase, forms urea and ornithine, the latter in presence of α -ketoglutarate being converted by ornithine δ -aminotransferase (OAT) into P5C and glutamate. While ProDH was recently described to be involved during senescence in fuelling mitochondrial respiration, only scarce information suggests a putative role of P5CDH and OAT in dark-induced senescence (DIS). In this study, metabolic reprogramming during DIS was studied in *Arabidopsis thaliana* leaves of Col-0 (WT) as well as in *prodh1prodh2*, *p5cdh*, and *oat* mutants. Progression of DIS was followed by measuring chlorophyll and proline contents for 5 days. Induction of ProDH, P5CDH, and OAT during DIS was observed by droplet digital PCR and western-blot. Metabolomic profiling revealed a similar behaviour of WT and *oat* mutant but distinct from *prodh1prodh2* and *p5cdh* mutants. P5C accumulates more in *p5cdh* than *prodh1prodh2* mutant, indicating a putative involvement of proline/P5C cycle during DIS, which may function as a P5C detoxification pathway. Both enzymatic activity and protein amount of ProDH1 and OAT were significantly down-regulated in *p5cdh* at day 4 of DIS, indicating mitochondrial P5C level must be tightly regulated during senescence.

Introduction

Leaf senescence is the final stage of leaf development and vital for the remobilization of valuable nutrients to other sink organs (Lim et al., 2007; Woo et al., 2019). As a highly organized and active physiological process, leaf senescence is essential to optimize nutrient reallocation for plant reproductive growth and for supporting plant adaptation under adverse environmental conditions (Noodén and Penney, 2001; Avila-Ospina *et al.*, 2014; Liebsch and Keech, 2016). It is controlled by the integration of various internal and external signals including developmental age, nutrition status, hormone signal, water status, light, hypoxia or temperature change (Woo *et al.*, 2019; Izumi and Ishida, 2019).

During senescence, leaf cells are subject to dramatic structural and metabolic changes. The breakdown of the chloroplast is the earliest and the most significant cellular structural alteration during senescence. In contrast, the mitochondrial integrity and energy status are maintained until the final stage of senescence, even if the number of mitochondria decreased by 30% (Keech *et al.*, 2007; Chrobok *et al.*, 2016). Alongside with the structural alteration, metabolic reprogramming from anabolism to catabolism is taking place in senescing leaf cells (Chrobok *et al.*, 2016). As the degradation of chloroplast occurs, senescing leaf cells are changing from photo-autotrophy to heterotrophy. When senescence is triggered, chloroplast degradation through autophagy allows the production of free amino acids as an alternative energy source in the mitochondria instead of amino acid biosynthesis (Chen *et al.*, 2017; Izumi and Ishida, 2019). Recently the major cysteine protease SAG12 was shown to participate in nitrogen remobilization that sustains grain production under nitrogen limiting conditions (James *et al.*, 2018). Indeed, most of nitrogen in leaves reside in chloroplasts (Makino and Osmond, 1991) and in C₃ plants, chloroplast proteins account for ~75% to 80% of the total leaf nitrogen (Makino and Osmond, 1991).

During developmental leaf senescence (DLS), mitochondria orchestrate catabolic processes of both amino acids and fatty acids and become energy-producing and metabolic hubs, facilitating the retrieval of nutrients from the senescing organ to the rest of the plant (Chrobok *et al.*, 2016). Many amino acid catabolic processes are up-regulated during DLS to produce glutamate, which has been proposed to play a central role in nitrogen remobilization during DLS. These processes include catabolism of lysine with lysine-ketoglutarate reductase/saccharopine dehydrogenase (LKR/SDH), branched-chain amino acids (BCAA) with branched-chain amino acid transaminase, arginine with ornithine δ -aminotransferase (OAT) and proline catabolism with proline dehydrogenase (ProDH) and Δ^1 -pyrroline-5-carboxylate dehydrogenase (P5CDH) (Chrobok *et al.*, 2016). Involvement of amino acid catabolism has also been described for senescence induced by light deprivation such as severe shading (SIS) or darkening of whole plants or leaves (DIS) (Liebsch and Keech, 2016). DIS of detached leaves has been shown to be highly effective in inducing senescence-associated genes (SAGs) and chlorophyll loss (Weaver and Amasino, 2001). DIS shares many features with DLS such as a differential regulation of common genes, but present also some important differences as well (Buchanan-Wollaston *et al.*, 2005; Graaff *et al.*, 2006).

Among amino acids whose oxidation is induced during senescence, proline is particularly interesting since it also contributes to osmotic adjustment, protein chaperoning, ROS signaling, redox homeostasis and energy production (Szabados and Saviouré, 2010; Liu and Phang,

2012; Silao *et al.*, 2019; Zheng *et al.*, 2021; Alvarez *et al.*, 2021). In higher plants, proline metabolism participates not only in plant adaptation in response to abiotic and biotic stresses but is also important for various developmental stages such as the formation of reproductive organs or flower petal senescence (Szabados and Saviouré, 2010; Cecchini *et al.*, 2011; Zhang and Becker, 2015; Mattioli *et al.*, 2018). Recent studies have shown that proline catabolism is induced not only during DLS (Chrobok *et al.*, 2016; Dellerio *et al.*, 2020) but also during DIS (Launay *et al.*, 2019) and during dark-induced energy deprivation (Dietrich *et al.*, 2011; Pedrotti *et al.*, 2018). Recently, proline has been described to be an alternative respiratory substrate to fuel mitochondrial respiration during senescence (Launay *et al.*, 2019).

In plants, proline is synthesized from glutamate in the cytosol via the sequential activities of Δ^1 -pyrroline-5-carboxylate (P5C) synthetase (P5CS) and P5C reductase (P5CR) (Funck *et al.*, 2020). Proline is oxidized in mitochondria by the sequential action of ProDH and P5CDH to release glutamate (Szabados and Saviouré, 2010). ProDH is a FAD-dependent enzyme, which catalyzes the first and rate-limiting step of proline oxidation to form P5C (Servet *et al.*, 2012), while P5CDH is a NAD-dependent enzyme which converts P5C to glutamate. Hence, by producing FADH₂ and NADH, proline catabolism is not only able to produce reducing power in the form of FADH₂ and NADH but is also capable of fuelling mitochondrial respiration (Launay *et al.*, 2019). P5C, the product of ProDH and the substrate of P5CDH, can also be generated by OAT, a pyridoxal-5'-phosphate dependent enzyme, which converts ornithine and α -ketoglutarate into P5C and glutamate in mitochondria (Winter *et al.*, 2015). Thus, P5CDH also participates in ornithine catabolism through the utilization of P5C produced by OAT. Ornithine is produced by arginase through the degradation of arginine in mitochondria. Arginine, which is synthesized from ornithine in chloroplasts, has been recognized as a storage form of organic nitrogen and plays a key role in nitrogen distribution and remobilization in plants. Additionally, aspartate and glutamine may also be essential precursors for arginine synthesis in chloroplasts (Winter *et al.*, 2015). Recently, it has been reported that OAT is crucial for nitrogen reutilization and plays a critical role in floret development and seed setting in *Oryza sativa* (Liu *et al.*, 2018). Transcripts of *OAT* have been reported to be induced during DLS in *Arabidopsis thaliana* (*Arabidopsis*) (Chrobok *et al.*, 2016). However, its role in senescence still remains elusive.

In *Arabidopsis*, two non-redundant ProDH isoforms are present but only one P5CDH and one OAT enzymes have been identified in *Arabidopsis* (Deuschle *et al.*, 2001, Funck *et al.*, 2008). Both *AtProDH1* and *AtProDH2* have been reported to be regulated by the heterodimer network of group C/S₁ bZIPs transcription factors (Weltmeier *et al.*, 2006) that have been described as central regulators of plant low-energy response under extended darkness, working

downstream of Snf1-Related Protein Kinase 1 (SnRK1) (Mair *et al.*, 2015; Pedrotti *et al.*, 2018). Furthermore, both SnRK1-signalling and group C/S₁ bZIPs are responsible for the metabolic reprogramming during DIS (Liebsch and Keech, 2016). This is consistent with the involvement of ProDH during DIS (Launay *et al.*, 2019).

Furthermore, light has been found to affect both proline biosynthesis and degradation in plants (Hanson and Tully, 1979; Sanada *et al.*, 1995; Hayashi *et al.*, 2000; Dubois *et al.*, 2017). Recently, it has been reported that Elongated Hypocotyl 5 (HY5), a bZIP-type transcription factor and a high hierarchical regulator of the photomorphogenesis (Lee *et al.*, 2007), directly binds the promoter of *ProDH1* and thus down-regulates the expression of *ProDH1* in response to light signal (Kovács *et al.*, 2019). Interestingly, *AtP5CDH* has also been shown to be negatively regulated by HY5 (Borsani *et al.*, 2005; Lee *et al.*, 2007). In addition, a large number of senescence-related genes have been reported to be under the control of HY5. However, its role in leaf senescence is not fully understood so far (Ay *et al.*, 2014).

Taken together, these findings build a strong metabolic connection between senescence and these three enzymes, ProDH, P5CDH, and OAT. This study aims to investigate the involvement and role of ProDH, P5CDH, and OAT during DIS in *Arabidopsis*. Analyses of transcripts, proteins and activities in wild-type plants (Col-0) as well in *prodh1prodh2*, *oat* and *p5cdh* mutants were carried out to assess their involvement during DIS. In addition, metabolic profile of these different genotypes was established in order to unravel their roles in proline oxidation.

Methods and Materials

Plant growth and dark-induced senescence treatment

The different *Arabidopsis thaliana* (*Arabidopsis*) mutant lines used in this study were in Columbia-0 (Col-0) genetic background. The *prodh1prodh2* double mutant was obtained by crossing the respective homozygous single knockout mutants *prodh1-4* (SALK_119334) and *prodh2-2* (GABI_328G05) as previously described by (Cabassa-Hourton *et al.*, 2016). The *oat-1* (SALK_033541) and *p5cdh-2* (SALK_018453) single knockout T-DNA insertion mutants have been described by Funck *et al.*, (2008) and Deuschle *et al.*, (2004) respectively. Seedlings were sown on soil and grown in growth chambers under 16 h light/8 h dark cycle with 80~100 $\mu\text{mol m}^{-2} \text{s}^{-1}$ light at 22°C for four weeks.

Dark-induced senescence (DIS) treatments were performed on excised 7th to 9th rosette leaves of 4-week-old *Arabidopsis* as described by Launay *et al.* (2019). Leaves of 4 plants per

each genotype were harvested from 4-week-old *Arabidopsis* and placed on wet Whatman® paper in Petri dishes. Plates were then placed in an opaque box and kept in the growth chamber for 24 h (D1), 48 h (D2), 72 h (D3), 96 h (D4) or 120 h (D5). Photographs of the excised leaves were taken at D0 and at each period of dark treatment. Thereafter, leaves were harvested, frozen and stored in liquid nitrogen until used.

Measurement of proline and chlorophyll contents

Measurements of the free proline and chlorophyll contents were carried out using 50-70 mg samples and 100 mg of fresh rosette leaf tissues, respectively as described in Launay *et al.* (2019). Measurement of proline contents was assessed using an acid-ninhydrin based method (Bates *et al.*, 1973). The absorbance of the proline–ninhydrin complex in toluene was measured at 520 nm using a NP80 Nanophotometer® (Implen). For measurement of chlorophyll contents, 100 mg of frozen leaves were ground to powder in liquid nitrogen and resuspended in 1 ml of 92% acetone. Samples were centrifuged for 10 min at 10000 $\times g$. The supernatants were collected and the volume adjusted to 2 ml with 80% acetone. The absorbance was read at 663 nm and 645 nm to determine chlorophyll concentrations.

Protein and mitochondria extraction

Frozen powder (100~200 mg) was suspended with 2 volumes of extraction buffer (50 mM DTT, 8 M urea, 5% (w/v) SDS, 40 mM Tris-HCl pH 6.8, 0.1 mM EDTA, 0.4 mg/ml bromophenol blue) supplemented with 1x protease inhibitor cocktail (Merck). Samples were shaken three times for 5 min at room temperature, following 5 min intervals on ice. The samples were then centrifuged at 18000 $\times g$ for 10 min at 10°C. The supernatants were transferred into new tubes for further SDS-PAGE and western-blot assay.

Mitochondria were isolated at 4°C from 3 g of fresh leaves of 4-week-old *Arabidopsis Col-0* lines and *prodh1prodh2*, *p5cdh* and *oat* mutants after 4 days of DIS. The harvested leaves were ground in a cold mortar with 30 ml of grinding buffer, and crude mitochondria were obtained by filtration followed by several differential centrifugation steps as described by Cabassa-Hourton *et al.* (2016). The mitochondrial protein concentration was determined according to Lowry *et al.* (1951) using BSA as a standard.

Western-blot assays

Protein samples were separated by SDS-PAGE either using manually casted polyacrylamide (Acrylamide/Bis-acrylamide 29:1, 30% solution, Sigma-Aldrich; 8.75% separation gel, and 4% stacking gel) or using 7.5% TGX Stain-Free™ FastCast™ Acrylamide Kit (Bio-Rad) in room temperature under 100 V. Proteins in SDS-PAGE were transferred to nitrocellulose or PVDF-LF membranes (Bio-Rad) in a Trans-Blot Semi-Dry Electrophoretic Transfer Cell (Bio-Rad) for 1 h at 100 V using transfer buffer (25 mM Tris-HCl, 192 mM glycine and 20% (v/v) ethanol, pH 8.3).

Equal protein loading and integrity of protein samples were checked by Ponceau S staining or Stain-Free channel by ChemiDoc (Bio-Rad). Immunodetection was performed using purified antibodies directed against either ProDH1, P5CDH, OAT, or SAG12. Primary antibody binding was detected either using StarBright fluorescent secondary antibodies (1:2500 dilution) by the ChemiDoc system (Bio-Rad) or a secondary antibody conjugated with a horseradish peroxidase (1:8000 dilution, SIGMA) detected by the ECL prime system (GE Healthcare).

ProDH and OAT activities measurements

ProDH activity was measured using the 2,6-dichlorophenolindophenol (DCIP)-based assay as described by Lebreton *et al.*, (2020). OAT activity was measured on crude mitochondria extracts in the presence of 25 mM ornithine and 25 mM α -ketoglutarate. The P5C formed is then quantified using its specific reaction with ninhydrin under hot and acid conditions (Funck *et al.*, 2008).

RNA extraction and droplet digital PCR analysis

RNAs were extracted from three leaves at the same developmental stage (~100 mg of plant tissue) that were ground in liquid nitrogen using a mixer mill (MM301; Retsch, Haan, Germany) according to Ben Rejeb *et al.* (2015). RNA quality and concentration were determined using a NP80 Nanophotometer® (Implen). cDNAs corresponding was prepared for each time point and used for droplet digital PCR (ddPCR). ddPCR was conducted and data were analysed using a QX200 ddPCR system (Bio-Rad) according to the manufacturer's protocol as described in Launay *et al.* (2019). All the primers used for ddPCR are given in Supplementary Table S1, where APT1 and UCR1-2 were used as a control

Metabolomic profiling using GC-MS

For each leaf position and each time point, the 7th to 9th rosette leaves from at least four plants during 5-days of DIS were mixed and frozen under liquid nitrogen. Sample preparation and analysis as well as data processing were performed as previously described by Fiehn (2006) and Fiehn *et al.* (2008).

Frozen powder from ground leaves (59.36 +/- 8.50, n=24) was resuspended in 1 mL of frozen (-20°C) water:acetonitrile:isopropanol (2:3:3) containing ribitol at 4 µg mL⁻¹ and extracted for 10 min at 4°C with shaking. Extracts were then centrifuged to remove insoluble material. Three blank tubes underwent the same steps as the samples. A quality control was made by pooling an equal volume of each condition. Fifty microliters were collected from each tube and dried overnight at 35°C in a vacuum centrifuge.

Derivatization was done according to Clément *et al.* (2018). Samples were analysed by an Agilent 7890A gas chromatograph coupled to an Agilent 5977B mass spectrometer in splitless and split 30 modes to get a proper quantification of low and high abundance compounds. The column was a Rxi-5SilMS from Restek (30 m with 10 m integraguard column). The liner (Restek # 20994) was changed before analysis. Oven temperature ramp was 70°C for 7 min then 10°C min⁻¹ to 330°C for 5 min (run length 38 min). Helium constant flow was 0.7 mL min⁻¹. Temperatures were the following: injector: 250°C, transfer line: 290°C, source: 250°C and quadripole 150°C. Five scans per second were acquired spanning a 50–600 Da range. Instrument was tuned with PFTBA with the 69 m/z and 219 m/z of equal intensities. The split mode conditions were 70°C for 2 min then 30°C per min to 330°C for 5 min. Helium constant flow 1 mL min⁻¹.

Raw Agilent data files were converted in NetCDF format and analyzed with AMDIS (<http://chemdata.nist.gov/mass-spc/amdis/>). A home retention indices/mass spectra library built from the NIST, Golm (<http://gmd.mpimp-golm.mpg.de/>) and Fiehn databases and standard compounds was used for metabolite identification. Peak areas were also determined with the Targetlynx software (Waters) after conversion of the NetCDF file in masslynx format. AMDIS, Target Lynx in splitless and split 30 mode data were compiled in one single Excel file for comparison. After blank mean subtraction, peak areas were normalized to ribitol and fresh weight. Determination of arginine with its related substances such as ornithine and citrulline faces major analytical difficulties as they are very polar in nature and therefore not easily separated. In addition, most of arginine is converted into ornithine and citrulline as well as five other uncharacterized decomposition products and this degradation is matrix dependent during the GC-MS

analysis. Therefore, only the kinetic of accumulation of these arginine-related compounds during DIS were taken into account. 117 metabolites were selected because they showed repeatable and significant differences (based on a t-test). A complete list of all metabolites that were detected is shown in Supplementary Data.

Data analysis

Statistics were performed using R3.6. To assess the general dynamics among the 117 metabolites that were identified, we computed a principal component analysis (PCA) using the package *ade4* in R, so that we obtained principal components (PCs), i.e., a few summarizing variables. To interpret the PCs, we then computed Pearson's correlation coefficient *R* between each of them and the values of each metabolite. Often, a metabolite would be significantly correlated to only one of the PC, indicating it covaries with this PC (and the other associated metabolites), but not with the other.

We also performed a two-way ANOVA (using an α risk of 0.050) to compare the amount of P5C, glutamate and proline between the four mutants, taking Day as the other factor. Computations were made using Generalized Least Squares (with adjustment for group variances when needed, package *nlme* in R), followed by pairwise comparisons (Zuur *et al.*, 2009).

Results

Knockout *Arabidopsis prodh1prodh2* and *p5cdh* mutants accumulate proline during dark-induced senescence

Dark-induced leaf senescence (DIS) was triggered on 7th to 9th leaves of 4-week-old Col-0 (WT), *prodh1prodh2*, *oat*, and *p5cdh* mutants as previously described by Launay *et al.* (2019). No difference in leaf phenotypes could be observed between Col-0 and the three mutant genotypes during DIS (Supplemental Figure 1). Progression of the senescence was followed by measuring the chlorophyll degradation. Chlorophyll contents progressively decreased during DIS but no statistically significant differences were observed between different genotypes within each time point (Figure 1). We also measured proline content during senescence and found a global difference (Figure 2, $F_{3,48}=74.938$, $p<0.001$). Significant 15-fold increase in proline accumulation at D4 was detected in *p5cdh* mutant compared to Col-0 for the global test ($p<0.001$). Both *prodh1prodh2* ($p<0.001$) and *oat* ($p<0.007$) mutants accumulated more proline

than Col-0 but to a lesser extent with 5-fold and 3-fold increases measured, respectively. Surprisingly, *p5cdh* mutant accumulated more proline than *prodh1prodh2* mutant ($p < 0.001$). These data suggest that ProDH, P5CDH and, to a lesser extent, OAT are involved in the oxidation of proline during DIS.

Involvement of P5C metabolism enzymes during DIS

Leaves from 4-week-old *Arabidopsis* were collected during senescence and transcript analyses were performed using the highly sensitive droplet digital PCR (ddPCR) method (Figure 3). First, the expression pattern of the senescence marker *SAG12* was examined. No *SAG12* transcript was present at D0 while an accumulation of *SAG12* transcripts was observed at D3 of DIS for all genotypes. The level of transcript was the same in *prodh1prodh2*, *p5cdh*, and *oat* mutants, but slightly lower than in WT. Expression of P5C metabolism genes, e.g., *ProDH*, *P5CDH* and *OAT*, was then followed during DIS. In WT leaves, *ProDH1*, *P5CDH*, and *OAT* were up-regulated after 3 d of DIS. As expected, *ProDH1* transcripts were not detectable at D0 but was triggered at D3 of DIS. A 5-fold and 10-fold increase was observed for *P5CDH* and *OAT* compared with Col-0 at D3, respectively. In order to know whether these up-regulations were affected in the mutant genotypes, transcript analysis was performed in leaves of *prodh1prodh2*, *p5cdh* and *oat* plants (Figure 3). Up-regulation was still observed but some differences appeared. While *OAT* transcript levels were not affected in *prodh1prodh2* and *p5cdh* mutants, *P5CDH* expression slightly decreased in *oat* mutant and *ProDH1* expression strongly increased in *p5cdh* mutant. As an accumulation of proline was observed in *prodh1prodh2* and *p5cdh* mutants upon senescence (Figure 2), the expression of *P5CS1* was also measured at D0 and D3 of DIS (Figure 3). Whatever the genotypes, a decrease of *P5CS1* content was observed at D3 in comparison to D0, with a highest decrease was measured for *p5cdh* and *oat* mutants and to a lesser extent for WT.

Next, protein levels of ProDH1, P5CDH, and OAT were investigated during DIS (Figure 4). Only ProDH1 but not ProDH2 protein levels were investigated because it was previously demonstrated that it is the main isoform that accumulates during DIS (Launay et al., 2019). Using total protein extracts of Col-0, *p5cdh* and *oat* (supplemental Figure S2), no ProDH1 was detected at D0 as expected. A faint signal corresponding to ProDH1 appeared at D2, which increased progressively to reach a plateau at D4 and D5. No clear difference was observed for ProDH1 protein abundance between crude extracts of WT, *p5cdh* and *oat* mutants. In addition, no ProDH1 signal could be detected in *prodh1prodh2* double mutant. In contrast, P5CDH signal

was already detectable at D0 in Col-0, *prodh1prodh2* and *oat* genotypes, but not in *p5cdh* mutant. Interestingly, P5CDH signal gradually increased to D4 and D5. Similarly, OAT was also detectable at D0 and increased to D4 in Col-0, *prodh1prodh2*, and *p5cdh*. No OAT signal could be detected in *oat* mutant. The protein profile of the senescence marker SAG12 was also examined. Gradual induction of SAG12 protein was found to be similar in the four tested genotypes suggesting that SAG12 expression may not be regulated by proline metabolism pathway. Taken together, these results indicate that ProDH1, P5CDH, and OAT were gradually induced during DIS suggesting their involvement during senescence in *Arabidopsis*. Moreover at D4, P5CS1 protein level was low in Col-0 and even lower in mutants compared to Col-0. P5CR was not differentially accumulated in Col-0, *prodh1prodh2*, *p5cdh*, and *oat* mutant (supplemental Figure S3). These results indicate that proline catabolism rather than biosynthesis was specifically triggered during DIS.

As ProDH1 and OAT, key enzymes for mitochondrial P5C production, were induced during DIS, we investigated their activities using crude mitochondrial extracts (Figure 5). First, the amount of ProDH1 and OAT protein levels was checked using crude mitochondria from the four genotypes. Western blot analyses at D4 showed slightly different protein profiles compared with total protein extracts. Lower ProDH1 and OAT signals were detected in *p5cdh* mutant in comparison to WT mitochondrial extracts. Whatever the genotypes, P5CDH protein level was constant. Next, ProDH and OAT enzymatic activities were investigated in crude mitochondrial extracts at D4 of DIS. Interestingly, ProDH activity decreased by 2.5-fold in *p5cdh* mutant but was not affected in *oat* mutant. No significant ProDH activity could be measured in the *prodh1prodh2* double mutant as previously reported by Cabassa-Hourton *et al.*, (2016). Measurement of OAT activity at D4 showed a 70% increase of activity in the *prodh1prodh2* double mutant but a 65% decrease of the OAT activity in the *p5cdh* mutant. No OAT activity was detected in the *oat* mutant.

Significant metabolic reprogramming of *prodh1prodh2* and *p5cdh* mutants during DIS evidenced by metabolomic profiling analysis

To gain more insights into the respective role of ProDH, P5CDH, and OAT during senescence, a metabolomic profiling analysis was carried out in detached 7th, 8th, and 9th leaves of WT, *prodh1prodh2*, *p5cdh*, and *oat* mutants during 5 days of DIS. A GC-MS untargeted approach identified 117 metabolites, including amino acids, organic acids mainly related to the TCA cycle, sugars, and some secondary metabolites. All of these metabolites were subjected

to Principal Component Analysis (PCA) to visualize the general trend of metabolic changes in respect to the genotypes during DIS (Figure 6). Three PCs could explain 77.1% of the variance of the 117 metabolites (divided in 54.2%, 13.5% and 9.4% for PC1, PC2 and PC3). Inspection of the scree plot (data not shown) confirmed that the three PCs are a good compromise. Supplementary Table 2 reports the classification of the metabolites in the different PCs. 78 out of 117 Metabolites could be assigned to a single PC and only 4 could not be associated to any PC. Interestingly, proline was significantly correlated only to PC1 ($R = 0.587$, $p = 0.003$; for PC2 and PC3, $p \geq 0.167$) and glutamate only to PC2 ($R = -0.886$, $p < 0.0001$; for PC1 or PC3 $p \geq 0.357$). As only 9 out of 117 metabolites are correlated to neither PC1 nor PC2, these correlations indicate that together these two specific metabolites are representative for most of the other, confirming their general interest in this study. Interestingly, P5C was not significantly correlated to any PC, although it barely missed significance for PC2 and PC3 (for PC1, $p = 0.301$; for PC2 $p = 0.075$; for PC3 $p = 0.053$). At D0, all the genotypes start at the same point although divergences appeared during the time course of senescence (Figure 6). When considering PC1 and PC2, *oat* mutant behaved as WT and different from *p5cdh* and *prodh1prodh2* mutants. In PC3, *oat* mutant appears to behave differently compared to Col-0, *prodh1prodh2* and *p5cdh* mutants, indicating a different involvement of OAT during senescence.

Furthermore, changes in different metabolites were studied in detail. In general, total amount of amino acids increased during DIS in all the genotypes (Figure 7A). A higher amino acid accumulation was detected in both *prodh1prodh2* and *p5cdh* mutants compared to WT at D4 and D5. In contrast, the accumulation pattern of global amino acids in *oat* mutant was similar to WT but started to be lower than WT from D3. Aromatic amino acids such as tryptophan (Trp), phenylalanine (Phe), and to a lesser extent tyrosine (Tyr) were observed to have significant increases. A similar pattern was observed with branched-chain amino acids (BCAAs) such as valine (Val), isoleucine (Ile), and leucine (Leu) (Figure 7B-C). No difference was observed for these amino acids between the four genotypes except a lower amount of both aromatic amino acids and BCAAs detected in *oat* mutant and higher amount for Tyr in *p5cdh* mutant.

Amount of Pro, Glu, Arg, Orn, which are directly linked to ProDH, P5CDH, and OAT were more affected in the tested mutants. Arg and Orn amounts increased significantly at D5 in *oat* mutant slightly in *p5cdh* mutant, while stayed constant in *prodh1prodh2* mutant and WT (Figure 7D). While Col-0 leaves did not accumulate proline during DIS, proline slightly increased in *oat* mutant and even more in *prodh1prodh2* double mutant as expected due to the lack of ProDH (Figure 8, $F_{3,15}=6.000$, $p=0.008$). Surprisingly, proline accumulation was much higher in *p5cdh* mutant during DIS compared to other groups ($p \leq 0.034$), including

prodh1prodh2 mutant (Figure 7D). Indeed, proline levels were 25- and 5- fold higher in *p5cdh* and *prodh1prodh2* mutants, respectively when compared to Col-0 at either D4 or D5 of DIS.

The amount of P5C, the product of ProDH or OAT and the substrate of P5CDH, was also altered differently in the different genotypes ($F_{3,15}=8.000$, $p=0.003$). No accumulation of P5C was observed in WT and *oat* mutant, while an increase until D3 then a decrease of P5C was observed in *prodh1prodh2* and *p5cdh* mutants; however, only *p5cdh* mutant reached significance in pairwise comparisons ($p\leq 0.010$ for *p5cdh*, and $p\geq 0.111$ in other comparisons). It is noteworthy that accumulation of P5C preceded the accumulation of Pro, which continues to accumulate when P5C started to decrease (Figure 7D).

Surprisingly, the amount of γ -aminobutyric acid (GABA) increased in the same way for all genotypes except for *oat* mutant. In this latter mutant, a slower and lower increase was observed for GABA compared to the others (Figure 7D); the overall difference is not significant ($F_{3,15}=2.000$, $p=0.150$). Hydroxy-proline accumulated in *prodh1prodh2* and *p5cdh* mutants in contrary to Col-0 and *oat* mutants ($F_{3,15}=15974799$, $p<0.001$); however, the difference was significant only for *p5cdh* ($p\leq 0.043$ versus Col-0 and *oat*, other comparisons ≥ 0.118). Glutamate level showed a two-step pattern of change, increased at the beginning of senescence, then decreasing in all genotypes. The maximum level of glutamate reached by *p5cdh* mutant is lower. By contrast, the accumulation of glutamate in *prodh1prodh2* mutant was prolonged to D4 and reached a higher level compared to the other genotypes. However, the differences were not statistically significant in pairwise comparisons ($F_{3,15}=5.586$, $p=0.009$ but $p\geq 0.081$ in global comparisons). The same pattern was observed for glutamine amount in *prodh1prodh2* and *p5cdh* mutants. A high accumulation of Glu, Gln, Asp, Asn, and Ser amino acids was also detected in *prodh1prodh2* mutant. In contrast, only high accumulation of Ser was detected in *p5cdh* mutant.

Besides amino acids, metabolomic data indicated increases in TCA intermediates, including citrate, malate, fumarate, succinate, and 2-oxoglutarate, during senescence for all genotypes (Figure 7E). The main difference was detected in *p5cdh* mutant, in which the amount of TCA intermediates decreased from D4 to D5. Moreover, all the TCA metabolites reached a lower level at D4 in *oat* mutant compared to the others. The more striking differences were observed at D4.

Other metabolites were differently affected between all the genotypes. In particular, pantothenate and β -alanine, precursors of Coenzyme-A, were accumulated only in *prodh1prodh2* and *p5cdh* mutants (Figure 7E). Nucleobases, adenine and uracil (Figure 7F) were also accumulated but to a lesser extent in *oat* mutant at D5. Some sugars like ribose and

xylulose were also more accumulated in *p5cdh* mutant compared to the others. Trehalose was more accumulated in both *prodh1prodh2* and *p5cdh* mutants. When glutamate is analysed in comparison to proline, Col-0 and oat mutant followed the same trend with a consumption of glutamate during DIS with no proline accumulation (Figure 8A). Interestingly a similar pattern is observed when P5C is compared to proline (Figure 8B).

Discussion

During senescence, nutrients such as nitrogen, carbon, phosphorus are remobilized from leaves to sink tissues and organs. Recently, proline catabolism has been shown to participate in plant senescence (Chrobok *et al.*, 2016; Launay *et al.*, 2019). ProDH, a key enzyme in proline oxidation, was recently shown to participate in nitrogen remobilization, fuelling mitochondrial respiration and the TCA cycle. ProDH activity leads to the production of P5C which is used by P5CDH to form glutamate. P5C is also produced by OAT from ornithine, thus connecting proline and arginine metabolisms. OAT has been described by some authors as an alternative route of proline synthesis (Hervieu *et al.*, 1995; Yang and Kao, 1999; Roosens *et al.*, 2002; Wu *et al.*, 2003). However, the involvement of OAT in proline biosynthesis upon salt stress was invalidated by Funck *et al.*, (2008). In this study, by complementing molecular and biochemical analyses with a metabolomic approach, we aimed at deciphering the role of the three mitochondrial enzymes involved in P5C metabolism, using knockout *prodh1prodh2*, *p5cdh*, and *oat* mutants in DIS.

As shown with the progressive and visible yellowing of *Arabidopsis* leaves during DIS, chlorophyll contents followed a similar trend in all genotypes. No significant differences of chlorophyll contents could be observed in Col-0 and mutants, indicating these enzymes are not involved directly or indirectly in this process. However, significant increase in proline accumulation was detected in *prodh1prodh2* and *p5cdh* and to a lower extent in *oat* mutant when compared with Col-0 by both GC-MS and colorimetric methods. The observed discrepancy for *oat*, depending on the method used for the determination of proline content, can be explained by the fact that the colorimetric ninhydrin assay is not totally specific of proline measurement. Indeed, ornithine, which is also accumulated in *oat* mutant, can react with ninhydrin at acid pH and interfere with the assay (Chinard, 1952). In this study, proline accumulation in *prodh1prodh2* followed a similar trend to what was previously reported by Launay *et al.* (2019), which demonstrates the involvement of ProDH during DIS.

Interestingly, higher proline accumulation was detected in *p5cdh* than in *prodh1prodh2* mutant. The origin of this striking proline accumulation in *p5cdh* mutant is intriguing because proline biosynthesis is not triggered during DIS, as shown by a constant and low level of P5CS1 and P5CR protein contents in all genotypes. In addition, *OAT* and to a higher extent *ProDH1* are expressed in *p5cdh* mutant. The increase in proline content may explain the higher amount of *ProDH1* transcript level in *p5cdh* mutant compared to Col-0 because proline is well known to trigger ProDH expression. However, ProDH1 and OAT amounts were similar in Col-0 and *p5cdh* mutant in crude protein extracts but lower in *p5cdh* crude mitochondria in comparison to Col-0. Interestingly ProDH and OAT activities were also decreased by around 2.5-fold in *p5cdh* mutant. The opposite expression pattern of ProDH1 and OAT transcript and protein levels indicates they may subject to either post-transcriptional or post-translational regulation in *p5cdh* mutant during DIS.

The increase in proline content in *p5cdh* mutant may originate from the activation of the putative proline-P5C cycle proposed in plants (Miller *et al.*, 2009). This cycle may allow the generation of proline from glutamate. P5C is an intermediate for both proline biosynthesis and proline oxidation. It is a product of ProDH in mitochondria and a substrate of P5CR in the cytosol. If P5C could move back and forth between the cytosol and the mitochondrial matrix, P5CR and ProDH would then form a metabolic ring, i.e., the proline-P5C cycle. However, the existence of this cycle in plant is not proven yet, because not only the fact that no transporter of P5C has been identified but also the movement of P5C between the two compartments has not been demonstrated yet (Zheng *et al.*, 2021). The proline-P5C cycle may compensate the disability of *p5cdh* mutant to remove unfavourable hyperaccumulated P5C/GSA during DIS. The toxicity of P5C/GSA has been proposed, whose accumulation has been reported to trigger a burst of ROS in both yeast and *Arabidopsis p5cdh* mutants (Deuschle *et al.*, 2001). ROS has been reported to trigger cell death among living organisms (Gill and Tuteja, 2010). Thus, ROS homeostasis must be maintained with care during senescence. Accordingly, co-induction of ProDH and P5CDH during DIS has been observed in Col-0, supporting the hypothesis that P5C/GSA accumulation is unfavourable for senescing Col-0 plants. Hence, in order to survive, *p5cdh* mutant senescing leaves may either induce alternative P5C detoxification pathway or inhibit the source of P5C to limit the accumulation of this unfavourable intermediate. Consistently, our results have shown that proline continuously accumulates in *p5cdh* mutant until D4 and D5, meanwhile P5C decreased at D4. Furthermore, the enzymatic activity and protein amount of both ProDH1 and OAT were downregulated in *p5cdh* mutant at D4, in an unknown regulatory manner. Taken together, these results suggest that the mitochondrial P5C must be

carefully limited during senescence, indicating that the full oxidation of proline to glutamate by ProDH and P5CDH is required during senescence.

Hence, mitochondrial P5C might be sequestered in a substrate channel by the interaction of P5CDH with ProDH and/or P5CDH with OAT. Consistently, substrate channelling has been reported in both PutA (Srivastava *et al.*, 2010; Singh *et al.*, 2014) and monofunctional TtProDH-TtP5CDH (Sanyal *et al.*, 2015) in *T. thermophilus*, although it has not been reported for OAT so far. Thus, one can speculate that ProDH and OAT may interact with P5CDH to sequester P5C/GSA during senescence in plants.

Furthermore, our results have shown the involvement of OAT during DIS. A 10-fold increase of *OAT* expression was observed after 3 days of DIS in all genotypes, while *OAT* protein amount as well as activity was lower in mitochondria of *p5cdh* mutant as also observed for ProDH1. However, according to the metabolomic data, the metabolome of *oat* is closer to Col-0 than to *prodh1prodh2* and *p5cdh* mutants. The global amino acid accumulation was decreased in *oat*, although its pattern was similar to Col-0, indicating a role of *OAT* and arginine for amino acid accumulation during senescence. Ornithine, the substrate of *OAT*, is an intermediate of the urea cycle and a central metabolite of arginine synthesis and degradation, arginine being recognized as a storage form of organic nitrogen and playing a key role in nitrogen distribution and remobilization in plants (Slocum, 2005; Winter *et al.*, 2015). *OAT* is then able to redirect ornithine into the proline metabolism and mobilize nitrogen from the urea cycle (Funck *et al.*, 2008; Blume *et al.*, 2019, page 2). Recently, it has been reported that *OAT* is crucial for nitrogen reutilization and plays a critical role in floret development and seed setting in *Oryza sativa* (Liu *et al.*, 2018). *OAT* is also linked to the polyamine (PA) metabolism even if no ornithine decarboxylase has been identified in *Arabidopsis* (Hanfrey *et al.*, 2001). Indeed, ornithine and arginine are both important precursors for PA biosynthesis.

A strong link has been found between PAs and DIS (Sequera-Mutiozabal *et al.*, 2016; Sobieszczuk-Nowicka *et al.*, 2016) and more generally with senescence (Moschou *et al.*, 2012; Sobieszczuk-Nowicka, 2017). More than the absolute contents of PAs, it is the dynamic of synthesis, degradation, attachment to other molecules and transport of the different PAs that are involved in senescence. In particular, PA catabolism leads to GABA production, an alternative source of succinate to TCA, as well as H₂O₂ release, which is involved in the programmed cell death response, and NH₄⁺ release (Moschou *et al.*, 2012; Tiburcio *et al.*, 2014). In addition, PAs are nitrogenous molecules that can contribute to nitrogen stockage and/or remobilization. As *OAT* uses ornithine, which comes from arginine degradation by arginase, we could hypothesize

that OAT affect nitrogen remobilization during DIS by this way. Anyway, the role of OAT needs more investigations and particularly through fluxomic approaches.

To conclude, our study demonstrates a key role of ProDH and P5CDH in proline oxidation during DIS. Interestingly, the use of either *prodh1prodh2* or *p5cdh* mutants differentially affect proline content during DIS, which may unravel the presence of a proline-P5C cycle. This cycle may allow the cell to regulate the accumulation of the toxic P5C/GSA. DIS appears to be an interesting physiological condition to decipher the existence of this cycle in plants. Our study also suggests that ProDH and P5CDH may function as a complex in order to channel P5C as shown in prokaryotes (Sanyal *et al.*, 2015). OAT pathway is not involved in this proline oxidation process during DIS and may be more linked to PA metabolism but further studies are needed to address this role.

Acknowledgements

This work received financial support from Sorbonne Université and a PhD fellowship to Y.Z. from the China Scholarship Council.

Conflict of interest

The authors declare that this research was conducted in the absence of any commercial or financial relationships that would cause any potential conflicts of interest.

Figures and tables

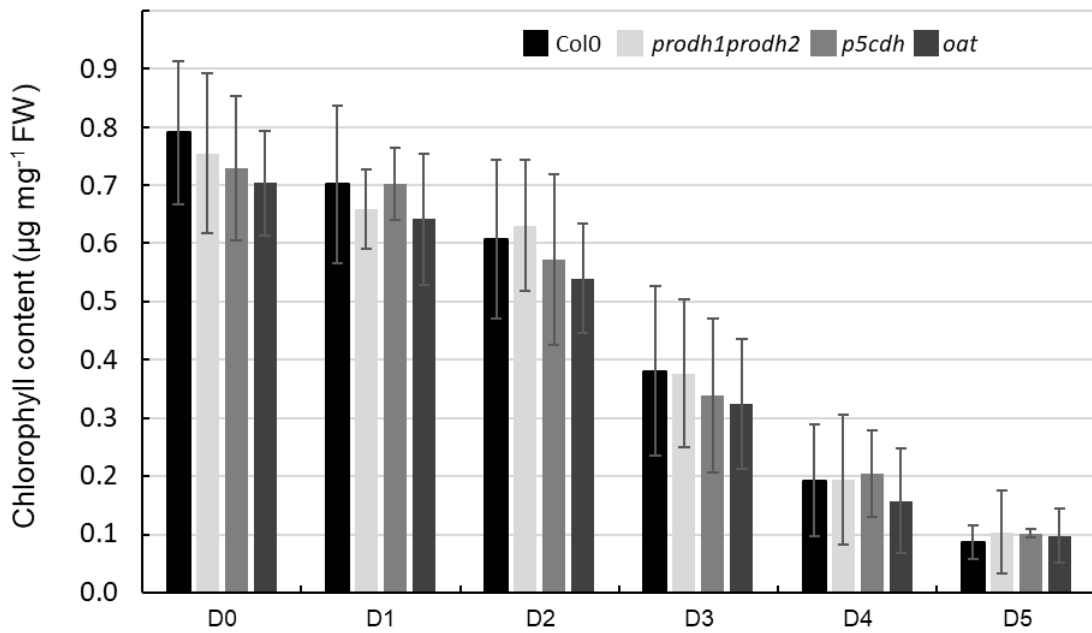


Figure 1. Total chlorophyll contents during dark-induced senescence in Arabidopsis. Total chlorophyll contents were measured in a time-course experiment during DIS in Col-0 (wild-type), *prodh1prodh2*, *p5cdh* and *oat* mutants. Data are means (\pm SD) of three independent measurements from three independent experiments. Variations of chlorophyll contents within each day time-point were not statistically different (ANOVA, $P > 0.05$).

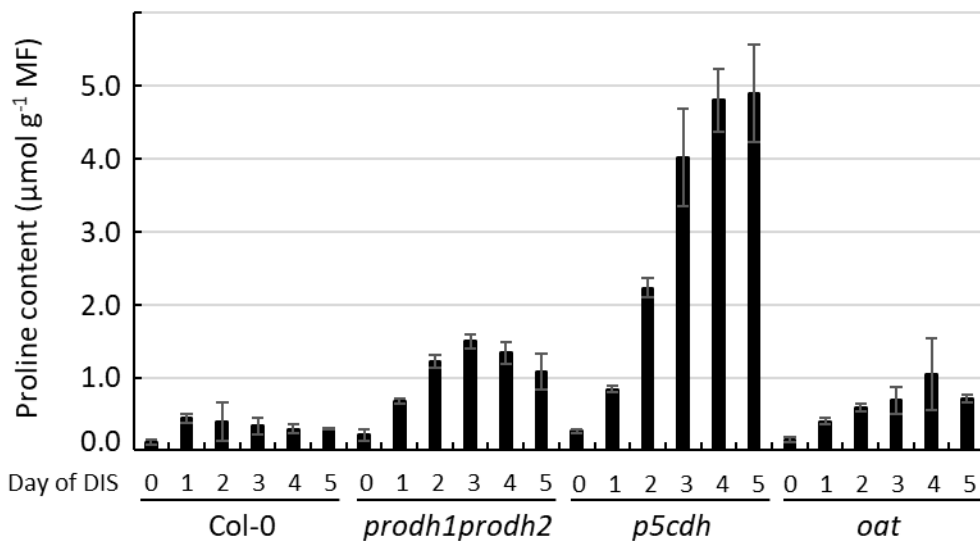


Figure 2. Proline contents during dark-induced senescence in Arabidopsis. Proline contents were measured in a time-course experiment during DIS in Col-0 (wild-type), *prodh1prodh2*, *p5cdh* and *oat* mutants. Data are means (\pm SD) of three independent measurements from three independent experiments.

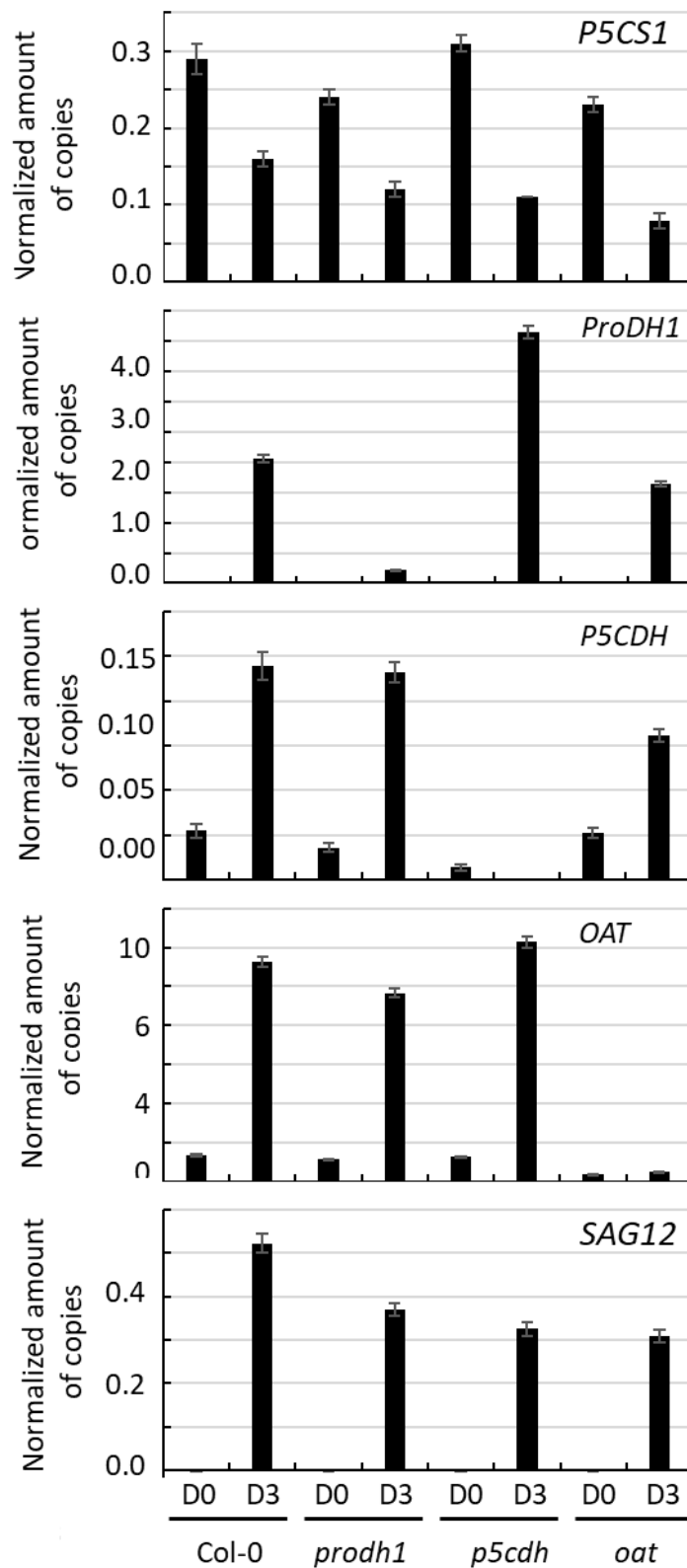


Figure 3. Transcript levels of P5CS1, ProDH1, P5CDH, and OAT during DIS. Transcript levels were quantified by droplet digital PCR after 0-5 days of DIS in WT, as well as *prodh1prodh2*, *p5cdh*, *oat* mutants. SAG12 is a marker that induced during senescence. Data are means \pm SD of normalized number of copies for a given genes (mean \pm SD).

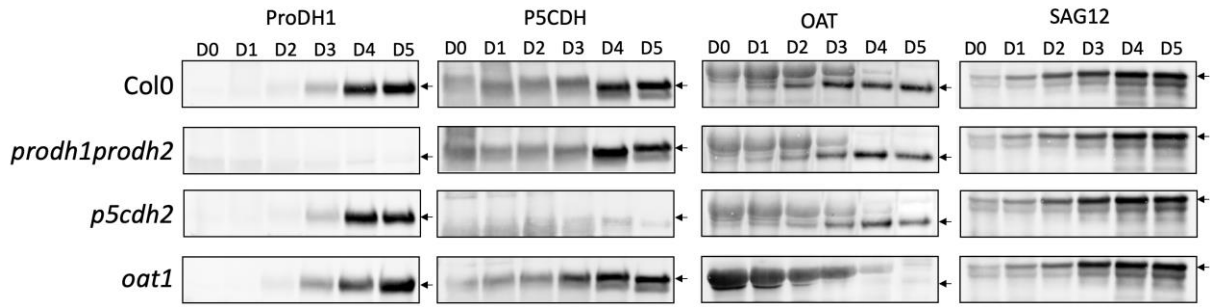


Figure 4. ProDH1, P5CDH, OAT and SAG12 protein levels during DIS in Arabidopsis. Western blots of total proteins extracted from 100 mg leaves 7 to 9 of WT, as well as *prodh1prodh2*, *p5cdh*, *oat* mutants after 0-5 days of DIS. Proteins from different genotypes were separated by Bio-Rad TGX Stain-Free PAGE gel and blots were probed with antibodies raised against ProDH1, P5CDH, OAT and SAG12.

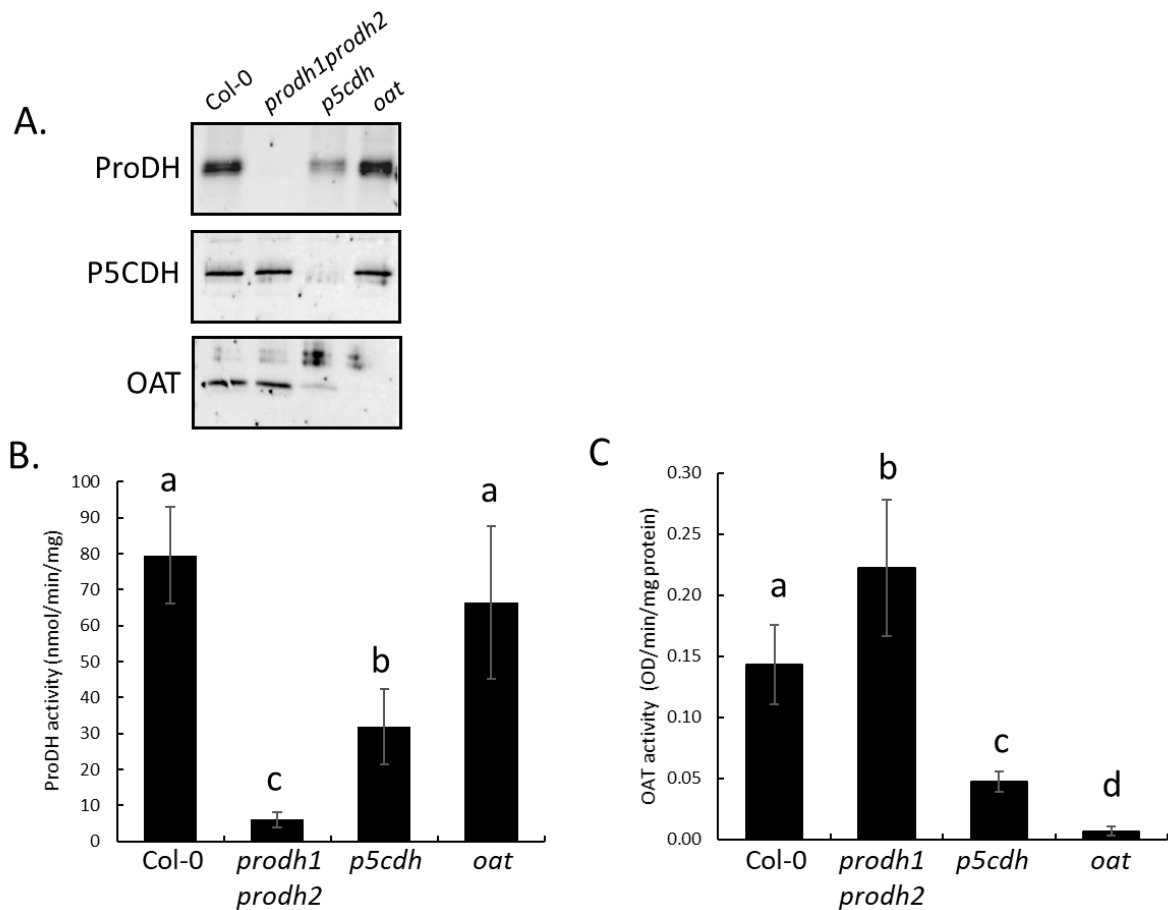


Figure 5. Protein amounts and enzymatic activities of ProDH and OAT were reduced in *p5cdh* at Day 4 of DIS. (A) Crude mitochondria extracted from 4-day DIS treated leaves of 4-week-old Col-0, *prodh1prodh2*, *oat*, and *p5cdh* plants. 5 μ g of proteins were loaded for each genotype on SDS-PAGE. Western-blot was probed with antibodies raised against ProDH1, P5CDH, or OAT, respectively. The enzymatic activities of ProDH (B) and OAT (C) were measured using crude mitochondria extracted from 4-day DIS-treated leaves of 4 genotypes.

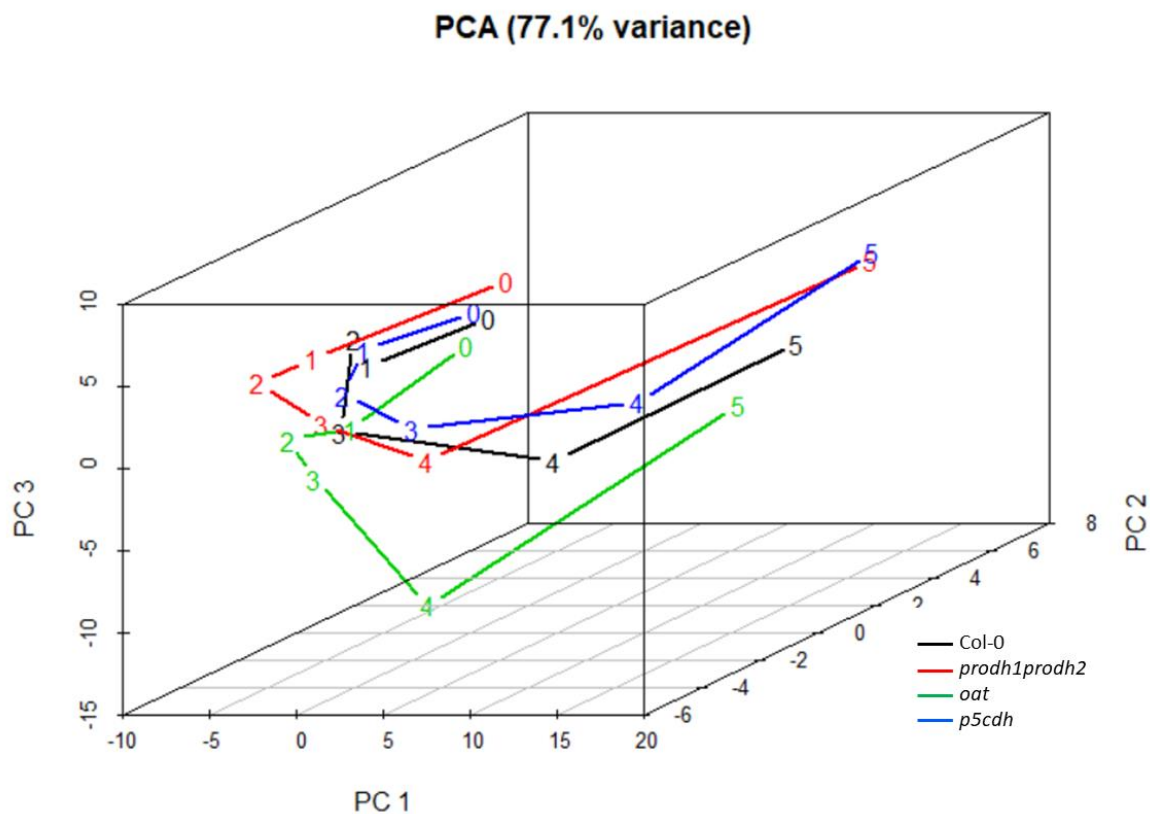
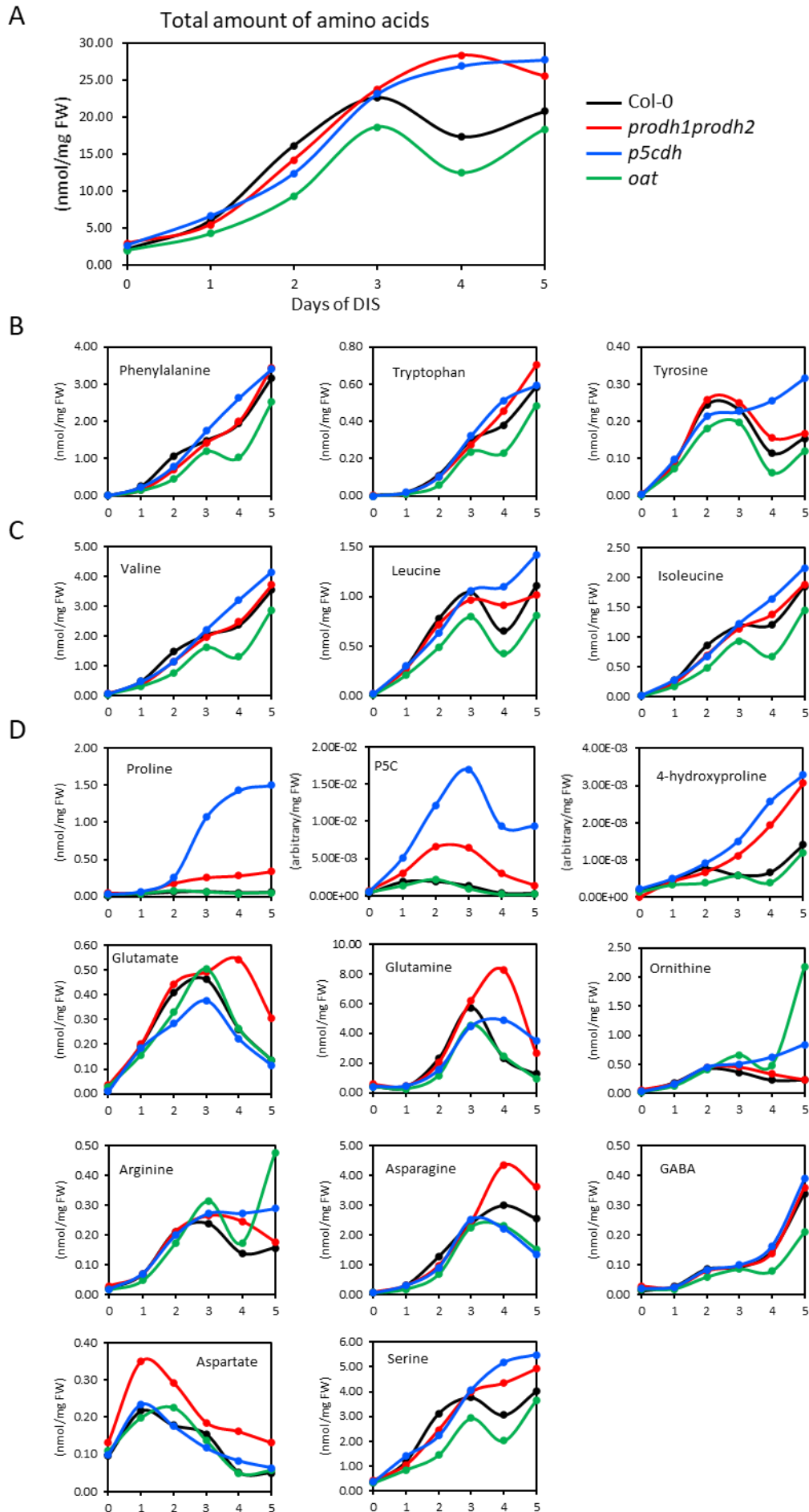


Figure 6. Principle component analysis (PCA) of metabolome during 0-5 days of DIS in *Arabidopsis*. The data matrix consisted of 117 metabolites characterized in our metabolomic data derived from DIS time-course samples in different genotypes. Zero to 5 labeled on the lines of each genotype indicates the time points (Day 0 to 5) of DIS time-course experiments. PC, principal components. The corresponding genotypes used for the PCA are shown on the right-down corner.



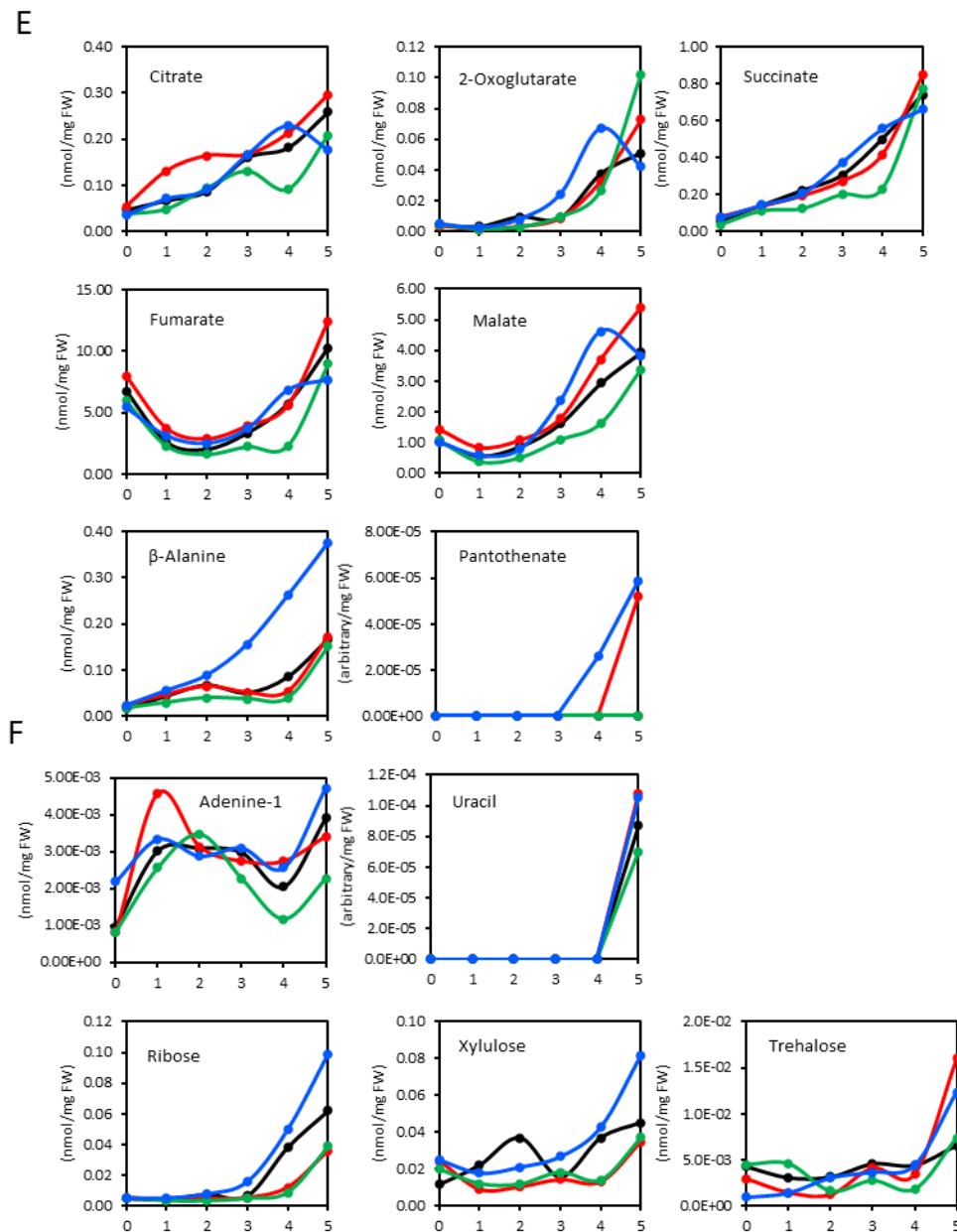


Figure 7. Contents of amino acids (AA), AA derived metabolites, and TCA metabolites in different genotypes during DIS. (A) Total amount of 20 proteinogenic amino acids detected in the metabolomic data of different genotypes during DIS. Contents of aromatic amino acids (B), of branched-chain amino acids (C), proline related metabolites (D), TCA metabolites (E) and nucleotides and sugars (F) detected in metabolome analysis are presented.

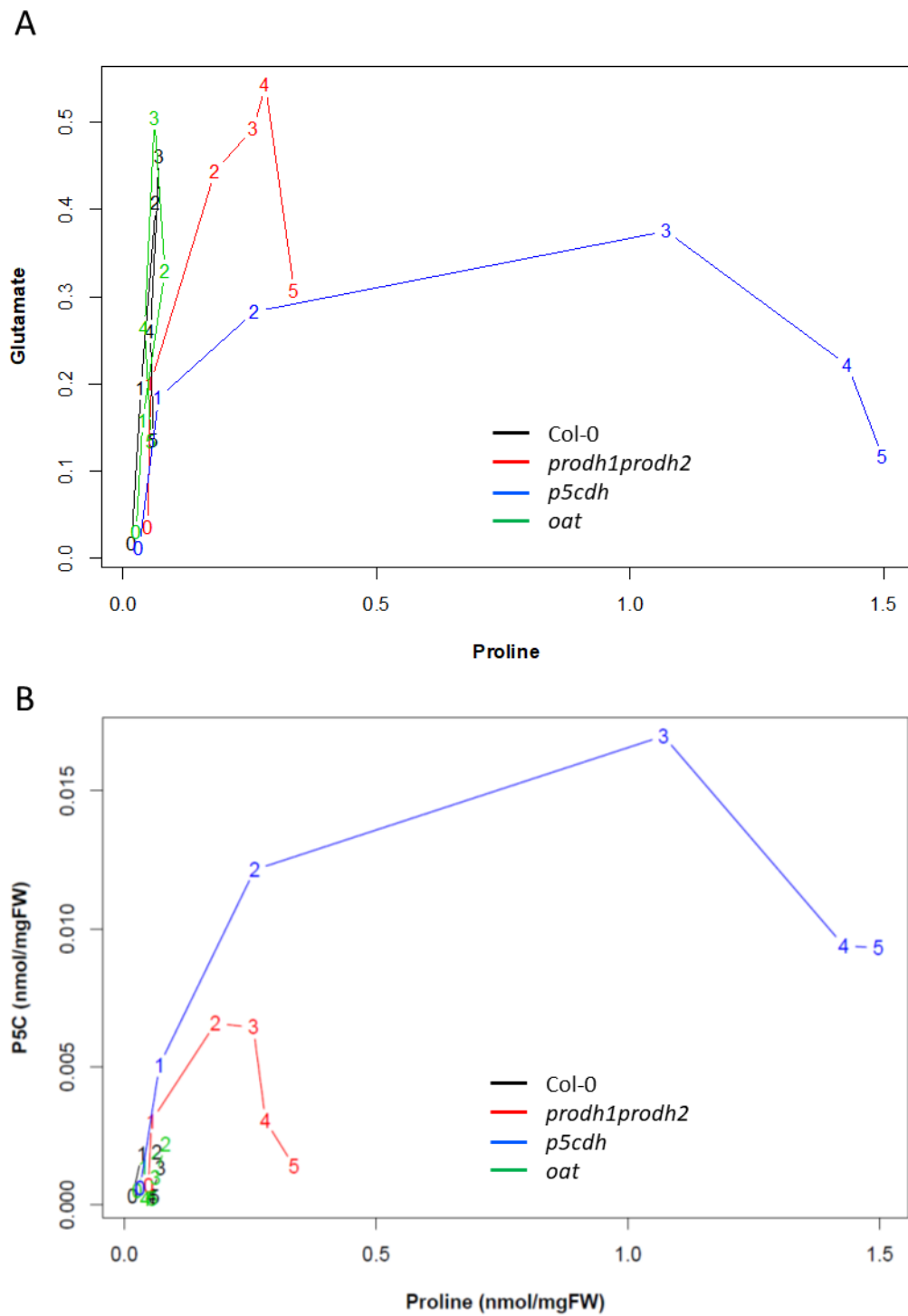
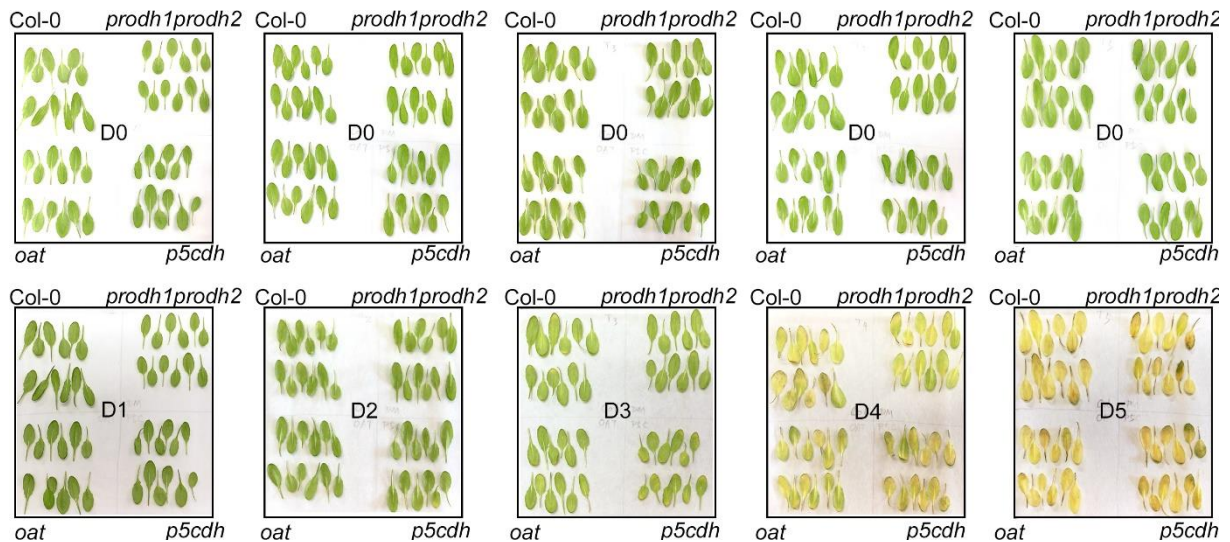
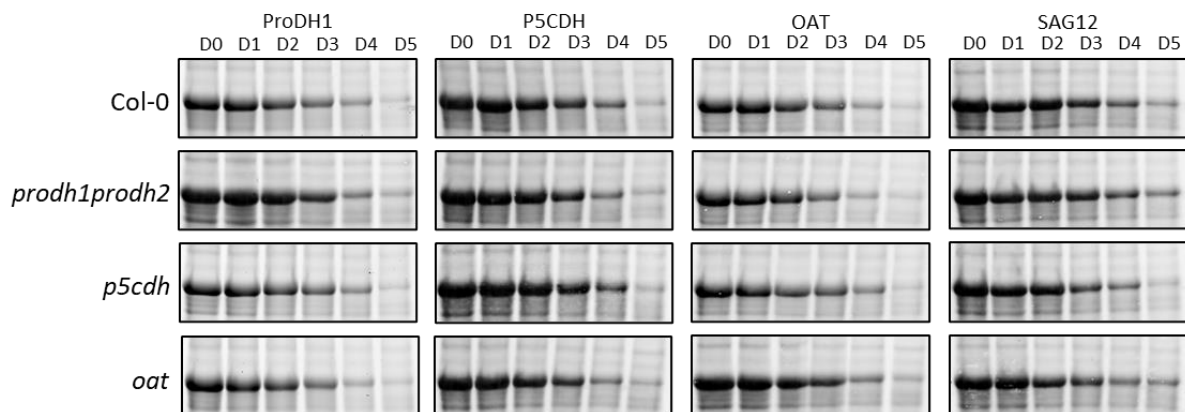


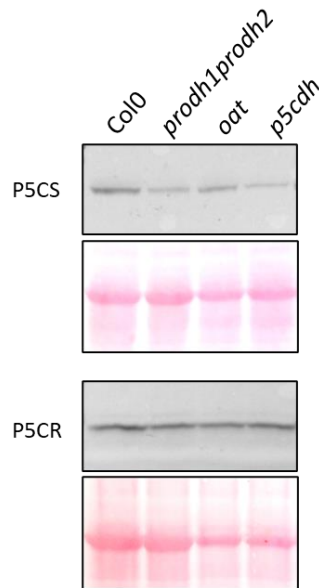
Figure 8. Correlation between glutamate and proline (A) as well as P5C and proline (B) during DIS in Arabidopsis. The abundance of proline in different genotypes during DIS is plotted on x-axis, and the abundance of glutamate or P5C is plotted on y-axis.



Supplemental Figure S1. Photographs of dark-induced leaf senescence during dark-induced leaf senescence in Arabidopsis. Col-0 (WT) as well as *prodh1prodh2*, *p5cdh* and *oat* mutant genotypes of the leaves is indicated in each corner of the photographs. Photographs were taken at D0, D1, D2, D3, D4 and D5 during DIS as indicated in the center of each panel.



Supplemental Figure S2. TGX Stain-Free membranes of total proteins extracted from Col-0, as well as *prodh1prodh2*, *p5cdh*, *oat* mutants after 0-5 days of DIS. TGX Stain-Free PAGE Gels were loaded with total proteins extracted from 100 mg leaves 7 to 9 of Col-0, as well as *prodh1prodh2*, *p5cdh*, *oat* mutants after 0-5 days of DIS.



Supplemental Figure S3. P5CS and P5CR protein contents at D3 of DIS in Arabidopsis. Western blots of total proteins extracted from 100 mg leaves 7 to 9 of Col-0, as well as *prodh1prodh2*, *p5cdh*, *oat* mutants at D3 of DIS. Proteins from different genotypes were separated by Bio-Rad TGX Stain-Free PAGE gel and blots were probed with antibodies raised against P5CS or P5CR.

Supplementary Table S1. List of primers

| Gene name | Gene ID number | Direction | Primer Name | Primer sequence 5' to 3' |
|-----------|----------------|-----------|----------------------|--------------------------|
| APT1* | At1g27450 | Forward | SHL604_APTI-QF1 | ACGACGCTTCTTCTCGACAC |
| | | Reverse | SHR605_APTI-QR1 | CACCAATAGCCAACGCAATAG |
| UCR1-2** | At5g13440 | Forward | SHL606_AT5G-QF1 | ACAAGCCAATTTTTGCTGAGC |
| | | Reverse | SHR607_AT5G-QR1 | ACAACAGTCCGAGTGTCATGGT |
| ProDH1 | At3g30775 | Forward | Q_PRODH1_VerF | AGCTGCCAAATCTTTACCAACATC |
| | | Reverse | Q_PRODH1_VerR | GCTTCATGAGAGTTTGAAGTTCG |
| ProDH2 | At5g38710 | Forward | Q_PRODH2_F | GCTGCTAAAACCCTACCTTCG |
| | | Reverse | Q_PRODH2_R | ACAGAGGACTTAAGCCGGAG |
| P5CDH | At5g62530 | Forward | SHL-494_P5CDH_Alva_F | GCGGTTCTTGGCACGGTCTT |
| | | Reverse | SHR-495_P5CDH_Alva_R | AGTCCACATCTTCAGCGGGTAAAC |
| OAT | At5g46180 | Forward | SHL496_OAT_Alva_F | TAACCGAGTGTGATCGCTGTGGAA |
| | | Reverse | SHR497_OAT_Alva_R | ACCGGTGCTGTGCCTATGGAAAT |
| SAG12 | At5g45890 | Forward | SH934L_SAG12 | TTGCCGGTTTCTGTTGACTG |
| | | Reverse | SH935R_SAG12 | ATCCATTAAACCGCCTTCGC |
| P5CS1 | At2g39800 | Forward | qP5CS1f | GAGCTAGATCGTTCACGTGCTTT |
| | | Reverse | qP5CS1r | ACAACCTGCTGTCCCAACCTTAAC |

*Adenine phosphoribosyl transferase 1 (APT1)

**Ubiquinol-cytochrome C reductase iron-sulfur subunit 1-2 (UCR1-2)

Supplementary Table 2. Distribution of the 117 metabolites across the 3 PCs.

| Grouping PCs | Metabolites |
|--------------|--|
| PC1 | 2-4-dihydroxybutanoate 2-Hydroxyglutarate 2-Oxoglutarate 4-hydroxyproline α -Amino adipate Agmatine(-NH ₃) Allantoin α -amino butyrate Anhydroglucose Arabitol Ascorbate Asparagine β -amino isobutyrate β -Alanine β -indole-3-acetonitrile β -Lactate β -Sitosterol Campesterol Citrate Cycloartenol Cys Dehydroascorbate Digalactosylglycerol Erythritol Fructose Fructose-6-P GABA Galacturonate γ -Tocopherol Gluconate Glucose Glucose-6-P Glucuronate Glutarate Glycine Histidine Isoleucine Leucine Linoleic acid Linolenic acid Malate Maleate Maltotriose Mannitol Methionine Monopalmitine myo-Inositol O-Acetyl-Serine Pantothenate Phenylalanine Porphine Proline Putrescine Ribose S-Methyl-L-cysteine Serine Sinapinate-cis Spermidine Stigmasterol Succinate Threonate Threonate-lactone Trehalose Tryptophan U1189.7/170(P5Cstandard) U1842.8/123 U1882.2/278 UGlucosinolatebreakdown140-1 Urea Valine Xylulose |
| PC2 | Glutamate Homoserine Mannose |
| PC3 | Galactonate Glycosylsalicylate Pipecolate |
| Multiple PCs | P5C (Δ^1-pyrroline-5-carboxylate) Alanine α -Tocopherol Arabinose Aspartate Citramalate Erythronate Fumarate Galactinol Galactose Galactosylglycerol Glucopyranose Glutamine Glycerate Glycerol-3-P Lysine Lyxonate Methionine sulfoxide Nicotinate Palmitelaidate Phosphate Phytol-2 Pyrrole-2-carboxylate Raffinose Rhamnose Ribonate Salicylate Shikimate Sinapinate-trans Sucrose Threitol Threonine Tyrosine U1297/1445(Norvaline) U1865.3/278 Uracil Urate Xylose |

References

- Alvarez ME, Savouré A, Szabados L. 2021. Proline metabolism as regulatory hub. Trends in Plant Science. *In press*. doi: 10.1016/j.tplants.2021.07.009
- Avila-Ospina L, Moison M, Yoshimoto K, Masclaux-Daubresse C. 2014. Autophagy, plant senescence, and nutrient recycling. *Journal of Experimental Botany* **65**, 3799–3811.

- Ay N, Raum U, Balazadeh S, Seidensticker T, Fischer A, Reuter G, Humbeck K.** 2014. Regulatory Factors of Leaf Senescence are Affected in Arabidopsis Plants Overexpressing the Histone Methyltransferase SUVH2. *Journal of Plant Growth Regulation* **33**, 119–136.
- Bates LS, Waldren RP, Teare ID.** 1973. Rapid determination of free proline for water-stress studies. *Plant and Soil* **39**, 205–207.
- Blume C, Ost J, Mühlenbruch M, Peterhänsel C, Laxa M.** 2019. Low CO₂ induces urea cycle intermediate accumulation in *Arabidopsis thaliana*. *PLOS ONE* **14**, e0210342.
- Borsani O, Zhu J, Verslues PE, Sunkar R, Zhu J-K.** 2005. Endogenous siRNAs Derived from a Pair of Natural cis-Antisense Transcripts Regulate Salt Tolerance in Arabidopsis. *Cell* **123**, 1279–1291.
- Buchanan-Wollaston V, Page T, Harrison E, et al.** 2005. Comparative transcriptome analysis reveals significant differences in gene expression and signalling pathways between developmental and dark/starvation-induced senescence in Arabidopsis. *The Plant Journal* **42**, 567–585.
- Cabassa-Hourton C, Schertl P, Bordenave-Jacquemin M, et al.** 2016. Proteomic and functional analysis of proline dehydrogenase 1 link proline catabolism to mitochondrial electron transport in *Arabidopsis thaliana*. *Biochemical Journal* **473**, 2623–2634.
- Cecchini NM, Monteoliva MI, Alvarez ME.** 2011. Proline Dehydrogenase Contributes to Pathogen Defense in Arabidopsis. *Plant Physiology* **155**, 1947–1959.
- Chen Y, Fu X, Mei X, Zhou Y, Cheng S, Zeng L, Dong F, Yang Z.** 2017. Proteolysis of chloroplast proteins is responsible for accumulation of free amino acids in dark-treated tea (*Camellia sinensis*) leaves. *Journal of Proteomics* **157**, 10–17.
- Chinard FP.** 1952. PHOTOMETRIC ESTIMATION OF PROLINE AND ORNITHINE. *Journal of Biological Chemistry* **199**, 91–95.
- Chrobok D, Law SR, Brouwer B, et al.** 2016. Dissecting the Metabolic Role of Mitochondria during Developmental Leaf Senescence. *Plant Physiology* **172**, 2132–2153.
- Dellero Y, Clouet V, Marnet N, Pellizzaro A, Dechaumet S, Niogret M-F, Bouchereau A.** 2020. Leaf status and environmental signals jointly regulate proline metabolism in winter oilseed rape. *Journal of Experimental Botany* **71**, 2098–2111.
- Deuschle K, Funck D, Hellmann H, Däschner K, Binder S, Frommer WB.** 2001. A nuclear gene encoding mitochondrial Δ^1 -pyrroline-5-carboxylate dehydrogenase and its potential role in protection from proline toxicity. *The Plant Journal* **27**, 345–356.
- Dietrich K, Weltmeier F, Ehlert A, Weiste C, Stahl M, Harter K, Dröge-Laser W.** 2011. Heterodimers of the Arabidopsis Transcription Factors bZIP1 and bZIP53 Reprogram Amino Acid Metabolism during Low Energy Stress. *The Plant Cell* **23**, 381–395.
- Dubois M, Claeys H, Broeck LV den, Inzé D.** 2017. Time of day determines Arabidopsis transcriptome and growth dynamics under mild drought. *Plant, Cell & Environment* **40**, 180–189.
- Fiehn O.** 2006. Metabolite Profiling in *Arabidopsis*. *Arabidopsis Protocols*. New Jersey: Humana Press, 439–448.
- Fiehn O, Wohlgemuth G, Scholz M, Kind T, Lee DY, Lu Y, Moon S, Nikolau B.** 2008. Quality control for plant metabolomics: reporting MSI-compliant studies. *The Plant Journal* **53**, 691–704.
- Funck D, Baumgarten L, Stift M, von Wirén N, Schönemann L.** 2020. Differential Contribution of P5CS Isoforms to Stress Tolerance in Arabidopsis. *Frontiers in Plant Science* **11**.
- Funck D, Stadelhofer B, Koch W.** 2008. Ornithine- δ -aminotransferase is essential for Arginine Catabolism but not for Proline Biosynthesis. *BMC Plant Biology* **8**, 40.
- Gill SS, Tuteja N.** 2010. Reactive oxygen species and antioxidant machinery in abiotic stress tolerance in crop plants. *Plant Physiology and Biochemistry* **48**, 909–930.
- Graaff E van der, Schwacke R, Schneider A, Desimone M, Flügge U-I, Kunze R.** 2006. Transcription Analysis of Arabidopsis Membrane Transporters and Hormone Pathways during Developmental and Induced Leaf Senescence. *Plant Physiology* **141**, 776–792.
- Hanfrey C, Sommer S, Mayer MJ, Burtin D, Michael AJ.** 2001. Arabidopsis polyamine biosynthesis: absence of ornithine decarboxylase and the mechanism of arginine decarboxylase activity. *The Plant Journal* **27**, 551–560.

- Hanson AD, Tully RE.** 1979. Light stimulation of proline synthesis in water-stressed barley leaves. *Planta* **145**, 45–51.
- Hayashi F, Ichino T, Osanai M, Wada K.** 2000. Oscillation and Regulation of Proline Content by P5CS and ProDH Gene Expressions in the Light/Dark Cycles in *Arabidopsis thaliana* L. *Plant and Cell Physiology* **41**, 1096–1101.
- Izumi M, Ishida H.** 2019. An additional role for chloroplast proteins—an amino acid reservoir for energy production during sugar starvation. *Plant Signaling & Behavior* **14**, 1552057.
- James M, Poret M, Masclaux-Daubresse C, Marmagne A, Coquet L, Jouenne T, Chan P, Trouverie J, Etienne P.** 2018. SAG12, a Major Cysteine Protease Involved in Nitrogen Allocation during Senescence for Seed Production in *Arabidopsis thaliana*. *Plant and Cell Physiology* **59**, 2052–2063.
- Keech O, Pesquet E, Ahad A, Askne A, Nordvall D, Vodnala SM, Tuominen H, Hurry V, Dizengremel P, Gardeström P.** 2007. The different fates of mitochondria and chloroplasts during dark-induced senescence in *Arabidopsis* leaves. *Plant, Cell & Environment* **30**, 1523–1534.
- Kovács H, Aleksza D, Baba AI, Hajdu A, Király AM, Zsigmond L, Tóth SZ, Kozma-Bognár L, Szabados L.** 2019. Light Control of Salt-Induced Proline Accumulation Is Mediated by ELONGATED HYPOCOTYL 5 in *Arabidopsis*. *Frontiers in Plant Science* **10**.
- Launay A, Cabassa-Hourton C, Eubel H, et al.** 2019. Proline oxidation fuels mitochondrial respiration during dark-induced leaf senescence in *Arabidopsis thaliana*. *Journal of Experimental Botany* **70**, 6203–6214.
- Lee J, He K, Stolc V, Lee H, Figueroa P, Gao Y, Tongprasit W, Zhao H, Lee I, Deng XW.** 2007. Analysis of Transcription Factor HY5 Genomic Binding Sites Revealed Its Hierarchical Role in Light Regulation of Development. *The Plant Cell* **19**, 731–749.
- Liebsch D, Keech O.** 2016. Dark-induced leaf senescence: new insights into a complex light-dependent regulatory pathway. *New Phytologist* **212**, 563–570.
- Lim PO, Kim HJ, Gil Nam H.** 2007. Leaf Senescence. *Annual Review of Plant Biology* **58**, 115–136.
- Liu W, Phang JM.** 2012. Proline dehydrogenase (oxidase) in cancer. *BioFactors* **38**, 398–406.
- Liu C, Xue Z, Tang D, Shen Y, Shi W, Ren L, Du G, Li Y, Cheng Z.** 2018. Ornithine δ -aminotransferase is critical for floret development and seed setting through mediating nitrogen reutilization in rice. *The Plant Journal* **96**, 842–854.
- Mair A, Pedrotti L, Wurzinger B, et al.** 2015. SnRK1-triggered switch of bZIP63 dimerization mediates the low-energy response in plants. *eLife* **4**, e05828.
- Makino A, Osmond B.** 1991. Effects of Nitrogen Nutrition on Nitrogen Partitioning between Chloroplasts and Mitochondria in Pea and Wheat. *Plant Physiology* **96**, 355–362.
- Mattioli R, Biancucci M, El Shall A, Mosca L, Costantino P, Funck D, Trovato M.** 2018. Proline synthesis in developing microspores is required for pollen development and fertility. *BMC Plant Biology* **18**, 356.
- Miller G, Honig A, Stein H, Suzuki N, Mittler R, Zilberstein A.** 2009. Unraveling Δ 1-Pyrroline-5-Carboxylate-Proline Cycle in Plants by Uncoupled Expression of Proline Oxidation Enzymes. *Journal of Biological Chemistry* **284**, 26482–26492.
- Moschou PN, Wu J, Cona A, Tavladoraki P, Angelini R, Roubelakis-Angelakis KA.** 2012. The polyamines and their catabolic products are significant players in the turnover of nitrogenous molecules in plants. *Journal of Experimental Botany* **63**, 5003–5015.
- Noodén LD, Penney JP.** 2001. Correlative controls of senescence and plant death in *Arabidopsis thaliana* (Brassicaceae). *Journal of Experimental Botany* **52**, 2151–2159.
- Pedrotti L, Weiste C, Nägele T, et al.** 2018. Snf1-RELATED KINASE1-Controlled C/S1-bZIP Signaling Activates Alternative Mitochondrial Metabolic Pathways to Ensure Plant Survival in Extended Darkness. *The Plant Cell* **30**, 495–509.
- Sanada Y, Ueda H, Kuribayashi K, Andoh T, Hayashi F, Tamai N, Wada K.** 1995. Novel Light-Dark Change of Proline Levels in Halophyte (*Mesembryanthemum crystallinum* L.) and Glycophytes (*Hordeum vulgare* L. and *Triticum aestivum* L.) Leaves and Roots under Salt Stress. *Plant and Cell Physiology* **36**, 965–970.

- Sanyal N, Arentson BW, Luo M, Tanner JJ, Becker DF.** 2015. First Evidence for Substrate Channeling between Proline Catabolic Enzymes: A VALIDATION OF DOMAIN FUSION ANALYSIS FOR PREDICTING PROTEIN-PROTEIN INTERACTIONS. *Journal of Biological Chemistry* **290**, 2225–2234.
- Sequera-Mutiozabal MI, Erban A, Kopka J, Atanasov KE, Bastida J, Fotopoulos V, Alcázar R, Tiburcio AF.** 2016. Global Metabolic Profiling of Arabidopsis Polyamine Oxidase 4 (AtPAO4) Loss-of-Function Mutants Exhibiting Delayed Dark-Induced Senescence. *Frontiers in Plant Science* **0**.
- Servet C, Ghelis T, Richard L, Zilberstein A, Savoure A.** 2012. Proline dehydrogenase: a key enzyme in controlling cellular homeostasis. *Front Biosci* **17**, 607–620.
- Silao FGS, Ward M, Ryman K, Wallström A, Brindefalk B, Udekwu K, Ljungdahl PO.** 2019. Mitochondrial proline catabolism activates Ras1/cAMP/PKA-induced filamentation in *Candida albicans*. *PLOS Genetics* **15**, e1007976.
- Singh H, Arentson BW, Becker DF, Tanner JJ.** 2014. Structures of the PutA peripheral membrane flavoenzyme reveal a dynamic substrate-channeling tunnel and the quinone-binding site. *Proceedings of the National Academy of Sciences* **111**, 3389–3394.
- Slocum RD.** 2005. Genes, enzymes and regulation of arginine biosynthesis in plants. *Plant Physiology and Biochemistry* **43**, 729–745.
- Sobieszczuk-Nowicka E.** 2017. Polyamine catabolism adds fuel to leaf senescence. *Amino Acids* **49**, 49–56.
- Sobieszczuk-Nowicka E, Kubala S, Zmienko A, Malecka A, Legocka J.** 2016. From Accumulation to Degradation: Reprogramming Polyamine Metabolism Facilitates Dark-Induced Senescence in Barley Leaf Cells. *Frontiers in Plant Science* **6**.
- Srivastava D, Schuermann JP, White TA, Krishnan N, Sanyal N, Hura GL, Tan A, Henzl MT, Becker DF, Tanner JJ.** 2010. Crystal structure of the bifunctional proline utilization A flavoenzyme from *Bradyrhizobium japonicum*. *Proceedings of the National Academy of Sciences* **107**, 2878–2883.
- Szabados L, Savouré A.** 2010. Proline: a multifunctional amino acid. *Trends in Plant Science* **15**, 89–97.
- Székely G, Ábrahám E, Cséplő Á, et al.** 2008. Duplicated P5CS genes of Arabidopsis play distinct roles in stress regulation and developmental control of proline biosynthesis. *The Plant Journal* **53**, 11–28.
- Tiburcio AF, Altabella T, Bitrián M, Alcázar R.** 2014. The roles of polyamines during the lifespan of plants: from development to stress. *Planta* **240**, 1–18.
- Weaver LM, Amasino RM.** 2001. Senescence Is Induced in Individually Darkened Arabidopsis Leaves, but Inhibited in Whole Darkened Plants. *Plant Physiology* **127**, 876–886.
- Weltmeier F, Ehlert A, Mayer CS, Dietrich K, Wang X, Schütze K, Alonso R, Harter K, Vicente-Carbajosa J, Dröge-Laser W.** 2006. Combinatorial control of Arabidopsis proline dehydrogenase transcription by specific heterodimerisation of bZIP transcription factors. *The EMBO Journal* **25**, 3133–3143.
- Winter G, Todd CD, Trovato M, Forlani G, Funck D.** 2015. Physiological implications of arginine metabolism in plants. *Frontiers in Plant Science* **6**.
- Woo HR, Kim HJ, Lim PO, Nam HG.** 2019. Leaf Senescence: Systems and Dynamics Aspects. , 33.
- Zhang L, Becker D.** 2015. Connecting proline metabolism and signaling pathways in plant senescence. *Frontiers in Plant Science* **6**.
- Zheng Y, Cabassa-Hourton C, Planchais S, Lebreton S, Savouré A.** 2021. The proline cycle as a eukaryotic redox valve. *Journal of Experimental Botany*. *In press*. doi: 10.1093/jxb/erab361
- Zuur AF, Ieno EN, Walker NJ, Saveliev AA, Smith GM.** 2009. Zero-Truncated and Zero-Inflated Models for Count Data. In: Zuur AF., In: Ieno EN., In: Walker N., In: Saveliev AA., In: Smith GM, eds. *Statistics for Biology and Health. Mixed effects models and extensions in ecology with R*. New York, NY: Springer, 261–293.

CHAPTER IV.

Pyrroline-5-carboxylate metabolism protein
complex detected in *Arabidopsis thaliana*
leaf mitochondria

Chapter 4. Pyrroline-5-carboxylate metabolism protein complex detected in *Arabidopsis thaliana* leaf mitochondria

In contrast to the emerging importance of proline catabolism, the regulation and organization of eukaryotic proline catabolic enzymes, ProDH and P5CDH, are still largely unknown so far. Indeed, most findings about proline catabolic enzymes are discovered in prokaryotic organisms.

The existence of bifunctional PutA (Srivastava *et al.*, 2010; Singh *et al.*, 2014) as well as the interaction of monofunctional prokaryotic proline catabolic enzymes in *Thermus thermophilus* (Sanyal *et al.*, 2015) prompted us to investigate whether eukaryotic ProDH and P5CDH could form a dynamic complex. As ProDH is not constitutively expressed and recent studies have shown the involvement of ProDH and P5CDH in leaf senescence (Chrobok *et al.*, 2016; Launay *et al.*, 2019), we decided to study proline catabolic enzymes under this physiological condition. Moreover, we have shown previously that OAT is also induced under DIS. As OAT converts ornithine into P5C, an unstable and toxic compound that is also the product of ProDH and the substrate of P5CDH, we consider that these three enzymes could form a dynamic complex.

At first, the sub-mitochondrial localization of ProDH, OAT, and P5CDH during DIS was investigated after sonication and ultracentrifugation of crude mitochondria. While ProDH was mainly associated to the membrane, P5CDH was found both in the matrix and associated to the membrane, and OAT mainly in the matrix. Interaction of ProDH, OAT, and P5CDH was then studied by Bimolecular Fluorescence Complementation (BiFC) assay in tobacco leaves. A binary interaction was observed for all the proteins as well as homo-oligomerization in mitochondria. In order to confirm these results, protein-protein interactions among these three proteins were further studied by 2D BN/SDS-PAGE, 2D Native/SDS-PAGE, complexome profiling and co-immunoprecipitation (co-IP) in *Arabidopsis* leaves under DIS. By these complementary approaches, we confirmed that ProDH1, P5CDH and OAT are involved in the same P5C metabolic complex. which probably pertain to a bigger complex containing additional partners. Taken together, our data provided the first evidence of a mitochondrial P5C metabolic complex in eukaryotes.

Article

Pyrroline-5-carboxylate metabolism protein complex detected in *Arabidopsis thaliana* leaf mitochondria

Yao Zheng¹, Cécile Cabassa-Hourton¹, Holger Eubel², Guillaume Chevreux³, Laurent Lignieres³, Emilie Crilat¹, Hans-Peter Braun², Sandrine Lebreton^{1,*}, Arnould Savouré^{1,*}

1 Sorbonne Université, UPEC, CNRS, IRD, INRAE, Institute of Ecology and Environmental Sciences of Paris (iEES), 75005 Paris, France

2 Institute of Plant Genetics, Leibniz Universität Hannover, Germany

3 ProteoSeine@IJM, Université de Paris/CNRS, Institut Jacques Monod, 75006 Paris, France

*Corresponding authors

sandrine.lanfranchi@sorbonne-universite.fr

arnould.savoure@sorbonne-universite.fr

Running title

Evidence of a plant pyrroline-5-carboxylate metabolism complex

Keywords: Ornithine δ -aminotransferase; Proline dehydrogenase; Pyrroline-5-carboxylate dehydrogenase; Proline catabolism

Author Contributions

S.L. and A.S. conceived the research plans and supervised the experiments; Y.Z. performed most of experiments; C.C.-H. and S.L. performed the experiments on enzyme activities; H.E., L.L. and H-P.B. performed the MS experiments and analyzed the data; L.L. provided technical assistance to G.C.; E.C. prepared gene constructs and transformed plants; Y.Z. drafted the manuscript, which was completed by A.S. and S.L. with contributions from all the authors.

Abstract

Proline dehydrogenase (ProDH) and pyrroline-5-carboxylate (P5C) dehydrogenase (P5CDH) catalyze the oxidation of proline into glutamate via the intermediates P5C and glutamate-semialdehyde (GSA), which spontaneously interconvert. P5C and GSA are also intermediates in the production of glutamate from ornithine and α -ketoglutarate catalyzed by ornithine δ -aminotransferase (OAT). ProDH and P5CDH form a fused bifunctional PutA enzyme in Gram-negative bacteria and are associated in a bifunctional substrate channelling complex in *Thermus thermophilus*, but the physical proximity of ProDH and P5CDH in eukaryotes has not been described. Here we report the first evidence of physical proximity and interactions between *Arabidopsis* ProDH, P5CDH, and OAT in the mitochondria of plants during dark-induced leaf senescence when all three enzymes are expressed. Pairwise interactions and localization of the three enzymes were investigated using bimolecular fluorescence complementation (BiFC) with confocal microscopy in tobacco and sub-mitochondrial fractionation in *Arabidopsis*. Evidence for a complex composed of ProDH, P5CDH, and OAT was revealed by co-migration of the proteins in native conditions in two-dimensional gel electrophoresis. Co-immunoprecipitation coupled with mass spectrometry analysis further confirmed the presence of the P5C metabolism complex in *Arabidopsis*. P5C metabolism complexes may channel P5C among the constituent enzymes and directly provide electrons to the respiratory electron chain via ProDH.

Introduction

Metabolism of the amino acid proline influences many cellular processes beyond protein synthesis, including stress responses, osmotic adjustment, protein chaperoning, reactive oxygen species (ROS) signalling, redox homeostasis and energy metabolism (Szabados and Savouré, 2010; Liu and Phang, 2012; Silao et al., 2019; Alvarez et al., 2021; Zheng et al., 2021). For example, proline metabolism participates in both biotic (Cecchini et al., 2011) and abiotic (Hayat et al., 2012) stress responses in plants and is critical in cancer reprogramming in humans (Phang, 2019). Proline is also a respiratory fuel for insect flight, for instance, in *Apis mellifera* (honeybee) (Teulier et al., 2016).

Proline can be synthesized from glutamate, which is first activated by phosphorylation and then reduced to glutamate semialdehyde (GSA) by pyrroline-5-carboxylate synthetase (P5CS) using NADPH as cofactor. GSA is in nonenzymatic equilibrium with pyrroline-5-

carboxylate (P5C). P5C reductase (P5CR), using NAD(P)H as a cofactor, reduces P5C to proline. When plant cells recover from stress, proline is rapidly oxidized by the action of proline dehydrogenase (ProDH), an FAD-dependent enzyme to give P5C/GSA, which is then oxidized by P5C dehydrogenase (P5CDH) using NAD as cofactor to produce glutamate. Alternatively, proline can be synthesized from ornithine. The δ -amino group of ornithine is transferred to α -ketoglutarate by ornithine δ -aminotransferase (OAT) forming P5C/GSA in equilibrium, which may be converted either to proline by P5CR or to glutamate by P5CDH. This alternative ornithine-derived proline biosynthesis pathway is likely to occur in bacteria, yeast and animals, but it is not clear if it occurs in plants (Mestichelli et al., 1979; Roosens et al., 2002; Funck et al., 2008).

The cellular compartmentalization of enzymes involved in eukaryotic proline metabolism is diverse (Szabados and Savouré, 2010). For proline anabolism, P5CS and P5CR were found in the cytosol of plants (Szabados and Savouré, 2010; Funck et al., 2020), while in humans P5CS was observed in mitochondria, and P5CR in both mitochondria and cytosol (Fichman et al., 2015; Phang, 2019). Proline catabolism has been detected in mitochondria from animals, yeasts, and plants (Fichman et al., 2015). ProDH is localized at the matrix-exposed surface of the mitochondrial inner membrane in several species (Brunner and Neupert, 1969; Elthon and Stewart, 1981; Cabassa-Hourton et al., 2016). P5CDH was reported to be associated with mitochondrial inner membranes in *Zea mays* (maize) (Elthon and Stewart, 1981) but in the mitochondrial matrix in animals (Brunner and Neupert, 1969). OAT is thought to be localized in the mitochondrial matrix in both animals (Doimo et al., 2013) and plants (Winter et al., 2015).

There are interesting differences in the respective protein structures of ProDH, P5CDH and OAT among species. In Gram-negative bacteria, the bifunctional enzyme known as proline utilization A (PutA) has an N-terminal (N-ter) ProDH domain and a C-terminal (C-ter) P5CDH domain. In some bacteria such as *Escherichia coli*, a DNA-binding domain is also present in the N-ter part of the bifunctional enzyme, which enables EcPutA to act as a transcriptional repressor of proline utilization genes (Gu et al., 2004). In some bacteria such as *Thermus thermophilus*, ProDH and P5CDH are monofunctional enzymes, which is also the case in eukaryotes (Tanner, 2008; Servet et al., 2012). OAT is thought to act as a monofunctional enzyme in all kingdoms (You et al., 2012; Anwar et al., 2018).

The oligomeric states of ProDH, P5CDH and OAT are notably diverse (for details see Table I-1). Dimeric and tetrameric structures were observed for PutA in bacteria and for ProDH in *Th. thermophilus* and *Trypanosoma cruzi*. A recent discovery is that ProDH proteins form oligomers via their N-terminal α helix. Dimeric, tetrameric and hexameric states have been

described for monofunctional P5CDH (Srivastava et al., 2012; Luo et al., 2013; Pemberton and Tanner, 2013; Korasick et al., 2019). Monomeric, dimeric, and tetrameric structure have also been reported for OAT (Sekhar et al., 2007; Jortzik et al., 2010; Stránská et al., 2010; Montioli et al., 2017).

The proximity of proline metabolism enzyme activities may have functional consequences. Dimerization of PutA in *Geobacter sulfurreducens* and *Bradyrhizobium japonicum* enables substrate-channelling to sequester P5C/GSA inside PutA (Srivastava et al., 2010; Singh et al., 2014). Similarly, in *Th. thermophilus*, monofunctional ProDH and P5CDH have been reported to interact with each other, forming a similar substrate channel to PutA (Sanyal et al., 2015). Some studies have suggested that the intermediate P5C, most probably in the GSA form, which is shared by proline and ornithine metabolism, is toxic for the cell (Deuschle et al., 2004; Lerma-Ortiz et al., 2016). Indeed, exogenous proline supply is lethal in both yeast and *Arabidopsis thaliana* (*Arabidopsis*) *p5cdh* mutants, as it causes a burst of ROS production (Deuschle et al., 2004). P5C/GSA has been reported to de-activate the OAT cofactor pyridoxal phosphate (Farrant et al., 2001), inhibit respiration and trigger a burst of superoxide anions in mitochondria (Nishimura et al., 2012), and participate in the apoptosis signalling pathway (Maxwell and Davis, 2000). Thus, P5C/GSA channelling could be a way to avoid P5C/GSA toxicity while tightly regulating proline catabolic flux, protecting cells from futile cycling between proline biosynthesis and catabolism. Eukaryotic proline catabolic enzymes possibly form complexes, as ProDH was found to be one component of an otherwise uncharacterized protein complex in proline-treated *Arabidopsis* (Cabassa-Hourton et al., 2016). There is little to no evidence to date of an interaction between proline catabolic enzymes and OAT.

Arabidopsis has two non-redundant ProDH1 and ProDH2 isoforms sharing 75% sequence identity (Servet et al., 2012), and one P5CDH and one OAT isoform that have been characterized (Deuschle et al., 2001; Funck et al., 2008). P5CDH is abundant in different organs in *Arabidopsis* under normal growth conditions (Deuschle et al., 2001; Funck et al., 2010). Expression of *ProDH1* encoding the main isoform of ProDH1 (Funck et al., 2010) and *OAT* is specifically regulated at different developmental stages and under stress conditions (Kiyosue et al., 1996; Funck et al., 2010). Our aim was to investigate whether *Arabidopsis* ProDH, P5CDH and OAT colocalize and/or interact with each other, knowing that they share the intermediate P5C. Bimolecular fluorescence complementation (BiFC) assays were carried out in *Nicotiana benthamiana* to test binary interactions between these enzymes. Proline catabolism can be induced in excised *Arabidopsis* leaves senescing in the dark (Chrobok et al., 2016; Launay et al., 2019), where proline acts as an alternative respiratory substrate in responding to energy

deprivation (Launay et al., 2019). Dark-induced senescence (DIS) was therefore chosen as the experimental condition to search for putative colocalization interaction between ProDH and P5CDH in *Arabidopsis* by subcellular fractionation of proteins from senescing leaves. Protein-protein interactions were further studied by two-dimensional (2D) blue native (BN) and native SDS-PAGE, complexome profiling and co-immunoprecipitation (co-IP). Our data provide evidence that a eukaryotic mitochondrial complex composed of ProDH1, P5CDH and OAT is present during proline catabolism.

Materials and Methods

Plant materials and growth conditions

Wild-type (WT) *Nicotiana benthamiana* (tobacco) plants were grown in growth chambers at 22°C with 16-h light/8-h dark cycles with 80-100 $\mu\text{mol m}^{-2} \text{s}^{-1}$ light for 4 weeks until used for leaf infiltration.

Arabidopsis thaliana (*Arabidopsis*) experiments were carried out using the Columbia-0 (Col-0) ecotype. The *prodh1 prodh2* (*prodh1/2*) double mutant was previously obtained by crossing the respective homozygous single knockout mutants *prodh1-4* (SALK_119334) and *prodh2-2* (GABI_328G05) as described by (Cabassa-Hourton et al., 2016). The *oat-1* (SALK_033541) and *p5cdh-2* (SALK_018453) single knockout T-DNA insertion mutants have been described previously by Funck et al. (2008) and Deuschle et al. (2004) respectively.

Arabidopsis seeds were sown on soil and grown in growth chambers at 22°C with 16-h light/8-h dark cycles with 80-100 $\mu\text{mol m}^{-2} \text{s}^{-1}$ light for 4 weeks. Dark-induced senescence (DIS) treatments were performed on excised rosette leaves of 4-week-old *Arabidopsis* as described before (Launay et al., 2019).

Bimolecular fluorescence complementation (BiFC) assays

Arabidopsis ProDH1 (AT3G30775), *P5CDH* (AT5G62530), and *OAT* (AT5G46180) cDNAs were inserted in the enhanced yellow fluorescent protein (eYFP) vectors pSPYNE173 and pSPYCE(M). pSPYNE173 encodes the N-ter part of eYFP and a Myc epitope tag while pSPYCE(M) encodes eYFP C-ter part and an HA epitope tag (Waadt et al., 2008). All constructs were verified by automated DNA sequencing. *Agrobacterium tumefaciens* strain GV3101 was transformed with each plasmid as described in Valsecchi et al. (2013). mCherry

(mt-rk, CD3-991) plasmid was used as a mitochondrial matrix marker (Nelson et al., 2007). Wild-type (WT) *Nicotiana benthamiana* (tobacco) was infiltrated with different combinations of the enzyme-eYFP constructs with the mCherry control as described in Valsecchi et al. (2013). Infiltrated tobacco plants were kept in a growth chamber at 22°C with 16-h light/8-h dark cycles for 3 days.

Images (8-bit) of fresh infiltrated tobacco samples were collected using a Leica ×40 oil immersion objective with an inverted Leica laser scanning confocal microscope TCS SP5 II (Leica Microsystems, Heidelberg, Germany). Infiltrated samples were fixed with fixation buffer (4% (w/v) formaldehyde, 1× PBS buffer, 0.01% (v/v) Tween) before acquisition of optical sections with z-spacing steps of 0.08 µm using a Leica ×63 oil immersion objective with the TCS SP5 II Leica confocal microscope. Confocal images of fixed tobacco samples were deconvoluted with the Huygens 3.7 software (Scientific Volume Imaging, Hilversum, the Netherlands).

For both fresh and fixed samples, fluorescence of YFP and mCherry was excited using a laser at 514 nm (15-20% laser power) and 561 nm (10-15% laser power), respectively. Detection ranges were set at 520-564 nm for YFP and 590-650 nm for mCherry and the same gain was chosen for all images. All images were captured in a temperature-controlled room at 21°C.

Transformation of Arabidopsis with transgenic GFP-fusion constructs

TurboGFP (tGFP, Chromotek), a bright dimeric green fluorescent protein (GFP) derived from the GFP of *Pontellina plumate*, was used as a protein tag. The cDNA sequence of Arabidopsis *P5CDH* (AT5G62530) was modified by site-directed mutagenesis to remove the *BsaI* restriction site, and cloned with addition of an enterokinase recognition and cleavage site into the entry plasmid pAGM1287 (MoClo Tool Kit, Addgene) (Weber et al., 2011) using the primers described in Supplemental Table S1. The C-ter fusion construct 35S:P5CDH-tGFP and the control 35S:tGFP were cloned respectively in the destination plasmid pICH86988 (MoClo Tool Kit, Addgene) using the Golden Gate Modular cloning toolbox for plants (Engler et al., 2014).

Vectors were verified by sequencing and transformed into *A. tumefaciens* GV3101, to then transform *p5cdh-2* with 35S:P5CDH-tGFP and Col-0 with 35S:tGFP by the floral-dip method (Bent, 2006). Transformants were selected on MS/2 media with 75 µg/ml kanamycin and transferred to soil for propagation until homozygous lines (35S:P5CDH-tGFP/*p5cdh* and 35S:tGFP/Col) were obtained. Functional complementation of the *p5cdh* phenotype by

35S:P5CDH-tGFP was checked in homozygous seedlings grown in the presence of proline (Supplemental Fig. S1).

Protein extraction for BiFC controls

Two to three tobacco leaves infiltrated as for BiFC were harvested, frozen with liquid nitrogen and ground to fine powder. Frozen powder (100-200 mg) was suspended in 2 volumes of extraction buffer (50 mM DTT, 8 M urea, 5% (w/v) SDS, 40 mM Tris-HCl pH 6.8, 0.1 mM EDTA, 0.4 mg/ml bromophenol blue) supplemented with 1× protease inhibitor cocktail (Merck). Samples were shaken three times for 5 min at room temperature after 5-min intervals on ice. The samples were then centrifuged at $18000 \times g$ for 10 min at 10 °C. Supernatants were transferred into new tubes for SDS-PAGE and western blots.

Extraction of crude mitochondria from Arabidopsis

Crude mitochondria were freshly prepared from 3 g of mature rosette leaves from 4-week-old *Arabidopsis* after 4 or 5 days of DIS as described before (Launay et al., 2019). The mitochondrial protein concentration was determined with the Lowry assay (Lowry et al., 1951) using BSA as a standard.

Fragmentation of Arabidopsis mitochondria for sub-mitochondrial fractionation

Mitochondrial matrix and membrane proteins were separated as described before (Cabassa-Hourton et al., 2016) with some modifications. *Arabidopsis* mitochondria samples (3 mg) were resuspended in 3 ml of sonication buffer (10 mM TES, 1 mM EDTA, 1 mM EGTA and 0.2 mM PMSF, pH 7.2). Mitochondria (1.5 ml of suspension) were broken by three freeze-thaw cycles and four 16-s sonication steps using an ultrasonic apparatus (Bioblock Scientific Vibracell 75041). Intact mitochondria were sedimented by centrifugation at $15000 \times g$ for 7 min at 4°C and removed. The supernatant was then ultra-centrifuged at $140000 \times g$ for 100 min at 4°C (Beckman Coulter Optima™ MAX ultracentrifuge, MLS-50 swinging rotor). The resulting pellet containing mitochondrial inner and outer membranes was resuspended in sonication buffer. The soluble fraction contained proteins of the mitochondrial matrix and inter membrane space. Samples were analysed by SDS-PAGE and western blots.

Western blot assays

Protein samples were separated by SDS-PAGE at 100 V at room temperature using either manually cast polyacrylamide gels (8.75% separation gel and 4% stacking gel, acrylamide/bis-acrylamide 29:1, 30% solution, Sigma-Aldrich) or the 7.5% TGX Stain-Free™ FastCast™ Acrylamide Kit (Bio-Rad). Separated proteins in gels were transferred to nitrocellulose or PVDF-LF membranes (Bio-Rad) in a Trans-Blot Semi-Dry Electrophoretic Transfer Cell (Bio-Rad) for 1 h at 100 V using transfer buffer (25 mM Tris-HCl, 192 mM glycine and 20% (v/v) ethanol, pH 8.3). Equal protein loading and integrity of protein samples were checked by Ponceau S staining or Stain-Free channel by ChemiDoc (Bio-Rad).

Immunodetection was performed using purified antibodies directed against either ProDH1, P5CDH, or OAT. The quality and purity of mitochondrial protein fractions were checked by western blots using alternative oxidase (AOX; Agrisera) and glycine decarboxylase (GDC; Agrisera) antibodies as controls for mitochondrial membrane and matrix fractions, respectively. Primary antibody binding was detected using either chemiluminescent secondary antibodies conjugated with a horseradish peroxidase (1:8000 dilution, SIGMA) and the ECL prime system (GE Healthcare) or using StarBright fluorescent secondary antibodies (1:2500 dilution) and the ChemiDoc system (Bio-Rad).

Two-dimensional PAGE

Separation of proteins from crude mitochondria was performed by 2D PAGE as described by Wittig et al. (2006). Mitochondrial protein samples were solubilized using 1% (w/v) digitonin solubilization buffer (30 mM HEPES, 150 mM potassium acetate, 10% (v/v) glycerol, pH 7.4) to a final protein concentration of 10 µg/µl, incubated for 20 min on ice, then centrifuged (10 min, 18300 × g, 4°C). Insoluble material was discarded and supernatants were analysed.

For the first dimension of BN PAGE, ~1000 µg of mitochondrial protein was solubilized per sample. The resultant supernatant was supplemented with 1 µl of Coomassie Blue loading buffer (750 mM aminocaproic acid, 5% (w/v) Coomassie blue 250 G) per 20 µl. Samples were directly loaded onto 4.5–16% (top to bottom) acrylamide gradient gels (acrylamide 4K-Solution 40%, 32:1) manually cast and electrophoresed using the PROTEAN II xi 2-D cell casting system (Bio-Rad). The same system was used for the second dimension of Tricine SDS-PAGE (Schägger, 2006) with 10% acrylamide separation and 8% acrylamide stacking gels. After

electrophoresis in both dimensions, gels were either used for western blot or stained with colloidal Coomassie blue (Schägger, 2006) for gel cutting.

For the first dimension of native PAGE, ~250 µg of mitochondrial protein was solubilized per sample. The resultant supernatant was mixed 3:1 (v/v) with 4 × native PAGE loading buffer (200 mM Tris-HCl pH 6.8, 40% (v/v) glycerol, 0.4% (w/v) bromophenol blue). Samples were directly loaded onto a native 4-15% (top to bottom) acrylamide gradient gel (Mini-PROTEAN TGX Stain-Free precast gel, Bio-Rad) and electrophoresed using the Mini-PROTEAN Tetra cell (Bio-Rad). The second dimension of SDS-PAGE was done using either the TGX Stain-Free™ FastCast™ Acrylamide Kit (7.5% acrylamide, Bio-Rad) or manually cast 8.75% acrylamide gels electrophoresed with the Mini-PROTEAN Tetra cell (Bio-Rad). After 2D electrophoresis, gels were either used for western blot or kept in water for gel cutting.

Tandem mass spectrometry (MS²) and complexome profiling

Gel spots (diameter 1 mm) were cut from gels after 2D BN/SDS-PAGE or 2D native/SDS-PAGE using sheared 100-µl disposable plastic pipettes. Gel slices (width 1 mm) were cut from gels after one dimensional (1D) BN-PAGE or native PAGE using a scalpel blade, which was thoroughly washed with ethanol for each cut (Senkler et al., 2017). Gel pieces were prepared for MS analyses by tryptic in-gel digestion and peptide extraction, as described before (Senkler et al., 2017).

MS-analysis was performed as outlined in Rugen et al. (2021) using an UltiMate 3000 nanoUPLC, coupled to a Q-Exactive mass spectrometer (both Thermo Fisher Scientific, Dreieich, Germany). In brief, peptides were first loaded onto a 2 cm trap column (inner diameter 100 µm, loaded with particles of 5 µm diameter and a pore size of 120 Å; Thermo Fisher Scientific, Dreieich, Germany). Separation was achieved on a 50 cm analytical column (inner diameter 75µm, loaded with particles of 3 µm diameter possessing a pore size of 120 Å; Thermo Fisher Scientific, Dreieich Germany) over a 60 min acetonitrile gradient (5.0% – 30.4% in 0.1% formic acid) using a flow rate of 250 nl/min . Transfer of positively charged peptides into the MS was accomplished using stainless steel emitters mounted in a Nanospray Flex source (Thermo Fisher Scientific) at 2.2 kV. Tandem MS² workflow employed a top-10 duty cycle. MS and MS² spectra were acquired using AGC targets of 10e6 and 10e5, and resolutions of 70,000 and 17,500, respectively. Raw files were processed using the MaxQuant software package (V2.0.1.0; Cox and Mann, 2008).

Complexome profiling was performed using hierarchical clustering as provided by the NOVA software (Giese et al., 2015) and is based on intensity based absolute quantification (iBAQ) values, as derived from MaxQuant using the following settings: method, hierarchic; linkage, average; distance function, Person correlation distance; normalization, none.

Co-immunoprecipitation (Co-IP) and LC-MS/MS analyses

Co-IP experiments were carried out with either total soluble proteins or mitochondrial proteins isolated from 35S:P5CDH-tGFP/*p5cdh* or 35S:tGFP/Col leaves after 4 days of DIS.

For co-IP from total proteins, 3 g of senescing leaves were ground in liquid nitrogen and resuspended in 15 ml of IP buffer (50 mM NaH₂PO₄, 150 mM NaCl, 0.5 mM EDTA, 5% glycerol, pH 7.5) supplemented with 0.1 mM PMSF and protease inhibitor cocktail (Sigma). The extract was then incubated with 1% (w/v) digitonin for 20 min at 4°C and centrifuged twice at 18300 × *g* for 10 min. The cleared supernatant was incubated with equilibrated 50 µl tGFP-Trap Agarose (Chromotek) for 2 h at 4 °C with end-over-end mixing. For co-IP from crude mitochondrial proteins, ~800 µg of 1% (w/v) digitonin-solubilized proteins were incubated with equilibrated 50 µl tGFP-Trap agarose (Chromotek) for 2 h at 4 °C. In both cases, tGFP-Trap Agarose was first saturated with 1% (w/v) BSA then equilibrated in IP buffer supplemented with 0.1% (w/v) digitonin before use.

After incubation, the supernatant was discarded. Beads were washed 4 times with 500 µl of IP buffer supplemented with 0.1% (w/v) digitonin, turning the tubes on a wheel for 5 min at 4°C between each washing step. The beads were resuspended in 1 × Laemmli buffer, boiled for 10 min and centrifuged for 2 min at 10000 × *g* to elute the dissociated proteins. Eluted proteins were subjected to SDS-PAGE and western blotting or analyzed by LC-MS/MS as described below.

A 1:1 (v/v) mixture of acetonitrile and 50 mM NH₄HCO₃ was used to destain gel plugs. Proteins in gel pieces were then digested overnight with either sequencing-grade trypsin (Promega) or chymotrypsin (ThermoFisher Scientific) at 37°C in 25mM NH₄HCO₃ buffer (20 µL final volume with 0.2 µg trypsin or 0.25 µg chymotrypsin). The resulting peptides were loaded and desalted on Evotips (Evosep, Odense, Denmark) according to the manufacturer's procedure.

Samples were analyzed on an Orbitrap Fusion mass spectrometer (ThermoFisher Scientific, Waltham, MA, USA) coupled with an Evosep One system (Evosep, Odense, Denmark) operating with the 30SPD method developed by the manufacturer. Briefly, the method is based

on a 44-min gradient and a total cycle time of 48 min with a C18 analytical column (0.15 × 150 mm, 1.9 μm beads, ref EV-1106) equilibrated at room temperature and operated at a flow rate of 500 nl/min with H₂O/0.1% formic acid as solvent A and acetonitrile/0.1% formic acid as solvent B. The mass spectrometer was operated in data-dependent MS/MS mode. Peptide masses were analyzed in the Orbitrap cell in full ion scan mode, at a resolution of 120,000, a mass range of m/z 350-1550 and an automatic gain control (AGC) target of 400000. MS/MS was performed in the top speed 3s mode. Peptides were selected for fragmentation by higher-energy C-trap dissociation with a normalized collisional energy of 27% and a dynamic exclusion of 60 s. Fragment masses were measured in an ion trap in the rapid mode, with an AGC target of 10000. Monocharged peptides and unassigned charge states were excluded from the MS/MS acquisition. The maximum ion accumulation times were set to 100 ms for MS and 35 ms for MS/MS acquisitions respectively.

Raw data processing was done using the PEAKS Studio XPro software (Bioinformatics Solutions Inc., Waterloo, ON, Canada). MS/MS spectra were searched against the UniprotKB protein database of *A. thaliana* (UP000006548, release 2020_11, 39345 Entries). A maximum of two missed cleavages were allowed, and precursor and fragment mass tolerances were set to respectively 15 ppm and 0.5 Da. Post-translational modifications (PTMs) were included with carbamidomethyl (C) as fixed and deamidation (NQ), and oxidation (M) as variable. The following variable PTMs were included in a second-round search using the PEAKS PTM module: acetylation (Protein N-term), acetylation (K), methylation (K, R), dimethylation (K, R), trimethylation (K, R) and phosphorylation (STY). The maximum of variable PTMs per peptide was set to 3 and MS/MS spectra were filtered at 1% FDR. Coverage and total intensities of the detected peptides were used to qualitatively assess the presence of differential (i.e. P5CDH interacting) proteins between J0 and J4 conditions.

Results

ProDH1, P5CDH and OAT interact in plant mitochondria

To test for putative interaction between *Arabidopsis* ProDH1, OAT, and P5CDH, a series of bimolecular fluorescence complementation (BiFC) assays was set up. This assay is based on producing the putative interacting protein partners fused with two non-fluorescent fragments of yellow fluorescent protein (YFP), YFP_N and YFP_C. If the proteins in question interact, they bring together YFP_N and YFP_C which fluoresce yellow when excited at the

appropriate wavelength. ProDH1, OAT, and P5CDH were each fused in frame with respectively YFP_N and YFP_C at the C-ter, thus keeping the mitochondrial targeting signals of the three enzymes intact at the N-ter of the fusions. *N. benthamiana* leaves were transformed with all possible combinations of the transgenic fusion constructs by infiltration. A binary plasmid encoding an mCherry-labelled mitochondrial matrix marker was also used as a control (Nelson et al., 2007) (Fig. 1, Supplemental Fig. S2 and S3).

Yellow fluorescence was observed in leaves over-expressing reciprocal fusions with the same enzyme, that is in leaves co-infiltrated with ProDH1-YFP_N and ProDH1-YFP_C, P5CDH-YFP_N and P5CDH-YFP_C, or OAT-YFP_N and OAT-YFP_C. The corresponding signals also co-localized with the fluorescence emitted by the mitochondrial mCherry marker (Fig. 1A). This indicates that all three enzymes can form homo-oligomers in plant mitochondria.

Yellow fluorescence signals were also observed in *N. benthamiana* leaves transiently transformed with the following combinations of fusion constructs: ProDH1-YFP_N and P5CDH-YFP_C, ProDH1-YFP_N and OAT-YFP_C, OAT-YFP_N and P5CDH-YFP_C (Fig.1), and P5CDH-YFP_N and OAT-YFP_C (Supplemental Fig. S2). Moreover, the YFP signals of these four co-infiltrations co-localized with signals from the mitochondrial marker (Fig. 1A, Supplemental Fig. S2).

As expected, no fluorescence was detected when leaves were co-infiltrated with a mixture of *A. tumefaciens* transformed with BiFC plasmids carrying the full-length cDNA of either *ProDH*, *P5CDH* or *OAT* and empty plasmids (Supplemental Fig. S2). Fusion protein expression in co-infiltrated leaves was examined by western blot for all infiltration combinations (Supplemental Fig. S3). Fusion proteins were detectable in all tested BiFC assays, though in variable amounts. Thus, the absence of YFP signal in some BiFC combinations was not due to the lack of protein expression. For example, YFP fluorescence was not detected in tobacco leaves infiltrated with P5CDH-YFP_N and ProDH1-YFP_C (Supplemental Fig. S2) or with OAT-YFP_N and ProDH1-YFP_C (data not shown), whereas the corresponding fusion proteins were properly expressed in these two combinations (Supplemental Fig. S3). These two negative fluorescence combinations were unexpected, but nevertheless demonstrate the specificity of the YFP fluorescence observed with the reciprocal construct combinations of ProDH1-YFP_N and P5CDH-YFP_C, and ProDH1-YFP_N and OAT-YFP_C (Figure 1). These results indicate that ProDH1, P5CDH, and OAT can interact with each other in pairs in mitochondria by forming hetero-oligomers (Fig. 1).

N. benthamiana leaves co-infiltrated with complementing combinations of YFP constructs were fixed with formaldehyde to immobilize mitochondria, which are usually

dynamic in living cells, in order to localise the fluorescence at the sub-mitochondrial level. This step made it possible to acquire high-resolution images of mitochondria by z-spacing confocal microscopy, such that the optical signals between mitochondrial matrix and inner membrane were distinguishable (Fig. 1B).

Localization of homo-oligomers of the three enzymes was assessed. Fluorescence signals of YFP and mCherry overlapped in leaves over-expressing *P5CDH-YFP_N* and *P5CDH-YFP_C* indicating that homo-oligomeric P5CDH is preferentially localized in the mitochondrial matrix (Fig. 1B). The fluorescence in leaves over-expressing *ProDH1-YFP_N* and *ProDH1-YFP_C* or *OAT-YFP_N* and *OAT-YFP_C* exhibited a mosaic pattern, which is consistent with a mitochondrial membrane localization. However, the mitochondria in these images of co-infiltrated cells were elongated and tubular, making it difficult to precisely determine the submitochondrial localization of P5CDH.

Confocal images of leaves overexpressing *ProDH1-YFP_N* and *P5CDH-YFP_C* exhibited clear mosaic patterns of fluorescence indicating that ProDH1 and P5CDH interacted in the mitochondrial membrane. For leaves over-expressing *ProDH1-YFP_N* and *OAT-YFP_C* or *OAT-YFP_N* and *P5CDH-YFP_C*, the fluorescence signal suggests the interacting proteins were localized in the matrix and membrane of mitochondria, which however had an atypical shape (Fig. 1B). These results show that the sub-mitochondrial localization of these proteins is more complex than previously described.

ProDH1, P5CDH and OAT are present in different sub-mitochondrial fractions during DIS in *Arabidopsis thaliana*

The sub-mitochondrial localization was further investigated in leaves of *Arabidopsis* Col-0, *prodh1prodh2*, *oat-1*, and *p5cdh-2* plants after 5 days of DIS, a condition in which the three P5C metabolism enzymes are expressed in WT and proline catabolism is underway (Kiyosue et al., 1996; Funck et al., 2010; Launay et al., 2019). Crude mitochondria from leaves were fragmented and the proteins fractionated according to their solubility. In order to evaluate the quality of mitochondrial sub-fractions and their degree of purity, alternative oxidase (AOX) and glycine decarboxylase complex (GDC) were used as markers of the mitochondrial inner membrane (Millenaar and Lambers, 2003) and mitochondrial matrix (Douce et al., 2001), respectively. AOX signal was only detected in membrane fractions, while GDC was only found in soluble fractions, indicating a distinct separation between mitochondrial membrane and soluble fractions (Fig. 2).

ProDH1 was predominantly localized in the mitochondrial membrane fraction. In contrast, OAT was predominantly localized in the soluble fraction, i.e., the mitochondrial matrix. P5CDH was observed in both fractions. These findings are fully consistent with the BiFC results from *N. benthamiana* for ProDH1, but only partially consistent for P5CDH and OAT (Fig. 1B), which may be due to the different physiological states of the leaves. The submitochondrial localizations of ProDH1, P5CDH, and OAT were the same in the different genetic backgrounds of the P5C metabolism mutants investigated. Taken together, these data provide direct molecular evidence for the differential but overlapping sub-mitochondrial localization of ProDH1, P5CDH, and OAT in the mitochondrial membrane and matrix.

Proteomic evidence for interactions between ProDH1, P5CDH and OAT during DIS in Arabidopsis leaves

To test whether the protein-protein interactions identified in the heterologous BiFC experiments reflected endogenous interactions, 2D BN/SDS-PAGE were performed using digitonin-solubilized crude mitochondria extracted from Arabidopsis Col-0 leaves incubated in DIS conditions. Two gels were run in parallel. After electrophoresis, one gel was stained with Coomassie blue and the other was used for blotted onto a nitrocellulose membrane and sequentially probed with primary antibodies directed against ProDH1, OAT, and P5CDH (Fig. 3B). Several signals for each protein of interest were revealed. Thirteen protein spots recognized by any of anti-ProDH, anti-P5CDH or anti-P5CDH sera were excised from the Coomassie blue stained gel (Fig. 3A) for analysis by mass spectrometry (MS) (Fig. 3C). ProDH1 was detected in 12 of the spots, OAT was detected in 5 spots (spots 5, 6, 9, 12, and 13), and P5CDH in 3 spots (spots 2, 3, and 4). These data confirmed the specificity of the immunoblotting.

ProDH1 signals were detected in a large gel area ranging from 70-300 kDa in the first dimension of the electrophoresis in BN conditions (hereafter designated 1D). In the second dimension of the electrophoresis in the presence of SDS (hereafter termed 2D), ProDH1 was detected at ~55 kDa as expected. Two signals of OAT were separated in 1D, one ranging from 70-146 kDa and the other around 146-200 kDa (Fig. 3B). Interestingly, all detected P5CDH signals in 1D were located around ~300 kDa. Molecular masses of these three proteins detected in 1D were higher than the theoretical molecular mass of their corresponding monomer. The difference is probably due to homo- or hetero-oligomerization.

In 1D, ProDH1 signals overlapped with OAT signals in the range 67-146 kDa and with P5CDH signals at around 300 kDa (Fig. 3A, C), which suggests that ProDH1 may interact with OAT and P5CDH during DIS.

If those two interactions do occur as the co-migration suggests, one cannot exclude the possibility that all three partners interact in a larger complex that may dissociate in the 1D due to the electrical repulsion generated by the negative charge of Coomassie blue (Eubel et al., 2005). To explore this possibility, 2D native/SDS-PAGE was performed using protein from crude mitochondria extracted from Col-0 DIS leaves (Fig. 4). In native PAGE (i.e. with no Coomassie blue), proteins are separated according to their net charge, size, and native structure, which preserves the native state of protein complexes during electrophoresis. The pattern of P5CDH after 2D native/SDS-PAGE is consistent with the BN/SDS-PAGE pattern (Fig. 4). One difference is that the ProDH1 signal is expanded in the native 1D gels, suggesting that ProDH1 may form other protein complexes. Significantly, the three proteins comigrated in 1D, suggesting they could form part of the same protein complex.

Identification of a P5CDH-interacting complex by complexome profiling

Complexome profiling was used to confirm whether ProDH1, P5CDH, and OAT interact in *Arabidopsis* mitochondria during DIS. Our approach was based on complementing *p5cdh* with a 35S:P5CDH-tGFP construct. The rationale was that P5CDH-interacting proteins, would exhibit a different migration pattern in 35S:P5CDH-tGFP/*p5cdh*, compared to WT P5CDH in Col-0. Crude mitochondria were extracted from Col-0 and 35S:P5CDH-tGFP/*p5cdh* leaves undergoing DIS. First, the transformation and complementation of *p5cdh* with P5CDH-tGFP construct was checked phenotypically *in vivo*. Although *p5cdh* mutant seedlings were unable to grow on MS media supplemented with proline 25 mM, *p5cdh* seedlings transformed with 35S:P5CDH-tGFP showed a WT phenotype in the presence of proline (Supplemental Fig. 1).

Next, mitochondria were isolated from the two genotypes and mitochondrial proteins were extracted then separated using 1D native PAGE. Gel lanes corresponding to each genotype were cut into 30 slices (1 mm), which were subjected to tryptic digestion and peptide identification by label-free quantitative MS. Based on the relative abundance of their constituent peptides (as estimated based on iBAQ values) in different gel slices, migration patterns for ProDH1, P5CDH and OAT were determined for the two genotypes (Fig. 5).

Several peaks in the migration profiles were observed for ProDH1 and OAT and to a lesser extent for P5CDH, which agrees with the native/SDS-PAGE results. The three proteins co-migrated at different positions and particularly in the gel slice number 18 in Col-0. In mitochondria extracted from 35S:P5CDH-tGFP/*p5cdh* leaves, the migration of P5CDH was clearly affected and shifted as predicted. Importantly, ProDH1 and OAT migration was also shifted, confirming that these three proteins interact in mitochondria of plants with a functioning P5CDH fusion protein. In particular, the peak observed in the gel slice 18 in Col-0 was shifted to slice 17 in P5CDH-tGFP/*p5cdh* samples. The migration profile of ProDH1 was more affected than that of OAT. Compared to Col-0, the migration pattern of ProDH1 was altered in P5CDH-tGFP/*p5cdh* samples in slices 9-16, indicating that migration of ProDH1 was affected by the change in the molecular mass of P5CDH-GFP. As a control, we checked whether these shifts were specific and several proteins with identical migration patterns in the two genotypes were identified (Supplemental Fig. S4). Notably some other proteins also had altered electrophoretic mobilities in P5CDH-tGFP/*p5cdh* samples, e.g., succinate dehydrogenase subunit SDH1-1 of respiratory chain Complex II (Supplemental Fig. S5).

ProDH1 and OAT co-immunoprecipitate with P5CDH-GFP

To further investigate the interaction between ProDH1, P5CDH and OAT, immunoprecipitation experiments were performed. Total digitonin-solubilized proteins extracted from 35S:tGFP/Col and 35S:P5CDH-tGFP/*p5cdh* leaves after 4 days of DIS were incubated with tGFP-Trap agarose beads. Immunoprecipitated proteins were separated by SDS-PAGE, transferred onto PVDF membrane, and probed with antibodies raised against ProDH1 (α -ProDH1) (Fig. 6A). A specific signal corresponding to ProDH1 was visible in immunoprecipitated samples from leaves overexpressing *P5CDH-tGFP*. This signal was absent in tGFP/Col-0 immunoprecipitated leaf protein samples, while two nonspecific bands were revealed in both samples.

Mitochondria were isolated from 35S:P5CDH-tGFP/*p5cdh* and WT leaves after 4 days of DIS (D4) and from non-treated 35S:P5CDH-tGFP/*p5cdh* leaves (D0) and solubilized as described above. Proteins immunoprecipitated with tGFP-Trap agarose beads (Fig. 6B) were electrophoresed through an SDS gel, transferred onto PVDF membrane, and probed first with α -ProDH1. In non-treated 35S:P5CDH-tGFP/*p5cdh* protein samples at D0, no ProDH1 was detected as expected, since ProDH1 expression is only induced upon senescence. The two bands detected in this sample are nonspecific because they appeared whatever the experimental

condition (Fig. 6A and 6B). In the control, ProDH1 did not interact with the tGFP-Trap agarose beads when WT mitochondrial fractions were used.

When immunoprecipitation was carried out on mitochondria extracted from 35S:P5CDH-tGFP/*p5cdh* leaves at D4, a major band corresponding to ProDH1 was observed, confirming that ProDH1 interacts with P5CDH during DIS. The presence of ProDH1 in this fraction and the absence in non-senescent mitochondria were confirmed by MS (Fig. 6D, Supplemental Table S2). The same PVDF membrane was then incubated with antibodies raised against OAT (Fig. 6C). A signal corresponding to OAT was revealed in protein samples of 35S:P5CDH-tGFP/*p5cdh* and WT leaves at D4 but not in 35S:P5CDH-tGFP/*p5cdh* mitochondria at D0. Only the immunoprecipitates corresponding to 35S:P5CDH-GFP/*p5cdh* mitochondria at D4 contained OAT. The presence of OAT in the D4 fraction and the absence in the non-senescent mitochondria were also confirmed by MS (Fig. 6D, Supplemental Table S2). Taken together, these results further demonstrate the interaction between ProDH1, P5CDH, and OAT during DIS *in vivo*.

Discussion

ProDH, P5CDH and OAT, all involved in P5C metabolism, share a common intermediate P5C/GSA, which may be toxic if not correctly regulated. Given that prokaryotic ProDH and P5CDH are sometimes in close proximity or physically interact, we hypothesized that coordination of the activities of the three eukaryotic P5C metabolism enzymes might rely on their physical interaction. In this study, using transgenic, imaging, biochemical and proteomic approaches, we demonstrate that ProDH1, P5CDH and OAT can interact and form a protein complex at least during DIS in leaves when all three enzymes are expressed.

ProDH1, P5CDH, and OAT interact in mitochondria during DIS.

We confirmed that ProDH1, P5CDH and OAT are expressed in mitochondria during DIS, and showed by BiFC that they are able to interact pairwise with themselves and each other. It was not surprising to observe homo-oligomerization since different oligomerization states have been previously described for ProDH1, P5CDH and OAT in several species (White et al., 2007; Luo et al., 2013; Montioli et al., 2017). Some combinations of fusion proteins involving ProDH1-YFP_C did not interact in the BiFC assays in tobacco leaves even though they were expressed and the corresponding hetero-oligomer formed in reciprocal assays (Supplemental

Fig. S2, Supplemental Fig. S3). This might be due to the structure of ProDH1-YFP_C, possibly preventing its interaction with P5CDH-YFP_N and OAT-YFP_N.

Sub-mitochondrial fractionation and confocal images of fixed BiFC samples indicate that ProDH1 is associated to the inner mitochondrial membrane. Indeed, the ProDH1 signal revealed by western blot is mainly in the membrane fraction and the BiFC results show that YFP and mCherry fluorescence signals did not overlap. ProDH1 has been described to localize in the matrix side of the mitochondrial inner membrane in both animals and plants (Brunner and Neupert, 1969; Elthon and Stewart, 1981; Cabassa-Hourton et al., 2016). Interactions between P5CDH and OAT could take place in the membrane or matrix since both proteins were found in these two compartments in this study. P5CDH was reported to associate with mitochondrial inner membrane in *Zea mays* (Elthon and Stewart, 1981) and the parasitic protozoan *Tr. cruzi* (Mantilla et al., 2015), but in the mitochondrial matrix in mouse (Brunner and Neupert, 1969). OAT is found in the mitochondrial matrix in animals (Doimo et al., 2013) and plants (Winter et al., 2015). The observed variability in submitochondrial localization could reflect differential protein-protein interactions that would target the proteins differently to the membrane or the matrix, possibly depending on cell physiology. For instance, our BiFC results showed that P5CDH homo-oligomers were localized in the matrix in plant cells, while P5CDH interacting with ProDH1 was more associated with membranes. This dual localization of P5CDH was also observed in sub-mitochondrial fractions evaluated by immunoblotting and in a *prodh1prodh2* mutant, indicating that ProDH alone cannot be responsible for the P5CDH interaction with membranes. As no transmembrane domain has been identified in P5CDH, it may rely on post-translational modifications, possibly triggered by DIS, to promote binding to the membrane. In particular, acylation could increase hydrophobicity of P5CDH and anchor P5CDH within the mitochondrial membrane (Chamberlain and Shipston, 2015). Interestingly, using biotin switch isobaric tagging to select S-acylated proteins from *Arabidopsis*, Hemsley (2015) identified 694 putative S-acylated proteins affecting diverse cellular processes, among them P5CDH. Further studies will be necessary to confirm that P5CDH can be anchored in mitochondrial membranes through S-acylation.

ProDH, P5CDH, and OAT can form a complex with other partners during DIS

The interaction between ProDH1 and P5CDH found in this study is consistent with the Rosetta Stone protein-protein interaction prediction that pairs of monofunctional homologs of fused bifunctional proteins in different organisms are likely to interact (Marcotte et al., 1999).

Moreover, such a bi-enzyme complex has been reported in *Th. thermophilus* (Sanyal et al., 2015). Kinetic data and surface plasmon resonance experiments were used to build a model showing one dimer of P5CDH associated to two monomers of ProDH. However, *in vivo* interactions between OAT and ProDH and/or P5CDH have never been described in any organism.

Native/SDS-PAGE and proteomic data suggest that ProDH, P5CDH, and OAT could be part of a larger complex. ProDH and to a lesser extent OAT have a widely spread pattern on 2D native gels, which could be due to dissociation of the complex during gel electrophoresis. We cannot exclude the possibility that only homo-oligomers dissociated, but some results suggest that a high-molecular-mass complex of these three enzymes and other partners could be present in mitochondria. First, in the co-IP experiments with P5CDH-tGFP, MS data indicate the presence of different subunits of succinate dehydrogenase, especially the SDH1-1 subunit mainly at D4 of DIS, and SDH2-1 and SDH2-2 at D0 (Supplemental Table S2). Interestingly, in native PAGE, SDH1-1 has a migration profile that overlaps with those of ProDH1, P5CDH, and OAT. In addition, the migration pattern of SDH1-1 was altered in P5CDH-tGFP/*p5cdh* samples, as was the case for ProDH1 and OAT. Taken together, these results support the theory that there is an interaction in mitochondria between Complex II of the respiratory chain and a P5C metabolic complex composed of ProDH1, P5CDH and OAT in *Arabidopsis*. Further investigation is needed but this hypothesis is consistent with other findings. For example, by using the membrane-permeable crosslinker DSP, Hancock et al. (2016) showed that ProDH can be co-immunoprecipitated with both SDH1 and SDH2 subunits in mouse mitochondria. P5CDH was also found to co-migrate with Complex II subunits in *Tr. cruzi* (Mantilla et al., 2015). In addition, succinate has been found to be a non-competitive inhibitor of ProDH in a cultured human colorectal cancer cells. In *Arabidopsis*, the respiratory rate of Complex II is significantly decreased in the *prodh1prodh2* double mutant compared with WT (Launay et al., 2019). Interaction with the Complex II might contribute to binding ProDH, P5CDH and OAT to the inner mitochondrial membrane.

The functional relevance of the association between ProDH, P5CDH and OAT during DIS is still unknown. Given that the complex tends to dissociate during electrophoresis, the dissociation constant (K_D) is probably high, but this needs to be determined experimentally *in vitro* in reconstitution assays with recombinant enzymes. A high K_D would be consistent with the likely dynamic behaviour of these interactions that could be modulated by post-translational modifications. Succinylation, acetylation and phosphorylation of P5CDH have been described in mouse (Park et al., 2013; Rardin et al., 2013; Zhou et al., 2013; Bian et al., 2014). Mouse

ProDH1 and OAT have also been reported to be acetylated (Rardin et al., 2013). In plants, as well as the aforementioned S-acylation of P5CDH in *Arabidopsis* (Hemsley, 2015), acetylation of P5CDH has been reported (König et al., 2014). Phosphorylation of the three proteins has also been described in plants (Wang et al., 2020) and some related phosphopeptides are present in the PhosPhAt database (Heazlewood et al., 2008).

One of the main benefits proposed for the association of enzymes catalysing sequential reactions is the channelling of intermediates (Sweetlove and Fernie, 2018). When ProDH oxidizes proline into GSA/P5C that is then converted into glutamate by P5CDH, NADH and FADH₂ are produced concomitantly, which impacts the mitochondrial electron transfer chain. OAT uses α -ketoglutarate, a compound of the TCA cycle, and ornithine to produce glutamate and P5C. The association between ProDH1, P5CDH and OAT could be a way to channel the inherently unstable and potentially toxic P5C/GSA to the appropriate enzyme and thus coordinate and regulate arginine and proline metabolisms. Substrate-channelling has been documented in both PutA (Srivastava et al., 2010; Singh et al., 2014) and the monofunctional ProDH-P5CDH complex of *Th. thermophilus* (Sanyal et al., 2015), but has not yet been reported for OAT. The physiological role of the interactions in the P5C metabolism complex detected in plants needs further investigation with fluxomics approaches, for example. To conclude, we show that ProDH1, P5CDH and OAT are able to interact in mitochondria of senescing *Arabidopsis* leaves.

Acknowledgements

We are grateful to Susanne Bolte and Jean-François Gilles from the IBPS imaging core facility for help with confocal microscopy and 3D rendering of organelles. This work was supported by Sorbonne University, Leibniz University Hannover, and the PROCOPE program between Germany and France (grant number 46711VJ). This work was supported by a grant from the China Scholarship Council to YZ. We thank Région Ile de France for financial support of ProteoSeine@IJM platform.

Figures and tables

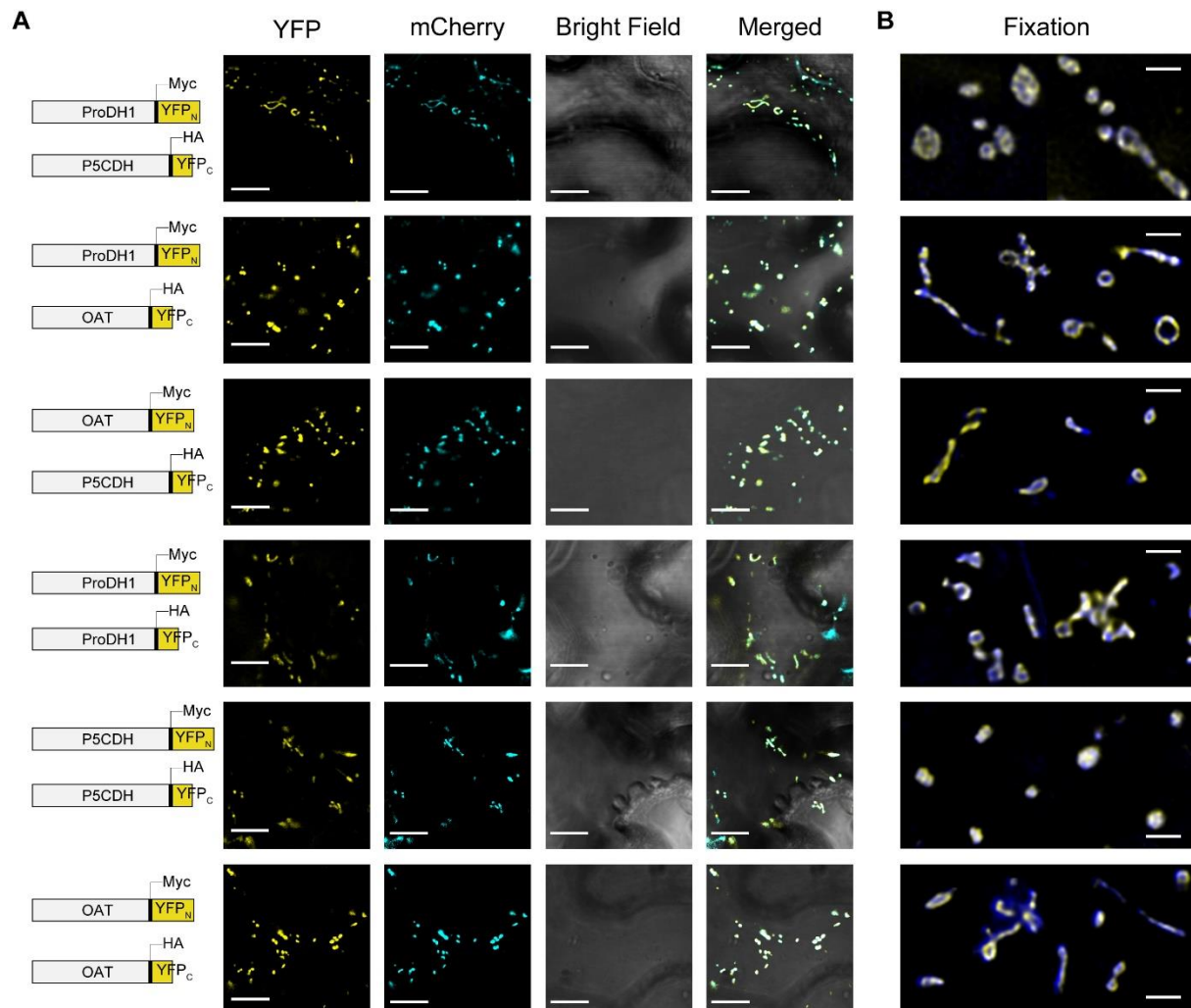


Figure 1. BiFC assays with ProDH1, P5CDH, and OAT in *Nicotiana benthamiana*

(A) Confocal analyses of living epidermal cells of *N. benthamiana* showing transient expression of the infiltrated plasmid combinations indicated schematically on the left of each panel. The size of each cassette is proportional to the corresponding CDS length. YFP panels show YFP fluorescent signals; mCherry panels indicate the position of mitochondria; bright field panels show the cellular structure of the tobacco epidermal cells under white light; and merged panels show merged images from the three channels. Bars = 10 µm. For control experiments, see Supplemental Fig. S2.

(B) Z-spacing confocal analyses coupled with image deconvolution of fixed epidermal cells of *N. benthamiana* infiltrated with the plasmid combinations indicated on the left as in (A). YFP signals, which indicate the localization of protein interaction, are yellow. mCherry signals from the matrix of mitochondria are blue. The overlap between YFP and mCherry signals are shown in white. Bars = 1.5 µm.

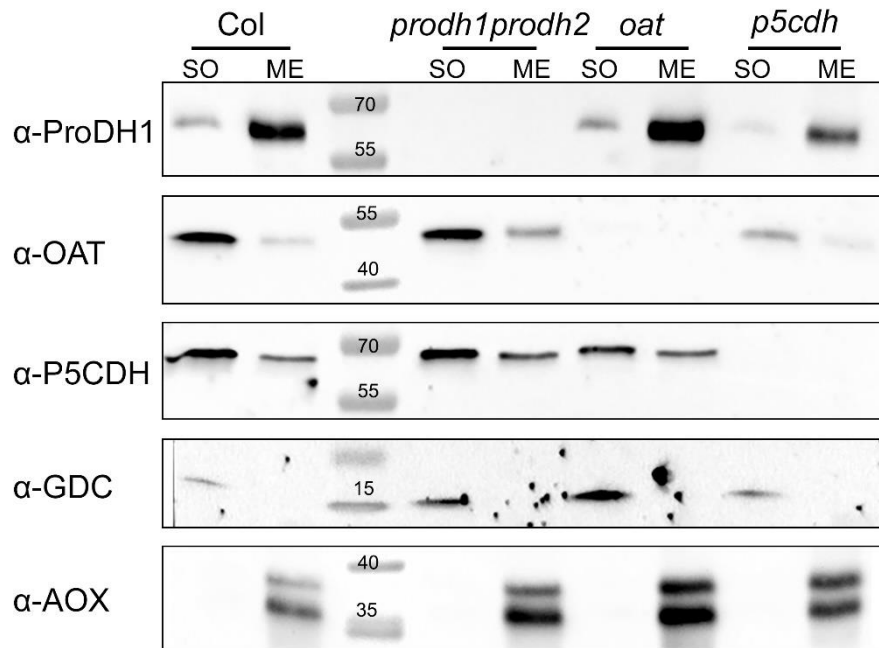


Figure 2. Sub-mitochondrial localization of ProDH1, P5CDH, and OAT in *Arabidopsis thaliana* during DIS

Crude mitochondria were isolated from 4-week-old *A. thaliana* plants of the indicated genotypes after 5 days of DIS. Crude mitochondria were subjected to sonication and ultra-centrifugation to separate mitochondrial membranes from matrix. The same amounts of protein were loaded into each well of SDS-polyacrylamide gels which were blotted onto nitrocellulose membrane. Blots were probed with antibodies against alternative oxidase (α -AOX), glycine decarboxylase complex (α -GDC), α -ProDH1, α -P5CDH and α -OAT. ME, membrane fraction containing proteins from the mitochondrial inner and outer membrane; SO, soluble fraction containing proteins from the mitochondrial intermembrane space and matrix.

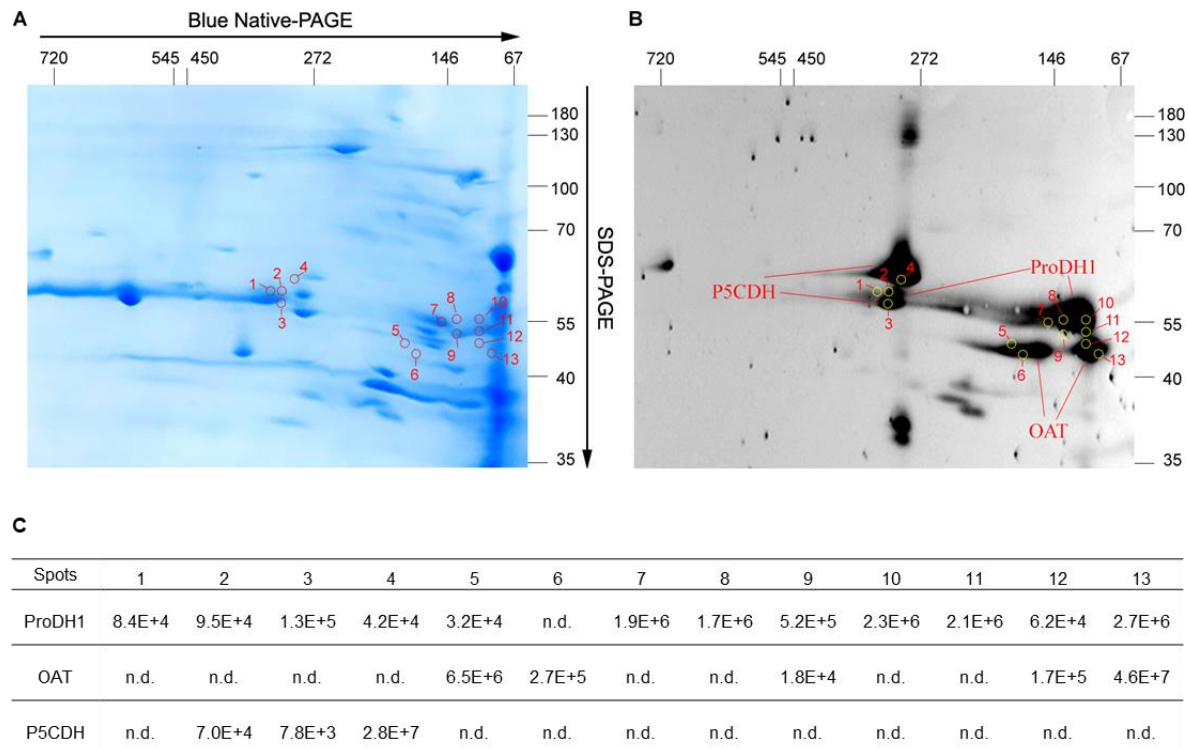


Figure 3. Proteomic analysis of ProDH1, P5CDH, and OAT in mitochondrial fractions of *Arabidopsis thaliana* using 2D BN/SDS-PAGE, immunoblotting and MS

Crude mitochondria were extracted from Col-0 leaves of *A. thaliana* after 5 days of DIS and solubilized by 1% (w/v) digitonin. Proteins were separated by 2D BN/SDS PAGE, loading 1 mg of mitochondrial protein on each of two gels run in parallel. After electrophoresis, one gel was stained with Coomassie blue (A), and the other was used for western blotting (B). The masses of standard proteins are given on the top and the right of each gel image (in kDa). In western blots (B), primary antibodies against ProDH1, OAT, and P5CDH were incubated sequentially with the same membrane, as labelled. Gel spots excised from the Coomassie blue stained gel (A) subjected to MS analysis are indicated by circles and numbered. iBAQ values obtained by MS analysis are shown in (C) for the abundance of ProDH1, OAT, and P5CDH peptides detected. The maximum iBAQ value of each protein is displayed in bold (C). N.d., not detected.

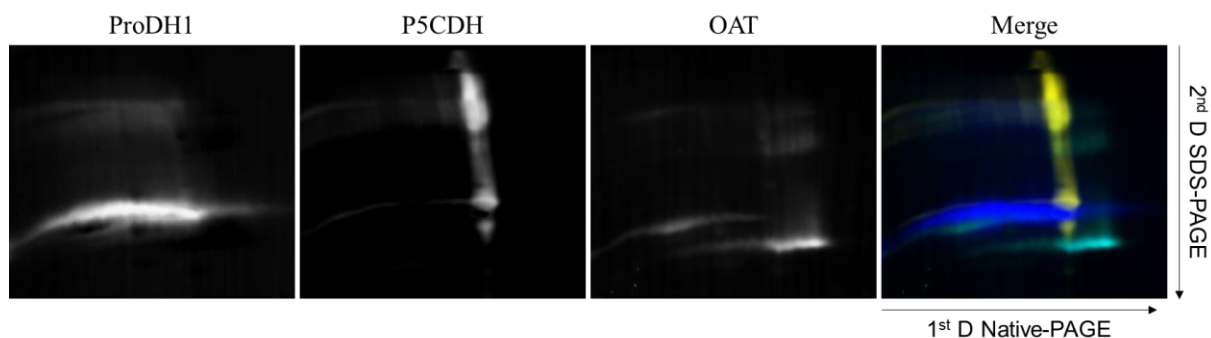


Figure 4. ProDH1, P5CDH, and OAT expressed during DIS in *Arabidopsis thaliana* co-migrate on 2D native/SDS gels

Crude mitochondria were extracted from Col-0 leaves of *Arabidopsis* after 5 days of DIS, and solubilized by 1% (w/v) digitonin. Mitochondrial protein (250 μ g) was separated by 2D native/SDS-PAGE, and the proteins transferred to a PVDF membrane, which was sequentially incubated with antibodies raised against ProDH1 (blue), OAT (cyan), and P5CDH (yellow) and analyzed using Image J.

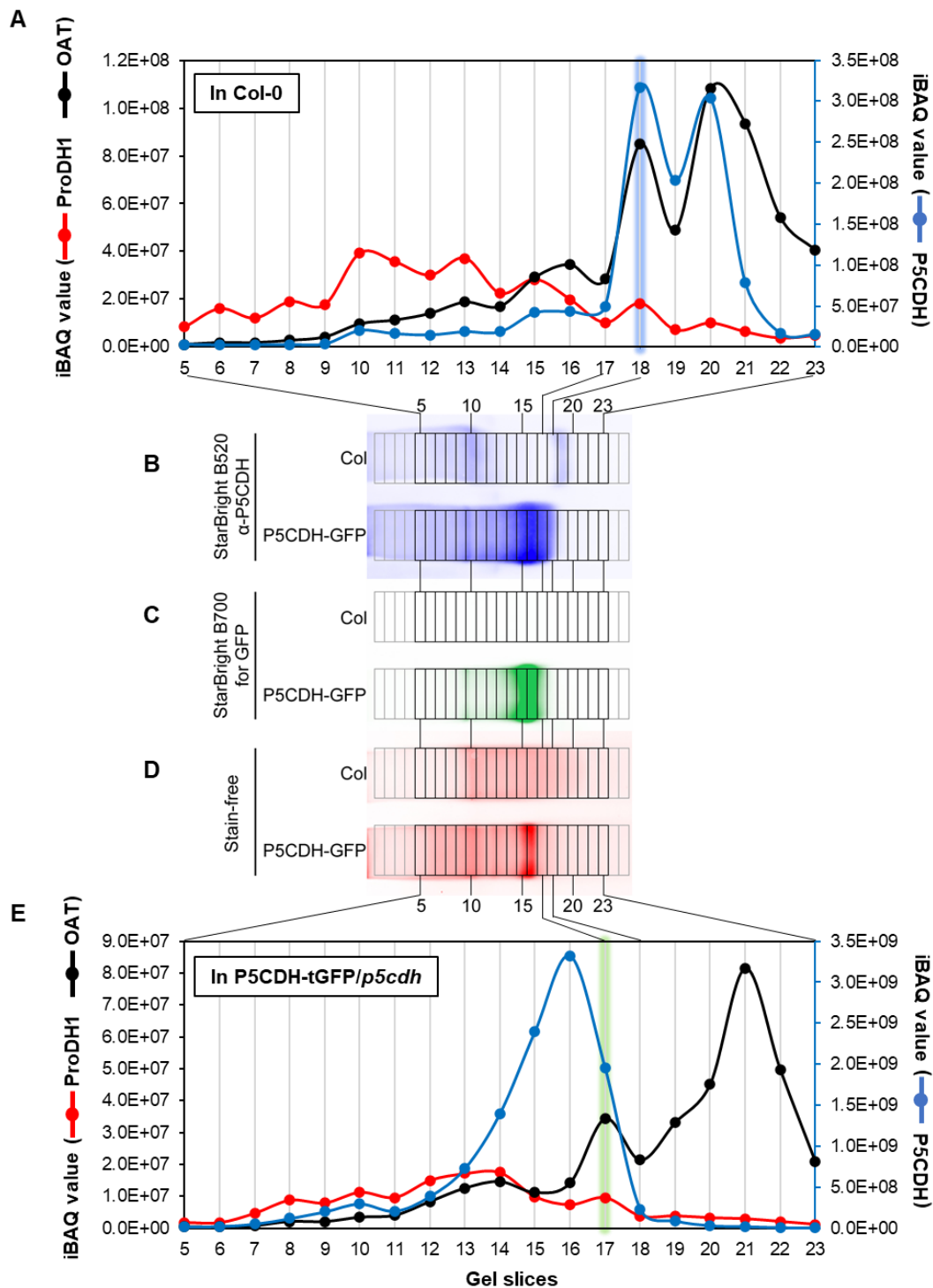


Figure 5. Comparative complexome profiling of mitochondria from two Arabidopsis lines

Crude mitochondria extracted from Col-0 and P5CDH-tGFP/p5cdh *Arabidopsis* leaves after 5 days of DIS were solubilized with 1% (w/v) digitonin and separated by 1D native-PAGE (130 μ g of mitochondrial protein). After electrophoresis, gels were incubated with Stain-free reagent, imaged, then blotted on to a membrane, which was probed with an antibody against P5CDH (B). Membranes or gels were visualized using the StarBright B700 channel for the GFP signal of the P5CDH-GFP protein (C) or the Stain-free channel for total protein (D). Gel slices were cut as indicated in (B-D); gel slices 5 to 23 were used for label-free MS analysis. The iBAQ values of ProDH1, P5CDH, and OAT in Col-0 (A) and P5CDH-tGFP/p5cdh (E) are visualized in the alignments shown in parts B-D of the Figure.

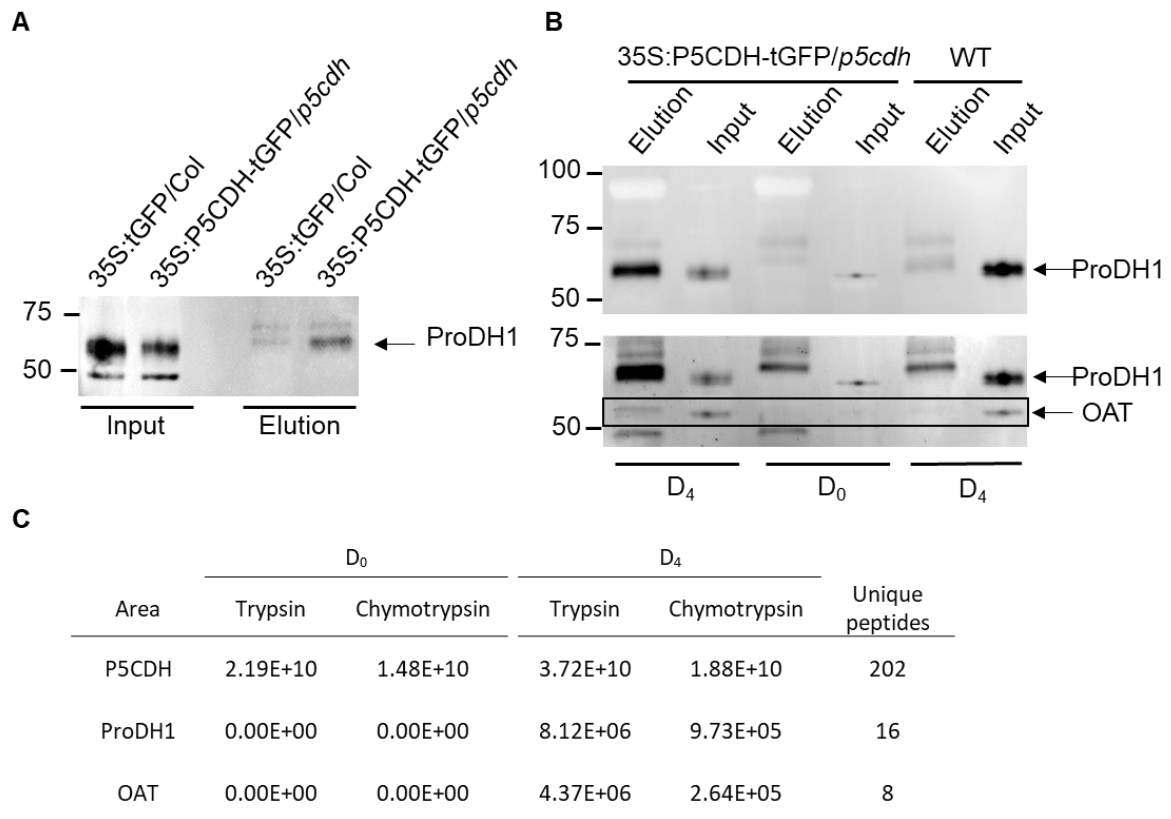
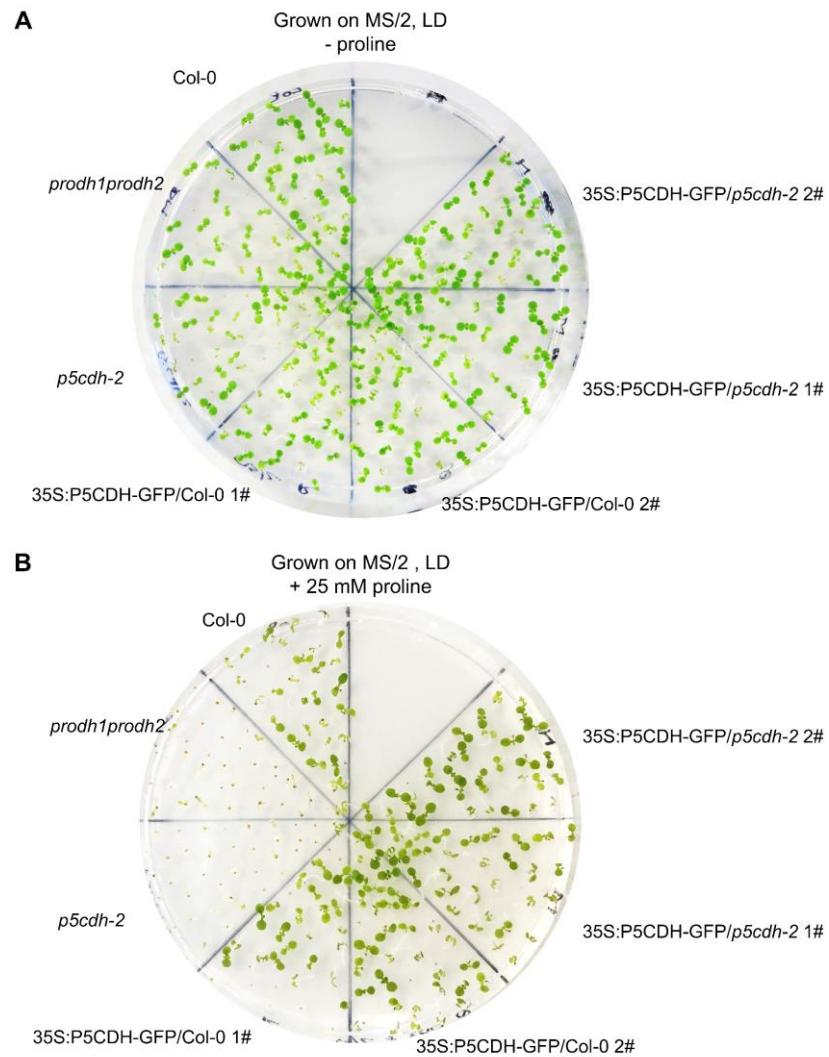


Figure 6. Co-immunoprecipitation (Co-IP) of ProDH1 and OAT with P5CDH-tGFP

(A) Co-IP using tGFP agarose beads from total proteins extracted from 35S:tGFP/Col and 35S:P5CDH-tGFP/*p5cdh* plants after 4 days of DIS. Western blots of total protein extract (Input) and the eluted fraction were probed with antibodies raised against ProDH1.

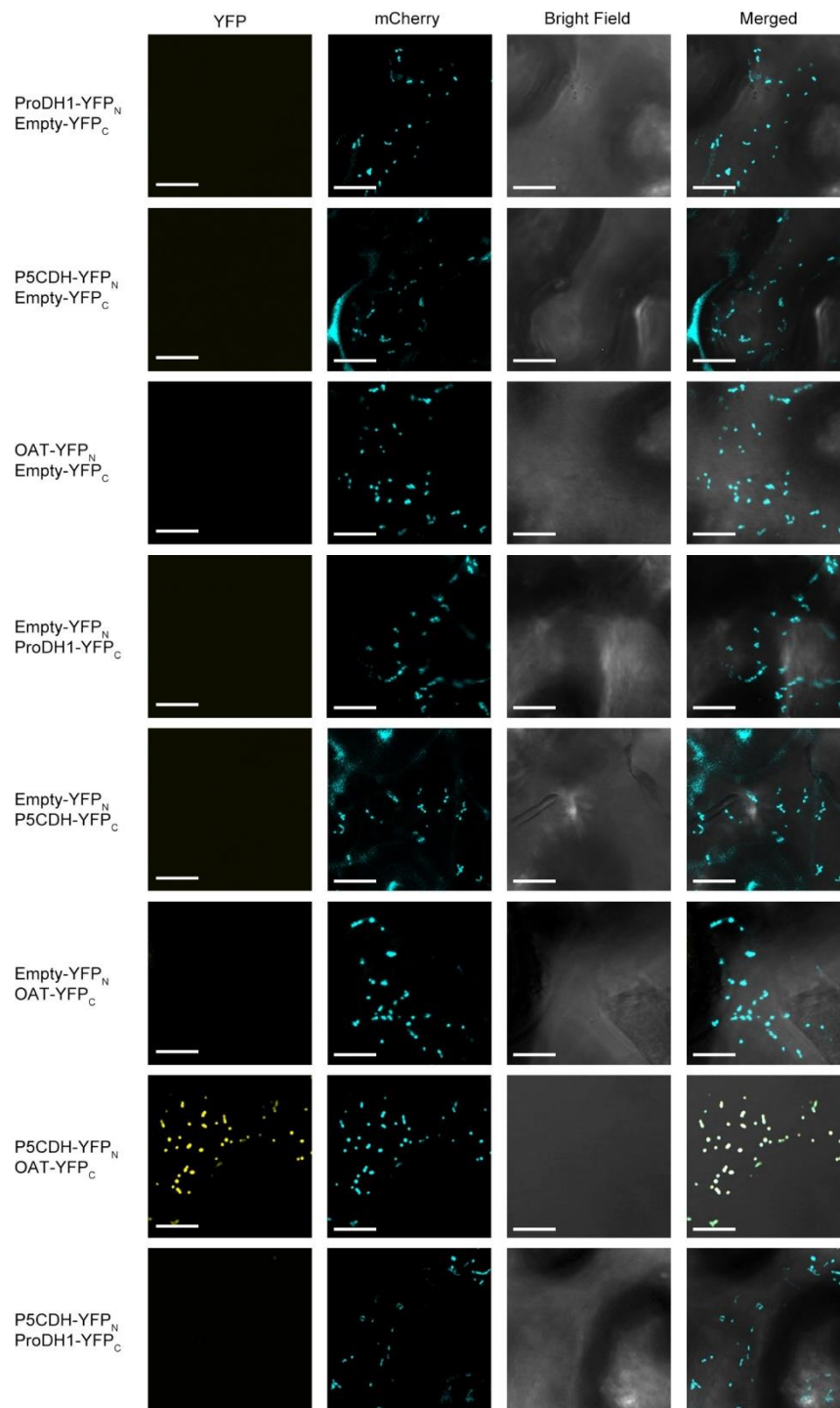
(B) Co-IP using tGFP agarose beads from mitochondrial extracts before (D₀) or after 4 days of DIS (D₄) from 35S:P5CDH-tGFP/*p5cdh* and/or WT leaves. Western blots of total protein extract (Input) and the eluted fraction were probed with antibodies raised against ProDH1. The same membrane was then incubated with antibodies raised against OAT. The white signal corresponds to P5CDH-tGFP.

(C) Mass spectrometry analysis of Co-IP from mitochondrial extracts from either D₀ or D₄ 35S:P5CDH-tGFP/*p5cdh* leaves.



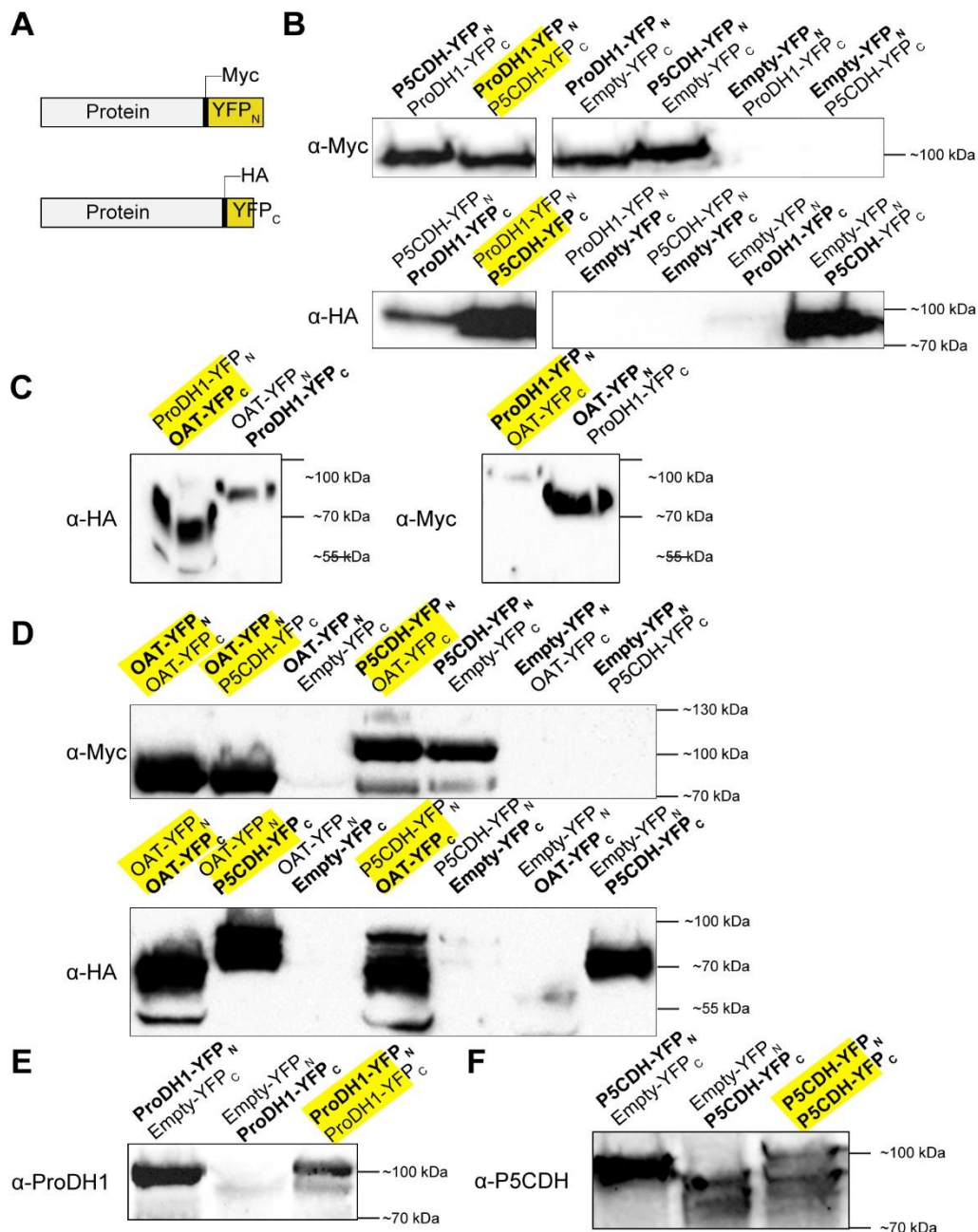
Supplemental Figure S1. Proline sensitivity of *p5cdh* was complemented in 35S:P5CDH-tGFP/*p5cdh* plants.

Seeds of different genotypes (as indicated in the Figure) were sterilized, stratified at 4°C for 72h and grown on MS/2 media supplemented without (A) or with 25 mM proline (B) for 7 days.



Supplemental Figure S2. Controls and additional BiFC assays in *Nicotiana benthamiana*.

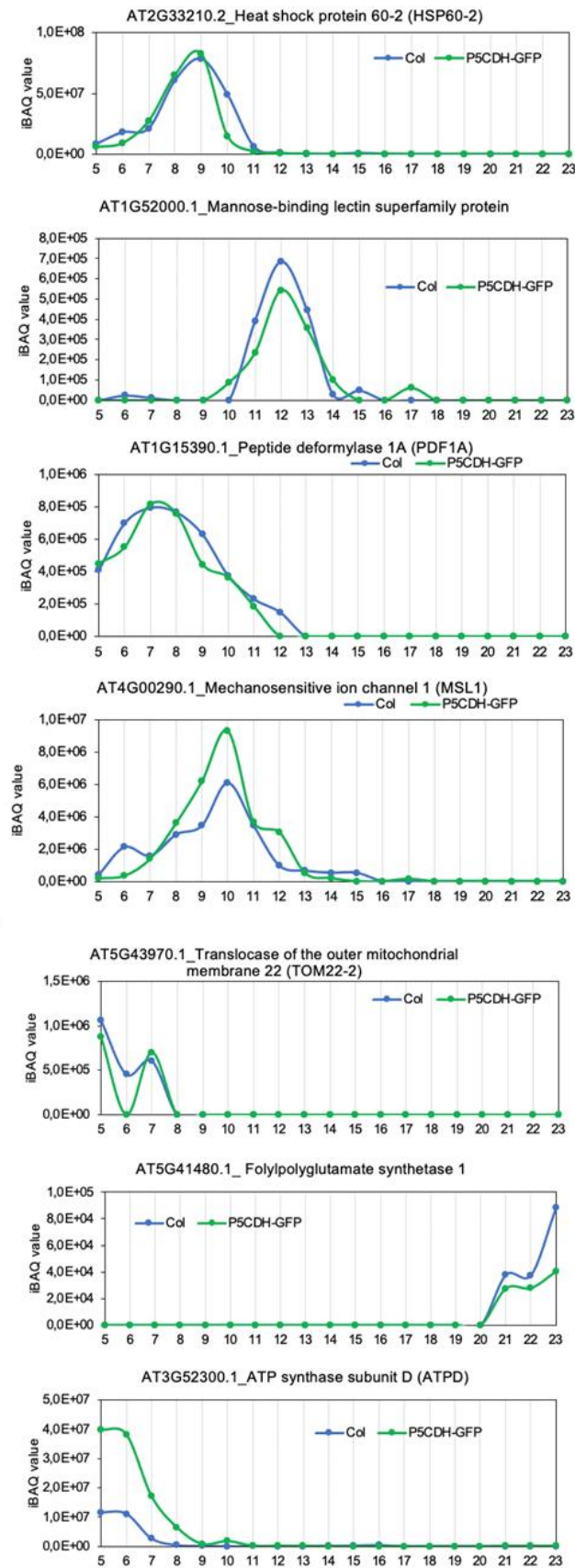
YFP channel shows YFP fluorescent signals; mCherry channel indicates the location of mitochondria; bright field channel shows the cellular structure of tobacco epidermal cell under white light; merged channel shows picture merged with other three channels. Bar = 10 μ m.



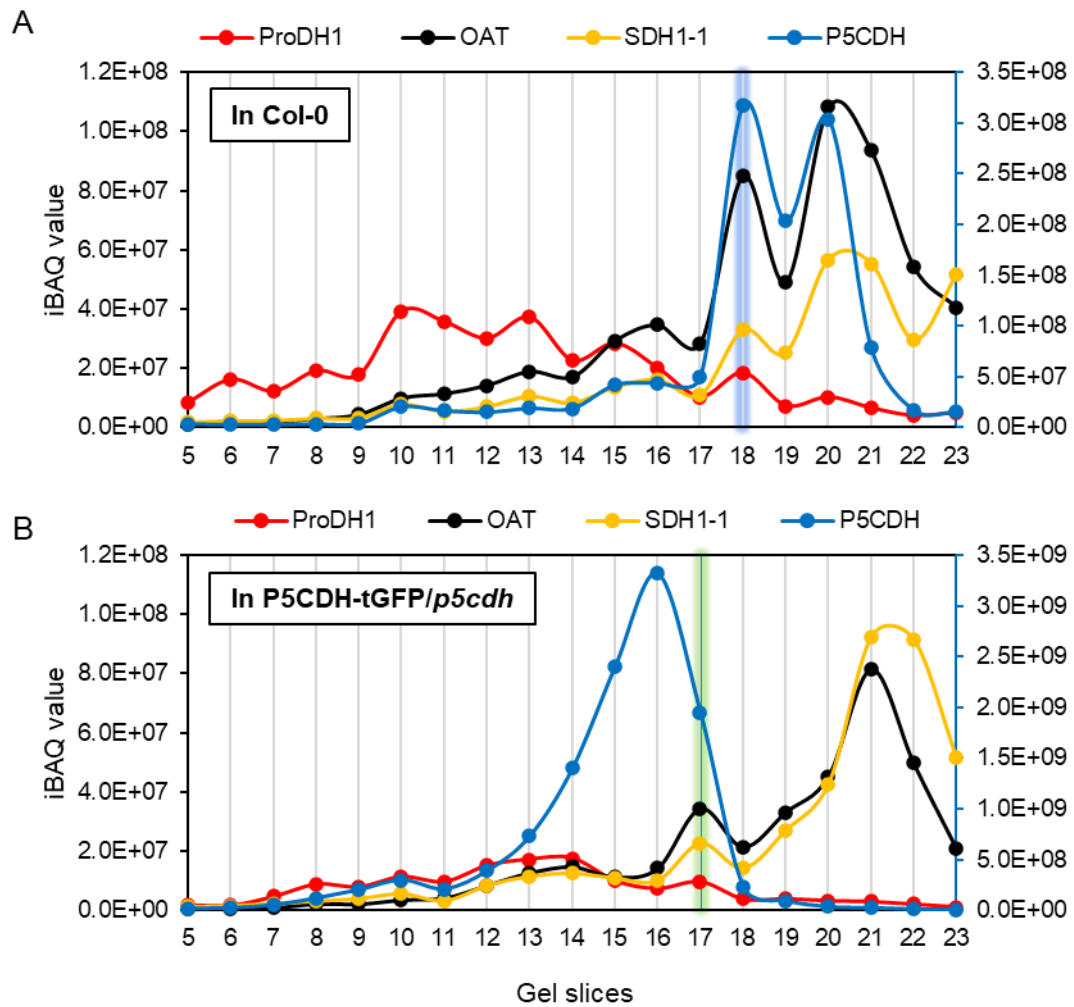
Supplemental Figure S3. Protein expression of BiFC infiltrated *Nicotiana benthamiana* leaves.

(A) Representative diagram of constructions used for BiFC assays. Cassettes are presented in 5' to 3' direction. The size of each cassette is based on their nucleic acid sequence length. Gray box, insertion of the CDS fragment of each construction; Myc, c-myc epitope tag; HA, hemagglutinin epitope tag; YFP_N, N-terminal fragment of eYFP; YFP_C, C-terminal fragment of eYFP.

(B-F) Total proteins were extracted from tobacco leaves infiltrated with the combination of plasmids indicated on the top of each western-blot. Same amount of proteins were loaded on SDS-PAGE gels, transferred onto a nitrocellulose membrane and revealed with antibodies raised against c-Myc or HA tags. Constructs with positive YFP signal are labelled with yellow backgrounds. The theoretical molecular weight of B4-ProDH1 is 73.7 kDa; B5-ProDH1, 65.6 kDa; B4-OAT, 70.9 kDa; B5-OAT, 62.8 kDa; B4-P5CDH, 80.5 kDa; B5-P5CDH, 72.4 kDa.



Supplemental Figure S4. Migration pattern of selected proteins not affected by P5CDH-tGFP. The iBAQ values of each protein in Col-0 and P5CDH-tGFP/*p5cdh* in different gel slices are shown.



Supplemental Figure S5. Complexome profiling for SDH1-1.

The iBAQ value of ProDH1, P5CDH, OAT, and succinate dehydrogenase 1-1 (SDH1-1) in Col-0 (A) and P5CDH-tGFP/p5cdh (B) are shown. The iBAQ values of P5CDH is shown on the right y-axis, iBAQ values of the other proteins are shown on the left y-axis.

Supplemental Table S1. List of primers used for cloning

| Gene name | Gene ID number | Direction | Primer Name | Primer sequence 5' to 3' |
|-----------|----------------|-----------|---------------------|--|
| P5CDH | At5g62530 | Forward | P5CDH-BiFC-BamHI-F | <u>CGGGATCCATGTATAGAGTTTTTGGC</u> |
| | | Reverse | P5CDH-BiFC-KpnI-R | <u>GGGGTACCAGTAGATGGAGGAAGTTC</u> |
| ProDH1 | At3g30775 | Forward | ProDH1-BiFC-BamHI-F | <u>CGGGATCCATGGCAACCCGTCTTCT</u> |
| | | Reverse | ProDH1-BiFC-KpnI-R | <u>GGGGTACCAATCCC GGCG</u> |
| OAT | At5g46180 | Forward | OAT-BamHI-F | <u>CGGGATCCATGGCAGCCACCACGAGAC</u> |
| | | Reverse | OAT-KpnI-R | <u>GGGGTACCAGCATAGAGGTTTCTTCCACAGC</u> |
| ProDH2 | At5g38710 | Forward | ProDH2-BiFC-BamHI-F | <u>CGGGATCCATGGCAAACCGTTTCCTCC</u> |
| | | Reverse | ProDH2-BiFC-KpnI-R | <u>GGGGTACCCCAAGCCATAACTCTT</u> |

Primers for directed mutagenesis to remove internal BsaI site, C-315-G, done on P5CDH-pET30b(+):

Forward GATTTGAAAGGGTTATGCAGACCATGTTTCGGGC
Reverse GCCCGAAACATGGTCTGCATAACCCTTTCAAATC

Primers for cloning in pAGM1287 (MoClo Tool Kit, Addgene) with BsaI + without STOP codon + addition of the Enterokinase recognition and cleavage site:

Forward TGGTCTCAAATGTATAGAGTTTTTTG
Reverse AGGTCTCACGAAGCCTTATCGTCATCGTCAGTAGATGGAGGAAG

Supplemental Table S2. LC-MS/MS data from gel slice analyses

Table S2 is an Excel file which will be available online after our manuscript is published.

References

- Alvarez ME, Savouré A, Szabados L** (2021) Proline metabolism as regulatory hub. Trends in Plant Science. *In press* doi: 10.1016/j.tplants.2021.07.009
- Anwar A, She M, Wang K, Riaz B, Ye X** (2018) Biological Roles of Ornithine Aminotransferase (OAT) in Plant Stress Tolerance: Present Progress and Future Perspectives. *International Journal of Molecular Sciences* **19**: 3681
- Bent A** (2006) *Arabidopsis thaliana* Floral Dip Transformation Method. *In* K Wang, ed, *Agrobacterium Protocols*. Humana Press, Totowa, NJ, pp 87–104
- Bian Y, Song C, Cheng K, Dong M, Wang F, Huang J, Sun D, Wang L, Ye M, Zou H** (2014) An enzyme assisted RP-RPLC approach for in-depth analysis of human liver phosphoproteome. *Journal of Proteomics* **96**: 253–262
- Brunner G, Neupert W** (1969) Localisation of proline oxidase and Δ -pyrroline-5-carboxylic acid dehydrogenase in rat liver. *FEBS Letters* **3**: 283–286
- Cabassa-Hourton C, Schertl P, Bordenave-Jacquemin M, Saadallah K, Guivarc'h A, Lebreton S, Planchais S, Klodmann J, Eubel H, Crilat E, et al** (2016) Proteomic and functional analysis of proline dehydrogenase 1 link proline catabolism to mitochondrial electron transport in *Arabidopsis thaliana*. *Biochemical Journal* **473**: 2623–2634
- Cecchini NM, Monteoliva MI, Alvarez ME** (2011) Proline Dehydrogenase Contributes to Pathogen Defense in *Arabidopsis*. *Plant Physiology* **155**: 1947–1959
- Chamberlain LH, Shipston MJ** (2015) The Physiology of Protein S-acylation. *Physiol Rev* **95**: 341–376
- Chrobok D, Law SR, Brouwer B, Lindén P, Ziolkowska A, Liebsch D, Narsai R, Szal B, Moritz T, Rouhier N, et al** (2016) Dissecting the Metabolic Role of Mitochondria during Developmental Leaf Senescence. *Plant Physiol* **172**: 2132–2153
- Cox J, Mann M** (2008) MaxQuant enables high peptide identification rates, individualized p.p.b.-range mass accuracies and proteome-wide protein quantification. *Nat Biotechnol* **26**: 1367–1372
- Deuschle K, Funck D, Forlani G, Stransky H, Biehl A, Leister D, Graaff E van der, Kunze R, Frommer WB** (2004) The Role of Δ 1-Pyrroline-5-Carboxylate Dehydrogenase in Proline Degradation. *The Plant Cell* **16**: 3413–3425
- Deuschle K, Funck D, Hellmann H, Däschner K, Binder S, Frommer WB** (2001) A nuclear gene encoding mitochondrial Δ^1 -pyrroline-5-carboxylate dehydrogenase and its potential role in protection from proline toxicity. *The Plant Journal* **27**: 345–356
- Doimo M, Desbats MA, Baldoin MC, Lenzini E, Basso G, Murphy E, Graziano C, Seri M, Burlina A, Sartori G, et al** (2013) Functional Analysis of Missense Mutations of OAT, Causing Gyrate Atrophy of Choroid and Retina. *Human Mutation* **34**: 229–236
- Elthon TE, Stewart CR** (1981) Submitochondrial Location and Electron Transport Characteristics of Enzymes Involved in Proline Oxidation. *PLANT PHYSIOLOGY* **67**: 780–784
- Engler C, Youles M, Gruetzner R, Ehnert T-M, Werner S, Jones JDG, Patron NJ, Marillonnet S** (2014) A Golden Gate Modular Cloning Toolbox for Plants. *ACS Synth Biol* **3**: 839–843
- Eubel H, Braun H-P, Millar Ah** (2005) Blue-native PAGE in plants: a tool in analysis of protein-protein interactions. *Plant Methods* **1**: 11
- Farrant RD, Walker V, Mills GA, Mellor JM, Langley GJ** (2001) Pyridoxal Phosphate De-activation by Pyrroline-5-carboxylic Acid: INCREASED RISK OF VITAMIN B6 DEFICIENCY AND SEIZURES IN HYPERPROLINEMIA TYPE II*. *Journal of Biological Chemistry* **276**: 15107–15116
- Fichman Y, Gerdes SY, Kovács H, Szabados L, Zilberstein A, Csonka LN** (2015) Evolution of proline biosynthesis: enzymology, bioinformatics, genetics, and transcriptional regulation. *Biological Reviews* **90**: 1065–1099
- Funck D, Baumgarten L, Stift M, von Wirén N, Schönemann L** (2020) Differential Contribution of P5CS Isoforms to Stress Tolerance in *Arabidopsis*. *Front Plant Sci*. doi: 10.3389/fpls.2020.565134

- Funck D, Eckard S, Müller G** (2010) Non-redundant functions of two proline dehydrogenase isoforms in *Arabidopsis*. *BMC Plant Biology* **10**: 70
- Funck D, Stadelhofer B, Koch W** (2008) Ornithine- δ -aminotransferase is essential for Arginine Catabolism but not for Proline Biosynthesis. *BMC Plant Biol* **8**: 40
- Giese H, Ackermann J, Heide H, Bleier L, Dröse S, Wittig I, Brandt U, Koch I** (2015) NOVA: a software to analyze complexome profiling data. *Bioinformatics* **31**: 440–441
- Gu D, Zhou Y, Kallhoff V, Baban B, Tanner JJ, Becker DF** (2004) Identification and Characterization of the DNA-binding Domain of the Multifunctional PutA Flavoenzyme. *Journal of Biological Chemistry* **279**: 31171–31176
- Hayat S, Hayat Q, Alyemeni MN, Wani AS, Pichtel J, Ahmad A** (2012) Role of proline under changing environments. *Plant Signaling & Behavior* **7**: 1456–1466
- Heazlewood JL, Durek P, Hummel J, Selbig J, Weckwerth W, Walther D, Schulze WX** (2008) PhosPhAt: a database of phosphorylation sites in *Arabidopsis thaliana* and a plant-specific phosphorylation site predictor. *Nucleic Acids Res* **36**: D1015–1021
- Hemsley PA** (2015) The importance of lipid modified proteins in plants. *New Phytol* **205**: 476–489
- Jortzik E, Fritz-Wolf K, Sturm N, Hipp M, Rahlfs S, Becker K** (2010) Redox Regulation of *Plasmodium falciparum* Ornithine δ -Aminotransferase. *Journal of Molecular Biology* **402**: 445–459
- Kiyosue T, Yoshiba Y, Yamaguchi-Shinozaki K, Shinozaki K** (1996) A nuclear gene encoding mitochondrial proline dehydrogenase, an enzyme involved in proline metabolism, is upregulated by proline but down-regulated by dehydration in *Arabidopsis*. *The Plant Cell* **8**: 1323–1335
- König A-C, Hartl M, Boersema PJ, Mann M, Finkemeier I** (2014) The mitochondrial lysine acetylome of *Arabidopsis*. *Mitochondrion* **19**: 252–260
- Korasick DA, Končítíková R, Kopečná M, Hájková E, Vigouroux A, Moréra S, Becker DF, Šebela M, Tanner JJ, Kopečný D** (2019) Structural and Biochemical Characterization of Aldehyde Dehydrogenase 12, the Last Enzyme of Proline Catabolism in Plants. *Journal of Molecular Biology* **431**: 576–592
- Launay A, Cabassa-Hourton C, Eubel H, Maldiney R, Guivarc'h A, Crilat E, Planchais S, Lacoste J, Bordenave-Jacquemin M, Clément G, et al** (2019) Proline oxidation fuels mitochondrial respiration during dark-induced leaf senescence in *Arabidopsis thaliana*. *Journal of Experimental Botany* **70**: 6203–6214
- Lerma-Ortiz C, Jeffryes JG, Cooper AJL, Niehaus TD, Thamm AMK, Frelin O, Aunins T, Fiehn O, de Crécy-Lagard V, Henry CS, et al** (2016) ‘Nothing of chemistry disappears in biology’: the Top 30 damage-prone endogenous metabolites. *Biochemical Society Transactions* **44**: 961–971
- Liu W, Phang JM** (2012) Proline dehydrogenase (oxidase) in cancer. *BioFactors* **38**: 398–406
- Lowry O, Rosebrough N, Farr AL, Randall R** (1951) Protein measurement with the Folin phenol reagent. *Journal of Biological Chemistry* **193**: 265–275
- Luo M, Singh RK, Tanner JJ** (2013) Structural Determinants of Oligomerization of Δ 1-Pyrroline-5-Carboxylate Dehydrogenase: Identification of a Hexamerization Hot Spot. *Journal of Molecular Biology* **425**: 3106–3120
- Mantilla BS, Paes LS, Pral EMF, Martil DE, Thiemann OH, Fernández-Silva P, Bastos EL, Silber AM** (2015) Role of Δ 1-Pyrroline-5-Carboxylate Dehydrogenase Supports Mitochondrial Metabolism and Host-Cell Invasion of *Trypanosoma cruzi**. *Journal of Biological Chemistry* **290**: 7767–7790
- Marcotte EM, Pellegrini M, Ng H-L, Rice DW, Yeates TO, Eisenberg D** (1999) Detecting Protein Function and Protein-Protein Interactions from Genome Sequences. *Science* **285**: 751–753
- Maxwell SA, Davis GE** (2000) Differential gene expression in p53-mediated apoptosis-resistant vs. apoptosis-sensitive tumor cell lines. *Proceedings of the National Academy of Sciences* **97**: 13009–13014
- Mestichelli LJ, Gupta RN, Spenser ID** (1979) The biosynthetic route from ornithine to proline. *Journal of Biological Chemistry* **254**: 640–647
- Montioli R, Zamparelli C, Borri Voltattorni C, Cellini B** (2017) Oligomeric State and Thermal Stability of Apo- and Holo- Human Ornithine δ -Aminotransferase. *Protein J* **36**: 174–185

- Nelson BK, Cai X, Nebenfuhr A** (2007) A multicolored set of in vivo organelle markers for co-localization studies in Arabidopsis and other plants. *Plant J* **51**: 1126–36
- Nishimura A, Nasuno R, Takagi H** (2012) The proline metabolism intermediate Δ 1-pyrroline-5-carboxylate directly inhibits the mitochondrial respiration in budding yeast. *FEBS Letters* **586**: 2411–2416
- Park J, Chen Y, Tishkoff DX, Peng C, Tan M, Dai L, Xie Z, Zhang Y, Zwaans BMM, Skinner ME, et al** (2013) SIRT5-Mediated Lysine Desuccinylation Impacts Diverse Metabolic Pathways. *Molecular Cell* **50**: 919–930
- Pemberton TA, Tanner JJ** (2013) Structural basis of substrate selectivity of Δ 1-pyrroline-5-carboxylate dehydrogenase (ALDH4A1): Semialdehyde chain length. *Archives of Biochemistry and Biophysics* **538**: 34–40
- Phang JM** (2019) Proline Metabolism in Cell Regulation and Cancer Biology: Recent Advances and Hypotheses. *Antioxidants & Redox Signaling* **30**: 635–649
- Rardin MJ, Newman JC, Held JM, Cusack MP, Sorensen DJ, Li B, Schilling B, Mooney SD, Kahn CR, Verdin E, et al** (2013) Label-free quantitative proteomics of the lysine acetylome in mitochondria identifies substrates of SIRT3 in metabolic pathways. *PNAS* **110**: 6601–6606
- Roosens NH, Bitar FA, Loenders K, Angenon G, Jacobs M** (2002) Overexpression of ornithine- δ -aminotransferase increases proline biosynthesis and confers osmotolerance in transgenic plants. *Molecular Breeding* **9**: 73–80
- Rugen N, Schaarschmidt F, Eirich J, Finkemeier I, Braun H-P, Eubel H** (2021) Protein interaction patterns in *Arabidopsis thaliana* leaf mitochondria change in dependence to light. *Biochimica et Biophysica Acta (BBA) - Bioenergetics* **1862**: 148443
- Sanyal N, Arentson BW, Luo M, Tanner JJ, Becker DF** (2015) First Evidence for Substrate Channeling between Proline Catabolic Enzymes: A VALIDATION OF DOMAIN FUSION ANALYSIS FOR PREDICTING PROTEIN-PROTEIN INTERACTIONS. *J Biol Chem* **290**: 2225–2234
- Schägger H** (2006) Tricine–SDS-PAGE. *Nature Protocols* **1**: 16–22
- Sekhar PN, Amrutha RN, Sangam S, Verma DPS, Kishor PBK** (2007) Biochemical characterization, homology modeling and docking studies of ornithine δ -aminotransferase—an important enzyme in proline biosynthesis of plants. *Journal of Molecular Graphics and Modelling* **26**: 709–719
- Senkler J, Senkler M, Eubel H, Hildebrandt T, Lengwenus C, Schertl P, Schwarzländer M, Wagner S, Wittig I, Braun H-P** (2017) The mitochondrial complexome of *Arabidopsis thaliana*. *The Plant Journal* **89**: 1079–1092
- Servet C, Ghelis T, Richard L, Zilberstein A, Savoure A** (2012) Proline dehydrogenase: a key enzyme in controlling cellular homeostasis. *Front Biosci* **17**: 607–620
- Silao FGS, Ward M, Ryman K, Wallström A, Brindefalk B, Udekwu K, Ljungdahl PO** (2019) Mitochondrial proline catabolism activates Ras1/cAMP/PKA-induced filamentation in *Candida albicans*. *PLOS Genetics* **15**: e1007976
- Singh H, Arentson BW, Becker DF, Tanner JJ** (2014) Structures of the PutA peripheral membrane flavoenzyme reveal a dynamic substrate-channeling tunnel and the quinone-binding site. *Proceedings of the National Academy of Sciences* **111**: 3389–3394
- Srivastava D, Schuermann JP, White TA, Krishnan N, Sanyal N, Hura GL, Tan A, Henzl MT, Becker DF, Tanner JJ** (2010) Crystal structure of the bifunctional proline utilization A flavoenzyme from *Bradyrhizobium japonicum*. *PNAS* **107**: 2878–2883
- Srivastava D, Singh RK, Moxley MA, Henzl MT, Becker DF, Tanner JJ** (2012) The Three-Dimensional Structural Basis of Type II Hyperprolinemia. *Journal of Molecular Biology* **420**: 176–189
- Stránská J, Tylichová M, Kopečný D, Snégaroff J, Šebela M** (2010) Biochemical characterization of pea ornithine- δ -aminotransferase: Substrate specificity and inhibition by di- and polyamines. *Biochimie* **92**: 940–948
- Sweetlove LJ, Fernie AR** (2018) The role of dynamic enzyme assemblies and substrate channelling in metabolic regulation. *Nat Commun.* doi: 10.1038/s41467-018-04543-8
- Szabados L, Savouré A** (2010) Proline: a multifunctional amino acid. *Trends in Plant Science* **15**: 89–97

- Tanner JJ** (2008) Structural biology of proline catabolism. *Amino Acids* **35**: 719–730
- Teulier L, Weber J-M, Crevier J, Darveau C-A** (2016) Proline as a fuel for insect flight: enhancing carbohydrate oxidation in hymenopterans. *Proceedings of the Royal Society B: Biological Sciences* **283**: 20160333
- Valsecchi I, Guittard-Crilat E, Maldiney R, Habricot Y, Lignon S, Lebrun R, Miginiac E, Ruelland E, Jeanette E, Lebreton S** (2013) The intrinsically disordered C-terminal region of *Arabidopsis thaliana* TCP8 transcription factor acts both as a transactivation and self-assembly domain. *Mol BioSyst* **9**: 2282–2295
- Waadt R, Schmidt LK, Lohse M, Hashimoto K, Bock R, Kudla J** (2008) Multicolor bimolecular fluorescence complementation reveals simultaneous formation of alternative CBL/CIPK complexes in planta. *Plant J* **56**: 505–16
- Wang P, Hsu C-C, Du Y, Zhu P, Zhao C, Fu X, Zhang C, Paez JS, Macho AP, Tao WA, et al** (2020) Mapping proteome-wide targets of protein kinases in plant stress responses. *Proc Natl Acad Sci U S A* **117**: 3270–3280
- Weber E, Engler C, Gruetzner R, Werner S, Marillonnet S** (2011) A Modular Cloning System for Standardized Assembly of Multigene Constructs. *PLOS ONE* **6**: e16765
- White TA, Krishnan N, Becker DF, Tanner JJ** (2007) Structure and Kinetics of Monofunctional Proline Dehydrogenase from *Thermus thermophilus*. *Journal of Biological Chemistry* **282**: 14316–14327
- Winter G, Todd CD, Trovato M, Forlani G, Funck D** (2015) Physiological implications of arginine metabolism in plants. *Frontiers in Plant Science*. doi: 10.3389/fpls.2015.00534
- Wittig I, Braun H-P, Schagger H** (2006) Blue native PAGE. *Nat Protoc* **1**: 418–428
- You J, Hu H, Xiong L** (2012) An ornithine δ -aminotransferase gene *OsOAT* confers drought and oxidative stress tolerance in rice. *Plant Science* **197**: 59–69
- Zheng Y, Cabassa-Hourton C, Planchais S, Lebreton S, Saviouré A** (2021) The proline cycle as a eukaryotic redox valve. *Journal of Experimental Botany*. *In press*. doi: 10.1093/jxb/erab361
- Zhou H, Di Palma S, Preisinger C, Peng M, Polat AN, Heck AJR, Mohammed S** (2013) Toward a Comprehensive Characterization of a Human Cancer Cell Phosphoproteome. *J Proteome Res* **12**: 260–271

4.1 Supplementary results

4.1.1 Heat map for proteins co-migrate with P5CDH

Apart from the SDH1-1 mentioned in the article, 14 proteins were identified that presented a migration pattern exhibiting a shift from gel slice 18 (in Col-0) to 17 (in P5CDH-GFP/*p5cdh*) (Fig. 1). These proteins belong to the same cluster with P5CDH in both Col-0 and P5CDH-GFP/*p5cdh* genotypes. They are promising candidates for P5CDH-interacting proteins.

However, the cluster analysis may not identify true putative interacting proteins. The cluster analysis calculate correlation according to the entire migration pattern of a given protein. If only part of the migration peak, instead of all peaks, overlapped between two proteins, the cluster analysis will assign them to different clusters. It is the reason that ProDH1 was not assigned to the same cluster as P5CDH. ProDH1 signals spread in most of gel slices, without a dominant peak. In contrast, P5CDH present dominant peaks. Thus, complexome profiling is a way to identify putative interacting protein partners but additional studies should be done to confirm these interactions.

4.1.2 Putative interaction between ProDH1 and SDH1-1 is strengthened by 1D BN-PAGE followed with MS

Prior to carry on the complexome profiling using 1D Native-PAGE, we have performed a primary experiment using 1D BN-PAGE followed with gel cutting and MS analysis (Fig. 2). In this study, P5CDH peaked in slice 10, while ProDH and OAT peaked in slice 40 (Fig. 2C). P5CDH overlapped with ProDH1 only in slice 10, while OAT overlapped with ProDH1 in slices 26, 27, 40, and 43 (Fig. 2C). This result was consistent with the 2D BN/SDS-PAGE result shown in the previous manuscript, where P5CDH was separated from ProDH and OAT indicating a putative dissociation among these proteins.

Moreover, subunits of Complex II were also detected in this experiment as the complexome profiling results in the article. Consistently, only SDH1-1 exhibited a clear and similar migration pattern with ProDH1 (Fig. 2D) in contrast to the other subunits of Complex II, further indicating putative interaction between SDH1-1 and ProDH1.

Chapter IV. Pyrroline-5-carboxylate metabolism protein complex detected in *Arabidopsis thaliana* leaf mitochondria

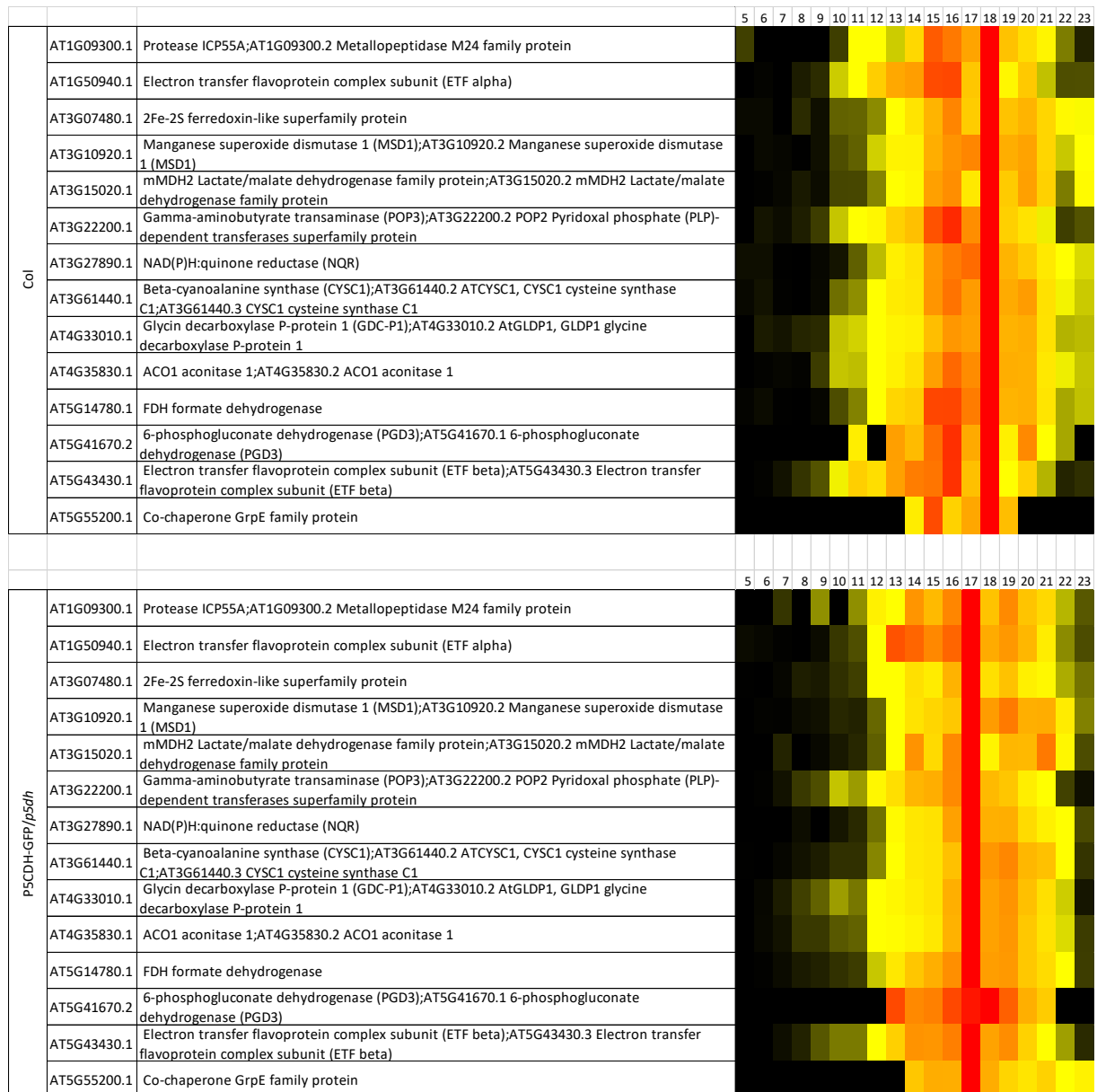


Figure 1. Heat map of proteins that co-migrate with P5CDH in the complexome profiling analysis. Data are from the complexome profiling indicated in Figure 5 in the previous article, which were normalized using maximum normalization and clustered using the Pearson Correlation distance function. Heat map of proteins that co-migrate with P5CDH in both Col-0 and P5CDH-GFP/p5cdh (as indicated on the left of this figure) is showed.

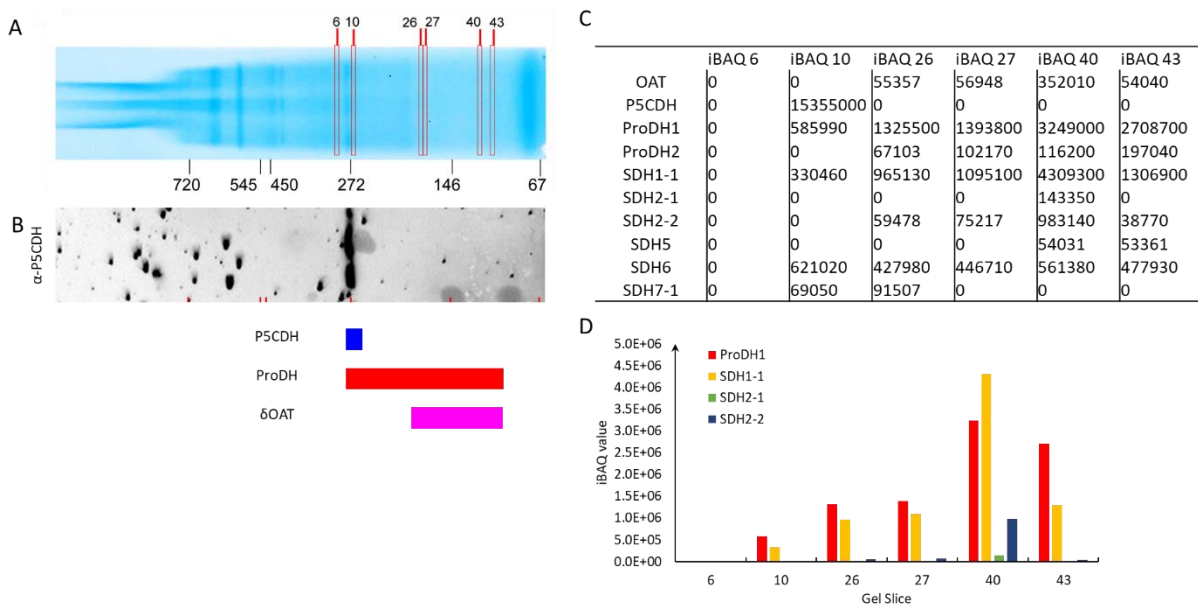


Figure 2. 1D BN-PAGE gel cutting followed with MS analysis. 500 μ g of mitochondrial proteins extracted from 5 d DIS treated leaves were solubilized with 1% digitonin and loaded on a 1D BN-PAGE gel for each lane. Two gel lanes were migrated at the same time. One gel lane was used for Coomassie Blue staining (A), the other one was subject to western-blot with antibody raised against P5CDH (B). The theoretical migration range of P5CDH, ProDH, and OAT deduced from previous experiments (data not shown) and western-blot of P5CDH (B) are shown below the western-blot in (B). The 1D BN-PAGE gel lane was cut as shown in (A). The resulting gel slices were analyzed by MS and the iBAQ value is shown in (C-D). Gel slice 6 is a negative control.

4.1.3 DSP crosslinking reveals high molecular weight complex of ProDH1, P5CDH, and OAT

TtProDH-TtP5CDH interaction found in *T. thermophilus* is transient and weak, whose dissociation constant is 3 μ M (Sanyal *et al.*, 2015). Protein dissociation found in our BN/SDS-PAGE results suggests that eukaryotic mitochondrial P5C metabolic complex identified in this study maybe also transient and weak. To improve its stability and identity other candidate partners of the complex, succinimidyl propionate (DSP) cross-linking experiments has been performed. DSP is a membrane-permeable and thiol-cleavable cross-linker, which is widely used for crosslinking of intracellular proteins (Gaucher *et al.*, 2006; Hancock *et al.*, 2016).

In addition, putative interaction submitochondrial localization of ProDH2, ProDH1, and P5CDH have been investigated by BiFC assay.

Crude mitochondria extracted from 5-day DIS-treated leaves were incubated with or without DSP. Samples were then either subjected or not to digitonin membrane protein

solubilization. Finally, all the samples were subjected to SDS-PAGE and Western-blot experiments (Fig. 3).

Optimal conditions for DSP treatment were determined with 5-day DIS treated Col crude mitochondria samples. Different concentrations of DSP (0.125 mM, 0.25 mM, 0.5 mM and 1 mM) and different incubating time (15 min, 30 min and 2h) were tested. A concentration as low as 0.125 mM for 15 min was sufficient to induce cross-linking of ProDH and P5CDH. Higher concentrations of DSP or longer incubation time will lead to the sequestration of our candidate proteins in the membrane fraction.

Experiments were first carried out on Col and subsequent Western blots were revealed with antibodies raised against ProDH1, P5CDH and OAT. For samples treated with DSP, different high molecular weight signals were observed whatever the antibodies used, which are disappeared after DTT treatment as expected. Some of them, especially with ProDH1 and P5CDH, were still present when no reducing agent was added even in the absence of DSP (Fig. 3). These results indicate that ProDH1, P5CDH and to a lesser extent OAT may form high MW complex(es) that could involve disulphide bonds.

The migration pattern of ProDH1 was different in *p5cdh* mutant mitochondria in presence of DSP. Higher MW bands appeared whereas low MW bands of ProDH1 disappeared in *p5cdh* mutant compared to Col, indicating the oligomerization states of ProDH1 was altered in *p5cdh* mutant (Fig. 4), which suggests the interaction between ProDH1 and P5CDH. In contrast, no obvious difference of the P5CDH migration pattern was observed between Col and *prodh1prodh2* mutant in presence of DSP (Fig. 3). This experiment suggests that P5CDH may homo-oligomerize as well as form complex with other partners than ProDH1. However, this cannot exclude the possibility that signals corresponding to ProDH1-P5CDH interaction could be masked by the signals of other complexes.

Aiming to study the submitochondrial localization of the high MW signals of ProDH1 and P5CDH, we performed DSP-crosslinking experiments without digitonin solubilization, using 3 cycles of freeze-thaw with liquid nitrogen to break mitochondria instead. Such that, the mitochondrial soluble proteins should be released, whereas membrane proteins will be removed by centrifugation.

Without digitonin solubilization, P5CDH was significantly less detectable in Col (Fig. 4a), whereas ProDH1 was not detectable (data not shown). These findings are consistent with the membrane localization of ProDH1 and the dual localisation of P5CDH evidenced by submitochondrial fragmentation results in the article. In contrast to previous results (Fig.1a), without digitonin solubilization P5CDH was hardly detected in absence of reducing reagents (Fig.

4a), suggesting the previous detected high MW P5CDH signals may be localized to mitochondrial membrane.

Taken together, our crosslinking results showed that (1) ProDH1, P5CDH and to a lesser extent OAT may form high MW complex(es) mediated by disulphide bonds; (2) the oligomerization states of ProDH1 was altered in *p5cdh*; (3) P5CDH may form complex with other partners than ProDH1; (4) high MW P5CDH signals may be localized to mitochondrial membrane.

4.1.4 ProDH2 may interact with ProDH1 and P5CDH in mitochondrial membrane

The interaction of ProDH2 with ProDH1 and P5CDH was studied by BiFC assay. Positive YFP signals were observed in *Nicotiana benthamiana* leaves co-infiltrated with the following combination: ProDH2-YFP_N/P5CDH-YFP_C, ProDH2-YFP_N/ProDH1-YFP_C, ProDH1-YFP_N/ProDH2-YFP_C, and ProDH2-YFP_N/ProDH2-YFP_C (Fig. 5a). As expected, no YFP signal was detectable in negative controls, where ProDH2-YFP_N-YFP_C co-infiltrated with corresponding empty plasmids (Fig. 5a). Moreover, YFP signals of these different BiFC co-infiltrations were overlapped with the mitochondrial marker mCherry signal (Fig. 5a). Protein expressions of all BiFC combinations in co-infiltrated leaves have been confirmed by Western-blot assay (Fig. 3c). These results indicate that ProDH2 seems to be able to interact with both ProDH1 and P5CDH as well as to homo-oligomerize in the mitochondrion.

However, YFP signal was not detected in P5CDH-YFP_N/ProDH2-YFP_C (data not shown) infiltrated tobacco leaves, even if P5CDH-YFP_N and ProDH2-YFP_C were properly expressed in this combination (Fig. 3c). This lack of interaction may result from poor accessibility of the interaction site in these fusion proteins.

Furthermore, YFP (yellow) and mCherry (blue) signals exhibited a mosaic pattern in fixed ProDH2-YFP_N/ProDH1-YFP_C and ProDH2-YFP_N/P5CDH-YFP_C samples (Fig. 3b), which mimics the results of ProDH1-YFP_N/ProDH1-YFP_C and ProDH1-YFP_N/P5CDH-YFP_C.

Taken together, these results suggest that ProDH2 may interact with ProDH1 and P5CDH in mitochondria. In addition, ProDH2 may also form homo-oligomers in mitochondria. Moreover, fixed BiFC assays suggest that the interactions of ProDH2-ProDH1 and ProDH2-P5CDH are likely associated to the mitochondrial membrane.

4.1.5 Figures

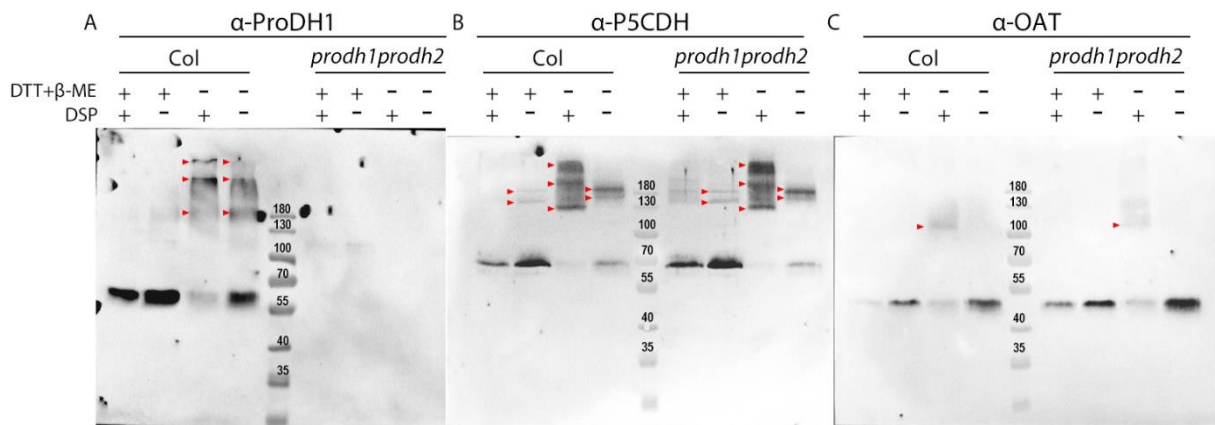


Figure 3. Putative complex evidenced by DSP cross-linking experiment. Crude mitochondria extracted from 5-day DIS treated Col and *prodh1prodh2* Arabidopsis leaves were cross-linked with 0.125 mM DSP for 15 mins. 5% digitonin were used to solubilized mitochondrial membrane proteins. Before loaded onto SDS-PAGE, cross-linked (+DSP) or not cross-linked (-DSP) protein samples were heated at 99°C for 5 mins with 4x laemmli loading buffer (1x final) with (+) or without (-) reducing reagents (DTT and β-ME) as indicated in the figures. In this experiment, ~22 μg mitochondrial proteins were loaded for ProDH1 group; ~50 μg mitochondrial proteins were loaded for P5CDH group; and ~28 μg for OAT group. DTT, dithiothreitol; β-me, β-mercaptoethanol. The monomeric P5CDH is ~62 kDa; the monomeric ProDH1 is ~55 kDa; the monomeric OAT is ~52 kDa. High molecular weight bands are indicated with red arrows.

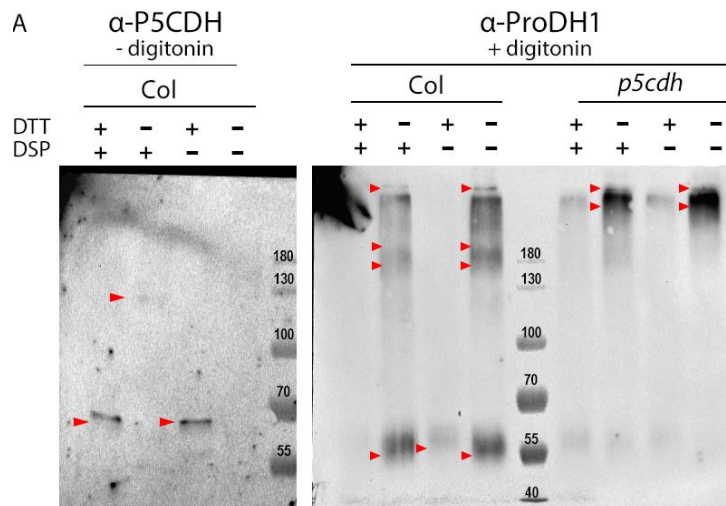


Figure 4. Putative ProDH1-P5CDH complex evidenced by DSP cross-linking experiment. Crude mitochondria extracted from 5-day DIS treated Col, *p5cdh*, and *prodh1prodh2* Arabidopsis leaves were cross-linked with 0.125 mM DSP for 15 mins. Cross-linked protein samples were either solubilized with (+ digitonin) 5% digitonin or not (- digitonin). Before loaded onto SDS-PAGE, protein samples were kept at room temperature for 30 mins with 4x laemmli loading buffer (1x final) with (+) or without (-) DTT as indicated in the figures. In this experiment, ~22 μg mitochondrial proteins were loaded for ProDH1 group; ~50 μg mitochondrial proteins were loaded for P5CDH group. DTT, dithiothreitol; β-me, β-mercaptoethanol. The monomeric P5CDH is ~62 kDa; the monomeric ProDH1 is ~55 kDa. Different bands are indicated with red arrows.

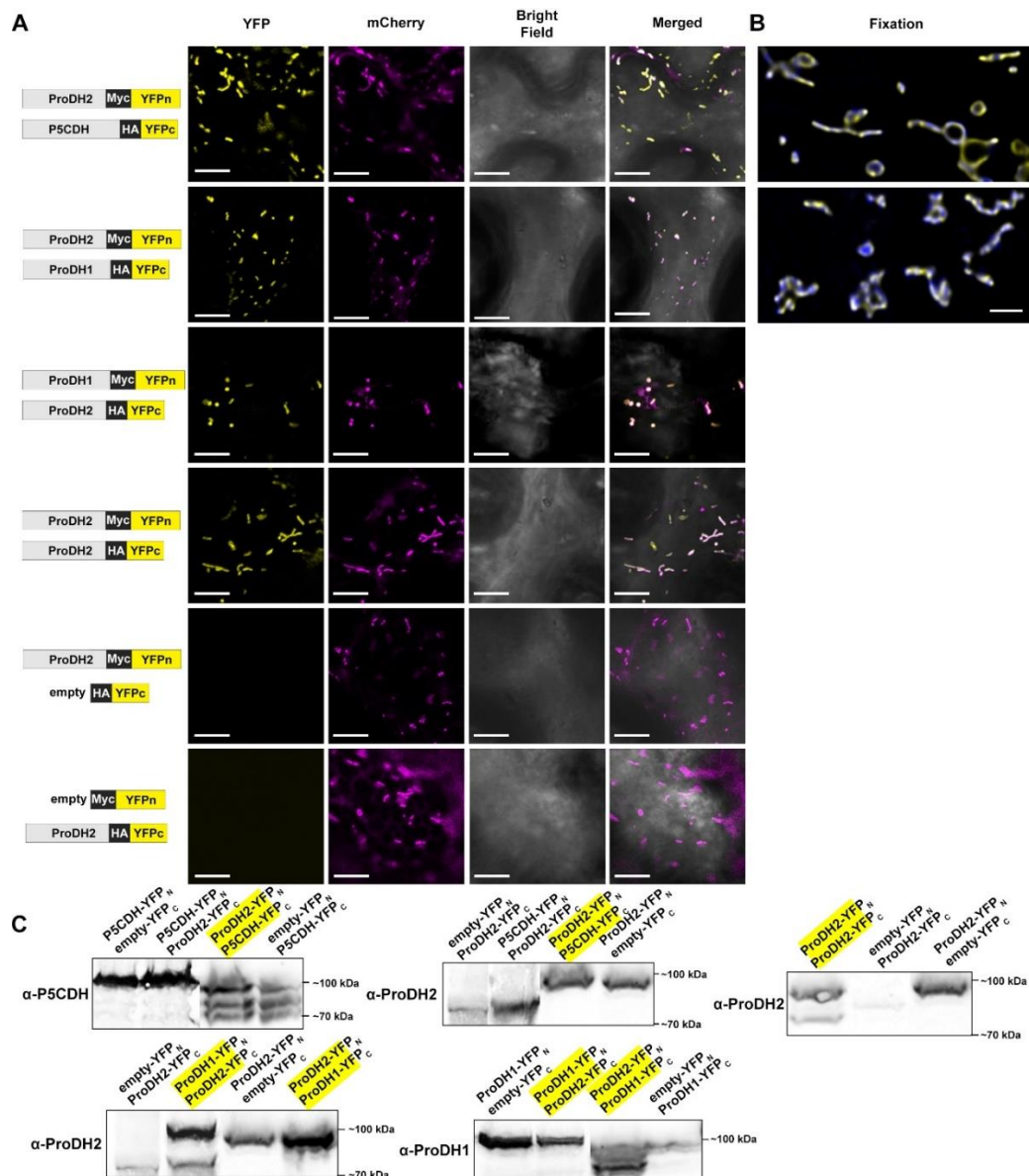


Figure 5. Hetero- and homo-oligomerization of ProDH2 by BiFC assay in *Nicotiana benthamiana*.

(A) Confocal analyses of living epidermal cells of *Nicotiana benthamiana* infiltrated with the schematic representation of plasmid combinations indicated on the left of each panel. The size of each cassette shown on the left is to mimic their CDS sequence length. YFP channel shows YFP fluorescent signals; mCherry channel indicates the location of mitochondria; bright field channel shows the cellular structure of tobacco epidermal cell under white light; merged channel shows picture merged with other three channels. Bar = 10 μ m.

(B) Z-spacing confocal analyses coupled with imaging deconvolution of fixed epidermal cells of *Nicotiana benthamiana* infiltrated with the plasmid combinations indicated on the left of each panel same as (A). YFP signals, which represent the localization of protein interaction, are labelled with yellow. mCherry signals, which represent the matrix of mitochondria, are labelled with blue. The overlap between YFP and mCherry signals are shown in white. Bar = 1.5 μ m.

(C) Full proteins were extracted from tobacco leaves infiltrated with the plasmid indicated in the picture. Constructs which are positive in YFP signal were marked by yellow backgrounds. SDS-PAGE and Western-blot was performed to examine the expression pattern of those proteins. Same amount of proteins was loaded on the SDS-PAGE gel. The theoretical molecular weight of B4-ProDH1 is 73.7 kDa; B5-ProDH1, 65.6 kDa; B4-ProDH2, 71.7 kDa; B5-ProDH2, 63.6 kDa; B4-P5CDH, 80.5 kDa; B5-P5CDH, 72.4 kDa. α -ProDH1, ProDH1 antibody; α -ProDH2, ProDH2 antibody; α -P5CDH, P5CDH antibody.

4.1.6 Supplementary materials and methods

Dithiobis succinimidyl propionate (DSP) is a commonly used crosslinker, which is a water-insoluble and membrane-permeable *N*-hydroxysuccinimide ester (NHS-ester). Therefore, it is useful for intracellular and intramembrane conjugation. Moreover, its disulfide bond in the spacer arm is readily cleaved by thiols, such as dithiothreitol (DTT) or β -mercaptoethanol (β -ME).

In this study, DSP (Thermo Scientific) was firstly dissolved in DMSO (until 20 mM), then added into crude mitochondria samples until final cross-linking concentration (0.125 mM). After incubation on the ice for 15 mins, 1M Tris-HCl pH 7.4 (20 mM final) was added into the sample to stop the cross-linking reaction. Finally, samples were subjected to centrifuge at 18300 x g, 4°C, for 10 min, to pellet down all the cross-linked crude mitochondria.

Afterwards, cross-linked mitochondrial proteins were either subject to (+ digitonin) membrane solubilization steps or not (- digitonin) as indicated in the figures. 1 μ l 5% digitonin per 10 μ g mitochondrial protein was added to resuspend the cross-linked mitochondrial pellet acquired above and incubated on ice for 20 mins. For samples without digitonin solubilization, 3 cycles of freeze-thaw with liquid nitrogen were performed in order to break mitochondria and release matrix proteins. Finally, samples were centrifuge at 18300 x g, 4°C, for 20 mins to remove insolubilized fractions.

Afterwards, 4x Laemmli loading buffer (1x final) with or without reducing reagents (DTT/ β -ME) was added into the protein samples as indicated in the figures. Then, protein samples were either heated at 99°C for 5 mins or kept at room temperature for 30 mins before loaded onto 8.75% SDS-PAGE gel.

CHAPTER V.
GENERAL DISCUSSION
AND
PERSPECTIVES

Chapter 5. General discussion and perspectives

In this study, by transcript analysis as well as biochemical, proteomic, and complexomic approaches, we have shown that ProDH1, P5CDH, and OAT are involved in dark induced senescence (DIS) in Arabidopsis and are able to interact together. The dynamic of this P5C metabolism complex and its putative biological functions will be discussed.

5.1 Temporal and spatial identification of ProDH1, P5CDH, and OAT

5.1.1 DIS triggers all three ProDH1, P5CDH, and OAT catabolic enzymes

The time-course experiment has shown that ProDH1, P5CDH, and OAT were gradually induced during DIS in Arabidopsis on both transcriptional and translational level. It is consistent with the previously reported accumulation of these three transcripts during developmental or induced senescence (Dietrich et al., 2011; Faës et al., 2015; Chrobok et al., 2016; Pedrotti et al., 2018; Launay et al., 2019). Surprisingly, protein amounts as well as activities of ProDH1 and OAT were affected by the absence of P5CDH in *p5cdh* knock-out mutant, indicating a crosstalk between these proteins. ProDH1 and OAT seem to be less stable in absence of P5CDH, which needs further investigation.

ProDH1 was first described as fuelling mitochondrial ETC as well as aiding nitrogen remobilization through proline oxidation and glutamate synthesis (Launay et al., 2019). Consecutively, the induction of P5CDH was then expected. When P5CDH is absent, an accumulation of proline much higher than in the *prodh1prodh2* mutant was observed. This indicates a proline-P5C cycle could exist in DIS in the *p5cdh* mutant. More information about P5C and proline transporters under DIS would be necessary to confirm this hypothesis as well as data about ProDH1 and P5CR activities during DIS *in vivo*. Moreover, fluxomic data would be also helpful to investigate the presence of hypothetical proline-P5C cycle.

During leaf senescence, carbon and nitrogen coming from chloroplast protein degradation have to be remobilized. Nitrogen is mainly remobilized from free amino acids by amino acids catabolism (Havé et al., 2016). The metabolomic results clearly indicate that amino acids metabolism is affected in *prodh1prodh2*, *p5cdh*, and *oat* mutants since the total amount of amino acids is higher in *prodh1prodh2* and *p5cdh* mutants and lower in *oat* mutant compared to WT. It has been reported that the most abundant amino acids in the phloem sap are glutamine,

glutamate, serine, asparagine, and aspartate, depending on plant species (Masclaux-Daubresse et al., 2006; Howarth et al., 2008; Zhang et al., 2010; Hu et al., 2016). Furthermore, glutamine and asparagine concentrations are increased in phloem during leaf senescence (Masclaux-Daubresse et al., 2006).

In plants, glutamine is synthesized by glutamine synthetase (GS) in both cytosol (GS1 and GS2) and chloroplasts (GS2). A dual targeting in cytosol and plastids has been described for GS2 (Taira et al., 2004). Cytosolic GS1, encoded by *GLN1*, plays an important role in nitrogen remobilization, which is preferentially expressed in the vascular tissues of leaves during senescence (Bernard and Habash, 2009; Guan et al., 2015). Antisense knock-down mutant of cytosolic GS1 in the *Nicotiana tabacum* phloem resulted in decreased proline production and impaired salt tolerance (Brugière et al., 1999). Moreover, knock-out mutant of plastidic GS2 in *Lotus japonicus*, *Ljgln2-2*, exhibited substantially decreased proline contents during drought stress compared to wild-type (Díaz et al., 2010). Moreover, glutamine synthesis is ATP-dependent and proline catabolism has been previously described as a source of ATP (Launay et al., 2019). Thus, a link clearly exists between proline metabolism and glutamine metabolism. This connection has also been reported in human cancer cells. Oncogenic transcription factor c-MYC has been reported to induce the expression of mitochondrial glutaminase, which converts glutamine to glutamate (Gao et al., 2009). c-MYC not only inhibited *POX/ProDH*, but also markedly induced the expression of *P5CS* and *PYCR1*. Moreover, MYC induced proline biosynthesis from glutamine was directly confirmed using ^{13}C , ^{15}N -glutamine as a tracer (Liu et al., 2012). However, the interplay between proline metabolism and glutamine metabolism during senescence is largely unknown.

So far, the connection between aspartate/asparagine and proline metabolism is not well documented. It has been reported in *Arabidopsis* that *ProDH1/2* and *ASPARAGINE SYNTHETASE1 (ASN1)* are activated by transcription factor bZIP11, which is repressed by sucrose (Hanson et al., 2008). Degradation of chloroplasts during senescence will lead to the arrest of photosynthesis and shortage of sugars, thus the co-activation of *ProDH1/2* and *ASN1* by bZIP11 may also occur during senescence. Moreover, *ASN1* is also ATP-dependent like GS (Lomelino et al., 2017). However, information about this co-activation is extremely limited so far. Fluxomic data will be instructive to discover the biological role of this co-activation.

In addition, arginine has been recognized as a storage form of organic nitrogen and plays a key role in nitrogen distribution and remobilization in plants (Slocum, 2005; Winter et al., 2015). Recently, it has been reported that *OAT* is crucial for nitrogen reutilization and plays a critical role in floret development and seed setting in *Oryza sativa* (Liu et al., 2018).

Accordingly, our metabolomic data has shown that the total amino acid content was substantially decreased in *oat* mutant compared to Col-0, suggesting a putative role of OAT in remobilizing nitrogen from arginine to produce other amino acids during DIS. However, the general metabolomic behaviour of *oat* is similar to Col-0 but different from *prodh1prodh2* and *p5cdh*, indicating the specific role of proline catabolism during DIS.

5.1.2 ProDH1, P5CDH, and OAT presents different submitochondrial localization

Next, we studied the submitochondrial localization of these three enzymes. Submitochondrial fragmentation results showed that AtProDH1, AtP5CDH, and AtOAT are detectable in both mitochondrial membrane fraction and soluble fraction during DIS with different distribution patterns, even if ProDH1 is mainly associated with the membrane. This result is partially consistent with previously reported submitochondrial localization of these enzymes. Since P5CDH was reported to associate with mitochondrial inner membrane in *Zea mays* (maize)(Elthon and Stewart, 1981) and parasitic protozoon *Trypanosoma cruzi* (Mantilla et al., 2015), but in mitochondrial matrix in mouse (Brunner and Neupert, 1969). Meanwhile, OAT is believed to localize in the mitochondrial matrix in both animals (Doimo et al., 2013) and plants (Winter et al., 2015).

No known transmembrane domains in these enzymes have been identified. Studies of prokaryotic PutA have shown that its N-terminal α domain is involved in membrane association (Zhu and Becker, 2003; Zhu and Becker, 2005). In the parasitic protozoon *Trypanosoma cruzi*, a putative transmembrane α -helix spanning domain (Phe198-Gly215) has been identified for TcP5CDH by bioinformatic prediction (Mantilla et al., 2015). However, no information for the presence of a transmembrane domain in eukaryotic ProDH is available.

Moreover, lipid PTMs, including S-acylation (palmitoylation), N-myristoylation, prenylation, and glycosylphosphatidylinositol (GPI) anchors are responsible for peripheral membrane localization of proteins (Chamberlain and Shipston, 2015; Hemsley, 2015). Among these lipid PTMs, S-acylation is the least understood in any organisms and the only one that is reversible (Hemsley, 2015). Dynamic S-acylation is emerging as a means of regulating protein function and modifying a protein's affinity for membranes (Hemsley, 2015). Interestingly, P5CDH has been identified as a putative S-acylated protein in root cell suspension cultures in *Arabidopsis* using proteomic approach (Hemsley et al., 2013). Thus, it will be interesting to investigate whether P5CDH, ProDH1, and OAT are subjected to S-acylation. Alternatively,

proteins can interact with membrane via amphipathic helices (Picot et al., 1994; Giménez-Andrés et al., 2018). It is interesting to check whether amphipathic helix is present in these enzymes using bioinformatic approach.

5.2 ProDH1, P5CDH, and OAT interact to form a P5C metabolic complex

Co-expression and partial co-localization of these three proteins during DIS provided a good foundation for their putative protein-protein interactions. The membrane localization of proteins can also help to increase their local concentration (Nooren and Thornton, 2003). As interactions and complexes are driven by the local concentration of proteins, this membrane localisation could thus facilitate the formation of the complex (Nooren and Thornton, 2003).

Using BiFC assays in *Nicotiana benthamiana*, we presented the first evidence of interaction between eukaryotic ProDH and P5CDH, which has never been reported before in contrary to procaryotic enzymes (Sanyal et al., 2015). The interactions of ProDH1 with ProDH2 and OAT as well as P5CDH with ProDH2 and OAT have also been evidenced by BiFC assay. During DIS, the interaction between ProDH1 and P5CDH and between ProDH1 and OAT was reinforced by BN/SDS-PAGE. Moreover, by co-immunoprecipitation assay, we have shown that both ProDH1 and OAT interact with P5CDH. In addition, the ternary complex of ProDH1, P5CDH, and OAT was evidenced by Native/SDS-PAGE and complexomic profiling.

The interaction between AtProDH1 and AtP5CDH identified in this study is consistent with the interaction of TtProDH-TtP5CDH found in *T. thermophilus* (Sanyal et al., 2015). It is also consistent with the Rosetta Stone (a.k.a. domain fusion) protein–protein interaction prediction using a combination of bioinformatics and structural biology data, which hypothesized that interacting proteins are sometimes fused into a single protein. This is actually the case for PutA in bacteria. Therefore the corresponding monofunctional homologs in another organism are likely to interact (Marcotte et al., 1999).

To our knowledge, interaction between OAT and ProDH1 and/or P5CDH have never been described in living organisms. Moreover, our Native/SDS-PAGE and complexome profiling results show the involvement of ProDH1, P5CDH, and OAT in the same complex. BiFC results also indicate that AtProDH1, AtP5CDH and AtOAT are able to homo-oligomerize.

The pattern of ProDH1 in the first dimension of Native/SDS-PAGE is particularly surprising since it appears as a huge smear, indicating the existence of oligomerization of ProDH1.

The long smear of ProDH1 suggests ProDH1 may also associate with additional partners that dissociate during migration. In addition, homo-oligomerization of ProDH1 cannot be excluded.

5.3 Proline catabolism has a close relationship with ETC and energy production

The ternary complex of ProDH1, P5CDH, and OAT could be part of a bigger complex that is not deciphered yet. Some candidates emerge from the IP-MS using P5CDH-tGFP and complexomic data. IP-MS analysis has identified SDH1-1, SDH2-1, SDH2-2, and SDH5 subunits of Complex II. Moreover, the complexomic data have revealed that SDH1-1 have the same migration pattern as ProDH1 in WT and P5CDH-tGFP overexpressing mitochondria.

Complex II in eukaryotes is classically composed of four subunits including a flavoprotein (SDH1) using FAD as cofactor, an iron–sulphur (Fe–S) protein (SDH2) that contains three Fe–S clusters, and two small integral membrane proteins (SDH3 and SDH4) that bind heme to form a b-type cytochrome (Huang and Millar, 2013). So far, the function of SDH5–8 subunits are still unclear. The sequences of SDH5–8 do not contain clear functional motifs, but together they may represent a secondary peripheral activity of the SDH complex in plants (Huang and Millar, 2013).

Consistently, the respiratory rate of Complex II has been found to significantly decrease in *prodh1prodh2* double mutant plants, compared with wildtype (Launay et al., 2019). In addition, succinate has been found to be an uncompetitive inhibitor of ProDH in human DLD colorectal cancer cell culture (Hancock et al., 2016). Furthermore, by using a membrane-permeable crosslinker DSP in mitochondria isolated from mouse liver, researchers have reported that ProDH can co-immunoprecipitate with both SDH1 and SDH2 subunits of Complex II (Hancock et al., 2016). P5CDH was also found co-migrating with complex II subunits in *Trypanosoma cruzi* (Mantilla et al., 2015). So far, it is still unclear whether this functional connection between ProDH and Complex II will affect the interaction between ProDH, P5CDH, and/or OAT. But taken together, these results support a putative interaction between Complex II and mitochondrial P5C metabolic complex in Arabidopsis.

As a flavoenzyme, ProDH has been speculated to transfer electrons to ETC. It has been reported that a functional ETC is necessary for *Saccharomyces cerevisiae* to utilize proline as a nitrogen source (Wang and Brandriss, 1987). To date, several studies have shown that the

oxidation of proline by ProDH is coupled with the reduction of UQ (Wanduragala et al., 2010; Becker et al., 2011; Goncalves et al., 2014; Hancock et al., 2016).

There are three possible mechanisms by which ProDH could transfer electrons to UQ. Firstly, ProDH could transfer electrons to UQ indirectly through ETF/ETF-QO system, like IVDH. However, this possibility has been ruled out by a study in yeast (Wanduragala et al., 2010).

Secondly, it is possible that ProDH may transfer electrons to UQ through Complex II. SDH2 subunit harbours 3x [Fe-S] clusters, which transfers electrons from FADH₂, produced by SDH1, to UQ. Both SDH1 and SDH2 have been detected in our IP-MS and complexomic data. This data suggest that ProDH may transfer electrons to UQ through interaction with SDH2.

A third possibility is that ProDH may transfer electrons directly to UQ. Accumulated researches have shown that ProDH can bind directly with UQ in *E. coli* (Moxley et al., 2011), *S. cerevisiae* (Wanduragala et al., 2010), mouse, and human (Hancock et al., 2016). Therefore, it is highly possible that plant ProDH should have a similar UQ binding capacity, which needs further experimental evidence *in planta*.

5.4 Mitochondrial P5C metabolic complex may allow P5C/GSA sequestration and fine regulation of proline catabolism

Among living organisms, proteins seldom act alone, but rather function in form of homo-/hetero-oligomeric complex (Marianayagam et al., 2004; Charbonnier et al., 2008; Matthews and Sunde, 2012). Temporary structural-functional complex formed between metabolically sequential enzymes, termed as metabolon, may allow channelling of substrates and intermediates within the complex (Srere, 1985; Sweetlove and Fernie, 2018; Zhang and Fernie, 2021). Moreover, the enzyme complex in a metabolon is assembled by transient, protein-surface, and structure-dependent interactions, thereby regulating metabolic flux through the dynamic association and dissociation of the components of the metabolon (Srere, 1985; Zhang and Fernie, 2021). The dissociation constant (K_D) of TtProDH-TtP5CDH complex in *T. thermophilus* is 3 μ M (Sanyal et al., 2015), indicating this complex is transient and weak (Perkins et al., 2010). In this study, the P5C metabolic complex was dissociated in BN/SDS-PAGE in comparison to Native/SDS-PAGE results, indicating this complex maybe also transient and weak, which could be beneficial to its dynamic regulation of the metabolic flux.

So far, dynamic assemblies of consecutive enzymes have been reported in a wide range of pathways, such as Calvin–Benson cycle (Gontero et al., 1988; Huege et al., 2011), TCA cycle (Robinson and Srere, 1985), glycolysis (Graham et al., 2007), mitochondrial electron transport chain (Lapuente-Brun et al., 2013), oxidative pentose phosphate pathway (Debnam et al., 1997), fatty acid β -oxidation (Ishikawa et al., 2004), and branched chain amino acid metabolism (Islam et al., 2007). However, evidence of dynamic protein-protein interactions is necessary but not sufficient to prove the presence of metabolon, because evidence for channelling of metabolites is mandatory. According to this criteria, the existence of metabolon was only demonstrated in glycolysis (Graham et al., 2007), TCA cycle (Zhang et al., 2017), phenylpropanoid biosynthesis (Achnine et al., 2004) and cyanogenic glucoside biosynthetic pathway (Laursen et al., 2016) in plants.

5.4.1 Substrate channelling

Studies have shown that transient complexes in metabolon can regulate metabolic flux through dynamic associations and/or dissociations (Zhang and Fernie, 2021). Moreover, various potential advantages of substrate channelling have been proposed such as: increasing catalytic efficiency, enriching local substrates, protecting cells from cytotoxic intermediates, preventing the decomposition of unstable compounds, overcoming the thermodynamically unfavourable equilibrium, avoiding competing pathways, reducing lag transients, and providing new means of metabolic regulation by modulation of enzyme associations (Spivey and Ovádi, 1999; Wheeldon et al., 2016; Zhang and Fernie, 2021).

For proline catabolism, substrate channelling has been reported in both PutA (Srivastava et al., 2010; Singh et al., 2014) and monofunctional TtProDH-TtP5CDH (Sanyal et al., 2015) in *T. thermophilus*. Eukaryotic ProDH-P5CDH interaction found in this study may also form substrate channelling to sequester P5C/GSA within the complex like its prokaryotic analogue. Although substrate channelling has not been reported for OAT so far, we can speculate that the possible biological function of OAT-P5CDH interaction is to sequester P5C/GSA within the complex as well.

In contrast, the OAT-ProDH1 interaction was not expected. One hypothesis is that OAT-ProDH1 interaction is beneficial for P5C/GSA sequestration, which is depending on the reverse catalytic activity of either OAT or ProDH1. If OAT/ProDH1 can catalyse P5C/GSA to produce ornithine or proline, thus their interaction would be beneficial to sequester P5C/GSA within the complex. However, no experimental data could support this reverse role of ProDH1

so far. Although OAT has been reported to catalyse the production of ornithine from GSA in mouse liver when GSA is in large excess (Strecker, 1965), this reverse activity of OAT unlikely exists in plants. Labelled precursors of proline applied to *p5cdh* mutant showed that proline accumulated was not degraded and stable over 48 hours, indicating the absence of alternative P5C or proline degradation pathway at least in Arabidopsis (Deuschle et al., 2004). Furthermore, extraordinary accumulation of P5C and proline has been observed in *p5cdh* mutant in our metabolomic data, suggesting that OAT is unable to catabolize P5C in plants during DIS as well. Taken together, the existence of substrate channelling in mitochondrial P5C metabolic complex still needs further investigation.

5.4.2 Co-regulation through interactions

In addition, protein oligomerization may allow concerted regulation of different components. Because it can generate new intermolecular interfaces, which may further produce sites for allosteric regulation, enabling cofactors to bind to non-substrate sites or facilitating substrate-induced cooperativity (Marianayagam et al., 2004). Protein-protein interaction may also generate new binding sites with other molecules and/or control the accessibility and specificity of active sites (Marianayagam et al., 2004).

In accordance with this notion, the redox state of FAD, cofactor of ProDH, instead of NAD⁺, cofactor of P5CDH, can regulate both membrane association affinity and oligomeric state of PutA. It has been reported that the reduction of FAD in PutA can dramatically change the conformation of FAD and initiate a global protein conformational change that enhances membrane association of PutA in *E. coli* (Zhu and Becker, 2003; Zhu et al., 2013). More recently, it has been reported that the oligomeric state of B_jPutA from *Bradyrhizobium japonicum* is also regulated by the redox state of FAD (Korasick et al., 2018). B_jPutA is dimeric at nanomolar concentration and forms a reversible dimer-tetramer equilibrium at higher concentration. Moreover, reduction of the FAD cofactor abrogates tetramerization of B_jPutA, producing primarily dimeric B_jPutA (Korasick et al., 2018).

It is possible that eukaryotic ProDH1 may cooperatively regulate its interactions with P5CDH, OAT, and P5CDH-OAT in response to FAD redox state. This hypothesis is more interesting for the regulation of OAT because, unlike P5CDH, OAT does not use either NAD(P) or FAD as cofactor suggesting that OAT may not be regulated by redox state. If this hypothesis is true, ProDH1 may allow OAT to be regulated by the redox state indirectly through its interaction.

5.4.3 P5CDH may function as a regulatory funnel during DIS

Interestingly, dramatic accumulation of proline has been detected in *p5cdh* mutant during DIS in our metabolomic data starting from Day 3 until Day 5, which is 4- to 5-fold of proline accumulation detected in *prodh1prodh2*. This is probably due to the toxicity of P5C, whose accumulation has been reported to trigger a burst of ROS in both yeast and Arabidopsis *p5cdh* mutants (Deuschle et al., 2001). The excessive production of ROS in plant cells is potentially harmful to nucleic acids, proteins, and lipids, which can lead to cell injury and cell death (Gill and Tuteja, 2010). Thus, ROS homeostasis must be maintained with care during senescence. Accordingly, co-induction of ProDH1 and P5CDH during DIS indicates that P5C/GSA accumulation might be unfavourable for senescing cells. However, in *p5cdh* mutant plants, senescing cells either induce alternative P5C detoxification pathway or inhibit the source of P5C to limit the accumulation of this unfavourable intermediate as much as possible. Consistently, our results have shown that the enzymatic activity and protein amount of both ProDH1 and OAT were downregulated in *p5cdh* mutant at Day 4. This suggests an increasingly important and putative regulatory role of P5CDH upon ProDH1 and OAT during DIS, due to the toxicity of P5C/GSA for senescing cells. In mitochondrial P5C catabolism during DIS, P5CDH may function as a funnel that gathering the P5C flux from both ProDH1 and OAT. Moreover, this is also consistent with the ProDH1-P5CDH-OAT complex identified in this study, which may allow P5C/GSA sequestration as discussed above.

5.5 Perspectives

Our work has shown for the first time the interaction of ProDH1, P5CDH, and OAT in eukaryotes during DIS. In the future, it will be interesting to work on the dynamic of this mitochondrial P5C metabolic complex, to investigate how this complex is regulated, and to figure out its relationship with Complex II.

5.5.1 Identify other partners of P5C metabolic complex

Firstly, it is important to identify other partners, such as subunits of Complex II, of this mitochondrial P5C metabolic complex using BiFC, Co-IP and/or Native/SDS-PAGE. Our DSP crosslinking experiments have shown that ProDH1, P5CDH and to a lesser extent OAT may involve in a high molecular weight complex mediated by disulphide bonds. Thus, it is promising to identify DSP crosslinked complex using MS analysis. Moreover, it is also necessary to

study the stoichiometry of each component of this complex by using approaches such as surface plasmon resonance (SPR) and size-exclusion chromatography (SEC). Dynamic assembly of P5C metabolic complex can be studied by using fluorescence lifetime imaging microscopy–Förster resonance energy transfer (FLIM/FRET) and/or bioluminescence resonance energy transfer (BRET).

5.5.2 Substrate channelling

Next, whether mitochondrial P5C metabolic complex can allow P5C/GSA sequestration in a substrate channelling manner still needs further study, for which fluxomic study will be highly informative. In addition, standard biochemical methods to evaluate substrate channelling including isotope dilution and enrichment studies, transient time analysis, resistance to a competing side reaction, resistance to a reaction inhibitor, and enzyme buffering analysis of channelling (Zhang and Fernie, 2021). Moreover, deciphering the crystal structure of eukaryotic ProDH will be highly informative to predict the putative substrate channelling. So far, crystal structure of plant P5CDH is available in *P. patens* and *Z. mays* (Korasick et al., 2019). However, as a membrane protein, eukaryotic ProDH is difficult to be expressed in soluble form in bacteria. During the past decade, attempts have been made to express recombinant eukaryotic ProDHs in bacteria (Wanduragala et al., 2010; Paes et al., 2013). However, this has not been fully achieved until Fabro et al., (2020). The authors reported a detail protocol to express AtProDH1/2 fused with a maltose binding protein (MBP) tag in *E. coli* (Fabro et al., 2020), which could facilitate the deciphering of the structure of eukaryotic ProDH.

5.5.3 Relationship with Complex II

Furthermore, it is also interesting to further study the relationship between P5C metabolic complex and Complex II. The interaction between subunits of Complex II and ProDH, P5CDH, or OAT should be studied using methods such as Co-IP and/or Native/SDS-PAGE. Moreover, it is also promising to study whether the inhibition of Complex II will affect the proline oxidation mediated electron transfer by Complex II inhibitors. Both 2-thenoyltrifluoroacetone (TTFA) and atpenin A5 (AA5) are inhibitors of the ubiquitin-binding site of Complex II (Hancock et al., 2016). Malonate inhibits the flavin site of Complex II in subunit SDH1 (Goncalves et al., 2014). It will be interesting to test whether the application of these inhibitors will affect proline oxidation. Furthermore, the inhibiting effect of succinate to ProDH found in

animals should be also investigated again in plants. It will be also necessary to study whether the inhibition of ProDH will impair its interaction with P5CDH and/or OAT.

In addition, *disrupted in stress responses 1 (dsr1)* is a point mutation of SDH1-1. This mutant presents a lower leaf ROS production after avirulent bacterial infection and exhibited increase susceptibility to specific fungal and bacterial pathogens (Gleason et al., 2011), indicating a role of Complex II in ROS production and pathogen resistance upon biotic stress. Moreover, proline catabolism and OAT have also been reported to participate in plant defence against pathogens through ROS production (Qamar et al., 2015). Control of proline catabolism through coordinated or uncoordinated expression of P5CDH, ProDH, and OAT under pathogen infection will lead to disease or defence reaction respectively (Qamar et al., 2015). However, in *Drosophila melanogaster* and human breast cancer cells, it has been reported that ProDH cannot produce ROS directly but mainly or exclusively through ETC (Goncalves et al., 2014). It is possible that proline catabolism mediated ROS production under pathogen infection in plants is originated from Complex II. Thus, it would be exciting to test whether Complex II participates in mediating pathogen responses from proline oxidation by using either inhibitors or mutants of Complex II.

5.5.4 PTMs

Moreover, PTMs might be responsible for the regulation of the dynamic of P5C metabolic complex. So far, direct study of ProDH, P5CDH, and OAT PTMs in plants is unavailable. By searching Arabidopsis protein phosphorylation site database (PhosPhAt 4.0) (Durek et al., 2010), there is one phosphorylation site experimentally confirmed for ProDH1 and 5 for ProDH2. Furthermore, disulphide bonds have been speculated to stabilize the quaternary structure of AtProDH (Fabro et al., 2020). According to sequence alignments, many conserved cysteine residues have been found in both ProDH and P5CDH in plants. Interestingly, AtP5CDH has been reported to be a target of thioredoxin in Arabidopsis roots (Marchand et al., 2010). P5CDH has also been identified as a putative S-acylated protein in root cell suspension cultures in Arabidopsis (Hemsley et al., 2013). In addition, PTMs including phosphorylation, acetylation, succinylation, and malonylation have been found in the subunits of Complex II (Beza-work-Geleta et al., 2017). Thus, the study of PTMs of P5C metabolic complex will be informative to unravel its dynamic organization, localization, functional regulation, and may help us further understand its connection with Complex II.

Taken together, further investigation of mitochondrial P5C metabolic complex will provide insights to better unravel its role in senescence, energy homeostasis, and plant defence in response to pathogen. Moreover, this mitochondrial P5C metabolic complex may also present in animals. The study of this complex would provide novel insights into the regulation and biological role of eukaryotic proline catabolism and may contribute to artificial engineering of proline catabolism for crop improvement and cancer therapy.

Annexes

ANNEXES

Alignments for ProDH

| | | |
|---------------------------------------|--|-----|
| <i>Saccharomyces cerevisiae</i> ProDH | MIASKSSLLVTKSRIPSLFPLIKRSYVSKTPTHSNTAANLMVETPAANANGNSVMA--- | 57 |
| <i>Homo sapiens</i> ProDH1 | ---MAL---RRALPALRPTIPRFVPLSTAPASREQFAA-----GPAAVPGGGSATAVR- | 47 |
| <i>Homo sapiens</i> ProDH2 | ---MAL---RRALPALRPTIPRFVQLSTAPASREQFAA-----GPAAVPGGGSATAVR- | 47 |
| <i>Zea mays</i> ProDH | -MAIASRATKR-----ALSTFAA--AKLPEEAIA-----ATAAVPV----- | 33 |
| <i>Oryza sativa Japonica</i> ProDH | -MAIASRIQKR-----VLASFAAAAAKLPEAAVA-----AAGGAAEAVEEV---- | 41 |
| <i>Medicago truncatula</i> ProDH1 | ---MATRVVPQKIKNLRFKTTTKPLN----SSH-PS-----ATAAVASLLEREQPSP | 45 |
| <i>Arabidopsis thaliana</i> ProDH2 | ---MANRFLRPNLIH---RFSTVSPVG---PPT-----TIIP EILSFDQPKP | 38 |
| <i>Arabidopsis thaliana</i> ProDH1 | ---MATRLLRNTNFIIRRSYRLPAFSPVG---PPTVTA-----STAVVPEILSFGQQAP | 46 |
| <i>Brassica napus</i> ProDH1 | ---MATRLLRNTNFIIRRPHEFSSLRPVG---SPTVTA-----STAAVPEILSFGQQAP | 46 |
| | | |
| <i>Saccharomyces cerevisiae</i> | -----PPNSINF-----LQTLPKKELFQ-----LGFIG-IATLNSFFLNTI | 92 |
| <i>Homo sapiens</i> ProDH1 | -----PPVPAVDVFNQAQAYRSRRTWELARSLLVLRLEAWPALLARHEQLLYVS | 96 |
| <i>Homo sapiens</i> ProDH2 | -----PPVPAVDVFNQAQAYRSRRTWELARSLLVLRLEAWPALLARHEQLLYVS | 96 |
| <i>Zea mays</i> ProDH | ---PLAPAPASSERALLQFEDTGRLFAGEPTPALRLTLAALQALSVGPLVDAATAA--LR | 88 |
| <i>Oryza sativa Japonica</i> ProDH | -ASSVQEQVQAQGAQVLEFGDTERLFAGERSTSLVRTLAVLQALSVGPLVDVATAA--LR | 98 |
| <i>Medicago truncatula</i> ProDH1 | PQ-----PSHQQPSYLDLNDGERLFSVPTSTLIRSSAVLHATAIGPVVDVGIWA--MQ | 97 |
| <i>Arabidopsis thaliana</i> ProDH2 | E-----VDLDSQARLFASVPISTLLRSTAILHATSIGPMVDLGSWL--MS | 83 |
| <i>Arabidopsis thaliana</i> ProDH1 | EPPLHHPKPTQSHDGLDLSQARLFSSIPTSDLLRSTAVLHAAAIGPMVDLGTWV--MS | 104 |
| <i>Brassica napus</i> ProDH1 | EPPLHHPKHNTQTHHDIDLSQARLFASVPTDLLRSTAVLHAAAIGPMVDVGSWV--MS | 103 |
| : : : | | |
| <i>Saccharomyces cerevisiae</i> | IKLF----PYIPIPVIKFVSSLYGGENFKEVIEGKRLQKRGISNMMLSLTIENSEG | 147 |
| <i>Homo sapiens</i> ProDH1 | RKLL---GQRLFNKLMKMTFYGFHVAGEDQESIQLPL-LRHYRAFVSAILDYGV EEDLS | 151 |
| <i>Homo sapiens</i> ProDH2 | RKLL---GQRLFNKLMKMTFYGFHVAGEDQESIQLPL-LRHYRAFVSAILDYGV EEDLS | 151 |
| <i>Zea mays</i> ProDH | SPAVAGSALG---RAAARATAYRHFAGETAGEAAAARRLWR-GMGGILDYGI EDAE- | 143 |
| <i>Oryza sativa Japonica</i> ProDH | SPAVAGSAG---RAAARATAYQHFAGETAEEAAAARRLWR-GMGGILDYGI EDAE- | 153 |
| <i>Medicago truncatula</i> ProDH1 | SKLLQGTGILKDAVMAVTKRTFYEHFCAGEDAITAGKSIRSVNE-AGLRGMLVFGVEDAH- | 155 |
| <i>Arabidopsis thaliana</i> ProDH2 | SKLMDTTVTRDLVLRIVKGTFFYDHFAGEDAAAAARRVSVYESTGLKGM LVYGV EHA E- | 142 |
| <i>Arabidopsis thaliana</i> ProDH1 | SKLMDASVTRGMVLGLVKSTFYDHFAGEDADAAAERVRSVYEATGLKGM LVYGV EHAD- | 163 |
| <i>Brassica napus</i> ProDH1 | SKLMDNALTRGMVLGLVKGTFFYDHFAGEDASAAAERVRSVYEATGLKGM LVYGV EHAD- | 162 |
| . : : .** : : * . : * | | |
| | | |
| <i>Saccharomyces cerevisiae</i> | TKSLSST-----PVDQI | 159 |
| <i>Homo sapiens</i> ProDH1 | PEEAHKEMESC TSAAERDGS GTNKRDKQYQAHWAFGDRRNGVISARTYFYANEAKDSDH | 211 |
| <i>Homo sapiens</i> ProDH2 | PEEAHKEMESC TSAAERDGS GTNKRDKQYQAHRAF GDRRNGVISARTYFYANEAKDSDH | 211 |
| <i>Zea mays</i> ProDH | -----DGGACDRN | 151 |
| <i>Oryza sativa Japonica</i> ProDH | -----DGPACDRN | 161 |
| <i>Medicago truncatula</i> ProDH1 | -----ENDGCDRN | 163 |
| <i>Arabidopsis thaliana</i> ProDH2 | -----DGGACDEN | 150 |
| <i>Arabidopsis thaliana</i> ProDH1 | -----DAVSCDDN | 171 |
| <i>Brassica napus</i> ProDH1 | -----DAASCDDN | 170 |
| * : | | |
| <i>Saccharomyces cerevisiae</i> | VKETISSVHNILLPNIIGQLESKPINDIAPGYIALKPSALVDNPHEVLYNFS--NPAYKA | 217 |
| <i>Homo sapiens</i> ProDH1 | METFRLC-----IEASGRVSDDG--FIAIKLTALGRPQFLLQFSEVLAKWRCFFHQMAV | 263 |
| <i>Homo sapiens</i> ProDH2 | METFRLC-----IEASGRVSDDG--FIAIKLTALGRPQFLLQFSEVLAKWRCFFHQMAV | 263 |
| <i>Zea mays</i> ProDH | AAGFASA-----VDVAAKLPPGSA-SVCIKITALCPVALLEKASD-LLRWQKRHPSLNL | 203 |
| <i>Oryza sativa Japonica</i> ProDH | AAGFLAA-----IDVAAALPPGSA-SVCIKITALCPVALLEKASD-LLRWQKHPATKL | 213 |
| <i>Medicago truncatula</i> ProDH1 | LKGFLLHT-----VDVSKSLPPSSVSVFVIVKITAIQPMALLERISD-LLRWQKDP SFNL | 216 |
| <i>Arabidopsis thaliana</i> ProDH2 | IQKFIET-----VEAAKTLPPSSLSVVVKITAIQPMNVLKRVSD-LLRWQYKPNPFKL | 203 |
| <i>Arabidopsis thaliana</i> ProDH1 | MQQFIRT-----IEAAKSLPTSHPSSVVVKITAIQPI SLLKRVSD-LLRWEYKSPNFKL | 224 |
| <i>Brassica napus</i> ProDH1 | MQHFLRT-----IEAAKSLPTSHPSSVVVKITAIQPI SLLKRVSD-LLRWEYKSKSFKL | 223 |
| : : : * : . : . : * . : | | |
| <i>Saccharomyces cerevisiae</i> | Q-----RDQLIEN | 225 |
| <i>Homo sapiens</i> ProDH1 | EQQGAGLAAMDTKLEVAVLQESVAKLGIASRAEIEDWF TAETLGVSGTMDLLDWSLIDS | 323 |
| <i>Homo sapiens</i> ProDH2 | EQQGAGLAAMDTKLEVAVLQESVAKLGIASRAEIEDWF TAETLGVSGTMDLLDWSLIDS | 323 |
| <i>Zea mays</i> ProDH | -----PWKTHD-----FPILSDS | 216 |
| <i>Oryza sativa Japonica</i> ProDH | -----PWKVHG-----FPVLCVS | 226 |
| <i>Medicago truncatula</i> ProDH1 | -----PWKQDS-----LPFSES | 229 |
| <i>Arabidopsis thaliana</i> ProDH2 | -----PWKLNS-----FPVFSGL | 216 |
| <i>Arabidopsis thaliana</i> ProDH1 | -----SWKLS-----FPVFSSES | 237 |
| <i>Brassica napus</i> ProDH1 | -----SWKLS-----FTVFSDS | 236 |
| : | | |
| <i>Saccharomyces cerevisiae</i> | CSKITK-----EIFELNQSLLKKYPERKAPFMVSTID | 257 |
| <i>Homo sapiens</i> ProDH1 | RTKLSKHLVVPNAQTGQLEPLL SRFTEEEELQMTRMLQRMVDVLAKKATEMGVRLMVDA-- | 381 |
| <i>Homo sapiens</i> ProDH2 | RTKLSKHLVVPNAQTGQLEPLL SRFTEEEELQMTRMLQRMVDVLAKKATEMGVRLMVDA-- | 381 |
| <i>Zea mays</i> ProDH | ----SPLHLTA---SEPP---ALSAAEERELELAHERVLAVCARCAERGVPPLL VDA-- | 262 |
| <i>Oryza sativa Japonica</i> ProDH | ----SPLYLTA---AEP---ALEAEEERELEMAHGRLLAIGERCAEYDIPLLVDA-- | 272 |
| <i>Medicago truncatula</i> ProDH1 | ----SPLYQTT---KKPE---PLTPQEESDFQLANQRLLQQLCKKQVEANMPLVDA-- | 275 |
| <i>Arabidopsis thaliana</i> ProDH2 | ----SPLYHTT---SEPE---PLTVEEERELEKAHERLKSVCRLKQESNVPLLIDA-- | 262 |
| <i>Arabidopsis thaliana</i> ProDH1 | ----SPLYHTN---SEPE---PLTAAEERELEAAHGRIQEI CRKQESNVPLLIDA-- | 283 |
| <i>Brassica napus</i> ProDH1 | ----SPLYHTN---SEPE---PLTAAEERELEAAHVRIQDI CRKQESNVPLLIDA-- | 282 |
| . : : * : : : : | | |

ANNEXES

| | | | |
|------------------------------------|---|-------------------------------------|-----|
| <i>Saccharomyces cerevisiae</i> | AEKYDLQENGVEYLQRIQLFQKFNPTSSKLIS | CVGTWQLYLRLDSGDHILHELKLAQENGYK | 317 |
| <i>Homo sapiens ProDH1</i> | -EQTYFQPAISR-LTLEMQRKFNV--E-KPLIFNTYQ | CYLKDAYDNVTLDELARREGWC | 436 |
| <i>Homo sapiens ProDH2</i> | -EQTYFQPAISR-LTLEMQRKFNV--E-KPLIFNTYQ | CYLKDAYDNVTLDELARREGWC | 436 |
| <i>Zea mays ProDH</i> | -EYAAVQPAIDY-LTLAGALACNA--E-RSIVHGTVQAYLRDARERLETMARGVERARVR | | 317 |
| <i>Oryza sativa Japonica ProDH</i> | -EYATVQPAIDY-FTFAGALAFNGG-G-RPIVHGTVQAYLRDARDRLEAMARAAQGERV | C | 328 |
| <i>Medicago truncatula ProDH1</i> | -EHTTVQPAIDY-FTYSSAIMHNKD-D-NPIVFGTIQTYLKDAKERLFLATKAAEKIGIP | | 331 |
| <i>Arabidopsis thaliana ProDH2</i> | -EDTILQPAIDY-MAYWSAIMFNADKD-RPIVYNTIQAYLRDAGERLHLALRESEKMNVP | | 319 |
| <i>Arabidopsis thaliana ProDH1</i> | -EDTILQPAIDY-MAYSSAIMFNADKD-RPIVYNTIQAYLRDAGERLHLAVQNAEKENVP | | 340 |
| <i>Brassica napus ProDH1</i> | -EDTILQPAIDY-MAYSSAIMFNADKD-RPIVYNTIQAYLRDAGERLHLVQEAKEGVP | | 339 |
| | * . * : * | * * * * : : . . | |
| <i>Saccharomyces cerevisiae</i> | LGLKLVRGAYIHSEKRNRIIF-----GDKTGTDENYDRIITQVVNDLIINGEDSYFGH | | 371 |
| <i>Homo sapiens ProDH1</i> | FGAKLVRGAYLAQERARAAEIGYEDPINPTYEATNAMYHR | CLDYVLEELKH----NAKAK | 492 |
| <i>Homo sapiens ProDH2</i> | FGAKLVRGAYLAQERARAAEIGYEDPINPTYEATNAMYHR | CLDYVLEELKH----NAKAK | 492 |
| <i>Zea mays ProDH</i> | LGVKLVRGAYLAREARVAALGVPSFVHGSIRETHD | CYNGCAAFLLDRVRR----GSAS- | 372 |
| <i>Oryza sativa Japonica ProDH</i> | LALKLVRGAYLAREARLAASLGVPSPVHRSIQDTHD | CYNGCAAFLLDRVRR----GAAA- | 383 |
| <i>Medicago truncatula ProDH1</i> | MGFKLVRGAYMSTESTLAESFGSKSPIHDTIKDTHN | CFNDCSSYLLEKFAN----GKGS- | 386 |
| <i>Arabidopsis thaliana ProDH2</i> | IGFKLVRGAYMSSEAKLADSLGKSPVHDTIQNTHD | CYNDCMSFLMEKASN----GSGIA | 375 |
| <i>Arabidopsis thaliana ProDH1</i> | MGFKLVRGAYMSSEASLADSLGKSPVHDTIQDTHS | CYNDGMTFLMEKASN----GSGFG | 396 |
| <i>Brassica napus ProDH1</i> | MGFKLVRGAYMSEGLKADSLGHKSPVHDTLQNTHAC | CYNDGMTFLMEKASN----GSGFG | 395 |
| | : . * * * * * : * | : * . : . : : . | |
| <i>Saccharomyces cerevisiae</i> | LVVASHNYQSQMLVTNLLKSTQDNSYAKSNIVLQQLGMADNVTYDLITNHGAKNI IKYV | | 431 |
| <i>Homo sapiens ProDH1</i> | VMVASHNEDTVRFALRRMEELGLHP-ADHQVYFGQLLGM | CDQISFPLG--QAGYPVYKYV | 549 |
| <i>Homo sapiens ProDH2</i> | VMVASHNEDTVRFALRRMEELGLHP-ADHQVYFGQLLGM | CDQISFPLG--QAGYPVYKYV | 549 |
| <i>Zea mays ProDH</i> | VVLATHNVESGQLAAARAEELGIPR-GDRNLQFAQLMGMDGLSLGLR--NAGFQVSKYL | | 429 |
| <i>Oryza sativa Japonica ProDH</i> | VTLATHNVESGQLAAARAEELGIGGGDRGLQFAQLMGMDGLSLGLR--NAGFQVSKYL | | 441 |
| <i>Medicago truncatula ProDH1</i> | VVLATHNIESGKLAARAEELGIGG--VNHKLEFAQL | CGMSDALS FGLS--KAGFRVSKYM | 443 |
| <i>Arabidopsis thaliana ProDH2</i> | VILATHNNTDSGKLGARKASELGINK-ENKIEFAQLYGMSDALS FGLK--RAGFNVSKYM | | 432 |
| <i>Arabidopsis thaliana ProDH1</i> | VVLATHNADSGRLASRKASDLGIDK-QNGKIEFAQLYGMSDALS FGLK--RAGFNVSKYM | | 453 |
| <i>Brassica napus ProDH1</i> | VVLATHNADSGRLASRKASELNINK-KNGTIEFAQLYGMSDALS FGLK--RAGFNVSKYM | | 452 |
| | : : * : * * : : : | : . : : * * * * : : * . . . : * * : | |
| <i>Saccharomyces cerevisiae</i> | PWGPPELETKDYLLRRLQENGDAVRS DNGWPLIKAIKSI PKRVGL----- | | 476 |
| <i>Homo sapiens ProDH1</i> | PYGPVMEVLPYLSRRALENSSLMKGTHRERQL--LWLELLRRLRTGNLFHRPA | | 600 |
| <i>Homo sapiens ProDH2</i> | PYGPVMEVLPYLSRRALENSSLMKGTHRERQL--LWLELLRRLRTGNLFHRPA | | 600 |
| <i>Zea mays ProDH</i> | PYGPVEQIVPYLIRRAEENRGLLSASSFDRQL--LREELVRRFKA AVLGRE-- | | 478 |
| <i>Oryza sativa Japonica ProDH</i> | PYGPVEQIIPYLIRRAEENRGLLSASSFDRQL--LRKELVRRFKAAMLGRE-- | | 490 |
| <i>Medicago truncatula ProDH1</i> | PFGPVEMVMPYLLRRAEENRGLLAASGFDRQL--IRRELGRRLKAAIF----- | | 489 |
| <i>Arabidopsis thaliana ProDH2</i> | PYGPVDTAIPYLIRRAYENRGMSTGALDRQL--MRKELKRRVMMAW----- | | 476 |
| <i>Arabidopsis thaliana ProDH1</i> | PFGPVATAIPYLIRRAYENRGMATGAHDRQL--MRMELKRRLIAGIA----- | | 499 |
| <i>Brassica napus ProDH1</i> | PFGPVETAIPYLIRRAYENRGMASGALDRQL--LRMELKRRLIAGIA----- | | 498 |
| | * : * * * * * * * * . : | : : : : * * * * : : * . . . : * * : | |

ANNEXES

Alignments for P5CDH

| | | |
|---------------------------------|---|-----|
| <i>Zea mays</i> | -----MS-RLLSRQH-LAA-----VRRSAPFAVSRWLHTPSFATVSPQEVSE----- | 40 |
| <i>Oryza sativa Japonica</i> | -----MS-LILSRRRLLAA-----VRRSGPAALASRWHTPPFATVSPQEIS----- | 41 |
| <i>Medicago truncatula</i> | -----MLNHFLTRASRVSSL----TKYNVLPANFNSRSVSSIPLATVEAEIEIS----- | 44 |
| <i>Arabidopsis thaliana</i> | -----MYRVFASRALRAKSLCDKSSST-SLASLTLSSLNHSIPFATVDAEELS----- | 46 |
| <i>Brassica napus</i> | -----MYRVLASRGLRAKSLCDNKASSFLASFTSSRLNHSIPFATVDAEIEIS----- | 47 |
| <i>Homo sapiens</i> | MLLPAPALRRALLSRPWTGAGLRW--KHT--S-SLKVANEPVLAFTQGS-PERDALQKAL | 54 |
| <i>Saccharomyces cerevisiae</i> | -----MDHHHHHHHHASENLYFQGHMK--P-PKHIRNEPVKPFNRNIDLKDWDLRLASL | 50 |
| : | : | : |
| <i>Zea mays</i> | ---GSSPAEVQNFVQGSWTASANWN---WIVDPLNG-DKFIKVAEVQGTEIKSFMESLSK | 93 |
| <i>Oryza sativa Japonica</i> | ---GSSPAEVQNFVQGSWTTSGNWN---WLVDPNG-EKFIKVAEVQEAIEKPFVESLSN | 94 |
| <i>Medicago truncatula</i> | ---GARPAEVLNLVHGKQWVSSNWN---TIVDPLNG-EFFIKVAEVDETGVPFVESLSS | 97 |
| <i>Arabidopsis thaliana</i> | ---GAHPAEVQSFVQGWIGSSNHN---TLLDPLNG-EFFIKVAEVEDSGTQPFVDSLSQ | 99 |
| <i>Brassica napus</i> | ---GAHPAEVQSFVQGWIGSSNHN---TLLDPLNG-EFFIKVAEVEESGVPFIESLAQ | 100 |
| <i>Homo sapiens</i> | KDLKGRMEATPQVVGDEEVWTSDVQ---YQVSPFNHGHKVAKCYADKSLNKAIEAALA | 111 |
| <i>Saccharomyces cerevisiae</i> | MKFKSSSLEVLVINGERYIDNNERALLFPQTNPANHQVLANVNTQATEKDVMMNAVKAAD | 110 |
| : | : | : |
| <i>Zea mays</i> | CPKHGLHNPLKAPERLYLMYGDISAKAAHMLGQPTVLDFFAKLIQRVSPKSYQQALAEVQV | 153 |
| <i>Oryza sativa Japonica</i> | CPKHGLHNPLKAPERLYLMYGDISAKAANMLGQPVVSDFFAKLIQRVSPKSYQQALAEVQV | 154 |
| <i>Medicago truncatula</i> | CPKHGLHNPFKAPERLYLMYGDISAKAAQMLSLPKVSEFFAKLIQRVSPKSYQQAEVYV | 157 |
| <i>Arabidopsis thaliana</i> | CPKHGLHNPFKSPERYLLYGDISTKAAHMLALPKVADFFARLIQRVAPKSYQQAAAGEVTV | 159 |
| <i>Brassica napus</i> | CPKHGLHNPFKSPERYLLYGDISTKAAHMLALPKVSDFFTRLIQRVAPKSYQQAAAGEVTV | 160 |
| <i>Homo sapiens</i> | ARKEWDLKPI-----ADRAQIFLKAADMLSGPRRAEILAKTMVGGKTVIQAEDIAAAE | 165 |
| <i>Saccharomyces cerevisiae</i> | AKKDWNLPF-----YDRSAIFLKAADLITKRYDMLAATMLGQGNVYQAEIDITE | 164 |
| : | : | : |
| <i>Zea mays</i> | SQKFLENFCGDQVRFRLARSFAVPGNHLGQRSNGYRWPYGPVAAIITPFNFPLEIPLQLMG | 213 |
| <i>Oryza sativa Japonica</i> | SQKFLENFCGDQVRFRLARSFAVPGNHLGQSSNGYRWPYGPVAAIITPFNFPLEIPLQLMG | 214 |
| <i>Medicago truncatula</i> | TQKFLENFCGDQVRFRLARSFAVPGNHLGQQSHGFRWPYGPVAAIITPFNFPLEIPLQLMG | 217 |
| <i>Arabidopsis thaliana</i> | TRKFLENFCGDQVRFRLARSFAIPGNHLGQQSHGYRWPYGPVTIVTTFNFPLEIPLQLMG | 219 |
| <i>Brassica napus</i> | TRKFLENFCGDQVRFRLARSFAVPGNHLGQQSHGYRWPYGPVTIVTTFNFPLEIPLQLMG | 220 |
| <i>Homo sapiens</i> | LIDFFRFNAKYAVELEGQ-QPISVPP-STNSTVYRLEGFVAAISPFNFATAIGNLA-GA | 222 |
| <i>Saccharomyces cerevisiae</i> | LSDFFRYYVKYASDLIYAQ-QVESADGTWNKAEYRPLEGFVYAVSPFNFTAIAANLI-GA | 222 |
| : | : | : |
| <i>Zea mays</i> | ALYMGNKPVLLKVDKSVSIVMEQMLRLLHDGLPAEDMDFINSDGAVMKNLLEAN-PKMT | 272 |
| <i>Oryza sativa Japonica</i> | ALYMGNKPVLLKVDKSVSIVMDQMLRLLHAGMPAEDVDFINSDGITMKNLLEAN-PKMT | 273 |
| <i>Medicago truncatula</i> | ALYMGNKPVLLKVDKSVSIVMEQMLRLLHSGLPVEDVDFINDGKTMKNLLEAN-PRMT | 276 |
| <i>Arabidopsis thaliana</i> | ALYMGNKPLLKVDKSVSIVMEQMMRLLHYGLPAEDVDFINSDGKTMKNLLEAN-PRMT | 278 |
| <i>Brassica napus</i> | ALYMGNKPLLKVDKSVSIVMEQMMRLLHYGLPVEDVDFINSDGKTMKNLLEAN-PRMT | 279 |
| <i>Homo sapiens</i> | PALMGNVVLLKVDKSVSIVMEQMLRLLHAGLPVEDVDFINSDGKTMKNLLEAN-PRMT | 282 |
| <i>Saccharomyces cerevisiae</i> | PALMGNTVVVKPSQTAALSNYLLMTVLEEAGLPKGVINFI PGDPVQVTDQVLADKDFGAL | 282 |
| : | : | : |
| <i>Zea mays</i> | LFTGSSRVAEKLAADLKGK-----VKLEDAGFDWKILGPDVQEVYVAVWQDQD | 321 |
| <i>Oryza sativa Japonica</i> | LFTGSSRVAEKLAADLKGK-----IKLEDAGFDWKILGPDVQEVYVAVWQDQD | 322 |
| <i>Medicago truncatula</i> | LFTGSSRVAEKLAADLKGK-----VKLEDAGFDWKILGPDVHQEDYTAVWQDQD | 325 |
| <i>Arabidopsis thaliana</i> | LFTGSSRVAEKLAADLKGK-----IRLEDAGFDWKVLPDQEVYVAVWQDQD | 327 |
| <i>Brassica napus</i> | LFTGSSRVAEKLAADLKGK-----IRLEDAGFDWKVLPDQEVYVAVWQDQD | 328 |
| <i>Homo sapiens</i> | NFTGSVPTFKHLWKVAVQ--LDRFHTFPRLAGEGGKNFHFVHRSAD-VESVSVGTLRS | 339 |
| <i>Saccharomyces cerevisiae</i> | HFTGSTNVFKSLYGIQSGVVEGKRYDPRIGETGGKNFHLVHPSAN-ISHAVLSTIRG | 341 |
| : | : | : |
| <i>Zea mays</i> | AYA SGQK SAQSVLFMHNWSSSGLLEKMKKLSERRKLE--D-----LTIGPV | 368 |
| <i>Oryza sativa Japonica</i> | AYA SGQK SAQSVLFMHNWSSSGLLDKMKLSERRKLE--D-----LTIGPV | 369 |
| <i>Medicago truncatula</i> | AYA SGQK SAQSVLFMHNWSSSGLLEKMKKLSERRKLE--D-----LTIGPV | 372 |
| <i>Arabidopsis thaliana</i> | AYA SGQK SAQSVLFMHNWSSSGLLEKMKKLSERRKLE--D-----LTIGPV | 374 |
| <i>Brassica napus</i> | AYA SGQK SAQSVLFMHNWSSSGLLEKMKKLSERRKLE--D-----LTIGPV | 375 |
| <i>Homo sapiens</i> | AFEYGGQKSAQSVLFMHNWSSSGLLEKMKKLSERRKLE--D-----LTIGPV | 391 |
| <i>Saccharomyces cerevisiae</i> | TFEFQGGKSAQSVLFMHNWSSSGLLEKMKKLSERRKLE--D-----LTIGPV | 401 |
| : | : | : |
| <i>Zea mays</i> | LTVTT-EAMIEHMNNLLKIRGSKVLFGGEPANHSIPKIYGAMKPTAVFVPLEEILKS-G | 426 |
| <i>Oryza sativa Japonica</i> | LTVTT-SSMIEHMNNLLKIPGSKVLFGGEPLENHSIPEIYGAFKPTAVFVPLEEILKS-G | 427 |
| <i>Medicago truncatula</i> | LTFTT-ESLLEHTKNLLEIPGAKLLFGGQPLEDHSIPHVYGAIKPTAVYVPIEEIVKD-K | 430 |
| <i>Arabidopsis thaliana</i> | LTFTT-EAMLEHMENLLQIPGSKLLFGGKELKNHSIPSIYGALEPTAVYVPIEEIILKDNK | 433 |
| <i>Brassica napus</i> | LTFTT-EAMVEHMENLLQIPGSKLLFGGKELKNHSIPSIYGALEPTAVYVPIEEIILKDSK | 434 |
| <i>Homo sapiens</i> | IDAKSFARIKKWLEHARSSPSLTLIAGGKDDSV-----GYFVEPIVSKDP | 439 |
| <i>Saccharomyces cerevisiae</i> | IHEQSFDKLVKVIEDAKKDPLEIILYGGQYDKSQ-----GWFVGTPIKAKRP | 449 |
| : | : | : |

References

- Alvarez ME, Savouré A, Szabados L.** 2021. Proline metabolism as regulatory hub. Trends in Plant Science. *In press*. doi: 10.1016/j.tplants.2021.07.009
- Ábrahám E, Rigó G, Székely G, Nagy R, Koncz C, Szabados L.** 2003. Light-dependent induction of proline biosynthesis by abscisic acid and salt stress is inhibited by brassinosteroid in Arabidopsis. *Plant Molecular Biology* **51**, 363–372.
- Achnine L, Blancaflor EB, Rasmussen S, Dixon RA.** 2004. Colocalization of l-Phenylalanine Ammonia-Lyase and Cinnamate 4-Hydroxylase for Metabolic Channeling in Phenylpropanoid Biosynthesis. *The Plant Cell* **16**, 3098–3109.
- Adams E, Frank L.** 1980. Metabolism of Proline and the Hydroxyprolines. *Annual Review of Biochemistry* **49**, 1005–1061.
- Atlante A, Passarella S, Pierro P, Martino CD, Quagliariello E.** 1996. The Mechanism of Proline/Glutamate Antipport in Rat Kidney Mitochondria. *European Journal of Biochemistry* **241**, 171–177.
- Avila-Ospina L, Moison M, Yoshimoto K, Masclaux-Daubresse C.** 2014. Autophagy, plant senescence, and nutrient recycling. *Journal of Experimental Botany* **65**, 3799–3811.
- Baena-González E, Rolland F, Thevelein JM, Sheen J.** 2007. A central integrator of transcription networks in plant stress and energy signalling. *Nature* **448**, 938–942.
- Baena-González E, Sheen J.** 2008. Convergent energy and stress signaling. *Trends in Plant Science* **13**, 474–482.
- Banerjee A, Roychoudhury A.** 2015. WRKY Proteins: Signaling and Regulation of Expression during Abiotic Stress Responses. *The Scientific World Journal* **2015**, 1–17.
- Bar-On YM, Phillips R, Milo R.** 2018. The biomass distribution on Earth. *Proceedings of the National Academy of Sciences* **115**, 6506–6511.
- Becker DF, Zhu W, Moxley MA.** 2011. Flavin Redox Switching of Protein Functions. *Antioxidants & Redox Signaling* **14**, 1079–1091.
- Ben Rejeb K, Abdelly C, Savouré A.** 2014. How reactive oxygen species and proline face stress together. *Plant Physiology and Biochemistry* **80**, 278–284.
- Berg JM, Tymoczko JL, Gatto GJ, Stryer L.** 2015. *Biochemistry*. New York: W.H. Freeman & Company, a Macmillan Education Imprint.
- Bernard SM, Habash DZ.** 2009. The importance of cytosolic glutamine synthetase in nitrogen assimilation and recycling. *New Phytologist* **182**, 608–620.
- Bezawork-Geleta A, Rohlena J, Dong L, Pacak K, Neuzil J.** 2017. Mitochondrial Complex II: At the Crossroads. *Trends in biochemical sciences* **42**, 312–325.
- Bian Y, Song C, Cheng K, Dong M, Wang F, Huang J, Sun D, Wang L, Ye M, Zou H.** 2014. An enzyme assisted RP-RPLC approach for in-depth analysis of human liver phosphoproteome. *Journal of Proteomics* **96**, 253–262.
- Borsani O, Zhu J, Verslues PE, Sunkar R, Zhu J-K.** 2005. Endogenous siRNAs Derived from a Pair of Natural cis-Antisense Transcripts Regulate Salt Tolerance in Arabidopsis. *Cell* **123**, 1279–1291.
- Brocker C, Vasiliou M, Carpenter S, et al.** 2013. Aldehyde dehydrogenase (ALDH) superfamily in plants: gene nomenclature and comparative genomics. *Planta* **237**, 189–210.
- Brugière N, Dubois F, Limami AM, Lelandais M, Roux Y, Sangwan RS, Hirel B.** 1999. Glutamine Synthetase in the Phloem Plays a Major Role in Controlling Proline Production. *The Plant Cell* **11**, 1995–2011.
- Brunner G, Neupert W.** 1969. Localisation of proline oxidase and Δ -pyrroline-5-carboxylic acid dehydrogenase in rat liver. *FEBS Letters* **3**, 283–286.

- Buchanan-Wollaston V, Page T, Harrison E, et al.** 2005. Comparative transcriptome analysis reveals significant differences in gene expression and signalling pathways between developmental and dark/starvation-induced senescence in *Arabidopsis*. *The Plant Journal* **42**, 567–585.
- Cabassa-Hourton C, Schertl P, Bordenave-Jacquemin M, et al.** 2016. Proteomic and functional analysis of proline dehydrogenase 1 link proline catabolism to mitochondrial electron transport in *Arabidopsis thaliana*. *Biochemical Journal* **473**, 2623–2634.
- Cecchini NM, Monteoliva MI, Alvarez ME.** 2011. Proline Dehydrogenase Contributes to Pathogen Defense in *Arabidopsis*. *Plant Physiology* **155**, 1947–1959.
- Chamberlain LH, Shipston MJ.** 2015. The Physiology of Protein S-acylation. *Physiological Reviews* **95**, 341–376.
- Charbonnier S, Gallego O, Gavin A-C.** 2008. The social network of a cell: Recent advances in interactome mapping. In: El-Gewely MR, ed. *Biotechnology Annual Review*. Elsevier, 1–28.
- Chen Y, Fu X, Mei X, Zhou Y, Cheng S, Zeng L, Dong F, Yang Z.** 2017. Proteolysis of chloroplast proteins is responsible for accumulation of free amino acids in dark-treated tea (*Camellia sinensis*) leaves. *Journal of Proteomics* **157**, 10–17.
- Chen S, Yang X, Yu M, et al.** 2019. SIRT3 regulates cancer cell proliferation through deacetylation of PYCR1 in proline metabolism. *Neoplasia* **21**, 665–675.
- Chen Q, Zheng Y, Luo L, Yang Y, Hu X, Kong X.** 2018. Functional FRIGIDA allele enhances drought tolerance by regulating the P5CS1 pathway in *Arabidopsis thaliana*. *Biochemical and Biophysical Research Communications* **495**, 1102–1107.
- Chiang H-H, Dandekar AM.** 1995. Regulation of proline accumulation in *Arabidopsis thaliana* (L.) Heynh during development and in response to desiccation. *Plant, Cell and Environment* **18**, 1280–1290.
- Christian JHB.** 1955. The Water Relations of Growth and Respiration of *Salmonella Oranienburg* At 30°C. *Australian Journal of Biological Sciences* **8**, 490–497.
- Chrobok D, Law SR, Brouwer B, et al.** 2016. Dissecting the Metabolic Role of Mitochondria during Developmental Leaf Senescence. *Plant Physiology* **172**, 2132–2153.
- Csonka LN, Hanson AD.** 1991. PROKARYOTIC OSMOREGULATION: Genetics and Physiology. *Annual Review of Microbiology* **45**, 569–606.
- Csonka LN, Leisinger T.** 2007. Biosynthesis of Proline. *EcoSal Plus* **2**.
- Debnam PM, Shearer G, Blackwood L, Kohl DH.** 1997. Evidence for Channeling of Intermediates in the Oxidative Pentose Phosphate Pathway by Soybean and Pea Nodule Extracts, Yeast Extracts, and Purified Yeast Enzymes. *European Journal of Biochemistry* **246**, 283–290.
- Delauney AJ, Hu CA, Kishor PB, Verma DP.** 1993. Cloning of ornithine delta-aminotransferase cDNA from *Vigna aconitifolia* by trans-complementation in *Escherichia coli* and regulation of proline biosynthesis. *Journal of Biological Chemistry* **268**, 18673–18678.
- Delauney AJ, Verma DPS.** 1993. Proline biosynthesis and osmoregulation in plants. *The Plant Journal* **4**, 215–223.
- Deuschle K, Funck D, Forlani G, Stransky H, Biehl A, Leister D, Graaff E van der, Kunze R, Frommer WB.** 2004. The Role of Δ^1 -Pyrroline-5-Carboxylate Dehydrogenase in Proline Degradation. *The Plant Cell* **16**, 3413–3425.
- Deuschle K, Funck D, Hellmann H, Däschner K, Binder S, Frommer WB.** 2001. A nuclear gene encoding mitochondrial Δ^1 -pyrroline-5-carboxylate dehydrogenase and its potential role in protection from proline toxicity. *The Plant Journal* **27**, 345–356.
- Di Martino C, Pizzuto R, Pallotta ML, De Santis A, Passarella S.** 2006. Mitochondrial transport in proline catabolism in plants: the existence of two separate translocators in mitochondria isolated from durum wheat seedlings. *Planta* **223**, 1123–1133.
- Díaz P, Betti M, Sánchez DH, Udvardi MK, Monza J, Márquez AJ.** 2010. Deficiency in plastidic glutamine synthetase alters proline metabolism and transcriptomic response in *Lotus japonicus* under drought stress. *New Phytologist* **188**, 1001–1013.

- Dietrich K, Weltmeier F, Ehlert A, Weiste C, Stahl M, Harter K, Dröge-Laser W.** 2011. Heterodimers of the Arabidopsis Transcription Factors bZIP1 and bZIP53 Reprogram Amino Acid Metabolism during Low Energy Stress. *The Plant Cell* **23**, 381–395.
- Dietz K-J, Vogel MO, Viehhauser A.** 2010. AP2/EREBP transcription factors are part of gene regulatory networks and integrate metabolic, hormonal and environmental signals in stress acclimation and retrograde signalling. *Protoplasma* **245**, 3–14.
- Dobrenel T, Caldana C, Hanson J, Robaglia C, Vincentz M, Veit B, Meyer C.** 2016. TOR Signaling and Nutrient Sensing. *Annual Review of Plant Biology* **67**, 261–285.
- Doimo M, Desbats MA, Baldoin MC, et al.** 2013. Functional Analysis of Missense Mutations of OAT, Causing Gyrate Atrophy of Choroid and Retina. *Human Mutation* **34**, 229–236.
- Dröge-Laser W, Weiste C.** 2018. The C/S1 bZIP Network: A Regulatory Hub Orchestrating Plant Energy Homeostasis. *Trends in Plant Science* **23**, 422–433.
- Dubois M, Claeys H, Broeck LV den, Inzé D.** 2017. Time of day determines Arabidopsis transcriptome and growth dynamics under mild drought. *Plant, Cell & Environment* **40**, 180–189.
- Durek P, Schmidt R, Heazlewood JL, Jones A, MacLean D, Nagel A, Kersten B, Schulze WX.** 2010. PhosphAt: the Arabidopsis thaliana phosphorylation site database. An update. *Nucleic Acids Research* **38**, D828–D834.
- Edman K, Ericson I, Møller IM.** 1985. The regulation of exogenous NAD(P)H oxidation in spinach (*Spinacia oleracea*) leaf mitochondria by pH and cations. *Biochemical Journal* **232**, 471–477.
- Elthon TE, Stewart CR.** 1981. Submitochondrial Location and Electron Transport Characteristics of Enzymes Involved in Proline Oxidation. *PLANT PHYSIOLOGY* **67**, 780–784.
- Fabro G, Cislighi AP, Condat F, Deza Borau G, Alvarez ME.** 2020. The N-terminal domain of Arabidopsis proline dehydrogenase affects enzymatic activity and protein oligomerization. *Plant Physiology and Biochemistry* **154**, 268–276.
- Fabro G, Kovács I, Pavet V, Szabados L, Alvarez ME.** 2004. Proline accumulation and AtP5CS2 gene activation are induced by plant-pathogen incompatible interactions in Arabidopsis. *Molecular Plant-Microbe Interactions* **17**, 343–350.
- Faës P, Deleu C, Ainouche A, et al.** 2015. Molecular evolution and transcriptional regulation of the oilseed rape proline dehydrogenase genes suggest distinct roles of proline catabolism during development. *Planta* **241**, 403–419.
- Farrant RD, Walker V, Mills GA, Mellor JM, Langley GJ.** 2001. Pyridoxal Phosphate De-activation by Pyrroline-5-carboxylic Acid: INCREASED RISK OF VITAMIN B6 DEFICIENCY AND SEIZURES IN HYPERPROLINEMIA TYPE II*. *Journal of Biological Chemistry* **276**, 15107–15116.
- Fedoroff NV, Battisti DS, Beachy RN, et al.** 2010. Radically Rethinking Agriculture for the 21st Century. *Science* **327**, 833–834.
- Fichman Y, Gerdes SY, Kovács H, Szabados L, Zilberstein A, Csonka LN.** 2015. Evolution of proline biosynthesis: enzymology, bioinformatics, genetics, and transcriptional regulation. *Biological Reviews* **90**, 1065–1099.
- Fischer W-N, Kwart M, Hummel S, Frommer WB.** 1995. Substrate Specificity and Expression Profile of Amino Acid Transporters (AAPs) in Arabidopsis*. *Journal of Biological Chemistry* **270**, 16315–16320.
- Frommer WB, Hummel S, Riesmeier JW.** 1993. Expression cloning in yeast of a cDNA encoding a broad specificity amino acid permease from Arabidopsis thaliana. *Proceedings of the National Academy of Sciences* **90**, 5944–5948.
- Fujii H, Chinnusamy V, Rodrigues A, Rubio S, Antoni R, Park S-Y, Cutler SR, Sheen J, Rodriguez PL, Zhu J-K.** 2009. In vitro reconstitution of an abscisic acid signalling pathway. *Nature* **462**, 660–664.
- Fujita T, Maggio A, Garcia-Rios M, Bressan RA, Csonka LN.** 1998. Comparative Analysis of the Regulation of Expression and Structures of Two Evolutionarily Divergent Genes for Δ^1 -Pyrroline-5-Carboxylate Synthetase from Tomato. *Plant Physiology* **118**, 661–674.
- Funck D, Eckard S, Müller G.** 2010. Non-redundant functions of two proline dehydrogenase isoforms in Arabidopsis. *BMC Plant Biology* **10**, 70.

- Funck D, Winter G, Baumgarten L, Forlani G.** 2012. Requirement of proline synthesis during Arabidopsis reproductive development. *BMC Plant Biology* **12**, 191.
- Fyhn HJ.** 1976. Holeuryhalinity and its mechanisms in a cirriped crustacean, *Balanus improvisus*. *Comparative Biochemistry and Physiology Part A: Physiology* **53**, 19–30.
- Gao P, Tchernyshyov I, Chang T-C, et al.** 2009. c-Myc suppression of miR-23a/b enhances mitochondrial glutaminase expression and glutamine metabolism. *Nature* **458**, 762–765.
- Ghars MA, Parre E, Debez A, Bordenave M, Richard L, Leport L, Bouchereau A, Savouré A, Abdelly C.** 2008. Comparative salt tolerance analysis between *Arabidopsis thaliana* and *Thellungiella halophila*, with special emphasis on K⁺/Na⁺ selectivity and proline accumulation. *Journal of Plant Physiology* **165**, 588–599.
- Ghars MA, Richard L, Lefebvre-De Vos D, Leprince A-S, Parre E, Bordenave M, Abdelly C, Savouré A.** 2012. Phospholipases C and D Modulate Proline Accumulation in *Thellungiella halophila/salsuginea* Differently According to the Severity of Salt or Hyperosmotic Stress. *Plant and Cell Physiology* **53**, 183–192.
- Gill SS, Tuteja N.** 2010. Reactive oxygen species and antioxidant machinery in abiotic stress tolerance in crop plants. *Plant Physiology and Biochemistry* **48**, 909–930.
- Gilles R, Schoffeniels E.** 1969. Isosmotic regulation in isolated surviving nerves of *eriocheir sinensis* Milne Edwards. *Comparative Biochemistry and Physiology* **31**, 927–939.
- Giménez-Andrés M, Čopič A, Antonny B.** 2018. The Many Faces of Amphipathic Helices. *Biomolecules* **8**, 45.
- Ginzberg I, Stein H, Kapulnik Y, Szabados L, Strizhov N, Schell J, Koncz C, Zilberstein A.** 1998. Isolation and characterization of two different cDNAs of $\Delta 1$ -pyrroline-5-carboxylate synthase in alfalfa, transcriptionally induced upon salt stress. *Plant Molecular Biology* **38**, 755–764.
- Girousse C, Bournoville R, Bonnemain JL.** 1996. Water Deficit-Induced Changes in Concentrations in Proline and Some Other Amino Acids in the Phloem Sap of Alfalfa. *Plant Physiology* **111**, 109–113.
- Gleason C, Huang S, Thatcher LF, Foley RC, Anderson CR, Carroll AJ, Millar AH, Singh KB.** 2011. Mitochondrial complex II has a key role in mitochondrial-derived reactive oxygen species influence on plant stress gene regulation and defense. *Proceedings of the National Academy of Sciences* **108**, 10768–10773.
- Goncalves RLS, Rothschild DE, Quinlan CL, Scott GK, Benz CC, Brand MD.** 2014. Sources of superoxide/H₂O₂ during mitochondrial proline oxidation. *Redox Biology* **2**, 901–909.
- Gontero B, Cárdenas ML, Ricard J.** 1988. A functional five-enzyme complex of chloroplasts involved in the Calvin cycle. *European Journal of Biochemistry* **173**, 437–443.
- Graaff E van der, Schwacke R, Schneider A, Desimone M, Flügge U-I, Kunze R.** 2006. Transcription Analysis of Arabidopsis Membrane Transporters and Hormone Pathways during Developmental and Induced Leaf Senescence. *Plant Physiology* **141**, 776–792.
- Graham JWA, Williams TCR, Morgan M, Fernie AR, Ratcliffe RG, Sweetlove LJ.** 2007. Glycolytic Enzymes Associate Dynamically with Mitochondria in Response to Respiratory Demand and Support Substrate Channeling. *The Plant Cell* **19**, 3723–3738.
- Grallath S, Weimar T, Meyer A, Gummy C, Suter-Grotemeyer M, Neuhaus J-M, Rentsch D.** 2005. The AtProT Family. Compatible Solute Transporters with Similar Substrate Specificity But Differential Expression Patterns. *Plant Physiology* **137**, 117–126.
- Gu D, Zhou Y, Kallhoff V, Baban B, Tanner JJ, Becker DF.** 2004. Identification and Characterization of the DNA-binding Domain of the Multifunctional PutA Flavoenzyme. *Journal of Biological Chemistry* **279**, 31171–31176.
- Guan M, Møller IS, Schjoerring JK.** 2015. Two cytosolic glutamine synthetase isoforms play specific roles for seed germination and seed yield structure in Arabidopsis. *Journal of Experimental Botany* **66**, 203–212.
- Hagedorn CH, Phang JM.** 1986. Catalytic transfer of hydride ions from NADPH to oxygen by the interconversions of proline and $\Delta 1$ -pyrroline-5-carboxylate. *Archives of Biochemistry and Biophysics* **248**, 166–174.
- Hancock CN, Liu W, Alvord WG, Phang JM.** 2016. Co-regulation of mitochondrial respiration by proline dehydrogenase/oxidase and succinate. *Amino Acids* **48**, 859–872.

- Hanson J, Hanssen M, Wiese A, Hendriks MMWB, Smeekens S.** 2008. The sucrose regulated transcription factor bZIP11 affects amino acid metabolism by regulating the expression of ASPARAGINE SYNTHETASE1 and PROLINE DEHYDROGENASE2: bZIP11 affects metabolism of amino acids. *The Plant Journal* **53**, 935–949.
- Hanson AD, Tully RE.** 1979. Light stimulation of proline synthesis in water-stressed barley leaves. *Planta* **145**, 45–51.
- Havé M, Marmagne A, Chardon F, Masclaux-Daubresse C.** 2016. Nitrogen remobilisation during leaf senescence: lessons from Arabidopsis to crops. *Journal of Experimental Botany*, erw365.
- Hayashi F, Ichino T, Osanai M, Wada K.** 2000. Oscillation and Regulation of Proline Content by P5CS and ProDH Gene Expressions in the Light/Dark Cycles in *Arabidopsis thaliana* L. *Plant and Cell Physiology* **41**, 1096–1101.
- Hemsley PA.** 2015. The importance of lipid modified proteins in plants. *New Phytologist* **205**, 476–489.
- Hemsley PA, Weimar T, Lilley KS, Dupree P, Grierson CS.** 2013. A proteomic approach identifies many novel palmitoylated proteins in Arabidopsis. *New Phytologist* **197**, 805–814.
- Hervieu F, Dily FL, Huault C, Billard J-P.** 1995. Contribution of ornithine aminotransferase to proline accumulation in NaCl-treated radish cotyledons. *Plant, Cell & Environment* **18**, 205–210.
- Hong Y, Zhang H, Huang L, Li D, Song F.** 2016. Overexpression of a Stress-Responsive NAC Transcription Factor Gene ONAC022 Improves Drought and Salt Tolerance in Rice. *Frontiers in Plant Science* **7**.
- Howarth JR, Parmar S, Jones J, et al.** 2008. Co-ordinated expression of amino acid metabolism in response to N and S deficiency during wheat grain filling. *Journal of Experimental Botany* **59**, 3675–3689.
- Hu C, Ham B-K, El-shabrawi HM, Alexander D, Zhang D, Ryals J, Lucas WJ.** 2016. Proteomics and metabolomics analyses reveal the cucurbit sieve tube system as a complex metabolic space. *The Plant Journal* **87**, 442–454.
- Huang S, Millar AH.** 2013. Succinate dehydrogenase: the complex roles of a simple enzyme. *Current Opinion in Plant Biology* **16**, 344–349.
- Huege J, Goetze J, Schwarz D, Bauwe H, Hagemann M, Kopka J.** 2011. Modulation of the Major Paths of Carbon in Photorespiratory Mutants of *Synechocystis*. *PLOS ONE* **6**, e16278.
- Huijbers MME, Berkel WJH van.** 2015. High yields of active *Thermus thermophilus* proline dehydrogenase are obtained using maltose-binding protein as a solubility tag. *Biotechnology Journal* **10**, 395–403.
- Huijbers MME, Berkel WJH van.** 2016. A more polar N-terminal helix releases MBP-tagged *Thermus thermophilus* proline dehydrogenase from tetramer-polymer self-association. *Journal of Molecular Catalysis B: Enzymatic* **134**, 340–346.
- Hur J, Jung K-H, Lee C-H, An G.** 2004. Stress-inducible OsP5CS2 gene is essential for salt and cold tolerance in rice. *Plant Science* **167**, 417–426.
- Igarashi Y, Yoshiba Y, Takeshita T, Nomura S, Otomo J, Yamaguchi-Shinozaki K, Shinozaki K.** 2000. Molecular Cloning and Characterization of a cDNA Encoding Proline Transporter in Rice. *Plant and Cell Physiology* **41**, 750–756.
- Ingeniis JD, Ratnikov B, Richardson AD, et al.** 2012. Functional Specialization in Proline Biosynthesis of Melanoma. *PLOS ONE* **7**, e45190.
- Ishikawa M, Tsuchiya D, Oyama T, Tsunaka Y, Morikawa K.** 2004. Structural basis for channelling mechanism of a fatty acid β -oxidation multienzyme complex. *The EMBO Journal* **23**, 2745–2754.
- Ishizaki K, Larson TR, Schauer N, Fernie AR, Graham IA, Leaver CJ.** 2005. The Critical Role of Arabidopsis Electron-Transfer Flavoprotein:Ubiquinone Oxidoreductase during Dark-Induced Starvation. *The Plant Cell* **17**, 2587–2600.
- Islam MM, Wallin R, Wynn RM, Conway M, Fujii H, Mobley JA, Chuang DT, Hutson SM.** 2007. A Novel Branched-chain Amino Acid Metabolite: PROTEIN-PROTEIN INTERACTIONS IN A SUPRAMOLECULAR COMPLEX*. *Journal of Biological Chemistry* **282**, 11893–11903.
- Izumi M, Ishida H.** 2019. An additional role for chloroplast proteins—an amino acid reservoir for energy production during sugar starvation. *Plant Signaling & Behavior* **14**, 1552057.

- Jarzyniak KM, Jasiński M.** 2014. Membrane transporters and drought resistance – a complex issue. *Frontiers in Plant Science* **5**.
- Jiang Y, Qiu Y, Hu Y, Yu D.** 2016. Heterologous Expression of AtWRKY57 Confers Drought Tolerance in *Oryza sativa*. *Frontiers in Plant Science* **7**.
- JL R, EM M.** 1998. The AP2/EREBP family of plant transcription factors. *Biological Chemistry* **379**, 633–646.
- Jortzik E, Fritz-Wolf K, Sturm N, Hipp M, Rahlfs S, Becker K.** 2010. Redox Regulation of Plasmodium falciparum Ornithine δ -Aminotransferase. *Journal of Molecular Biology* **402**, 445–459.
- Katchalsky A, Paecht M.** 1954. Phosphate Anhydrides of Amino Acids. *Journal of the American Chemical Society* **76**, 6042–6044.
- Keech O, Pesquet E, Ahad A, Askne A, Nordvall D, Vodnala SM, Tuominen H, Hurry V, Dizengremel P, Gardeström P.** 2007. The different fates of mitochondria and chloroplasts during dark-induced senescence in *Arabidopsis* leaves. *Plant, Cell & Environment* **30**, 1523–1534.
- Kemble AR, Macpherson HT.** 1954. Liberation of amino acids in perennial rye grass during wilting. *Biochemical Journal* **58**, 46–49.
- Kesari R, Lasky JR, Villamor JG, Des Marais DL, Chen Y-JC, Liu T-W, Lin W, Juenger TE, Verslues PE.** 2012. Intron-mediated alternative splicing of Arabidopsis P5CS1 and its association with natural variation in proline and climate adaptation. *Proceedings of the National Academy of Sciences of the United States of America* **109**, 9197–9202.
- Kiyosue T, Yoshiba Y, Yamaguchi-Shinozaki K, Shinozaki K.** 1996. A nuclear gene encoding mitochondrial proline dehydrogenase, an enzyme involved in proline metabolism, is upregulated by proline but down-regulated by dehydration in *Arabidopsis*. *The Plant Cell* **8**, 1323–1335.
- Korasick DA, Campbell AC, Christgen SL, Chakravarthy S, White TA, Becker DF, Tanner JJ.** 2018. Redox Modulation of Oligomeric State in Proline Utilization A. *Biophysical Journal* **114**, 2833–2843.
- Korasick DA, Gamage TT, Christgen S, Stiers KM, Beamer LJ, Henzl MT, Becker DF, Tanner JJ.** 2017. Structure and characterization of a class 3B proline utilization A: Ligand-induced dimerization and importance of the C-terminal domain for catalysis. *Journal of Biological Chemistry* **292**, 9652–9665.
- Korasick DA, Končítíková R, Kopečná M, Hájková E, Vigouroux A, Moréra S, Becker DF, Šebela M, Tanner JJ, Kopečný D.** 2019. Structural and Biochemical Characterization of Aldehyde Dehydrogenase 12, the Last Enzyme of Proline Catabolism in Plants. *Journal of Molecular Biology* **431**, 576–592.
- Kovács H, Aleksza D, Baba AI, Hajdu A, Király AM, Zsigmond L, Tóth SZ, Kozma-Bognár L, Szabados L.** 2019. Light Control of Salt-Induced Proline Accumulation Is Mediated by ELONGATED HYPOCOTYL 5 in *Arabidopsis*. *Frontiers in Plant Science* **10**.
- Krishnan N, Dickman MB, Becker DF.** 2008. Proline modulates the intracellular redox environment and protects mammalian cells against oxidative stress. *Free Radical Biology and Medicine* **44**, 671–681.
- Lagautriere T, Bashiri G, Baker EN.** 2015. Use of a “silver bullet” to resolve crystal lattice dislocation disorder: A cobalamin complex of $\Delta 1$ -pyrroline-5-carboxylate dehydrogenase from *Mycobacterium tuberculosis*. *Journal of Structural Biology* **189**, 153–157.
- Lapiente-Brun E, Moreno-Loshuertos R, Acín-Pérez R, et al.** 2013. Supercomplex Assembly Determines Electron Flux in the Mitochondrial Electron Transport Chain. *Science* **340**, 1567–1570.
- Launay A, Cabassa-Hourton C, Eubel H, et al.** 2019. Proline oxidation fuels mitochondrial respiration during dark-induced leaf senescence in *Arabidopsis thaliana*. *Journal of Experimental Botany* **70**, 6203–6214.
- Laursen T, Borch J, Knudsen C, et al.** 2016. Characterization of a dynamic metabolon producing the defense compound dhurrin in sorghum. *Science* **354**, 890–893.
- Lee J, He K, Stolc V, Lee H, Figueroa P, Gao Y, Tongprasit W, Zhao H, Lee I, Deng XW.** 2007. Analysis of Transcription Factor HY5 Genomic Binding Sites Revealed Its Hierarchical Role in Light Regulation of Development. *The Plant Cell* **19**, 731–749.
- Lee Y-H, Tegeder M.** 2004. Selective expression of a novel high-affinity transport system for acidic and neutral amino acids in the tapetum cells of *Arabidopsis* flowers. *The Plant Journal* **40**, 60–74.
- Lehmann S, Funck D, Szabados L, Rentsch D.** 2010. Proline metabolism and transport in plant development. *Amino Acids* **39**, 949–962.

- Li C, Ng CK-Y, Fan L-M.** 2015. MYB transcription factors, active players in abiotic stress signaling. *Environmental and Experimental Botany* **114**, 80–91.
- Liebsch D, Keech O.** 2016. Dark-induced leaf senescence: new insights into a complex light-dependent regulatory pathway. *New Phytologist* **212**, 563–570.
- Lim PO, Kim HJ, Gil Nam H.** 2007. Leaf Senescence. *Annual Review of Plant Biology* **58**, 115–136.
- Liu W, Hancock CN, Fischer JW, Harman M, Phang JM.** 2015. Proline biosynthesis augments tumor cell growth and aerobic glycolysis: involvement of pyridine nucleotides. *Scientific Reports* **5**, 17206.
- Liu W, Le A, Hancock C, Lane AN, Dang CV, Fan TW-M, Phang JM.** 2012. Reprogramming of proline and glutamine metabolism contributes to the proliferative and metabolic responses regulated by oncogenic transcription factor c-MYC. *Proceedings of the National Academy of Sciences* **109**, 8983–8988.
- Liu X, Liu S, Wu J, Zhang B, Li X, Yan Y, Li L.** 2013. Overexpression of *Arachis hypogaea* NAC3 in tobacco enhances dehydration and drought tolerance by increasing superoxide scavenging. *Plant Physiology and Biochemistry* **70**, 354–359.
- Liu W, Phang JM.** 2012. Proline dehydrogenase (oxidase) in cancer. *BioFactors* **38**, 398–406.
- Liu C, Xue Z, Tang D, Shen Y, Shi W, Ren L, Du G, Li Y, Cheng Z.** 2018. Ornithine δ -aminotransferase is critical for floret development and seed setting through mediating nitrogen reutilization in rice. *The Plant Journal* **96**, 842–854.
- Lomelino CL, Andring JT, McKenna R, Kilberg MS.** 2017. Asparagine synthetase: Function, structure, and role in disease. *Journal of Biological Chemistry* **292**, 19952–19958.
- Luo M, Gamage TT, Arentson BW, Schlasner KN, Becker DF, Tanner JJ.** 2016. Structures of Proline Utilization A (PutA) Reveal the Fold and Functions of the Aldehyde Dehydrogenase Superfamily Domain of Unknown Function. *Journal of Biological Chemistry* **291**, 24065–24075.
- Luo M, Singh RK, Tanner JJ.** 2013. Structural Determinants of Oligomerization of Δ 1-Pyrroline-5-Carboxylate Dehydrogenase: Identification of a Hexamerization Hot Spot. *Journal of Molecular Biology* **425**, 3106–3120.
- Ma Y, Szostkiewicz I, Korte A, Moes D, Yang Y, Christmann A, Grill E.** 2009. Regulators of PP2C Phosphatase Activity Function as Abscisic Acid Sensors. *Science* **324**, 1064–1068.
- Madeira F, Park YM, Lee J, et al.** 2019. The EMBL-EBI search and sequence analysis tools APIs in 2019. *Nucleic acids research* **47**, W636–W641.
- Mair A, Pedrotti L, Wurzinger B, et al.** 2015. SnRK1-triggered switch of bZIP63 dimerization mediates the low-energy response in plants. *eLife* **4**, e05828.
- Makino A, Osmond B.** 1991. Effects of Nitrogen Nutrition on Nitrogen Partitioning between Chloroplasts and Mitochondria in Pea and Wheat. *Plant Physiology* **96**, 355–362.
- Makino A, Sato T, Nakano H, Mae T.** 1997. Leaf photosynthesis, plant growth and nitrogen allocation in rice under different irradiances. *Planta* **203**, 390–398.
- Mantilla BS, Paes LS, Pral EMF, Martil DE, Thiemann OH, Fernández-Silva P, Bastos EL, Silber AM.** 2015. Role of Δ 1-Pyrroline-5-Carboxylate Dehydrogenase Supports Mitochondrial Metabolism and Host-Cell Invasion of *Trypanosoma cruzi**. *Journal of Biological Chemistry* **290**, 7767–7790.
- Mao X, Jia D, Li A, Zhang H, Tian S, Zhang X, Jia J, Jing R.** 2011. Transgenic expression of TaMYB2A confers enhanced tolerance to multiple abiotic stresses in *Arabidopsis*. *Functional & Integrative Genomics* **11**, 445–465.
- Marchand CH, Vanacker H, Collin V, Issakidis-Bourguet E, Maréchal PL, Decottignies P.** 2010. Thioredoxin targets in *Arabidopsis* roots. *PROTEOMICS* **10**, 2418–2428.
- Marcotte EM, Pellegrini M, Ng H-L, Rice DW, Yeates TO, Eisenberg D.** 1999. Detecting Protein Function and Protein-Protein Interactions from Genome Sequences. *Science* **285**, 751–753.
- Marianayagam NJ, Sunde M, Matthews JM.** 2004. The power of two: protein dimerization in biology. *Trends in Biochemical Sciences* **29**, 618–625.
- Masclaux-Daubresse C, Reisdorf-Cren M, Pageau K, Lelandais M, Grandjean O, Kronenberger J, Valadier M-H, Feraud M, Joulet T, Suzuki A.** 2006. Glutamine Synthetase-Glutamate Synthase Pathway and

REFERENCES

- Glutamate Dehydrogenase Play Distinct Roles in the Sink-Source Nitrogen Cycle in Tobacco. *Plant Physiology* **140**, 444–456.
- Matthews JM, Sunde M.** 2012. Dimers, Oligomers, Everywhere. In: Matthews JM, ed. *Advances in Experimental Medicine and Biology. Protein Dimerization and Oligomerization in Biology*. New York, NY: Springer, 1–18.
- Mattioli R, Costantino P, Trovato M.** 2009a. Proline accumulation in plants. *Plant Signaling & Behavior* **4**, 1016–1018.
- Mattioli R, Falasca G, Sabatini S, Altamura MM, Costantino P, Trovato M.** 2009b. The proline biosynthetic genes P5CS1 and P5CS2 play overlapping roles in Arabidopsis flower transition but not in embryo development. *Physiologia Plantarum* **137**, 72–85.
- Mattioli R, Marchese D, D'Angeli S, Altamura MM, Costantino P, Trovato M.** 2008. Modulation of intracellular proline levels affects flowering time and inflorescence architecture in Arabidopsis. *Plant Molecular Biology* **66**, 277–288.
- Maxwell SA, Davis GE.** 2000. Differential gene expression in p53-mediated apoptosis-resistant vs. apoptosis-sensitive tumor cell lines. *Proceedings of the National Academy of Sciences* **97**, 13009–13014.
- McKenna MC, Waagepetersen HS, Schousboe A, Sonnewald U.** 2006. Neuronal and astrocytic shuttle mechanisms for cytosolic-mitochondrial transfer of reducing equivalents: Current evidence and pharmacological tools. *Biochemical Pharmacology* **71**, 399–407.
- Mezl VA, Knox WE.** 1977. Metabolism of arginine in lactating rat mammary gland. *Biochemical Journal* **166**, 105–113.
- Miller G, Honig A, Stein H, Suzuki N, Mittler R, Zilberstein A.** 2009. Unraveling Δ^1 -Pyrroline-5-Carboxylate-Proline Cycle in Plants by Uncoupled Expression of Proline Oxidation Enzymes. *Journal of Biological Chemistry* **284**, 26482–26492.
- Mondal WA, Dey BB, Choudhuri MA.** 1985. Proline accumulation as a reliable indicator of monocarpic senescence in rice cultivars. *Experientia* **41**, 346–348.
- Monteoliva MI, Rizzi YS, Cecchini NM, Hajirezaei M-R, Alvarez ME.** 2014. Context of action of Proline Dehydrogenase (ProDH) in the Hypersensitive Response of Arabidopsis. *BMC Plant Biology* **14**, 21.
- Montioli R, Zamparelli C, Borri Voltattorni C, Cellini B.** 2017. Oligomeric State and Thermal Stability of Apo- and Holo- Human Ornithine δ -Aminotransferase. *The Protein Journal* **36**, 174–185.
- Moxley MA, Tanner JJ, Becker DF.** 2011. Steady-state kinetic mechanism of the proline:ubiquinone oxidoreductase activity of proline utilization A (PutA) from *Escherichia coli*. *Archives of Biochemistry and Biophysics* **516**, 113–120.
- Nanjo T, Kobayashi M, Yoshiba Y, Sanada Y, Wada K, Tsukaya H, Kakubari Y, Yamaguchi-Shinozaki K, Shinozaki K.** 1999. Biological functions of proline in morphogenesis and osmotolerance revealed in antisense transgenic Arabidopsis thaliana. *The Plant Journal* **18**, 185–193.
- Nishimura A, Nasuno R, Takagi H.** 2012. The proline metabolism intermediate Δ^1 -pyrroline-5-carboxylate directly inhibits the mitochondrial respiration in budding yeast. *FEBS Letters* **586**, 2411–2416.
- Noodén LD, Penney JP.** 2001. Correlative controls of senescence and plant death in *Arabidopsis thaliana* (Brassicaceae). *Journal of Experimental Botany* **52**, 2151–2159.
- Nooren IMA, Thornton JM.** 2003. Diversity of protein–protein interactions. *The EMBO Journal* **22**, 3486–3492.
- Ostrovsky PC, Maloy S.** 1995. Protein phosphorylation on serine, threonine, and tyrosine residues modulates membrane-protein interactions and transcriptional regulation in *Salmonella typhimurium*. *Genes & Development* **9**, 2034–2041.
- Paes LS, Mantilla BS, Zimbres FM, Pral EMF, Melo PD de, Tahara EB, Kowaltowski AJ, Elias MC, Silber AM.** 2013. Proline Dehydrogenase Regulates Redox State and Respiratory Metabolism in *Trypanosoma cruzi*. *PLOS ONE* **8**, e69419.
- Palmieri F, Rieder B, Ventrella A, et al.** 2009. Molecular Identification and Functional Characterization of *Arabidopsis thaliana* Mitochondrial and Chloroplastic NAD⁺ Carrier Proteins. *Journal of Biological Chemistry* **284**, 31249–31259.

- Pandey N, Ranjan A, Pant P, Tripathi RK, Ateek F, Pandey HP, Patre UV, Sawant SV.** 2013. CAMTA 1 regulates drought responses in *Arabidopsis thaliana*. *BMC Genomics* **14**, 216.
- Park J, Chen Y, Tishkoff DX, et al.** 2013. SIRT5-Mediated Lysine Desuccinylation Impacts Diverse Metabolic Pathways. *Molecular Cell* **50**, 919–930.
- Park S-Y, Fung P, Nishimura N, et al.** 2009. Abscisic Acid Inhibits Type 2C Protein Phosphatases via the PYR/PYL Family of START Proteins. *Science* **324**, 1068–1071.
- Parre E, Ghars MA, Leprince A-S, Thiery L, Lefebvre D, Bordenave M, Richard L, Mazars C, Abdely C, Savouré A.** 2007. Calcium Signaling via Phospholipase C Is Essential for Proline Accumulation upon Ionic But Not Nonionic Hyperosmotic Stresses in *Arabidopsis*. *Plant Physiology* **144**, 503–512.
- Pedrotti L, Weiste C, Nägele T, et al.** 2018. Snf1-RELATED KINASE1-Controlled C/S1-bZIP Signaling Activates Alternative Mitochondrial Metabolic Pathways to Ensure Plant Survival in Extended Darkness. *The Plant Cell* **30**, 495–509.
- Pemberton TA, Srivastava D, Sanyal N, Henzl MT, Becker DF, Tanner JJ.** 2014. Structural Studies of Yeast Δ^1 -Pyrroline-5-carboxylate Dehydrogenase (ALDH4A1): Active Site Flexibility and Oligomeric State. *Biochemistry* **53**, 1350–1359.
- Pemberton TA, Tanner JJ.** 2013. Structural basis of substrate selectivity of Δ^1 -pyrroline-5-carboxylate dehydrogenase (ALDH4A1): Semialdehyde chain length. *Archives of Biochemistry and Biophysics* **538**, 34–40.
- Perkins JR, Diboun I, Dessailly BH, Lees JG, Orengo C.** 2010. Transient Protein-Protein Interactions: Structural, Functional, and Network Properties. *Structure* **18**, 1233–1243.
- Phang JM.** 2019. Proline Metabolism in Cell Regulation and Cancer Biology: Recent Advances and Hypotheses. *Antioxidants & Redox Signaling* **30**, 635–649.
- Phang JM, Liu W, Zabirnyk O.** 2010. Proline Metabolism and Microenvironmental Stress. *Annual Review of Nutrition* **30**, 441–463.
- Piao S, Liu Q, Chen A, Janssens IA, Fu Y, Dai J, Liu L, Lian X, Shen M, Zhu X.** 2019. Plant phenology and global climate change: Current progresses and challenges. *Global Change Biology* **25**, 1922–1940.
- Picot D, Loll PJ, Garavito RM.** 1994. The X-ray crystal structure of the membrane protein prostaglandin H 2 synthase-1. *Nature* **367**, 243–249.
- Qamar A, Mysore K, Senthil-Kumar M.** 2015. Role of proline and pyrroline-5-carboxylate metabolism in plant defense against invading pathogens. *Frontiers in Plant Science* **6**.
- Rardin MJ, Newman JC, Held JM, et al.** 2013. Label-free quantitative proteomics of the lysine acetylome in mitochondria identifies substrates of SIRT3 in metabolic pathways. *Proceedings of the National Academy of Sciences* **110**, 6601–6606.
- Rasmusson A, Møller IM.** 2015. Transport Into and Out of Plant Mitochondria. *Plant physiology and development*. Sinauer Associates, Inc., Publishers, Online Topic 12.5.
- Rentsch D, Hirner B, Schmelzer E, Frommer WB.** 1996. Salt stress-induced proline transporters and salt stress-repressed broad specificity amino acid permeases identified by suppression of a yeast amino acid permease-targeting mutant. *The Plant Cell* **8**, 1437–1446.
- Reversade B, Escande-Beillard N, Dimopoulou A, et al.** 2009. Mutations in PYCR1 cause cutis laxa with progeroid features. *Nature Genetics* **41**, 1016–1021.
- Robinson JB, Srere PA.** 1985. Organization of Krebs tricarboxylic acid cycle enzymes in mitochondria. *Journal of Biological Chemistry* **260**, 10800–10805.
- da Rocha IMA, Vitorello VA, Silva JS, Ferreira-Silva SL, Viégas RA, Silva EN, Silveira JAG.** 2012. Exogenous ornithine is an effective precursor and the δ -ornithine amino transferase pathway contributes to proline accumulation under high N recycling in salt-stressed cashew leaves. *Journal of Plant Physiology* **169**, 41–49.
- Roosens NH, Bitar FA, Loenders K, Angenon G, Jacobs M.** 2002. Overexpression of ornithine- δ -aminotransferase increases proline biosynthesis and confers osmotolerance in transgenic plants. *Molecular Breeding* **9**, 73–80.

- Ruberti C, Barizza E, Bodner M, La Rocca N, De Michele R, Carimi F, Schiavo FL, Zottini M. 2014. Mitochondria Change Dynamics and Morphology during Grapevine Leaf Senescence (D Bassham, Ed.). PLoS ONE 9, e102012.
- Samach A, Onouchi H, Gold SE, Ditta GS, Schwarz-Sommer Z, Yanofsky MF, Coupland G. 2000. Distinct Roles of CONSTANS Target Genes in Reproductive Development of Arabidopsis. Science 288, 1613–1616.
- Sanada Y, Ueda H, Kuribayashi K, Andoh T, Hayashi F, Tamai N, Wada K. 1995. Novel Light-Dark Change of Proline Levels in Halophyte (*Mesembryanthemum crystallinum* L.) and Glycophytes (*Hordeum vulgare* L. and *Triticum aestivum* L.) Leaves and Roots under Salt Stress. Plant and Cell Physiology 36, 965–970.
- Sanyal N, Arentson BW, Luo M, Tanner JJ, Becker DF. 2015. First Evidence for Substrate Channeling between Proline Catabolic Enzymes: A VALIDATION OF DOMAIN FUSION ANALYSIS FOR PREDICTING PROTEIN-PROTEIN INTERACTIONS. Journal of Biological Chemistry 290, 2225–2234.
- Satoh R, Fujita Y, Nakashima K, Shinozaki K, Yamaguchi-Shinozaki K. 2004. A Novel Subgroup of bZIP Proteins Functions as Transcriptional Activators in Hypoosmolarity-Responsive Expression of the ProDH Gene in Arabidopsis. Plant and Cell Physiology 45, 309–317.
- Satoh R, Nakashima K, Seki M, Shinozaki K, Yamaguchi-Shinozaki K. 2002. ACTCAT, a Novel cis-Acting Element for Proline- and Hypoosmolarity-Responsive Expression of the *ProDH* Gene Encoding Proline Dehydrogenase in Arabidopsis. Plant Physiology 130, 709–719.
- Savouré A, Hua X-J, Bertauche N, Montagu MV, Verbruggen N. 1997. Abscisic acid-independent and abscisic acid-dependent regulation of proline biosynthesis following cold and osmotic stresses in Arabidopsis thaliana. Molecular and General Genetics MGG 254, 104–109.
- Schertl P, Braun H-P. 2014. Respiratory electron transfer pathways in plant mitochondria. Frontiers in Plant Science 5.
- Schertl P, Cabassa C, Saadallah K, Bordenave M, Savouré A, Braun H-P. 2014. Biochemical characterization of proline dehydrogenase in Arabidopsis mitochondria. FEBS Journal 281, 2794–2804.
- Schulze E-D (Ed.). 2001. *Global biogeochemical cycles in the climate system*. San Diego: Academic Press.
- Schulze W, Schulze E-D, Stadler J, Heilmeier H, Stitt M, Mooney HA. 1994. Growth and reproduction of *Arabidopsis thaliana* in relation to storage of starch and nitrate in the wild-type and in starch-deficient and nitrate-uptake-deficient mutants. Plant, Cell and Environment 17, 795–809.
- Schwacke R, Grallath S, Breitzkreuz KE, Stransky E, Stransky H, Frommer WB, Rentsch D. 1999. LeProT1, a Transporter for Proline, Glycine Betaine, and γ -Amino Butyric Acid in Tomato Pollen. The Plant Cell 11, 377–391.
- Sekhar PN, Amrutha RN, Sangam S, Verma DPS, Kishor PBK. 2007. Biochemical characterization, homology modeling and docking studies of ornithine δ -aminotransferase—an important enzyme in proline biosynthesis of plants. Journal of Molecular Graphics and Modelling 26, 709–719.
- Servet C, Ghelis T, Richard L, Zilberstein A, Savoure A. 2012. Proline dehydrogenase: a key enzyme in controlling cellular homeostasis. Front Biosci 17, 607–620.
- Sharma S, Villamor JG, Verslues PE. 2011. Essential Role of Tissue-Specific Proline Synthesis and Catabolism in Growth and Redox Balance at Low Water Potential. Plant Physiology 157, 292–304.
- Shetty K. 2004. Role of proline-linked pentose phosphate pathway in biosynthesis of plant phenolics for functional food and environmental applications: a review. Process Biochemistry 39, 789–804.
- Shinde S, Villamor JG, Lin W, Sharma S, Verslues PE. 2016. Proline Coordination with Fatty Acid Synthesis and Redox Metabolism of Chloroplast and Mitochondria. Plant Physiology 172, 1074–1088.
- Shinozaki K, Yamaguchi-Shinozaki K. 2007. Gene networks involved in drought stress response and tolerance. Journal of Experimental Botany 58, 221–227.
- Silao FGS, Ward M, Ryman K, Wallström A, Brindefalk B, Udekwu K, Ljungdahl PO. 2019. Mitochondrial proline catabolism activates Ras1/cAMP/PKA-induced filamentation in *Candida albicans*. PLOS Genetics 15, e1007976.

- Singh H, Arentson BW, Becker DF, Tanner JJ.** 2014. Structures of the PutA peripheral membrane flavoenzyme reveal a dynamic substrate-channeling tunnel and the quinone-binding site. *Proceedings of the National Academy of Sciences* **111**, 3389–3394.
- Singh RK, Larson JD, Zhu W, Rambo RP, Hura GL, Becker DF, Tanner JJ.** 2011. Small-angle X-ray Scattering Studies of the Oligomeric State and Quaternary Structure of the Trifunctional Proline Utilization A (PutA) Flavoprotein from *Escherichia coli*. *Journal of Biological Chemistry* **286**, 43144–43153.
- Slocum RD.** 2005. Genes, enzymes and regulation of arginine biosynthesis in plants. *Plant Physiology and Biochemistry* **43**, 729–745.
- Smirnoff N, Cumbes QJ.** 1989. Hydroxyl radical scavenging activity of compatible solutes. *Phytochemistry* **28**, 1057–1060.
- Smith RJ, Phang JM.** 1979. The importance of ornithine as a precursor for proline in mammalian cells. *Journal of Cellular Physiology* **98**, 475–481.
- Spicer PO de, Maloy S.** 1993. PutA protein, a membrane-associated flavin dehydrogenase, acts as a redox-dependent transcriptional regulator. *Proceedings of the National Academy of Sciences* **90**, 4295–4298.
- Spivey HO, Ovádi J.** 1999. Substrate Channeling. *Methods* **19**, 306–321.
- Srere PA.** 1985. The metabolon. *Trends in Biochemical Sciences* **10**, 109–110.
- Srivastava D, Schuermann JP, White TA, Krishnan N, Sanyal N, Hura GL, Tan A, Henzl MT, Becker DF, Tanner JJ.** 2010. Crystal structure of the bifunctional proline utilization A flavoenzyme from *Bradyrhizobium japonicum*. *Proceedings of the National Academy of Sciences* **107**, 2878–2883.
- Srivastava D, Singh RK, Moxley MA, Henzl MT, Becker DF, Tanner JJ.** 2012. The Three-Dimensional Structural Basis of Type II Hyperprolinemia. *Journal of Molecular Biology* **420**, 176–189.
- Stines AP, Naylor DJ, Høj PB, Heeswijck R van.** 1999. Proline Accumulation in Developing Grapevine Fruit Occurs Independently of Changes in the Levels of $\Delta 1$ -Pyrroline-5-Carboxylate Synthetase mRNA or Protein. *Plant Physiology* **120**, 923–923.
- Stránská J, Kopečný D, Tylichová M, Snégaroff J, Šebela M.** 2008. Ornithine δ -aminotransferase. *Plant Signaling & Behavior* **3**, 929–935.
- Stránská J, Tylichová M, Kopečný D, Snégaroff J, Šebela M.** 2010. Biochemical characterization of pea ornithine- δ -aminotransferase: Substrate specificity and inhibition by di- and polyamines. *Biochimie* **92**, 940–948.
- Strecker HJ.** 1965. Purification and Properties of Rat Liver Ornithine δ -Transaminase. *Journal of Biological Chemistry* **240**, 1225–1230.
- Strizhov N, Ábrahám E, Ökrész L, Blickling S, Zilberstein A, Schell J, Koncz C, Szabados L.** 1997. Differential expression of two P5CS genes controlling proline accumulation during salt-stress requires ABA and is regulated by ABA1, ABI1 and AXR2 in *Arabidopsis*. *The Plant Journal* **12**, 557–569.
- Sweetlove LJ, Fernie AR.** 2018. The role of dynamic enzyme assemblies and substrate channelling in metabolic regulation. *Nature Communications* **9**, 2136.
- Szabados L, Savouré A.** 2010. Proline: a multifunctional amino acid. *Trends in Plant Science* **15**, 89–97.
- Székely G, Ábrahám E, Cséplő Á, et al.** 2008. Duplicated P5CS genes of *Arabidopsis* play distinct roles in stress regulation and developmental control of proline biosynthesis. *The Plant Journal* **53**, 11–28.
- Szoke A, Miao G-H, Hong Z, Verma DPS.** 1992. Subcellular Location of $\Delta 1$ -Pyrroline-5-Carboxylate Reductase in Root/Nodule and Leaf of Soybean. *Plant Physiology* **99**, 1642–1649.
- Taira M, Valtersson U, Burkhardt B, Ludwig RA.** 2004. *Arabidopsis thaliana* GLN2-Encoded Glutamine Synthetase Is Dual Targeted to Leaf Mitochondria and Chloroplasts. *The Plant Cell* **16**, 2048–2058.
- Taji T, Seki M, Satou M, Sakurai T, Kobayashi M, Ishiyama K, Narusaka Y, Narusaka M, Zhu J-K, Shinozaki K.** 2004. Comparative Genomics in Salt Tolerance between *Arabidopsis* and *Arabidopsis*-Related Halophyte Salt Cress Using *Arabidopsis* Microarray. *Plant Physiology* **135**, 1697–1709.
- Takagi H.** 2008. Proline as a stress protectant in yeast: physiological functions, metabolic regulations, and biotechnological applications. *Applied Microbiology and Biotechnology* **81**, 211–223.

- Tallarita E, Pollegioni L, Servi S, Molla G.** 2012. Expression in *Escherichia coli* of the catalytic domain of human proline oxidase. *Protein Expression and Purification* **82**, 345–351.
- Tanner JJ.** 2008. Structural biology of proline catabolism. *Amino Acids* **35**, 719–730.
- Tanner JJ.** 2017. Structural Biology of Proline Catabolic Enzymes. *Antioxidants & Redox Signaling* **30**, 650–673.
- Teulier L, Weber J-M, Crevier J, Darveau C-A.** 2016. Proline as a fuel for insect flight: enhancing carbohydrate oxidation in hymenopterans. *Proceedings of the Royal Society B: Biological Sciences* **283**, 20160333.
- Thiery L, Leprince A-S, Lefebvre D, Ghars MA, Debarbieux E, Savouré A.** 2004. Phospholipase D Is a Negative Regulator of Proline Biosynthesis in *Arabidopsis thaliana*. *Journal of Biological Chemistry* **279**, 14812–14818.
- Ueda A, Shi W, Sanmiya K, Shono M, Takabe T.** 2001. Functional Analysis of Salt-Inducible Proline Transporter of Barley Roots. *Plant and Cell Physiology* **42**, 1282–1289.
- Waditee R, Hibino T, Tanaka Y, et al.** 2002. Functional Characterization of Betaine/Proline Transporters in Betaine-accumulating Mangrove*. *Journal of Biological Chemistry* **277**, 18373–18382.
- Wanduragala S, Sanyal N, Liang X, Becker DF.** 2010. Purification and characterization of Put1p from *Saccharomyces cerevisiae*. *Archives of Biochemistry and Biophysics* **498**, 136–142.
- Wang SS, Brandriss MC.** 1987. Proline utilization in *Saccharomyces cerevisiae*: sequence, regulation, and mitochondrial localization of the PUT1 gene product. *Molecular and Cellular Biology* **7**, 4431–4440.
- Wang CY, Cheng SH, Kao CH.** 1982. Senescence of Rice Leaves: VII. PROLINE ACCUMULATION IN SENESCING EXCISED LEAVES. *Plant Physiology* **69**, 1348–1349.
- Wang C, Deng P, Chen L, et al.** 2013. A Wheat WRKY Transcription Factor TaWRKY10 Confers Tolerance to Multiple Abiotic Stresses in Transgenic Tobacco (X Zhang, Ed.). *PLoS ONE* **8**, e65120.
- Weaver LM, Amasino RM.** 2001. Senescence Is Induced in Individually Darkened *Arabidopsis* Leaves, but Inhibited in Whole Darkened Plants. *Plant Physiology* **127**, 876–886.
- Weltmeier F, Ehlert A, Mayer CS, Dietrich K, Wang X, Schütze K, Alonso R, Harter K, Vicente-Carbajosa J, Dröge-Laser W.** 2006. Combinatorial control of *Arabidopsis* proline dehydrogenase transcription by specific heterodimerisation of bZIP transcription factors. *The EMBO Journal* **25**, 3133–3143.
- Wheeldon I, Minter SD, Banta S, Barton SC, Atanassov P, Sigman M.** 2016. Substrate channelling as an approach to cascade reactions. *Nature Chemistry* **8**, 299–309.
- White TA, Krishnan N, Becker DF, Tanner JJ.** 2007. Structure and Kinetics of Monofunctional Proline Dehydrogenase from *Thermus thermophilus*. *Journal of Biological Chemistry* **282**, 14316–14327.
- Winter G, Todd CD, Trovato M, Forlani G, Funck D.** 2015. Physiological implications of arginine metabolism in plants. *Frontiers in Plant Science* **6**.
- Woo HR, Kim HJ, Lim PO, Nam HG.** 2019. Leaf Senescence: Systems and Dynamics Aspects. , 33.
- Wu L, Fan Z, Guo L, Li Y, Zhang W, Qu L-J, Chen Z.** 2003. Over-expression of an *Arabidopsis* δ -OAT gene enhances salt and drought tolerance in transgenic rice. *Chinese Science Bulletin* **48**, 2594–2600.
- Xiong H, Li J, Liu P, Duan J, Zhao Y, Guo X, Li Y, Zhang H, Ali J, Li Z.** 2014. Overexpression of OsMYB48-1, a Novel MYB-Related Transcription Factor, Enhances Drought and Salinity Tolerance in Rice (H Yang, Ed.). *PLoS ONE* **9**, e92913.
- Yang A, Dai X, Zhang W-H.** 2012. A R2R3-type MYB gene, OsMYB2, is involved in salt, cold, and dehydration tolerance in rice. *Journal of Experimental Botany* **63**, 2541–2556.
- Yang C-W, Kao CH.** 1999. Importance of ornithine- δ -aminotransferase to proline accumulation caused by water stress in detached rice leaves. *Plant Growth Regulation* **27**, 191–194.
- Yoo JH, Park CY, Kim JC, et al.** 2005. Direct Interaction of a Divergent CaM Isoform and the Transcription Factor, MYB2, Enhances Salt Tolerance in *Arabidopsis**. *Journal of Biological Chemistry* **280**, 3697–3706.
- Yoshida Y, Kiyosue T, Katagiri T, Ueda H, Mizoguchi T, Yamaguchi-Shinozaki K, Wada K, Harada Y, Shinozaki K.** 1995. Correlation between the induction of a gene for Δ 1-pyrroline-5-carboxylate

- synthetase and the accumulation of proline in *Arabidopsis thaliana* under osmotic stress. *The Plant Journal* **7**, 751–760.
- You J, Hu H, Xiong L.** 2012. An ornithine δ -aminotransferase gene OsOAT confers drought and oxidative stress tolerance in rice. *Plant Science* **197**, 59–69.
- Zarattini M, Forlani G.** 2017. Toward Unveiling the Mechanisms for Transcriptional Regulation of Proline Biosynthesis in the Plant Cell Response to Biotic and Abiotic Stress Conditions. *Frontiers in Plant Science* **8**.
- Zhang Y, Beard KFM, Swart C, et al.** 2017. Protein-protein interactions and metabolite channelling in the plant tricarboxylic acid cycle. *Nature Communications* **8**, 1–11.
- Zhang Y, Fernie AR.** 2021. Metabolons, enzyme–enzyme assemblies that mediate substrate channeling, and their roles in plant metabolism. *Plant Communications* **2**, 100081.
- Zhang B, Tolstikov V, Turnbull C, Hicks LM, Fiehn O.** 2010. Divergent metabolome and proteome suggest functional independence of dual phloem transport systems in cucurbits. *Proceedings of the National Academy of Sciences* **107**, 13532–13537.
- Zheng Y, Cabassa-Hourton C, Planchais S, Lebreton S, Savouré A.** 2021. The proline cycle as a eukaryotic redox valve. *Journal of Experimental Botany*. *In press*. doi: 10.1093/jxb/erab361
- Zhou H, Di Palma S, Preisinger C, Peng M, Polat AN, Heck AJR, Mohammed S.** 2013. Toward a Comprehensive Characterization of a Human Cancer Cell Phosphoproteome. *Journal of Proteome Research* **12**, 260–271.
- Zhou Y, Zhu W, Bellur PS, Rewinkel D, Becker DF.** 2008. Direct linking of metabolism and gene expression in the proline utilization A protein from *Escherichia coli*. *Amino Acids* **35**, 711–718.
- Zhu J-K.** 2016. Abiotic Stress Signaling and Responses in Plants. *Cell* **167**, 313–324.
- Zhu W, Becker DF.** 2003. Exploring the proline-dependent conformational change in the multifunctional. *Biochemistry* **42**, 5469–5477.
- Zhu W, Becker DF.** 2005. Exploring the Proline-Dependent Conformational Change in the Multifunctional PutA Flavoprotein by Tryptophan Fluorescence Spectroscopy. *Biochemistry* **44**, 12297–12306.
- Zhu W, Haile AM, Singh RK, Larson JD, Smithen D, Chan JY, Tanner JJ, Becker DF.** 2013. Involvement of the β 3- α 3 Loop of the Proline Dehydrogenase Domain in Allosteric Regulation of Membrane Association of Proline Utilization A. *Biochemistry* **52**, 4482–4491.
- Zhu Q, Zhang J, Gao X, Tong J, Xiao L, Li W, Zhang H.** 2010. The *Arabidopsis* AP2/ERF transcription factor RAP2.6 participates in ABA, salt and osmotic stress responses. *Gene* **457**, 1–12.

Abstract

The proteinogenic amino acid proline plays a crucial role for cellular metabolism in living organisms. In mitochondria, proline is oxidized to glutamate by the sequential action of proline dehydrogenase (ProDH) and pyrroline-5-carboxylate (P5C) dehydrogenase (P5CDH). In addition, ornithine δ -aminotransferase (OAT) also participates in P5C formation through the conversion of ornithine and α -ketoglutarate into glutamate and P5C. Using mutants and biochemical approaches, ProDH1, P5CDH, and OAT were shown to be involved during dark-induced leaf senescence (DIS) in *Arabidopsis thaliana*. Striking accumulation of P5C and proline was observed in *p5cdh* mutant and to a lesser extent in *prodh1prodh2* mutant, suggesting a putative proline-P5C cycle. Metabolomic analysis indicated that *prodh1prodh2* and *p5cdh* have a similar metabolomic profile, but significantly different from wild-type and *oat* mutant, demonstrating the role of proline oxidation during DIS. ProDH1 was shown to be preferentially associated to the mitochondrial membrane fraction, while P5CDH and OAT are more evenly distributed between matrix and membrane fractions. Homo- and hetero-oligomerizations of ProDH1, P5CDH, and OAT were revealed using Bimolecular Fluorescence Complementation (BiFC) assay of infiltrated tobacco leaves. Interactions between P5C metabolism enzymes were further highlighted in DIS leaves using proteomics approaches coupled with mass spectrometry. Our work demonstrates that these three enzymes form P5C metabolic complex(es) involved in the oxidation of proline to fuel mitochondrial electron transfer chain to support the energy needs of senescent cells.

Résumé

La proline, acide aminé protéino-gène, joue un rôle crucial dans le métabolisme cellulaire. Dans les mitochondries, la proline est oxydée en glutamate par l'action séquentielle de la proline déshydrogénase (ProDH) et de la pyrroline-5-carboxylate (P5C) déshydrogénase (P5CDH). L'ornithine- δ -aminotransférase (OAT) participe également à la formation de P5C via la conversion de l'ornithine et de l' α -cétoglutarate en glutamate et P5C. L'utilisation de mutants et d'approches biochimiques a révélé que ProDH1, P5CDH et OAT sont impliquées dans la sénescence des feuilles induite à l'obscurité (DIS) chez *Arabidopsis thaliana*. Une accumulation importante de P5C et de proline est observée chez le mutant *p5cdh* et, dans une moindre mesure chez le mutant *prodh1prodh2*, suggérant un cycle proline-P5C. Les mutants *prodh1prodh2* et *p5cdh* ont un profil métabolomique similaire qui diffère de celui du WT et de *oat*, démontrant ainsi le rôle de l'oxydation de la proline au cours de la sénescence. Nous avons montré que ProDH1 est essentiellement associée à la membrane mitochondriale, tandis que P5CDH et OAT sont plus uniformément réparties entre la matrice et la membrane. L'oligomérisation de ProDH1, P5CDH et OAT a été révélée à l'aide d'une analyse de complémentation bimoléculaire de fluorescence (BiFC). Les interactions entre ces enzymes du métabolisme du P5C ont été confirmées par des approches de protéomique couplée à la MS en condition de sénescence chez *A. thaliana*. Ces trois enzymes forment un(des) complexe(s) impliqué(s) dans l'oxydation de la proline pour alimenter la chaîne de transfert d'électrons mitochondriale afin de pourvoir aux besoins énergétiques des cellules sénescents.